GHENT UNIVERSITY

FACULTY OF PHARMACEUTICAL SCIENCES

Laboratory for General Biochemistry and Physical Pharmacy
nanomedicines & biophotonics

The repurposing of low molecular weight drugs to induce lysosomal release of siRNA and *in vitro* approaches to probe the toxicity of inorganic nanoparticles.

Freya Joris

Pharmacist
Master of Science in Drug Development

2017

Thesis submitted to obtain the degree of
Doctor in Pharmaceutical Sciences

Proefschrift voorgedragen tot het bekomen van de graad van
Doctor in de Farmaceutische Wetenschappen

Dean

Prof.dr.apr. Jan Van Bocxlaer

Promotors

Prof.dr.apr. Stefaan De Smedt

Prof.dr.apr. Koen Raemdonck

Members of the Exam Committee:

Prof.dr.apr. **Serge Van Calenbergh** (chairman)	Ghent University
Prof.dr.apr. **Christophe Stove** (secretary)	Ghent University
Prof.dr.apr. **Tom Coenye**	Ghent University
Prof.dr. **Arwyn Jones**	Cardiff University
Prof.dr.apr. **Véronique Préat**	Université catholique de Louvain
Prof.dr. **Roos Vandenbroucke**	VIB-Ghent University

Ghent, March 9th 2017

Promotors

Prof.dr.apr. Stefaan De Smedt

Prof.dr.apr. Koen Raemdonck

Author

Apr. Freya Joris

– The journey is the reward –

Steve Jobs, 1983

TABLE OF CONTENTS

LIST OF ABBREVIATIONS

PART I: THE REPURPOSING OF LOW MOLECULAR WEIGHT DRUGS TO INDUCE LYSOSOMAL RELEASE OF SIRNA

2OHOA	2-hydroxy oleic acid
5A2dC	5-aza-2'-deoxycytidine
Ago2	Argonaute 2
ASM	Acid sphingomyelinase
ASO	Antisense oligonucleotide
BMP	Bis(monoacylglycero)phosphate
CAD	Cationic amphiphilic drug
CaP	Calcium phosphate
CD	Carvedilol
CHAP31	Cyclic hydroxamic acid containing peptide 31
Chol-siRNA	Cholesterol-siRNA conjugate
CLQ	Chloroquine
CPP	Cell penetrating peptide
CRISPR	Clustered regularly interspaced short palindromic repeats
Dex-HEMA	Dextran hydroxyethyl methacrylate
Dex-NGs	Dextran nanogels
DL	Desloratadine
DLS	Dynamic light scattering
DMSO	Dimethylsulfoxide
DNMT	DNA methyl transferase
DPC	Dynamic polyconjugate
DOPE	1,2-dioleoyl-sn-glycero-3-phosphoethanolamine
DOTAP	(2,3-dioleoyloxy-propyl)-trimethylammonium

DSF	Disulfiram
dsRNA	Double stranded RNA
DX	Dextrometorphan
eGFP	Enhanced green fluorescent protein
FBS	Fetal bovine serum
FD	FITC-labeled dextran
FIASMA	Functional inhibitor of the acid sphingomyelinase
GalNAc	N-acetylgalactosamine
GR	Glucocorticoid receptor
HDAC	Histon deacetylase
HEPES	N-2-hydroxyethylpiperazine-N'-2-ethanesulfonic acid
i.t.	Intratumoral
LDR	Lysotracker® Deep Red
LMP	Lysosomal membrane permeabilization
LNP	Lipid nanoparticle
LPS	Liposome
LPX	Lipoplex
LSCM	Laser scanning confocal microscope
LSD	Lysosomal storage disorder
MFI	Mean fluorescence intensity
miRNA	microRNA
mRNA	messenger RNA
MTOC	Microtubule-organizing center
NA	Nucleic acid
NG	Nanogel
NM	Nanomedicine
NP	Nanoparticle
NPC1	Niemann-Pick C1

NPD	Niemann-Pick disease
NT	Nortriptyline
ON	Oligonucleotide
PAMAM	Poly(amidoamine)
PBS	Phosphate buffered saline
pDNA	Plasmid DNA
PEG	Polyethylene glycol
PEI	Polyethylenimine
PFA	Paraformaldehyde
PLA2	Phospholiase A2
PLD	Phospholipidosis
PLK1	Polo-like kinase 1
Pre-miRNA	Precursor microRNA
pri-miRNA	Primary microRNA
PTX	Paclitaxel
RISC	RNA-induced silencing complex
RNAi	RNA interference
SEM	Standard error of the mean
shRNA	Short hairpin RNA
siCTRL	Scrambled control siRNA duplex
sieGFP	siRNA duplex targeting eGFP
siNG	siRNA-loaded nanogel
siPLK1	siRNA duplex targeting PLK1
siRNA	Small interfering RNA
SSC	Side scatter
siSTABLE	Nuclease-stabilized siRNA duplex
SM	Sphingomyelin
SMoC	Small molecule carrier

SNALP	Stable nucleic acid lipid nanoparticle
SSO	Splice switching oligonucleotide
ST	Salmeterol
TM	Tobramycin
TMAEMA	2-(methacryloyloxy)ethyl)trimethylammonium chloride
TSA	Trichostatin A

PART II: *IN VITRO* APPROACHES TO PROBE THE TOXICITY OF INORGANIC NANOPARTICLES

$\Delta\Psi_m$	mitochondrial membrane potential
$[Ca^{2+}]_c$	Cytosolic free calcium concentration
AgNP	Silver nanoparticle
ATP	Adenosine triphosphate
AuNP	Gold nanoparticle
Ca^{2+}	Calcium
Cd	Cadmium
CeO_2NP	Cerium oxide nanoparticle
CNT	Carbon nanotube
d_c	Core diameter
DLS	Dynamic light scattering
DMSA	2,3-meso-dimercaptosuccinic acid
ECM	Extracellular matrix
ER	Endoplasmatic reticulum
GI	Gastro-intestinal
HCS	High content screening
hNSC	Human neural stem cell
ISDD	*In vitro* sedimentation, diffusion and dosimetry model

IONP	Iron oxide nanoparticle
MDDC	Monocyte derived dendritic cell
MDM	Monocyte derived macrophage
mNSC	Murine neural stem cell
MRI	Magnetic resonance imaging
NM	Nanomaterial
NP	Nanoparticle
NOAEL	No observed adverse effect level
NSC	Neural stem cell
NTC	Not treated control
OECD	Organization for Economic Cooperation and Development
PMA	poly(isobutylene-*alt*-maleic anhydride)
QD	Quantum dot
QSAR	Quantitative structure-activity relationship
REACH	Registration, Evaluation, Approval and Restriction of Chemicals
ROS	Reactive oxygen species
SiO_2NP	Silica nanoparticle
SEM	Standard error of the mean
SS	Shear stress
TEM	Transmission electron microscopy
TiO_2NP	Titanium dioxide nanoparticle
TNF_α	Tumor necrosis factor α
ZnONP	Zinc oxide nanoparticle

AIM & OUTLINE

Nanotechnology is one of the main drivers of the current scientific advancements. Indeed, by engineering materials in the nanoscale range, materials may acquire unique properties that allow the development of novel and innovative applications for sometimes well-known materials. Distinct nanoparticles enjoy widespread popularity as they are being exploited by various industries, such as the automotive, aerospace, chemical, textile and cosmetic industry. In this spirit, the use of organic and inorganic nanoparticles (NPs) is also being avidly explored for biomedical use. NPs can be applied to improve biomarker detection, enhance imaging-mediated diagnosis or improve treatment strategies. Overall organic nanoparticles have evolved further in their clinical development, whereas the elusive safety profiles of inorganic nanoparticles hinder their clinical implementation. In this thesis we will look into the origin of the questionable safety of inorganic NPs and how the optimization of nanotoxicity testing may bring solace. First, we look into the use of organic particles as nanocarriers for nucleic acids (NA), and how their delivery potential could be enhanced using low molecular weight adjuvants.

The therapeutic potential of nucleic acids has been well established for a myriad of disorders. In contrast, few NA-based therapeutics managed to transfer to the clinic. This can mainly be attributed to delivery challenges, as NA require delivery to their cytosolic or nuclear site of action to evoke a therapeutic effect. Nanocarriers were initially believed to be the magic bullet towards efficient delivery of NA. However, the intracellular endo-lysosomal entrapment upon endocytosis severely hampers their delivery efficiency. Indeed, only a minor fraction of the internalized NA dose manages to reach its intracellular site of action, whereas the bulk is destined for lysosomal degradation. Hence, escape to the cytosol remains a major intracellular hurdle, which we aim to tackle by improving cytosolic NA release through the repurposing of cationic amphiphilic drugs (CADs).

This method was initially investigated in the context of small interfering (si)RNA delivery, using dextran nanogels (NG) as a model nanocarrier. In **Chapter 1** we provide a general introduction to NA delivery by nanocarriers, focussing on the abovementioned NGs. In addition, we discuss the molecular RNA interference pathway, which is triggered upon

successful cytosolic delivery of siRNA and allows sequence-specific post-transcriptional gene silencing. Finally, we introduce the use of CADs as low molecular weight adjuvants and explain their molecular action, which is hypothesized to improve siRNA delivery. In **Chapter 2** we review literature on the use of low molecular weight adjuvants to improve NA delivery. More specifically, we describe how the delivery by distinct nanocarriers or the transfection efficiency of certain NA can be improved through the action of specific small molecules.

In **Chapter 3** we investigated whether CADs could be repurposed to improve the cytosolic siRNA delivery upon transfection with NGs in cancer cells. We furthermore assessed the effect of the CADs on the endo-lysosomal compartment in an attempt to elucidate how CADs facilitate siRNA transfer to the cytosol. Moreover, we evaluated whether additional CAD treatments at later time points could further induce cytosolic delivery of siRNA, thereby exploiting the lysosomes as an intracellular NA depot. Finally, we established the therapeutic potential of the adjuvant approach by enhancing the effect of an anti-cancer siRNA in non-small cell lung cancer cells.

Given the promising observations in **Chapter 3,** we aimed to establish the broader applicability of the adjuvant approach in terms of the adjuvant, NA cargo and nanocarrier. More specifically, in **Chapter 4** we examined if additional low molecular weight molecules without CAD properties could equally improve siRNA delivery. In addition, we assessed whether CADs could improve messenger RNA delivery and looked into the effect of CADs on the delivery by lipid-based formulations and a cholesterol-siRNA conjugate.

Several inorganic nanoparticles can equally be applied as delivery vehicles. Iron oxide (IO)NPs are for instance being developed for magnetism-guided drug delivery and gold and silica NPs are investigated for their NA delivery potential. Additional potential applications comprise imaging, biomarker detection and cancer treatment (through hyperthermia). Despite the large body of research on the potential biomedical use of distinct inorganic NPs, few are currently applied in the clinic. Overall, the main setback towards clinical translation remains the questionable safety, which can at least in part be attributed to the publication of conflicting and inconsistent data. Hence, standardization of *in vitro* nanotoxicity assessments became a hot topic with various research groups pinpointing drawbacks in the current testing paradigm and identifying parameters that require optimization. We aimed to

contribute to the optimization effort by assessing the importance of the applied cell model in mechanistic nanotoxicity evaluations and NP optimization studies.

In **Chapter 5** we first provided a general introduction into the field of nanotoxicity by discussing several mechanisms through which inorganic NPs may affect the cell homeostasis and the conventional *in vitro* assays applied to study cell-NP interactions. Moreover, intrinsic shortcomings to these methods are highlighted and recently developed assays are introduced. Finally, we provide insights into how the *in vitro* cell model complexity affects NP uptake and toxicity.

In **Chapter 6** we studied the interaction of iron oxide (IO)NPs with six related neural cell types, namely neural stem cells, a neural progenitor cell line and neuroblastoma cell line derived from both humans and mice. In short, we assessed the IONP-induced cytotoxicity, production of reactive oxygen species and the impact of IONPs on the calcium homeostasis, mitochondrial health and cell morphology. Hereby, we aimed to unveil whether the cell type and species extensively influence the outcome of *in vitro* nanotoxicity studies and if the cell model should be standardized, just like many other elements of the *in vitro* nanotoxicity testing paradigm. In a follow-up study, presented in **Chapter 7**, we investigated if the selected cell model affects the nanosafety optimization of inorganic NPs for biomedical use. Hereto we evaluated cell-NP interactions in the same setup as described in **Chapter 6** and looked into the cell-NP interaction of differentially coated IONPs.

Thus in this thesis we aim to tackle an important short coming to of both organic and inorganic NPs, being the low delivery efficiency and the optimization of nanotoxicity assessments, respectively. In a final chapter **(Chapter 8)** we discuss the broader international context and commercial incentive towards the use of both types of NPs. Finally, we look into the clinical development of inorganic NPs and nanoconstructs for siRNA delivery and discuss how research on both topics should be continued.

PART I

The repurposing of low molecular weight drugs to induce lysosomal release of siRNA.

CHAPTER 1

General introduction to RNA interference, nanogels as nanocarriers and functional inhibitors of acid sphingomyelinase.

Freya Joris, Stefaan C. De Smedt, Koen Raemdonck.

Lab of General Biochemistry and Physical Pharmacy, Faculty of Pharmaceutical Sciences, Ghent University, B9000 Ghent, Belgium.

Table of contents

ABSTRACT

RNA interference (RNAi) is a highly conserved biological process applied by the cell to regulate gene expression in a sequence specific fashion at the post-transcriptional level. Ever since the discovery of this phenomenon, researchers have set out to use it to their advantage as a lab tool or a novel therapeutic strategy. In this thesis we triggered the RNAi pathway with short interfering RNA (siRNA). Given the issues connected to nucleic acid delivery, an appropriate carrier was applied to obtain intracellular siRNA delivery. More specifically, we applied dextran nanogels in the majority of the experiments. In this general introduction we supply the reader with background information on the RNAi pathway, its effectors – including siRNA – and the nanocarriers that can be applied to deliver siRNA, with a focus on dextran nanogels. In a final section, we focus on the use of functional inhibitors of the acid sphingomyelinase to enhance cytosolic siRNA delivery.

1. RNA INTERFERENCE

RNA interference (RNAi) is a mechanism through which gene expression can sequence-specifically be modulated at the post-transcriptional level. This process is highly evolutionary conserved, given its important function in the endogenous regulation of gene expression and the defense against viral infections and foreign genetic material, such as transposons.[1-3]

RNAi was first witnessed in plants in 1990.[4] Nearly a decade later Fire and Mello showed that exogenous double stranded RNA (dsRNA) silenced an endogenous gene in a sequence specific way in *C. elegans*.[5] For their pioneer work, both gentleman were rewarded the Nobel Prize for Physiology and Medicine in 2006. Soon after these observations, RNAi was shown to modulate gene expression in mammalian cells.[6] From this point onwards, research into this pathway with regard to both the elucidation of the molecular mechanism and the potential applications fiercely increased. The first report on RNAi-mediated gene silencing in human cells appeared in 2004.[7] One year earlier, a first successful *in vivo* study was published, which systemically applied naked siRNA in a murine acute liver failure model.[8] In 2004, Acuity Pharmaceuticals commenced a first Phase I clinical trial where naked siRNA targeting the VEGF pathway was injected intravitreally for the treatment of age-related macular degeneration.[9] Soon afterwards stable nucleic acid lipid nanoparticles (SNALP) were applied to deliver 1-2.5 mg/kg siRNA *via* an intravenous injection in non-human primates, leading to >90% apolipoprotein B silencing in the liver 48h post injection.[10] Intranasally administrated siRNA was reported to be safe and well tolerated in 2008.[11] The final glass ceiling was breached in 2010 with the report on the first clinical Phase I study in humans providing a proof-of-concept that systemically administrated siRNAs can silence target genes in human beings.[12]

As a lab tool RNAi can be applied to elucidate protein functions or to create knock-down models mimicking certain disorders.[13, 14] More importantly, RNAi modulators can be applied as a therapeutic strategy for a vast diversity of disorders, such as viral infections, hereditary and autoimmune diseases or cancer.[15, 16] In this section we will introduce the RNAi pathway as well as its effectors.

1.1. Mechanism

The RNAi pathway can be triggered by different categories of effector molecules, including microRNA (miRNA) and short interfering RNA (siRNA). Although both groups share certain steps in the pathway, both their biogenesis and final effect on the target messenger RNA (mRNA) differ (Figure 1.1).[17]

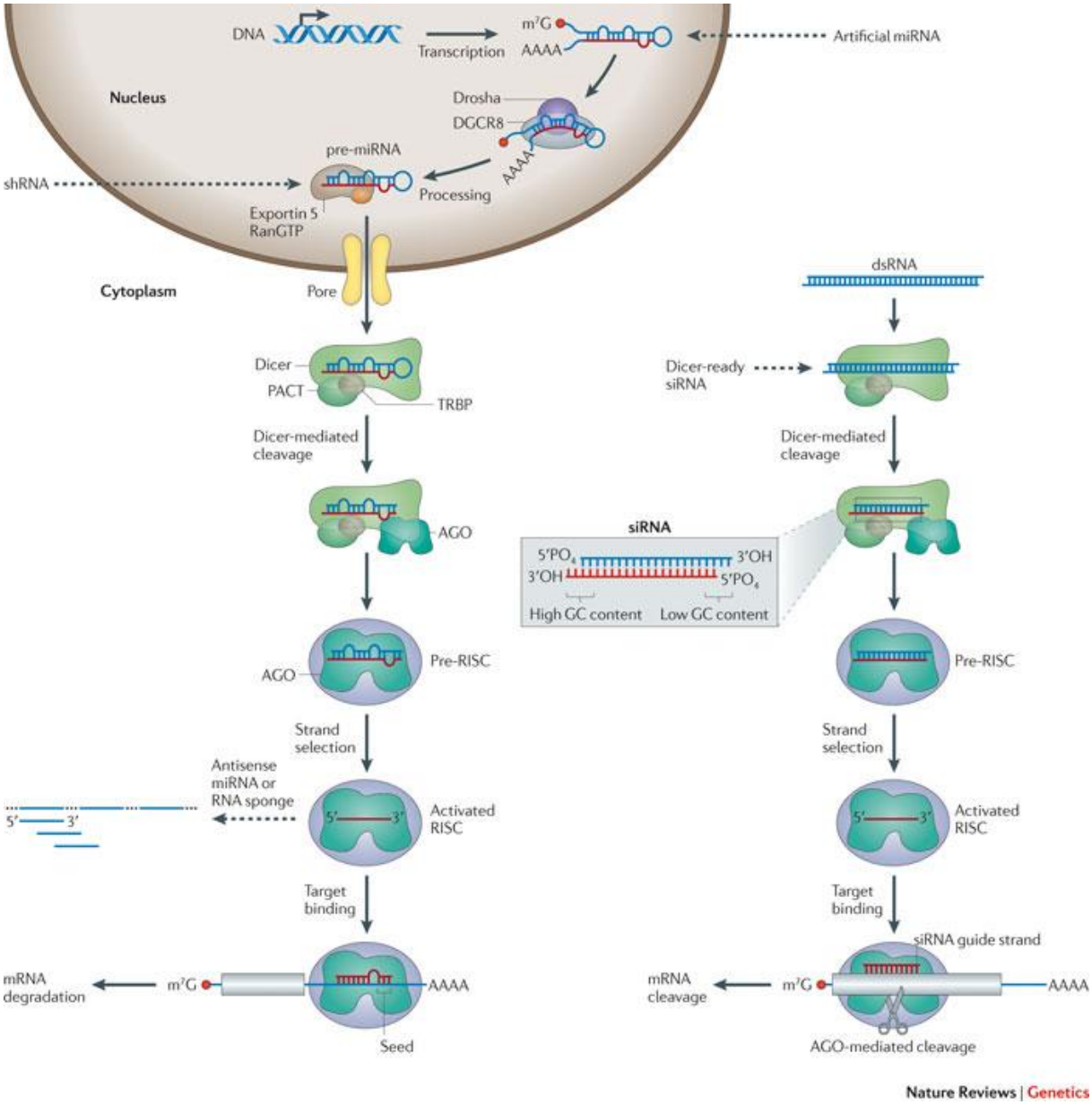

Figure 1.1. miRNA biogenesis and the RNAi molecular pathway followed by miRNA (left) and siRNA (right). This figure is reproduced from Davidson et al.[18] © Nature Publishing group 2011.

First, siRNA is mainly exogenous in source whereas miRNA stem from endogenously expressed transcripts.[19] Primary miRNA (pri-miRNA) is generated through transcription by RNA polymerase II and folded into a stem-loop structure with bulges due to occasional base pair mismatches.[20] This pri-miRNA is subsequently transferred to the microprocessor complex, where Drosha cleaves the pri-miRNA into a shorter precursor miRNA (pre-miRNA).[17, 21] Next, pre-miRNA is shuttled from the nucleus to the cytosol by Exprotin-5.[22-24] Once in the cytosol, the pre-miRNA is processed by Dicer, which produces mature ˜22 nucleotides long miRNA duplexes and removes the loop structure.[20]

Where miRNA mainly stems from endogenously expressed transcripts, siRNA generally enters the cytosol as a long dsRNA molecule upon a viral infection. As for pre-miRNA, the dsRNA is cleaved by Dicer at ˜22 nucleotide intervals to generate mature siRNA duplexes with 2 nucleotide overhangs at the 3' end.[25] In contrast to miRNA, the base pairs in the siRNA molecule show complete complementarity wherefore no bulges are present in the mature duplexes.[17, 20]

From this point onwards, both the mature siRNA and miRNA follow similar processing down the RNAi pathway. First, Argonaute 2 (Ago2) associates with the RNase complex containing Dicer to facilitate transfer of the mature siRNA or miRNA duplex to Ago2 in the so-called pre-RNA-induced silencing complex (pre-RISC). Here, the mature duplexes are unwound in an ATP-dependent process.[17] Next, the guide strand is selected based on the thermodynamic stability of both strands, with the strand with the more stable base pairs at its 5' end being more likely to become the passenger strand.[25, 26] The latter is subsequently discarded from pre-RISC or cleaved by Ago2 in case of miRNA or siRNA, respectively, whereby activated RISC* is obtained.[27, 28] The guide strand subsequently directs RISC* towards the target mRNA, which is recognized through Watson and Crick base pairing.[17]

From this point onwards the pathways for siRNA- and miRNA-mediated gene silencing once again diverge. In general, siRNA shows complete complementarity with its target mRNA and the phosphodiester bond of the target nucleotides associated with nucleotide 10 and 11 of the siRNA guide strand (counting from the 5' end) is cleaved by Ago 2.[29] Hereby, unprotected ends are created in the mRNA strand, which leaves it vulnerable to further degradation by exonucleases in the cytosol.[30]

Complete complementarity is in contrast not a prerequisite for miRNA-mediated gene silencing, as the target mRNA is generally recognized through complementarity with bases 2 to 8 of the miRNA guide strand, also known as the seed region.[31] Consequently, the target mRNA will either be degraded or its translation will be inhibited, based on the extent of base complementarity in the miRNA-mRNA duplex.[20, 32] In case of complete complementarity, Ago2 cleaves the mRNA similar to silencing by siRNA.[29, 33] However, in most cases incomplete complementarity leads to bulges in the mRNA-miRNA duplex, which hampers cleaving by Ago2. The consequent mechanism of gene silencing is still under debate. One possibility may be the inhibition of translation initiation by blocking the association of the 40S and 60S ribosome subunits.[34] The mRNA may in turn be shuttled towards the processing bodies (p-bodies) where it can be deadenylated and degraded.[17, 20]

This last distinction between siRNA- and miRNA-mediated gene silencing implicates that siRNA will theoretically silence a single target gene whereas a single miRNA can affect the expression of multiple genes.[15] An overview of the distinctions between siRNA and miRNA is provided in Table 1.1. SiRNA was selected for our work given its increased specificity.

Table 1.1. Distinctions between siRNA and miRNA source, processing and effect.

	siRNA	**miRNA**
Source	Exogenous ➔ Viral, transposons ➔ Synthetic dsRNA or siRNA	Endogenous ➔ Transcription by RNA polymerase II
Processing	Dicer: dsRNA -> siRNA	Drosha: Pri-mirNA -> pre-miRNA Dicer: Pre-miRNA -> miRNA
Structure mature duplex	˜22 base pairs 3’ 2 nucleotide overhang Complete complementarity	18-25 base pairs 3’ 2 nucleotide overhang Incomplete complementarity
Target recognition	Complete complementarity	Complementarity in seed region
# mRNA targets	One	Multiple
Mechanism of gene silencing	Ago2 cleaves target mRNA	Ago2 cleaves target mRNA Repress initiation translation Processing by p-bodies

1.2. RNAi triggers

Based upon the current knowledge of the RNAi pathway, several RNAi triggers could be developed. These include plasmid DNA (pDNA) or synthetic siRNA molecules, being either dsRNA or ˜22 base pair duplexes.[15] Of note, by synthesizing RNAi triggers with the proper sequence any given mRNA molecule can theoretically be targeted.

In case of pDNA, transcription of the transgene renders a short hairpin (sh)RNA molecule mimicking the pre-miRNA intermediate in the miRNA biogenesis. This shRNA is subsequently processed like miRNA but will cleave the target mRNA similar to siRNA.[35, 36] Interestingly, prolonged gene silencing can be achieved *via* this method when stable transgene expression is obtained.[37] Despite the fact that this strategy can be interesting for chronic disorders, this method also poses several challenges. First, in order to influence the target gene expression, the shRNA has to run through the entire miRNA pathway wherefore the extent of the effect largely depends on the kinetics of the various enzymes necessary for shRNA processing. Competition of the shRNA with endogenous pre-miRNA for exportin-5 and additional downstream enzymes may consequently affect the cellular RNAi homeostasis and cause severe adverse effects.[22, 38] Secondly, pDNA nuclear entry is a predicament for a successful therapy. Hence, the nuclear envelope needs to be crossed for successful delivery, which is one of the more difficult biological barriers to overcome during transfection.[39, 40]

Overall, the use of synthetic siRNA and especially that of ˜22 base pair duplexes is the preferred strategy. Such oligonucleotides can be easily produced on a large scale and are more easily transfected into the cytosol. Chemical modifications can furthermore reduce potential adverse events and improve the stability.[16, 41] Initially 25 to 27 base pair 'Dicer-ready' duplexes were applied. However, these duplexes still required Dicer mediated cleaving, which is not the case when applying synthetic ˜22 base pair duplexes mimicking mature siRNA molecules.[42] Hence, the latter are the overall selected weapon of choice. Indeed, by applying an effector that only enters the pathway at its final stage, a minimum effect on the cellular RNAi homeostasis is anticipated.[42]

2. NANOCARRIERS

Naked unmodified siRNA duplexes, as applied in preliminary work, largely failed to strongly influence gene expression. Two main factors were held responsible: namely the limited stability and the physicochemical properties of the duplex. Indeed, unmodified siRNA is prone to nuclease-mediated degradation and the large size and negative charge limit cellular siRNA internalization through passive diffusion.[43] The issue of siRNA degradation was in part resolved by chemical modifications of the siRNA bases whereas nanoparticles, the so-called nanocarriers, are most often applied to ensure internalization. In this section we provide a short overview of avidly applied nanoparticles for siRNA delivery, with a focus on the dextran nanogels (dex-NGs) used in the majority of the experimental work presented in the first part of this thesis.

2.1. Overview

Nanoparticles for nucleic acid delivery, from here on forward referred to as nanocarriers, can be divided into two main subgroups: viral and non-viral nanocarriers. Viral vectors allow great transfection efficiencies, but their use has been correlated with insertional mutagenesis and immunogenicity.[44] Non-viral vectors are in contrast considered to be a safer alternative although the main limitation remains their limited transfection efficiency. Thus, no ideal nanocarrier exists as of today.

Since the applied dex-NGs belong to the non-viral carriers, this subgroup will be further highlighted. In general, non-viral carriers can be subdivided in lipid-based, polymer-based and inorganic nanocarriers, all of which have shown potential to deliver siRNA.[2] Here, we provide a short introduction to the different nanocarriers for siRNA delivery. For more detailed information and extensive reviews on distinct formulations, the reader is referred to various recent reviews.[2, 3, 9, 41, 45]

Lipid-based carriers are most widely applied and have advanced furthest in their development.[41] Concurrently, most siRNA-formulations evaluated in clinical trials are lipid-based.[16, 41, 46, 47] The *in vitro* standard for siRNA transfection is Lipofectamine RNAiMAX, where lipids and siRNA are mixed to form lipoplexes.[2] Amphiphilic lipids are furthermore often applied as they spontaneously arrange in micellar or liposomal structures when dispersed in aqueous media.[48] Cationic lipids are generally added as liposome (LPS)

constituents to ensure siRNA complexation.[49, 50] Helper lipids can furthermore be included to improve the LPS stability (cholesterol) or endosomal escape efficiency (DOPE).[2, 49, 51] Many different synthetic and naturally occurring lipids (e.g. phospholipids, sphingolipids, cholesterol, etc.) can be applied to synthesize LPS, explaining the plethora of reported formulations.[2] Efforts on formulation optimization lead to the development of stable nucleic acid lipid particles (SNALP). This LPS consists of lipids that become charged in an acidic environment to promote escape and encapsulates the siRNA in its aqueous core. The LPS is furthermore stabilized by polyethylene glycol (PEG) and is readily degradable. In general, good *in vitro* and *in vivo* transfection results were obtained with SNALP, explaining its avid use in clinical trials.[10, 52, 53] More recently, Akinc *et al.* developed biodegradable lipid-like molecules, the so-called 'lipidoids'.[54] More than 1200 lipidoids could be created by combining hydrophobic alkylacrylate or –acrylamide chains of different lengths (C10-18) with various primary or secondary amine structures. A screening approach revealed the most efficient lipidoid-based carrier for siRNA delivery, which successfully induced gene silencing in hepatocytes *in vitro*, in mice and in non-human primates.[55, 56]

A second ominously applied strategy is the use of polymer-based nanocarriers.[3] Such carriers come in distinct structures depending on the applied polymer, with the most frequently reported ones being polyplexes, polymeric micelles, dendrimers and nanospheres.[2, 41] First, polyplexes are - similar to lipoplexes - prepared by simply mixing nucleic acids with the cationic polymer. The first polymer to be applied in this context was poly-L-lysine.[57, 58] Probably the best-known polymer applied in this way is polyethylene imine (PEI). The many amine groups are suggested to act as a proton sponge in the endosomal environment, which facilitates endosomal escape.[59, 60] However, the strong positive charge responsible for PEI-related cytotoxicity reduces its applicability.[61] Consequently, recent reports rather incorporate PEI into a formulation (lipid-based, polymer-based or inorganic nanocarriers) to enhance the escape properties of the latter rather than applying it on its own.[41, 62, 63] Secondly, polymeric micelles are generally prepared through self-assembly by introducing amphiphilic polymers (mainly tri-block polymers) into an aqueous milieu.[41] A third category comprises of dendrimers, which are repetitively branched molecules, with the most well-known example being the poly(amidoamine) (PAMAM) dendrimers. These are reported to promote endosomal escape through a proton sponge mechanism, but are on the downside

not biodegradable and are reported to evoke adverse effects.[2, 41] A final main category consists of the nanospheres, where the nucleic acids are electrostatically attached to the polymer throughout the entire sphere.[3] A popular polymer applied to prepare nanospheres is poly(lactic-co-glycolic acid) (PLGA). The biodegradable feature of this FDA-approved polymer allows to synthesize controlled release formulations, which consequently show excellent biocompatibility.[64, 65] The downsides of this polymer are its anionic charge and hydrophobic nature implying the necessity to introduce a cationic element to ensure NA complexation.[2, 41] The nanogels applied in this thesis furthermore belong to this category and will be discussed in detail in section 2.2.

In addition to the use of the abovementioned synthetic polymers various groups apply naturally occurring polymers.[2, 3] The polysaccharide chitosan is for instance avidly used given its excellent biocompatibility and abundance of amine groups allowing siRNA complexation.[66] Secondly, the cyclic oligosaccharides, also known as cyclodextrins, can be applied for siRNA delivery.[66, 67] A final category comprises the cell penetrating peptides (CPP). In this regard, a large variety of CPPs has been reported since the structure and size can be tuned by varying the amino acid number and composition.[68, 69]

Finally, inorganic nanoparticles (NPs) are considered interesting delivery vehicles, as their size and surface properties are to a large extent tunable.[2, 45] Nowadays these NPs are employed either alone or in combination with lipids or polymers. In the latter case, the NPs can either be the core of the construct or be present at the surface of the polymer- or lipid-based carrier. Overall, gold and mesoporous silica NPs are chiefly reported as NA delivery vehicles.[2, 45] Interestingly, gold NPs bind the NA through thiol linkages, which are revoked in the reducing cellular environment.[70] The mesoporous silica NPs are in turn applied for their good biocompatibility, their ease of surface functionalization and their large NA loading capacity.[71, 72]

2.2. Dextran-nanogels

The dex-NGs can be classified as nanospheres and more specifically as hydrogels. They consist of 2-(methacryloyloxy)ethyl)trimethylammonium chloride (TMAEMA) and dextran hydroxyethyl methacrylate (dex-HEMA) monomers that are cross-linked *via* an inverse emulsion photopolymerization method (Figure 1.2A).[66] The obtained dex-NGs are a 3D hydrophilic network, which can absorb large quantities of water and the positive charge, necessary to allow siRNA loading stems from the TMAEMA monomers.[66]

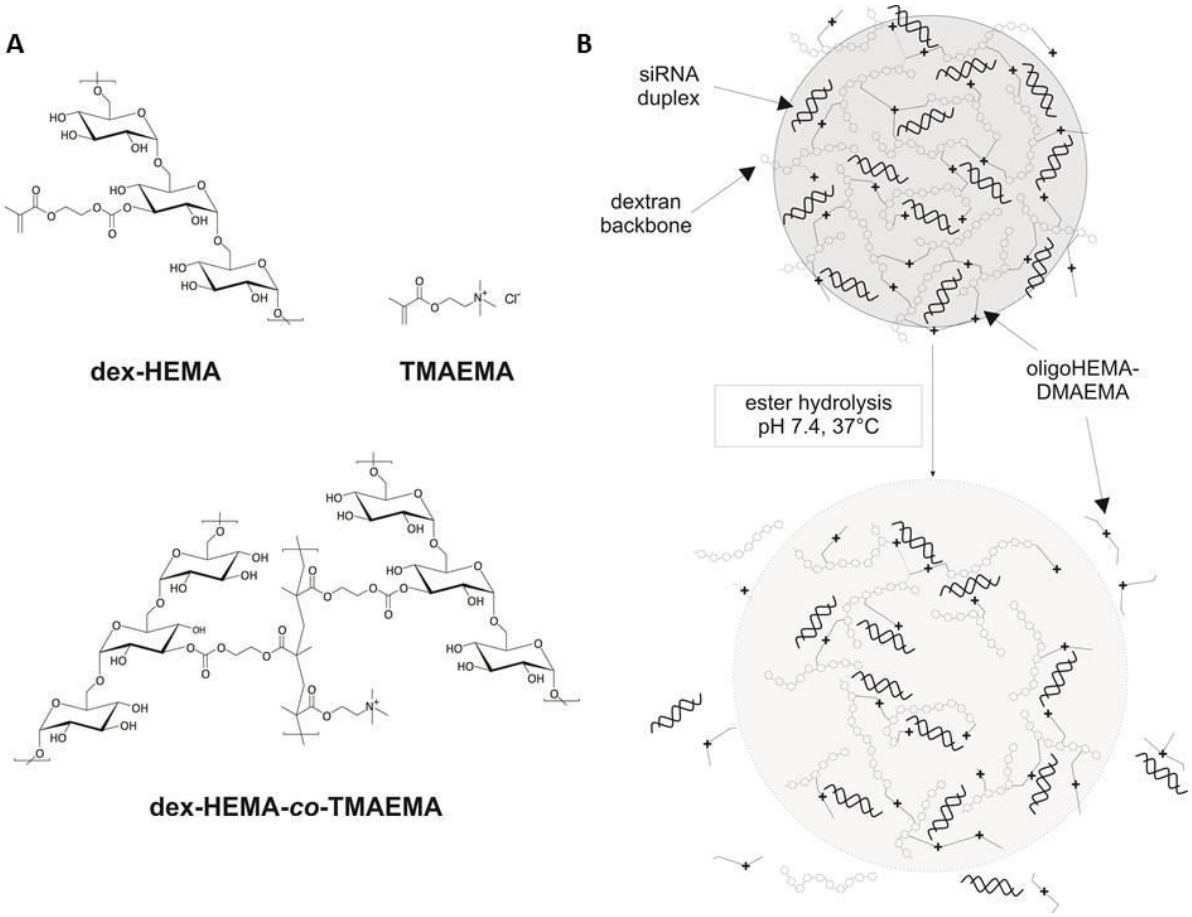

Figure 1.2. (A) Chemical structures of the dex-HEMA and TMAEMA monomers, and the three-dimensional nanogel network of dex-HEMA copolymerized with TMAEMA (dex-HEMA-co-TMAEMA) (B) Overview of the nanogel degradation process under physiological conditions (pH 7,4; 37°C). This figure is adapted from Raemdonck et al.[66, 73] © John Wiley & Sons 2009 and Elsevier 2010.

Previous work from our group highlighted the potential of these dex-NGs as a nanocarrier for siRNA delivery.[66, 74] They showed a high loading capacity, as up to 50 pmol siRNA can be complexated to 1 µg of lyophilized dex-NGs.[66, 74] The positive charge furthermore ensures good cellular uptake.[74] Once inside the cell, the carbonate ester linkages in the dex-HEMA monomers are prone to hydrolysis, especially at physiological pH (Figure 1.2B). Hydrolysis is in contrast slowed down in the acidic environment of the endo-lysosomes, thereby

protecting the dex-NGs and its siRNA cargo from rapid degradation.[74] Due to this hydrolysis, increasing amounts of water dilate the pores in the gel network, causing the particle to swell, degrade and release siRNA. Interestingly, this biodegradation can be tuned by varying the crosslinking degree in the dex-HEMA monomers.[66] Hence, dex-NGs with a proper crosslinking density can potentially be applied as a depot for prolonged intracellular siRNA release.

Previous work showed that the dex-NGs are internalized through endocytosis, stimulated by the interaction between the cationic dex-NGs and the negative membrane lipids. The majority of the internalized dex-NGs are subsequently trafficked to the lysosomal compartment.[74] During this process a certain amount of siRNA is able to reach the cytosol and induce gene silencing. However, relatively large siRNA doses are required to obtain the desired effect as cytosolic delivery remains incomplete. Hence, we evaluated if cytosolic siRNA delivery could be enhanced by a small molecular adjuvant strategy.

3. FUNCTIONAL INHIBITORS OF ACID SPHINGOMYELINASE

The evaluated small molecular adjuvants to boots siRNA delivery are functional inhibitors of the acid sphingomyelinase (ASM, FIASMA). FIASMAs are structurally diverse compounds from distinct drug classes. However, all known FIASMAs are cationic amphiphilic drugs (CADs), which implies that they contain a basic amine group and a hydrophobic segment. Hence, all FIASMAs are characterized by a pKa of at least 7.4 and a LogP > 3.[75, 76]

Due to these physicochemical properties, CADs preferentially accumulate in the acidic organelles. Indeed, the lysosomes can contain up to 100-fold higher CAD concentrations than the cytosol. It is in these lysosomes that the FIASMAs inhibit ASM.[75]ASM is a positively charged membrane bound enzyme that is anchored to the abundant negatively charged bis(monoacylglycero)phosphate (BMP) through electrostatic interactions. ASM requires this interaction for its protection against enzymatic degradation as well as its enzymatic action, being the hydrolysis of sphingomyeline into ceramide and phosphorylcholine.[77]

Upon lysosomal accumulation, the FIASMAs insert into the lysosomal membrane through their hydrophobic segment. They preferentially accumulate at the negative BMP regions due to electrostatic interactions with their positive amine groups. Upon sufficient accumulation, the electrostatic anchoring of ASM is perturbed and the latter is released from the membrane, followed by enzymatic degradation in the lysosomal lumen (Figure 1.3).[78] Hence, the FIASMA do not inhibit ASM through a key-lock mechanism, but sufficiently high concentrations are required to ensure functional inhibition, which is obtained through the lysomotrophic nature of the compounds. Consequently, sphingomyelin accumulates leading to a perturbed lipid balance with an increased sphingomyelin/ceramide ratio. This in turn causes lysosomal membrane destabilization and even permeabilization.[79, 80]

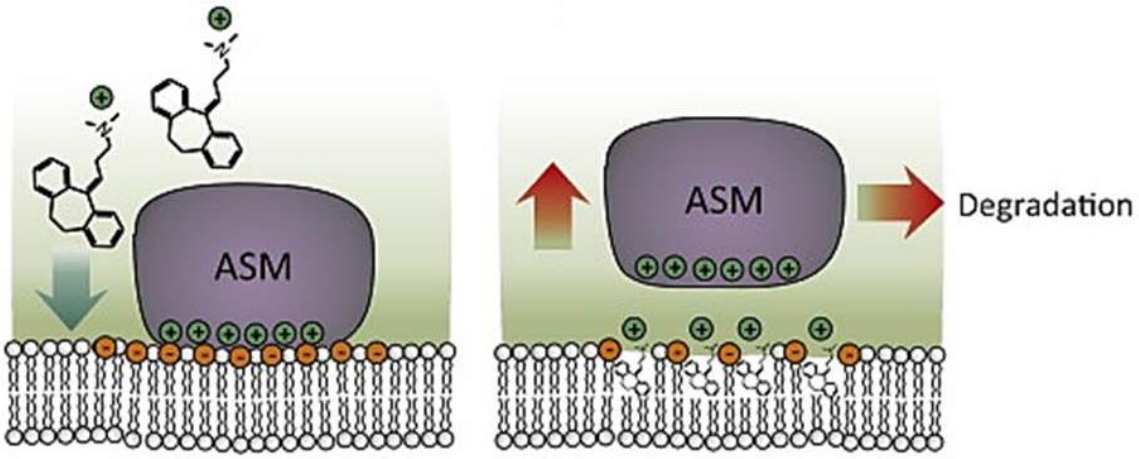

Figure 1.3. ASM is electrostatically anchored to the negative BMP region of the lysosomal membrane. FIASMAs insert into the membrane and interfere with the electrostatic interaction between BMP and ASM. Functional inhibition is obtained through ASM is release into the lysosomal lumen followed by cathepsin-mediated degradation. This figure is adapted from Kornhuber et al.[78] © Elsevier 2014.

Cancer cells are reported to be more sensitive towards perturbation of the lysosomal compartment.[80, 81] Due to their enhanced metabolic needs, cancer cells contain more and enlarged lysosomes, which are less stable and have a higher cathepsin content. In addition, cancer lysosomes contain less sphingomyelin and express lower ASM levels. Hence, lower FIASMA concentrations are required to functionally inhibit ASMs.[80] Indeed, several reports revealed CAD-mediated cancer-cell selective lysosomal membrane permeabilization (LMP).[82, 83] In turn, we investigated whether this phenomenon could be applied to induce cytosolic siRNA delivery of lysosomally accumulated siRNA.

REFERENCES

1. Hannon, G. J. *Nature* **2002,** 418, (6894), 244-51.
2. Tan, S. J.; Kiatwuthinon, P.; Roh, Y. H.; Kahn, J. S.; Luo, D. *Small* **2011,** 7, (7), 841-56.
3. Cun, D.; Jensen, L. B.; Nielsen, H. M.; Moghimi, M.; Foged, C. *J Biomed Nanotechnol* **2008,** 4, (3), 258-275.
4. Napoli, C.; Lemieux, C.; Jorgensen, R. *Plant Cell* **1990,** 2, (4), 279-289.
5. Fire, A.; Xu, S.; Montgomery, M. K.; Kostas, S. A.; Driver, S. E.; Mello, C. C. *Nature* **1998,** 391, (6669), 806-11.
6. Elbashir, S. M.; Harborth, J.; Lendeckel, W.; Yalcin, A.; Weber, K.; Tuschl, T. *Nature* **2001,** 411, (6836), 494-8.
7. Morris, K. V.; Chan, S. W.; Jacobsen, S. E.; Looney, D. J. *Science* **2004,** 305, (5688), 1289-92.
8. Song, E. W.; Lee, S. K.; Wang, J.; Ince, N.; Ouyang, N.; Min, J.; Chen, J. S.; Shankar, P.; Lieberman, J. *Nature Medicine* **2003,** 9, (3), 347-351.
9. Whitehead, K. A.; Langer, R.; Anderson, D. G. *Nat Rev Drug Discov* **2009,** 8, (2), 129-38.
10. Zimmermann, T. S.; Lee, A. C.; Akinc, A.; Bramlage, B.; Bumcrot, D.; Fedoruk, M. N.; Harborth, J.; Heyes, J. A.; Jeffs, L. B.; John, M.; Judge, A. D.; Lam, K.; McClintock, K.; Nechev, L. V.; Palmer, L. R.; Racie, T.; Rohl, I.; Seiffert, S.; Shanmugam, S.; Sood, V.; Soutschek, J.; Toudjarska, I.; Wheat, A. J.; Yaworski, E.; Zedalis, W.; Koteliansky, V.; Manoharan, M.; Vornlocher, H. P.; MacLachlan, I. *Nature* **2006,** 441, (7089), 111-4.
11. DeVincenzo, J.; Cehelsky, J. E.; Alvarez, R.; Elbashir, S.; Harborth, J.; Toudjarska, I.; Nechev, L.; Murugaiah, V.; Van Vliet, A.; Vaishnaw, A. K.; Meyers, R. *Antiviral Res* **2008,** 77, (3), 225-31.
12. Davis, M. E.; Zuckerman, J. E.; Choi, C. H.; Seligson, D.; Tolcher, A.; Alabi, C. A.; Yen, Y.; Heidel, J. D.; Ribas, A. *Nature* **2010,** 464, (7291), 1067-70.
13. Moffat, J.; Sabatini, D. M. *Nat Rev Mol Cell Bio* **2006,** 7, (3), 177-187.
14. Dorsett, Y.; Tuschl, T. *Nat Rev Drug Discov* **2004,** 3, (4), 318-329.
15. Kim, D. H.; Rossi, J. J. *Biotechniques* **2008,** 44, (5), 613-616.
16. Wittrup, A.; Lieberman, J. *Nat Rev Genet* **2015,** 16, (9), 543-52.
17. Carthew, R. W.; Sontheimer, E. J. *Cell* **2009,** 136, (4), 642-55.
18. Davidson, B. L.; McCray, P. B., Jr. *Nat Rev Genet* **2011,** 12, (5), 329-40.
19. Saini, H. K.; Griffiths-Jones, S.; Enright, A. J. *Proc Natl Acad Sci U S A* **2007,** 104, (45), 17719-24.
20. Wilson, R. C.; Doudna, J. A. *Annu Rev Biophys* **2013,** 42, 217-239.
21. Kim, Y. K.; Kim, V. N. *Embo J* **2007,** 26, (3), 775-783.
22. Yi, R.; Qin, Y.; Macara, I. G.; Cullen, B. R. *Genes Dev* **2003,** 17, (24), 3011-6.
23. Lund, E.; Guttinger, S.; Calado, A.; Dahlberg, J. E.; Kutay, U. *Science* **2004,** 303, (5654), 95-98.
24. Lund, E.; Dahlberg, J. E. *Cold Spring Harb Sym* **2006,** 71, 59-66.
25. Schwarz, D. S.; Hutvagner, G.; Du, T.; Xu, Z. S.; Aronin, N.; Zamore, P. D. *Cell* **2003,** 115, (2), 199-208.
26. Khvorova, A.; Reynolds, A.; Jayasena, S. D. *Cell* **2003,** 115, (4), 505-505.
27. Leuschner, P. J. F.; Ameres, S. L.; Kueng, S.; Martinez, J. *Embo Rep* **2006,** 7, (3), 314-320.
28. Tang, G. L. *Trends Biochem Sci* **2005,** 30, (2), 106-114.
29. Meister, G.; Landthaler, M.; Patkaniowska, A.; Dorsett, Y.; Teng, G.; Tuschl, T. *Mol Cell* **2004,** 15, (2), 185-197.
30. Orban, T. I.; Izaurralde, E. *Rna* **2005,** 11, (4), 459-469.
31. Bartel, D. P. *Cell* **2004,** 116, (2), 281-297.
32. Green, D.; Dalmay, T.; Chapman, T. *Heredity* **2016,** 116, (2), 125-134.
33. Bagga, S.; Bracht, J.; Hunter, S.; Massirer, K.; Holtz, J.; Eachus, R.; Pasquinelli, A. E. *Cell* **2005,** 122, (4), 553-563.
34. Dalmay, T. *Essays Biochem* **2013,** 54, 29-38.

35. Rao, D. D.; Vorhies, J. S.; Senzer, N.; Nemunaitis, J. *Adv Drug Deliver Rev* **2009,** 61, (9), 746-759.
36. Moore, C. B.; Guthrie, E. H.; Huang, M. T.; Taxman, D. J. *Methods Mol Biol* **2010,** 629, 141-58.
37. Vorhies, J. S.; Nemunaitis, J. *Expert Rev Anticancer Ther* **2007,** 7, (3), 373-82.
38. Grimm, D.; Streetz, K. L.; Jopling, C. L.; Storm, T. A.; Pandey, K.; Davis, C. R.; Marion, P.; Salazar, F.; Kay, M. A. *Nature* **2006,** 441, (7092), 537-41.
39. Zhou, X.; Liu, X.; Zhao, B.; Liu, X.; Zhu, D.; Qiu, N.; Zhou, Q.; Piao, Y.; Zhou, Z.; Tang, J.; Shen, Y. *J Control Release* **2016,** 234, 90-7.
40. Yin, H.; Kanasty, R. L.; Eltoukhy, A. A.; Vegas, A. J.; Dorkin, J. R.; Anderson, D. G. *Nat Rev Genet* **2014,** 15, (8), 541-55.
41. Juliano, R. L. *Nucleic Acids Res* **2016,** 44, (14), 6518-48.
42. Foster, D. J.; Barros, S.; Duncan, R.; Shaikh, S.; Cantley, W.; Dell, A.; Bulgakova, E.; O'Shea, J.; Taneja, N.; Kuchimanchi, S.; Sherrill, C. B.; Akinc, A.; Hinkle, G.; White, A. C. S.; Pang, B.; Charisse, K.; Meyers, R.; Manoharan, M.; Elbashir, S. M. *Rna* **2012,** 18, (3), 557-568.
43. Chiu, Y. L.; Rana, T. M. *Rna* **2003,** 9, (9), 1034-1048.
44. Zhi, D.; Zhao, Y.; Cui, S.; Chen, H.; Zhang, S. *Acta Biomater* **2016,** 36, 21-41.
45. Jiang, Y.; Huo, S.; Hardie, J.; Liang, X. J.; Rotello, V. M. *Expert Opin Drug Deliv* **2016,** 13, (4), 547-59.
46. Bobbin, M. L.; Rossi, J. J. *Annu Rev Pharmacol* **2016,** 56, 103-122.
47. Barata, P.; Sood, A. K.; Hong, D. S. *Cancer Treat Rev* **2016,** 50, 35-47.
48. Balazs, D. A.; Godbey, W. *J Drug Deliv* **2011,** 2011, 326497.
49. Felgner, J. H.; Kumar, R.; Sridhar, C. N.; Wheeler, C. J.; Tsai, Y. J.; Border, R.; Ramsey, P.; Martin, M.; Felgner, P. L. *J Biol Chem* **1994,** 269, (4), 2550-61.
50. Bouxsein, N. F.; McAllister, C. S.; Ewert, K. K.; Samuel, C. E.; Safinya, C. R. *Biochemistry* **2007,** 46, (16), 4785-92.
51. Gao, X.; Huang, L. *Gene Ther* **1995,** 2, (10), 710-22.
52. Heyes, J.; Palmer, L.; Bremner, K.; MacLachlan, I. *J Control Release* **2005,** 107, (2), 276-87.
53. Ozcan, G.; Ozpolat, B.; Coleman, R. L.; Sood, A. K.; Lopez-Berestein, G. *Adv Drug Deliv Rev* **2015,** 87, 108-19.
54. Akinc, A.; Zumbuehl, A.; Goldberg, M.; Leshchiner, E. S.; Busini, V.; Hossain, N.; Bacallado, S. A.; Nguyen, D. N.; Fuller, J.; Alvarez, R.; Borodovsky, A.; Borland, T.; Constien, R.; de Fougerolles, A.; Dorkin, J. R.; Narayanannair Jayaprakash, K.; Jayaraman, M.; John, M.; Koteliansky, V.; Manoharan, M.; Nechev, L.; Qin, J.; Racie, T.; Raitcheva, D.; Rajeev, K. G.; Sah, D. W.; Soutschek, J.; Toudjarska, I.; Vornlocher, H. P.; Zimmermann, T. S.; Langer, R.; Anderson, D. G. *Nat Biotechnol* **2008,** 26, (5), 561-9.
55. Love, K. T.; Mahon, K. P.; Levins, C. G.; Whitehead, K. A.; Querbes, W.; Dorkin, J. R.; Qin, J.; Cantley, W.; Qin, L. L.; Racie, T.; Frank-Kamenetsky, M.; Yip, K. N.; Alvarez, R.; Sah, D. W.; de Fougerolles, A.; Fitzgerald, K.; Koteliansky, V.; Akinc, A.; Langer, R.; Anderson, D. G. *Proc Natl Acad Sci U S A* **2010,** 107, (5), 1864-9.
56. Whitehead, K. A.; Dorkin, J. R.; Vegas, A. J.; Chang, P. H.; Veiseh, O.; Matthews, J.; Fenton, O. S.; Zhang, Y.; Olejnik, K. T.; Yesilyurt, V.; Chen, D.; Barros, S.; Klebanov, B.; Novobrantseva, T.; Langer, R.; Anderson, D. G. *Nat Commun* **2014,** 5, 4277.
57. Wu, G. Y.; Wu, C. H. *Biochemistry* **1988,** 27, (3), 887-92.
58. Wu, C. H.; Wilson, J. M.; Wu, G. Y. *J Biol Chem* **1989,** 264, (29), 16985-7.
59. Boussif, O.; Lezoualc'h, F.; Zanta, M. A.; Mergny, M. D.; Scherman, D.; Demeneix, B.; Behr, J. P. *Proc Natl Acad Sci U S A* **1995,** 92, (16), 7297-301.
60. Martens, T. F.; Remaut, K.; Demeester, J.; De Smedt, S. C.; Braeckmans, K. *Nano Today* **2014,** 9, (3), 344-364.
61. Moghimi, S. M.; Hunter, A. C.; Murray, J. C. *FASEB J* **2005,** 19, (3), 311-30.
62. Choi, M.; Lee, M.; Rhim, T. *Biomaterials* **2013,** 34, (30), 7453-61.
63. Chen, Z.; Zhang, L.; He, Y.; Li, Y. *ACS Appl Mater Interfaces* **2014,** 6, (16), 14196-206.

64. Sandor, M.; Mehta, S.; Harris, J.; Thanos, C.; Weston, P.; Marshall, J.; Mathiowitz, E. *J Drug Target* **2002,** 10, (6), 497-506.
65. Danhier, F.; Ansorena, E.; Silva, J. M.; Coco, R.; Le Breton, A.; Preat, V. *J Control Release* **2012,** 161, (2), 505-22.
66. Raemdonck, K.; Naeye, B.; Buyens, K.; Vandenbroucke, R. E.; Hogset, A.; Demeester, J.; De Smedt, S. C. *Adv Funct Mater* **2009,** 19, (9), 1406-1415.
67. Islam, M. A.; Park, T. E.; Singh, B.; Maharjan, S.; Firdous, J.; Cho, M. H.; Kang, S. K.; Yun, C. H.; Choi, Y. J.; Cho, C. S. *J Control Release* **2014,** 193, 74-89.
68. Lehto, T.; Ezzat, K.; Wood, M. J.; El Andaloussi, S. *Adv Drug Deliv Rev* **2016,** 106, (Pt A), 172-182.
69. Kurrikoff, K.; Gestin, M.; Langel, U. *Expert Opin Drug Deliv* **2016,** 13, (3), 373-87.
70. Oishi, M.; Nakaogami, J.; Ishii, T.; Nagasaki, Y. *Chem Lett* **2006,** 35, (9), 1046-1047.
71. Xia, T. A.; Kovochich, M.; Liong, M.; Meng, H.; Kabehie, S.; George, S.; Zink, J. I.; Nel, A. E. *Acs Nano* **2009,** 3, (10), 3273-3286.
72. Li, X.; Xie, Q. R.; Zhang, J. X.; Xia, W. L.; Gu, H. C. *Biomaterials* **2011,** 32, (35), 9546-9556.
73. Raemdonck, K.; Naeye, B.; Hogset, A.; Demeester, J.; De Smedt, S. C. *J Control Release* **2010,** 145, (3), 281-8.
74. De Backer, L.; Braeckmans, K.; Demeester, J.; De Smedt, S. C.; Raemdonck, K. *Nanomedicine (Lond)* **2013,** 8, (10), 1625-38.
75. Kornhuber, J.; Muehlbacher, M.; Trapp, S.; Pechmann, S.; Friedl, A.; Reichel, M.; Muhle, C.; Terfloth, L.; Groemer, T. W.; Spitzer, G. M.; Liedl, K. R.; Gulbins, E.; Tripal, P. *PLoS One* **2011,** 6, (8), e23852.
76. Kornhuber, J.; Tripal, P.; Gulbins, E.; Muehlbacher, M. *Handb Exp Pharmacol* **2013**, (215), 169-86.
77. Jenkins, R. W.; Canals, D.; Hannun, Y. A. *Cell Signal* **2009,** 21, (6), 836-846.
78. Kornhuber, J.; Muller, C. P.; Becker, K. A.; Reichel, M.; Gulbins, E. *Trends Pharmacol Sci* **2014,** 35, (6), 293-304.
79. Giraldo, A. M. V.; Appelqvist, H.; Ederth, T.; Ollinger, K. *Biochem Soc T* **2014,** 42, 1460-1464.
80. Gulbins, E.; Kolesnick, R. N. *Cancer Cell* **2013,** 24, (3), 279-281.
81. Saftig, P.; Sandhoff, K. *Nature* **2013,** 502, (7471), 312-313.
82. Ellegaard, A. M.; Dehlendorff, C.; Vind, A. C.; Anand, A.; Cederkvist, L.; Petersen, N. H. T.; Nylandsted, J.; Stenvang, J.; Mellemgaard, A.; Osterlind, K.; Friis, S.; Jaattela, M. *Ebiomedicine* **2016,** 9, 130-139.
83. Petersen, N. H.; Olsen, O. D.; Groth-Pedersen, L.; Ellegaard, A. M.; Bilgin, M.; Redmer, S.; Ostenfeld, M. S.; Ulanet, D.; Dovmark, T. H.; Lonborg, A.; Vindelov, S. D.; Hanahan, D.; Arenz, C.; Ejsing, C. S.; Kirkegaard, T.; Rohde, M.; Nylandsted, J.; Jaattela, M. *Cancer Cell* **2013,** 24, (3), 379-93.

CHAPTER 2

Boosting non-viral nucleic acid delivery and transfection efficiency: small molecules aid to convey big messages.

Manuscript in preparation.

Freya Joris, Stefaan C. De Smedt, Koen Raemdonck.

Lab of General Biochemistry and Physical Pharmacy, Faculty of Pharmaceutical Sciences, Ghent University, B9000 Ghent, Belgium.

Table of contents

ABSTRACT

There is no doubt regarding the great therapeutic potential of nucleic acids (NA). To be functional, NA require delivery into the cytosol or nucleus of the target cell. To first ensure cellular internalization, NA are generally packaged into nanomedicines. However, many nanomedicines largely fail to deliver the bulk of their NA cargo to its intracellular site of action. Indeed, escape from the endosomal lumen following nanomedicine uptake through endocytosis, remains an inefficient process. Interestingly, increasing evidence exists that major NA delivery hurdles can in part be overcome through helpful biological functions of distinct classes of small molecules. Our literature study revealed how various (classes of) small molecular compounds can intervene at distinct stages of the delivery pathway. Small molecules are reported to influence processes including nanomedicine internalization, endosomal escape, intracellular trafficking and transgene expression. Of note, a number of compounds exert their effect by simultaneously affecting several of these elements. Interestingly, the small molecular adjuvants were incorporated into the nanocarrier, conjugated to the nucleic acid or added before, during or after nanocarrier administration, indicating the versatility of this approach.

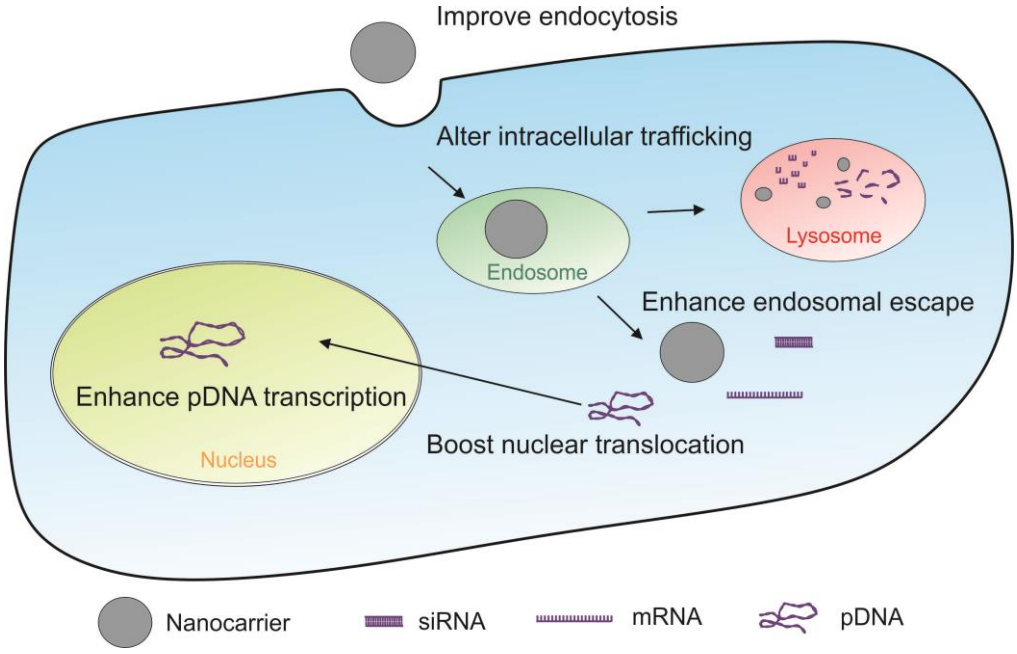

1. INTRODUCTION

The potential of nucleic acid (NA) therapeutics to treat a plethora of disorders has been clearly established in the course of the past three decades.[1] For instance, plasmid (p)DNA and messenger (m)RNA can be administered to restore protein expression. Splice switching oligonucleotides (SSO) in turn correct aberrant pre-mRNA splicing or induce alternative splicing to restore protein function.[2] Furthermore, antisense oligonucleotides (ASO) and RNA interference (RNAi) triggers, such as small interfering (si)RNA, short hairpin (sh)RNA and micro (mi)RNA, can be applied to silence disease-promoting genes.[3] However, relatively few NA drugs were successfully translated from bench to bedside.[4] This can mainly be attributed to the difficulty of safely and effectively delivering NA therapeutics to the desired (intracellular) target site, given the many extra- and intracellular barriers (Figure 2.1).[1, 5]

NA therapeutics encounter various extracellular barriers upon systemic administration. For one, most naked NA are readily attacked by nucleases present in the blood stream and can induce an innate immune response.[1] In addition, smaller NA are prone to glomerular filtration and renal elimination. Hence, naked NA suffer from rapid clearance, as evidenced by their short half-life of ˜10 minutes.[1] Both issues of the enzymatic degradation and the immunogenic character could at least in part be tackled by chemical modifications.[3, 6] However, such modifications do not affect the NA size to reduce rapid clearance. Hence, suitable delivery agents are required to prolong the circulation time and ensure NA internalization. Both viral and non-viral nanocarriers are being developed in parallel, but only the latter is discussed in this overview. Although non-viral nanocarriers protect the NA cargo from nucleases in the bloodstream and rapid renal clearance, the nanocarrier itself faces several extra- and intracellular obstacles that hamper efficient delivery.[5] Upon systemic administration, proteins rapidly adsorb onto the nanocarrier surface. *Via* this protein corona, nanocarriers are recognized and internalized by macrophages of the mononuclear phagocyte system (MPS).[5] Next, the nanocarrier needs to reach its target through extravasation, unless endothelial or circulating cells are targeted.[7, 8] The ease of extravasation is in part determined by the size of the endothelial fenestrations. The latter are reported to be enlarged in for instance inflamed tissues and solid tumors, which facilitates passive targeting.[1, 5] The nanocarrier should subsequently be distributed throughout the target tissue, which is influenced by the interstitial pressure, cell density and extracellular matrix.[5]

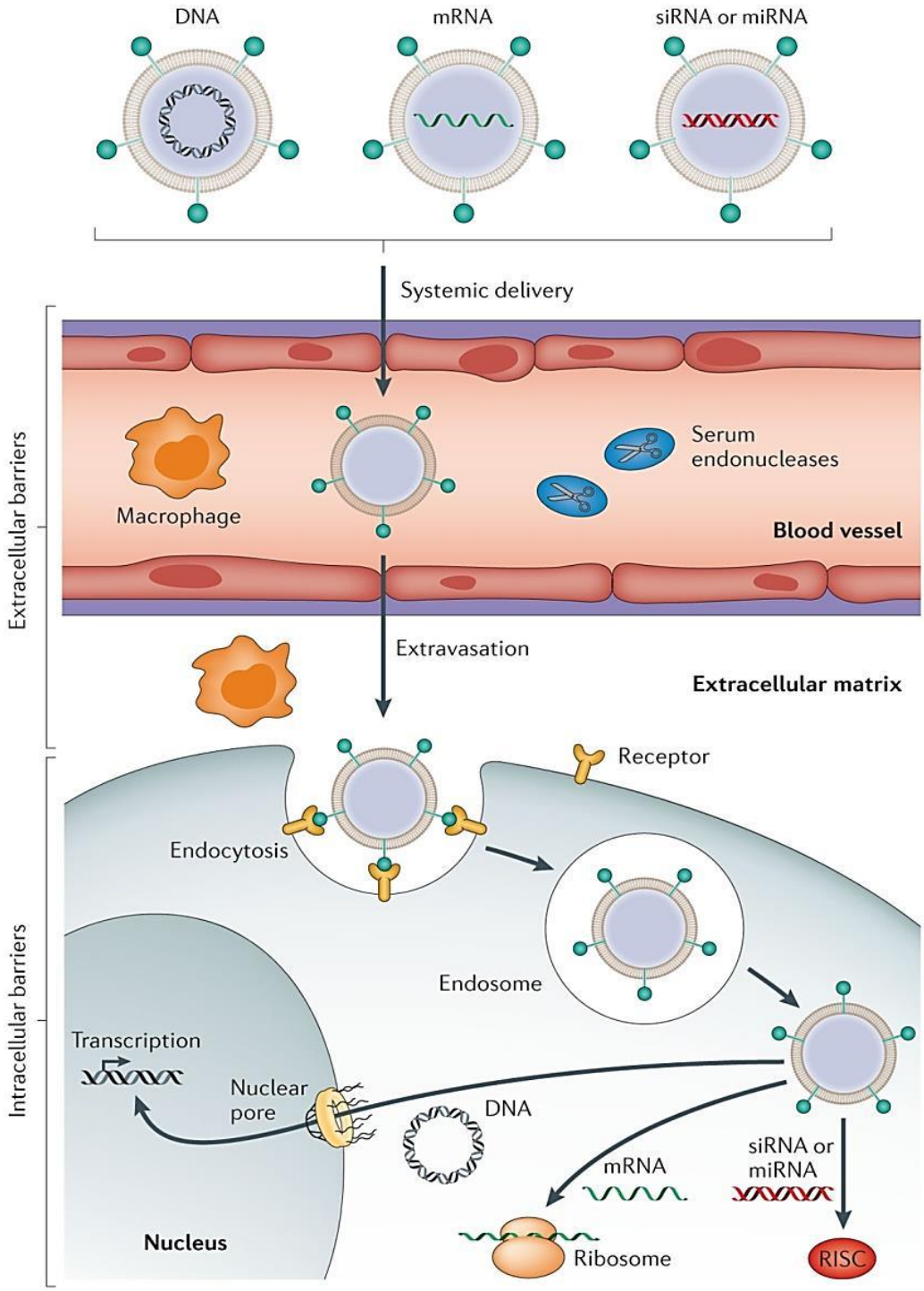

Figure 2.1. Intra- and extracellular barriers limit successful in vivo NA delivery via non-viral carriers. The latter need to overcome extracellular barriers, such as (i) degradation by serum endonucleases, (ii) immune detection, (iii) renal clearance and (iv) nonspecific interactions. Subsequently, the carriers must in most cases extravasate to reach their target tissue. Next, The nanocarriers should have sufficient mobility in the tissue extracellular matrix to reach the target cells. From this point onwards the cell membrane and entrapment in the endo-lysosomes pose major intracellular barriers. Finally, following endosomal escape, the NA need to reach their site of action. For siRNA and miRNA mimics this implies loading into the RNA-induced silencing complex (RISC), mRNA must interact with the translational machinery and DNA needs to cross the nuclear envelope in order to exert its function. This figure is adapted from Yin et al.[1] © Nature Publishing group 2014.

Once the nanocarrier has successfully reached the target cell, it additionally encounters several (intra)cellular barriers. The first is the cell membrane over which the nanocarrier is generally internalized *via* endocytosis. Consequently, the nanocarrier is captured in endosomal vesicles and will chiefly be trafficked to the lysosomes, where the acidic pH and lysosomal hydrolases can degrade both the carrier and cargo.[1] In contrast, NA require cytosolic or even nuclear localization to exert their function. Unfortunately, even for state of the art delivery systems endosomal escape remains a major bottleneck.[9, 10] For those NA that require nuclear translocation, the nuclear envelope presents a final important barrier towards successful transfections.[1]

Overall, the low delivery efficiency of non-viral carriers remains the major bottleneck. To meet this impediment, several strategies were suggested to overcome various extra- and intracellular barriers. An ideal carrier size range was for instance defined to improve their pharmacokinetic profile. Indeed, nanocarriers with a diameter below 20 nm are prone to renal clearance, while nanocarriers larger than 200 nm undergo hepatic clearance or are more easily removed by MPS.[1] Potentially the most widely applied strategy to arm the nanocarrier against rapid clearance by MPS, is to avoid opsonization with a polyethylene glycol (PEG) coating.[5] Moreover, targeting ligands were included to increase the tissue specificity. Such active targeting approaches theoretically improve carrier uptake *via* receptor-mediated endocytosis. However, a recent sobering report indicated that only a limited delivery advantage is obtained by actively targeting solid tumors.[11] On the intracellular level, many groups in turn focused on improving endosomal escape. Among others, such methods include the use of nanocarriers containing positively charged polymers or lipids with a high buffer capacity to induce the so-called proton sponge effect. In turn, fusogenic or lysogenic lipids or peptides and cell penetrating peptides are applied to increase the permeability of the endosomal membrane.[10, 12]

As an alternative to the abovementioned strategies, small molecules can be applied to improve NA delivery. Since the very start of LNP-mediated pDNA transfections, several groups experimented with the concept of low molecular weight adjuvants to increase the transfection efficiency. For instance, Fraley and colleagues were the first to report enhanced pDNA transfection *in vitro* upon a chloroquine (CLQ) pretreatment in 1981.[13] In 1994, Malone *et al.* found subcutaneous dexamethasone injections to improve the transfection by

intrahepatically injected pDNA.[14] Despite an initial wave of promising results, this concept left the foreground of the delivery field. However, many groups did combine low molecular weight drugs and NA as a possible anti-cancer treatment.[15] Here, the NA aid the drug through a synergistic effect on cell viability or reverting multidrug resistance. In recent years, the interest in the use of low molecular weight adjuvants to improve NA delivery was renewed, with several large-scale compound screenings identifying novel NA delivery enhancers.[16-18] This chapter bundles both the initial and recent reports to provide a general overview on low molecular weight adjuvants improving the therapeutic potential of NA.

2. SMALL MOLECULES IMPROVE NUCLEIC ACID UPTAKE

First, literature revealed that small molecules can boost NA internalization. On the one hand, adjuvants can enhance carrier distribution throughout the tumor tissue. On the other hand, small molecules can be incorporated in the nanocarrier as targeting ligands to boost uptake through receptor-mediated endocytosis. Furthermore, carbohydrates stimulate the cell to more avidly internalize NA. Finally, small molecules can modify the physicochemical properties of the carrier, thereby improving its uptake kinetics.

2.1. Small molecules enhance tumor penetration

The therapeutic potential of systemic NA therapies to treat cancer is widely investigated. To achieve an optimal therapeutic effect, the carrier needs to be evenly distributed throughout the tumor tissue. However, the mobility of nanocarriers in the tumor interstitium following extravasation is severely hindered by the high cell density, dense fibrotic extracellular matrix and high interstitial pressure, especially in solid tumors.[19, 20] Indeed, Kataoka's group showed that 70 nm micelles are confined to the vicinity of the tumor vessels, whereas 30 nm micelles can penetrate deeper into the tumor tissue.[21] Unfortunately, the size of most nanocarriers largely exceeds 30 nm, thereby severely limiting their tumor penetration.

Matrix modifiers, such as relaxin and bacterial collagenase, were initially investigated as penetration enhancers to improve delivery to solid tumors.[20] However alternative small molecules were evaluated, given the reported toxicity and the increased risk of tumor progression of the former. Losartan was for instance put forward due to its antifibrotic activity. Indeed, losartan doses with a minimal effect on blood pressure reduced the

intratumoral collagen I production in mice. Consequently, the tumor penetration and accumulation of intravenously (i.v.) or intratumorally (i.t.) injected 100 nm fluorescent nanoparticles (NPs) was significantly increased in three different tumor models. In contrast, NPs were found at the i.t. injection site or in the periphery of the untreated tumors following i.v. administration.[20] Losartan pretreatment clearly enhanced the *in vivo* efficacy of Doxil® liposomes (LPS) and could equally improve the delivery of NA loaded nanocarriers.

In addition, the group of Jessie Au introduced the concept of tumor priming. Here, tumors are pretreated with an apoptosis inducing agent to improve delivery.[22] More specifically, a single paclitaxel (PTX) administration prior to the nanocarrier treatment induces apoptosis in >10% of the tumor cells. Consequently, the cell density is reduced and the interstitial space is enlarged, becomes more porous and less tortuous in favor of interstitial nanocarrier transport. In addition, a PTX pretreatment increases the blood vessel radius, thereby improving tumor perfusion and increasing the nanocarrier supply.[19] This strategy was initially applied to successfully improve the efficacy of protein-bound drugs and Doxil® LPS.[19, 22] More recently, Wong *et al.* showed that PTX pretreatment enhanced the depth of LPS penetration in a 3D spheroid and tumor fragment histoculture.[23] A PTX pretreatment in turn improved the siRNA-mediated gene silencing in mice thereby reducing tumor growth and increasing survival, which underscored the therapeutic potential of tumor priming.[24, 25] In confirmation, docetaxel pre- or co-treatment improved the tumor distribution of LNPs in a mouse xenograft model.[26]

2.2. Small molecules improve NA internalization

2.2.1. The application of small molecules as targeting ligands

The success of a systemic NA therapeutic furthermore depends on its targeting efficiency. To date, satisfactory delivery could chiefly be obtained in the liver and spleen, given the preferential accumulation of most nanocarriers.[27-29] Unfortunately, many carriers fail to identify their target tissue, which results in nonspecific accumulation in off-target tissues.[30, 31] To overcome this impediment, it was proposed to apply targeting moieties. In theory, active targeting improves tissue specific biodistribution by enhancing interactions with the target cell surface and subsequent receptor-mediated endocytosis.[3] Initial targeting approaches mainly applied antibodies, peptides or antibody- or peptide-fragments.

However, several drawbacks included immune responses upon repeated administration, expensive manufacturing processes and non-straightforward formulation and characterization. Subsequently, small molecules were put forward as an alternative since they are less immunogenic, show better biodegradability and are easier to manufacture, characterize and integrate into a formulation.[31] In this regard, the small molecule can either be present on the nanocarrier surface or directly conjugated to the NA.

Probably, the best-known low molecular weight targeting ligand is folate. It is often applied to obtain cancer cell-specific uptake, as the folate receptor is overexpressed on the cell surface of various tumor cell types compared to normal tissue. Tumor targeting with folate can be obtained *via* many different strategies, as elaborately reviewed elsewhere.[30, 32]

A second popular targeting approach is the use of carbohydrates. For instance, mannose targets the lectin-like receptor on tumor cells, galactose and lactose interact with the asialoglycoprotein receptor to facilitate uptake in hepatocytes and stellate cells and fructose improves targeting of the hepatic Kupffer cells.[30] Furthermore, Akinc *et al.* synthesized a trivalent N-acetylgalactosamine (GalNAc) cluster, which can be conjugated to LNP or siRNA (Figure 2.2). GalNAc avidly binds the asialoglycoprotein receptor thereby promoting receptor-mediated uptake of the complex in hepatocytes in mice.[33] The GalNAc-siRNA conjugate recently advanced into Phase III clinical evaluation.[34] However, reanalysis of the Phase II data revealed higher mortality in the GalNAc-conjugate treated group, wherefore the Phase III study was prematurely terminated.[35]

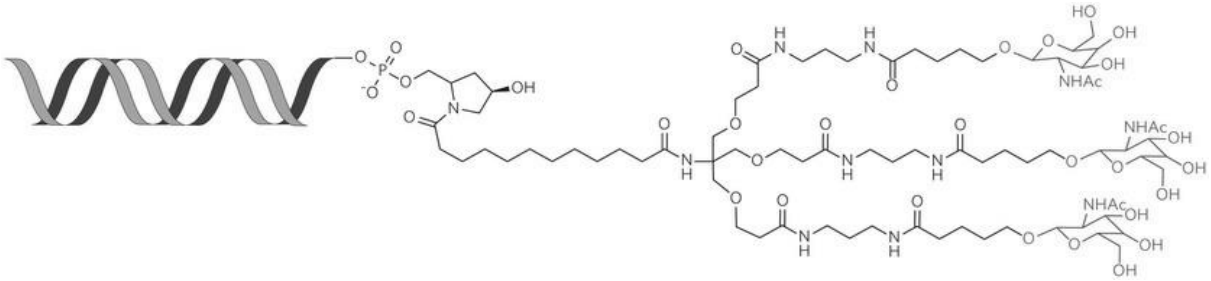

Figure 2.2. Molecular structure of a GalNAc-siRNA conjugate. This figure is reproduced from Kanasty et al.[36] ©Nature publishing group 2013.

Appropriate small molecular ligands are furthermore suggested to target tumors overexpressing the sigma receptor at their cell surface. For instance, Mukherjee *et al.* incorporated haloperidol – a high affinity ligand of the sigma receptor – in their formulation

for pDNA delivery and clearly observed improved transgene expression for the targeted formulation compared to the untargeted LPS or Lipofectamine® 2000. In addition, this improvement was blocked by treatment with free haloperidol and no differences in transgene expression were obtained for targeted and non-targeted LPS in CHO cells, which express low sigma receptor levels.[37] Subsequently, the group of Leaf Huang proposed the use of anisamide as a sigma-1 receptor ligand.[38] Incorporation of anisamide into their lipid-based carrier, improved siRNA delivery by 4-fold in B16F10 murine melanoma cells. These results were confirmed in mice, as tumor-specific uptake was obtained along with 70-80% luciferase silencing.[39] A follow-up study underscored the potential of this approach since anisamide-targeting of a carrier containing siRNA against MDM2, c-myc and VEGF markedly reduced lung metastasis and prolonged the mean animal survival time with 30%.[40] Nakagawa *et al.* furthermore conjugated a trivalent anisamide construct to SSO, which enhanced both the internalization and the biological effect of this complex *in vitro*.[41] However, the use of anisamide was recently put to question, as the interaction between the intracellular sigma-1 receptor and surface-bound anisamide may be unlikely and given the variable *in vivo* efficacy of anisamide-decorated nanocarriers.[42] Of note, the efficiency of active solid tumor targeting strategies was generally questioned since a recent meta-analysis revealed that active targeting moieties could not strongly augment the median internalized NA dose compared to non-targeted nanocarriers.[11]

Finally, Tam *et al.* recently reported a screening of 800 compounds to identify LNP uptake enhancers. Out of the 7 components that most significantly improved LNP uptake in HeLa cells by their presence during transfection, 3 were cardiac glycosides. These molecules bind to the extracellular region of the Na^+/K^+ ATPase pump, which induces endocytosis of the latter. Thus, the glycoside co-treatment likely improved LNP uptake *via* increased plasma membrane turnover. Accordingly, when strophanthindin (a cardiac glycoside) was incorporated into the LNP bilayer, the carrier internalization and gene silencing were improved *in vitro*. Given the general recurrence of the Na^+/K^+ ATPase pump throughout the body, the authors argued that this strategy could potentially be applied as a generic strategy to improve LNP uptake.[43] However, the limited selectivity could likewise imply the induction of off-target effects, thereby limiting the applicability of this approach for systemically administered nanocarriers.

2.2.2. Additional methods to improve nucleic acid uptake

In 1981, Fraley *et al.* showed that carbohydrates can additionally stimulate nanocarrier endocytosis.[13] Much more recently, Han *et al.* applied a similar approach to improve ASO delivery in muscle cells of a Duchenne muscular dystrophy mouse model. More specifically, intramuscular (i.m.) co-injection of ASO and a mixture of 2.5% glucose and 2.5% fructose enhanced the exon skipping activity of the former, resulting in a remarkable functional improvement at low ASO doses. The cellular metabolism of the injected hexoses produced excess ATP that subsequently supported the energy-dependent ASO uptake in energy deficient muscle cells. Of note, this approach could potentially be generally applicable to stimulate NA uptake in muscles and other energy-dependent tissues.[44]

In addition, several small molecules boost NA uptake through direct interaction with the carrier or NA, thereby altering the physicochemical characteristics in favor of cellular internalization. For instance, Osborn *et al.* identified Guanabenz (Wytensin^{TM}) as a delivery enhancer for cholesterol-conjugated siRNA (chol-siRNA). Guanabenz markedly improved chol-siRNA uptake in an siRNA sequence-independent, but NA-specific way, hypothetically by shielding the negative siRNA charge. However, the independent modulation of cellular processes involved in chol-siRNA uptake by Guanabenz could not be excluded.[18] Likewise, Gilleron *et al.* identified several hit compounds that significantly improved chol-siRNA uptake upon co-incubation through unidentified mechanisms. The same accounted for LNP, although little overlap was found between the hits for both constructs. Interestingly, a number of molecules improved LNP uptake when the molecules were added to the LNP dispersion prior to the transfection. An overnight incubation allowed direct interaction between the small molecule and the LNP, resulting in LNP size reduction and improved uptake kinetics.[16]

3. SMALL MOLECULES ENHANCE ENDOSOMAL ESCAPE

As mentioned in the introduction, NA enclosed in a nanocarrier are mainly internalized through endocytosis and become sequestered in the endosomal compartment. However, NA need to reach the cytosol or nucleus in order to achieve a therapeutic effect. Unfortunately, the amount of NA effectively reaching its intracellular site of action is dramatically low and the bulk of the carrier and cargo either leaves the cell *via* exocytosis or faces degradation in

the lysosomes.[9, 45] Hence, timely escape of the NA, preferably from the endosomal compartment to avoid exposure to lysosomal hydrolases, is one of the biggest challenges in the delivery field. In an effort to overcome this hurdle, various physical and chemical techniques were proposed to promote release by inducing a burst of the endosome, creating pores in the endosomal membrane or fusion of the carrier with the endosomal membrane (Figure 2.3).[10]

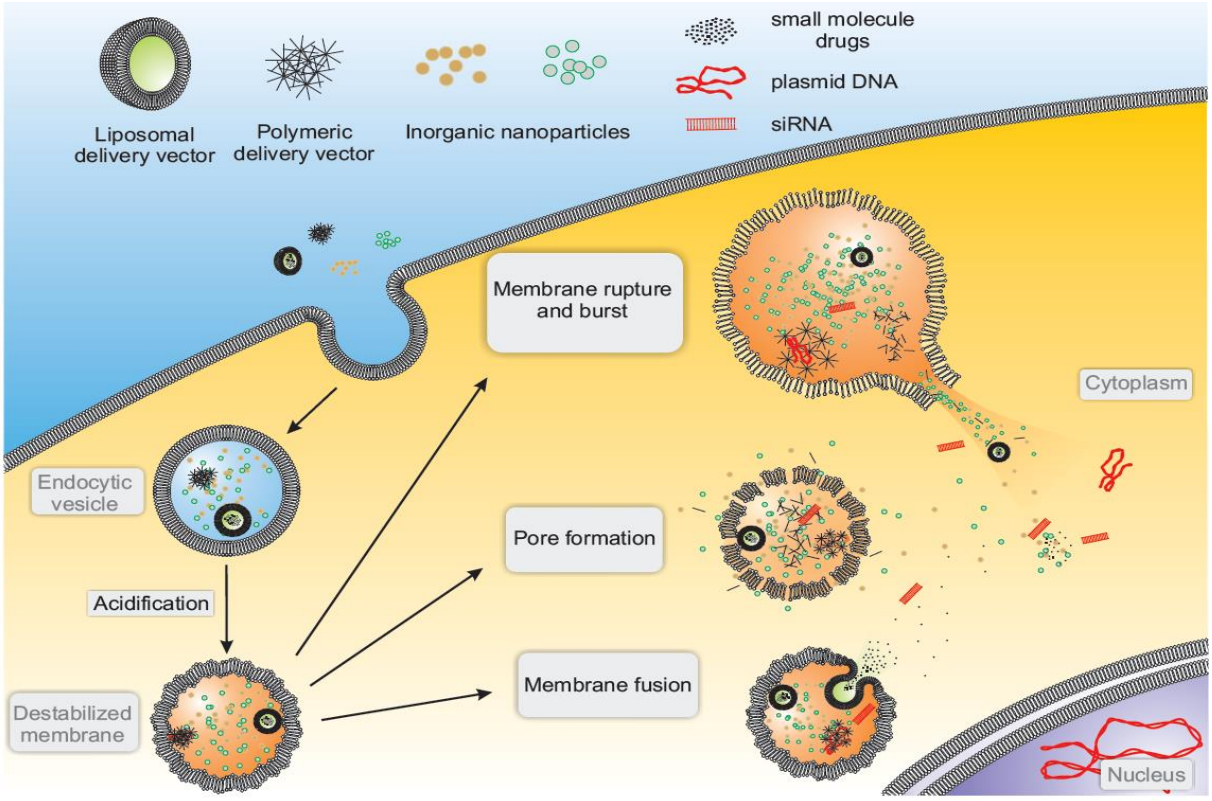

Figure 2.3. Nanocarriers are taken up by endocytosis and sequestered in the endosomal compartment (blue vesicle). From here on, vesicles gradually acidify (orange vesicle) and the cargo can be released through a burst of the endosomal membrane, the formation of pores or fusion of the lipid-based carrier with the endosomal membrane. This figure is adapted from Martens et al.[10] ©Elsevier 2014.

Interestingly, several small molecules were recently proposed to positively influence endosomal escape and reduce the chances of lysosomal entrapment. Yu *et al.* showed that exposure of the endosomal membrane to amphotericin B promotes endosomal escape through the formation of pores in the endosomal membrane. Upon inclusion of the compound in a micelle, siRNA delivery was markedly enhanced. In contrast, free amphotericin B failed to improve siRNA delivery and elicited toxicity, most probably by damaging the plasma membrane.[46] Furthermore, the plant glycoside SO1861 (known to trigger cytosolic delivery of the plant toxin saporin) improved the endosomal escape of

plasmid (p)DNA, mini circle (mc)DNA and siRNA delivered by lipid- and peptide-based carriers. Of note, siRNA-mediated gene silencing was to a lesser extent improved than transgene expression. Additionally, only a glycoside treatment post transfection positively influenced siRNA delivery, whereas glycoside presence during or after transfection as well as incorporation into the carrier improved DNA delivery. The glycoside was proposed to improve delivery via interactions with the endosomal membrane, though this remains to be experimentally confirmed.[47]

In an effort to identify small molecules that reduce the cytotoxic effect of bacterial toxins, Retro-1 was discovered. This molecule blocks retrograde trafficking by interfering with the shuttling from the late endosomes to the Golgi apparatus. Subsequently, Ming *et al.* evaluated the potential of this molecule to improve NA delivery and found that Retro-1 treatment post transfection improved NA release by preferential destabilization of the late endosomal compartment. Of note, Retro-1 improved the action of SSO and ASO but not of siRNA, which could potentially be attributed to limited uptake of the unstabilized siRNA. Furthermore, Retro-1 improved the *in vivo* activity of SSO in mice.[48] In a follow-up screening, more than 100.000 compounds were evaluated for their potential to improve the delivery of SSO, ASO and chol-siRNA. The identified hits improved the action of all three NA tested and were more potent than Retro-1. Similar to Retro-1, the hit compounds targeted the late endosomes to facilitate cytosolic NA release. However, only partial release was obtained since the bulk of the internalized NA dose remained entrapped in the late endosomes. It was not clear whether only a specific subset of endosomes was affected or if all endosomes were equally affected to a limited extent. Despite the fact that the exact impact on the endosomal membrane remains to be elucidated, the hits were proposed to enhance escape by (i) inducing defects in vesicle fusion, (ii) destabilizing the endosomal membrane or (iii) increasing the rate or extent of tubulation and budding of the carrier-containing vesicles.[17] In turn, the screening performed by Gilleron *et al.* furthermore identified hits that improved the escape of the LNP-encapsulated siRNA or chol-siRNA. Hit compounds could be subdivided according to their effect on the endosomal system, which was correlated to the possible mechanism through which escape was improved. These included: (i) interference with endosomal vesicle acidification or maturation, (ii) effects on intracellular trafficking or (iii) membrane destabilization.[16]

4. SMALL MOLECULES INTERFERE WITH INTRACELLULAR TRAFFICKING

Upon internalization through endocytosis, nanocarriers are sequestered in the early endosomes. From this point onwards, intracellular trafficking determines the cellular location of the carrier and its cargo. Initially the early endosomes mature to late endosomes, wherefrom the carrier is mainly trafficked to the lysosomes.[9, 45] The minor fraction of NA that is able to escape these compartments in turn needs to travel through the cytosol to reach its site of action. Small RNA molecules, such as siRNA, can freely diffuse through the dense cytosol, whereas NA larger than 2000 bases require active transport mechanisms.[49] In general, the cytosolic transport of both larger NA and endo-lysosomal vesicles containing NA-loaded nanocarriers occurs *via* microtubules.[50] Hence, scientists investigated whether microtubule (de)stabilizing agents can influence NA delivery.

The first report on this hypothesis was published in 1996, where Chowdhury *et al.* evaluated if a single intraperitoneal (i.p.) colchicine injection 30 minutes prior to the i.v. injection of a pDNA-asialoglycoprotein-polylysine complex improved the hepatic transgene expression in rats. Colchicine, which disrupts the microtubule network, increased the residence time of the delivered pDNA in the liver, accompanied by prolonged transgene expression up to 14 weeks compared to 48h in control rats.[51] Subsequently, Hasewaga *et al.* observed that a 60-minute nocodazole (microtubule disruptor) or taxol (microtubule stabilizer) pretreatment altered the cellular lipoplex (LPX) distribution. In untreated cells, the internalized LPX were trafficked over the microtubuli to the lysosomes, which in turn concentrated in the microtubule-organizing center (MTOC). Upon nocodazole treatment, the LPX and lysosomes were freely distributed throughout the cytosol without co-localization. In case of taxol, the LPX still preferentially resided in the perinuclear region without co-localizing with the lysosomes or the MTOC. Thus, the 2-fold improved transgene expression obtained with either compound could be explained by the prevention of lysosomal degradation due to alternate intracellular trafficking.[50] These findings were recently corroborated, as nocodazole pretreatment improved transgene expression by 8- and 40-fold, respectively, for Lipofectamine and LPX-mediated delivery *via* altering the LPX transport and intracellular destination.[52] In turn, Lindberg *et al.* confirmed the results on nocodazole whereas no improvement could be obtained with taxol.[53] The potential to enhance transgene expression was furthermore shown to be cell type-dependent: colchicine increased the LPS-mediated

pDNA transfection to varying extents in A549, H1299 and Chang Liver cells whereas PTX, which stabilizes the microtubuli, only enhanced transfection in the A549 cells.[54]

Wang and MacDonald evaluated a larger set of molecules known to specifically bind tubulin and inhibit its polymerization, namely colchicine, vinblastine, vincristine, nocodazole and podophyllotoxin. Pretreatment with each molecule dramatically enhanced the transgene expression (from 25- up to 39-fold) following transfection with cationic LPX.[55] The greater enhancement compared to Hasegawa *et al.* could potentially be explained by the prolonged pre-incubation time (3h vs 1h), the distinct cell type or differences in LPX compositions. Interestingly, colchicine failed to enhance transgene expression when present during transfection. Of note, inhibition of actin polymerization by cytochalasin B did not affect the transfection efficiency, underscoring that vesicle and pDNA transport occurs on microtubules. Interestingly, three molecules known to prevent endo-lysosomal fusion through distinct mechanisms improved the transfection efficiency, highlighting the importance of avoiding lysosomal sequestration.[55]

In addition, microtubule-stabilizing agents improve transgene expression following electroporation or microinjection. Indeed, the presence of taxol immediately after electroporation increased transgene expression by 4.5-fold, while nocodazole remained without effect.[56] Vaughan *et al.* furthermore hypothesized that histon deacetylase 6 (HDAC6) inhibitors influence cytosolic pDNA transport. The latter enhance microtubule acetylation, which improves the microtubule stability and results in the attraction of motor proteins. In confirmation, pDNA was trafficked to the nucleus remarkably quicker in a HDAC6 knock down model. Furthermore, taxol and the HDAC6 inhibitor NCT-10b had a similar positive effect on transgene expression following pDNA delivery *via* electroporation.[57]

The presence of microtubule stabilizing agents during polymer-mediated transfection also augmented transgene expression. For example, a 40-fold increased luciferase expression was obtained in PC3 cells with the HDAC6 inhibitor tubacin. This was correlated to the altered intracellular polyplex distribution, as the polyplexes were diffusely present in the cytosol in tubacin treated cells in contrast to the perinuclear condensation to the MTOC in untreated cells.[58] Similarly, PTX significantly enhanced transgene expression when present during polyethylenimine (PEI):pDNA transfection. In accordance with previous findings, actin

depolymerization by cytochalasin B had no influence on the transfection efficiency. Of note, microtubule disruption by colchicine strongly reduced the delivery efficiency of the PEI polyplexes in contrast to the significant improvement observed for lipid-based carriers.[59] The opposite effects of microtubule (de)stabilizing agents for lipid- and polymer-based carriers can presumably be explained by their intrinsic differences in intracellular trafficking and escape mechanism. PEI-based polyplexes likely require a certain extent of intracellular trafficking and vesicle acidification to facilitate pDNA release, which could be hampered by microtubule depolymerization. In turn, PTX promotes vesicle trafficking without advancing to endo-lysosomal fusion.[50] Thus, endosomal escape could still occur followed by improved pDNA transport to the nucleus over stabilized microtubuli.[59]

Although all molecules are applied to improve the transfection efficiency by preventing trafficking to the lysosomes, the effect of microtubule (de)stabilizing agents on transgene expression clearly depends on the cell type, carrier and applied small molecule. For lipid-based carriers, pretreatment with microtubule destabilizing agents provides the best results whereas polymer-based carriers require co-incubation with compounds that promote microtubule stability.

In addition, certain kinases influence intracellular trafficking. Consequently, pre-inhibition of protein kinase A with H89 promoted the transfection efficiency of branched PEI polyplexes 2- to 3-fold by inhibiting trafficking to the lysosomes. Although H89 pretreatment equally altered the trafficking pattern of linear PEI polyplexes and Lipofectamine, no influence on transfection efficiency could be detected for these carriers.[60]

Next to lysosomal routing, the carrier and cargo can be recycled to the extracellular milieu by exocytosis. Of note, up to 70% of the internalized siRNA dose can be exported, which is in part controlled by the endo-lysosomal Niemann-Pick C1 (NPC1) membrane protein.[45] Accordingly, NPC1 inhibition by NP3.47 delayed the recycling, which enhanced the silencing potential up to 4-fold in HeLa cells. The improved therapeutic potential was explained in terms of increased chances of endosomal escape by the prolonged cellular retention and reduced trafficking to the lysosomes.[61]

5. SMALL MOLECULES BOOST TRANSGENE EXPRESSION

When free pDNA in the cytosol is able to cross the nuclear envelope, the negatively charged pDNA associates with positive histones to form nucleosomes.[62] This inclusion of exogenous pDNA into the nuclear chromatin structure hampers efficient transgene expression and explains the gradual transgene silencing.[63] From this point onwards, the transgene expression is furthermore subjected to epigenetic regulation mechanisms.[64] Histone hyperacetylation is typically associated with gene expression by facilitating access of transcription factors and RNA polymerase to the unwound DNA.[38, 65] In contrast, histone deacetylation and methylation of a pDNA promoter region silences transgene expression.[66] Hence, various studies report on the use of epigenetic expression modulators in an effort to improve transgene expression. Of note, in contrast to the cytosolic HDAC6, the HDAC inhibitors described in this section target nuclear HDACs.

In 2000, Yamano and colleagues were the first to report the beneficial effect of the HDAC inhibitor depsipeptide on transgene expression. Co-exposure to LPS and depsipeptide significantly enhanced transgene expression *in vitro* through improved transcription, without affecting the number of pDNA copies in the nucleus. Transgene expression was additionally improved *in vivo* upon i.t. co-injection. However, a separate i.p. depsipeptide injection or inclusion of depsipeptide into the LPS failed to enhance transgene expression.[67] Subsequently, Liu *et al.* showed that i.v. co-injection of PEI:pDNA polyplexes and depsipeptide improved transgene expression in the liver, spleen and lungs of healthy mice. In tumor bearing mice, the expression was in turn preferentially enhanced in the metastatic breast cancer cells without affecting normal cells.[38] Besides depsipeptide, trichostatin A (TSA) and cyclic hydroxamic acid containing peptide 31 (CHAP31) improved transgene expression *in vitro* more efficiently in the human keratinocyte cell line (HaCaT) than in normal human keratinocytes. The expression in normal dermal fibroblast was to an even greater extent improved.[62, 65, 67] The enhanced transgene expression was cell type-dependent, which was explained by variations in the basal transgene expression levels and the availability of the transcription apparatus.[67] In addition, HDAC inhibitors enhanced transgene expression to a greater extent in more rapidly dividing cells, which can be explained by the improved nuclear translocation of pDNA during mitosis.[68] Hence, rapidly

dividing cells acquire more nuclear pDNA copies that are prone to enhanced transcription upon HDAC inhibition.

Additional studies report on the combination of various HDAC inhibitors with different delivery vehicles in diverse cell models. For instance, post transfection treatment with TSA, valeric acid, caproic acid, 4-phenyl butyric acid and butyric acid enhanced transgene expression following LPS-mediated pDNA delivery in CHO cells.[69] Kim *et al.* in turn found TSA, sodium butyrate and valproic acid to improve GFP expression in embryonic stem cells following transfection with the commercial carriers Lipofectamine® 2000 and FuGENE®.[70] A valproic acid treatment post transfection furthermore improved expression of a transgene delivered *via* PEI complexes in CHO cells.[71] Finally, the presence of etinostat during and post transfection with different polymer-based carriers enhanced luciferase expression up to 25-fold in bladder and prostate cancer cells.[62]

In general, these HDAC inhibitors increased the expression of successfully delivered but poorly expressed transgenes. They are suggested to improve expression through (i) the prevention of histone deacetylation, (ii) the acetylation (activation) of transcription factors and (iii) their influence on the expression of genes that in turn regulate transgene expression.[38, 65, 67] Thus, HDAC inhibition increases mRNA levels without affecting pDNA uptake, stability or translocation to the nucleus. This is a general phenomenon, independent of the applied promoter region or carrier. Initiation of adjuvant treatment more than 24 hours post transfection did not result in enhanced transgene expression.[63] Presumably, the applied molecules mainly keep the de novo synthesized histones, needed to form nucleosomes, acetylated.[69] When treatment initiation is delayed, many of the histones may have undergone deacetylation, leaving no room for a potential adjuvant effect.

Besides histone (de)acetylation, epigenetic gene regulation involves additional processes like DNA methylation, which is involved in gradual silencing of stably and transiently transfected genes.[66, 72] Consequently, Choi *et al.* showed that 5-aza-2'-deoxycytidine (5A2dC), a DNA methyl transferase (DNMT) inhibitor, could reactivate the transcription of stably transfected genes. Of note, the combination of 5A2dC with sodium butyrate or TSA resulted in a synergistic reactivation of the transgene.[72] Interestingly, 5A2dC could also improve the therapeutic potential of DNA vaccines both *in vitro* and *in vivo*. Indeed, a 5A2dC treatment

prior to vaccine delivery by gene gun increased the expression of the transgene-encoded antigen, resulting in reduced tumor growth and prolonged survival.[73] This strategy was furthermore tested in the context of polymer-based pDNA delivery. Backliwal *et al.* evaluated the potential of 4 HDAC inhibitors and 4 DNMT inhibitors to enhance transgene expression in CHO and HEK293 cells. Small molecule treatment was initiated 3 hours post transfection with PEI:DNA polyplexes. HDAC inhibitors were more efficient than DNMT inhibitors in HEK293 cells, whereas both groups equally efficient improved transgene expression in the CHO cells. Here, HDAC inhibitor and DNMT inhibitor combinations resulted in additive enhancement of gene expression. The variations between both cell types were explained in terms of relative abundance of HDAC and DNMT. In turn, histon deacetylation is a reversible process whereas DNA can only be demethylated upon replication, which may explain the variations in efficacy for both inhibitors observed in the HEK293 cells.[64]

Finally, Ishiguro and Sartorelli defined two additional (classes of) molecules with the potential to enhance transgene expression when added post transfection. The first molecule is phorbol 12-myristate 13-acetate, which presumably affects transgene transcription through the activation of protein kinase C. The second group – consisting of hexamethylene bisacetamide, diazepam, hypoxantine and 6-thioguanine – promotes the initiation of transcription potentially by destabilizing the chromatin structure.[63, 74]

6. ALTERNATIVE MECHANISMS TO IMPROVE THE TRANSFECTION EFFICIENCY

An additional major issue to NA delivery is the induction of an innate immune response upon recognition of the cationic carrier or NA cargo by pattern recognition receptors on the cell membrane or in the endo-lysosomes.[75-77] This immune response is reported to decrease the magnitude and duration of the NA effect, thereby severely reducing the therapeutic potential.[75, 77] Consequently, various groups evaluated the potential of small molecules to mitigate the immune response by blocking key proteins involved in NA recognition.[75] However, a successfully reduced innate immune response was not always clearly correlated to improved transfection efficiencies.[78-80] In contrast, Awe *et al.* applied BAY11 during and post transfection with RNAiMAX® to enhance mRNA-mediated reprogramming of adult human skin cells to pluripotency. BAY11 inhibits the NF-κβ-based immune response pathway, thereby significantly increasing the relative protein expression levels of the mRNA-

encoded reprogramming factors. Of note, the effect could be retained upon sustained BAY11 exposure. The exact mechanism for the enhanced trans-mRNA expression remains to be elucidated, although an enhanced mRNA stability (due to reduced immune response-mediated decay), improved translation and/or transfection efficiency were proposed.[81]

In addition, NA are subjected to degradation by endo-lysosomal nucleases. Indeed, Howell *et al.* showed that the success of pDNA transfection was reduced or enhanced in DNAse II overexpressing or knock out cells, respectively.[82] In corroboration, the naturally occurring endo-lysosomal DNAse II inhibitor, DMI-2, improved the expression of chloramphenicol acetyl transferase *in vitro*. Of note, the expression was 10-fold enhanced upon transfection with protein-A-poly-lysine conjugates, whereas the expression was only 1.5-fold improved upon lipofection and the transfection potential of calcium phosphate precipitates was not altered.[83] Hence, the adjuvant effect of the DNAse inhibitor DMI-2 was clearly carrier specific, potentially depending on (i) the ability of the carrier to shield the NA and (ii) the amount of NA released from the carrier available for degradation by endo-lysosomal nucleases.

Since many kinases are known to regulate different cellular processes that may influence the NA therapeutic efficiency, such as endocytosis, cell proliferation and gene transcription, Christensen *et al.* hypothesized that certain kinase inhibitors may positively influence transgene delivery and expression.[84] Kinase inhibitors with a positive impact on transgene expression affected cell cycle kinases, signal transducers and growth factor receptors. The Polo-like kinase 1 (PLK1) inhibitors altered the polyplex distribution from confinement in the MTOC to a diffuse presence in the cytosol. In addition, PLK1 inhibitors induced cell cycle arrest in the G2/M phase, where cells are more susceptive to transfection given the compromised nuclear membrane.[84] Likewise, synchronization of the cells in the G2/M phase prior to transfection can be applied to improve the pDNA transfection efficiency. Indeed, when removing the reversible inhibitor of cyclin-dependent kinase 1 (RO-3306) during transfection, the cells synchronously enter mitosis. During mitosis the nuclear envelope is compromised, which allows increased nuclear translocation of the pDNA followed by enhanced transgene expression.[68]

Finally, Kendall *et al.* reported that several small molecules improve ASO-mediated exon skipping in Duchenne muscular dystrophy. Most identified hits were compounds known to modulate the intracellular calcium level. More specifically, three compounds target the ryanodine receptor thereby potentially altering the calcium homeostasis in the nucleus in favor of exon skipping. Of note, the most potent adjuvant, dantrolene, enhanced exon skipping both *in vitro* and *in vivo*, leading to rescue of muscle function in mice.[85]

7. SMALL MOLECULES AS A NANOCARRIER

A nanocarrier should fulfill several functions, namely (i) tightly package the NA cargo, (ii) ensure stability in a biological environment, (iii) selectively deliver the payload to the target tissue, (iv) interact with the cell surface to initiate internalization and (v) induce endosomal escape.[86, 87] To meet these requirements, nanocarriers are often complex formulations consisting of several components, each with a specific function. For instance, cationic lipids or polymers are included to complex the NA, a hydrophilic polymer (e.g. PEG) assures colloidal stability and mitigates unspecific interactions, and ligands at the nanocarrier surface improve interaction with the cell surface and initiate receptor-mediated endocytosis.[88] In contrast, Gooding *et al.* proposed to apply a simple small molecule carrier (SMoC), with the small molecule consisting of cationic guanidine groups linked to a biphenyl backbone. This positively charged low molecular weight construct binds negatively charged NA and shields its charge.[89] The structure of the SMoC is based on cell penetrating peptides (CPP), which enter the cell through macropinocytosis upon binding of glycosaminoglycan chains of the proteoglycans on the cell surface. The guanidine rich SMoC mimics this CPP feature to ensure cellular internalization. The functionality of this SMoC for siRNA delivery was demonstrated *in vitro* by similar transfection efficiencies for both the SMoC and Lipofectamine, despite lower internalization of the former.[86]

8. PLEIOTROPIC ADJUVANTS

Finally, several molecules are able to improve the potential of NA therapeutics through various mechanisms. The previously mentioned molecule TSA belongs to this group, as it improves transgene expression through inhibition of nuclear HDAC and interferes with trafficking by inhibition of the cytosolic HDAC6.[57, 73] CLQ is potentially the most well-known compound in this category, besides dexamethasone and other steroids.

8.1. Chloroquine

Many reports can be found on the use of CLQ as an enhancer for NA delivery. In 1981, Fraley *et al.* were the first to report that CLQ pretreatment of glycerol-stimulated cells enhanced liposome-mediated pDNA delivery *in vitro*.[13] Combined efforts from different groups elucidated the mechanisms through which CLQ influences transgene expression. On the one hand, CLQ intercalates double stranded NA structures. This facilitates displacement from the carrier, prevents enzymatic degradation and recognition by toll like receptor 9 (TLR9), thereby preventing the initiation of an innate immune response. On the other hand, CLQ is reported to buffer the endosomes. Consequently, both the NA recognition by TLR9 and NA progression to the degrading lysosomal compartment are hampered, as they require an acidic pH.[90, 91]

The group of John Fabre showed the potential of a CLQ treatment during transfection to improve transgene expression in various cell models, such as corneal endothelial cells, primary rat neural cells and primary vascular smooth muscle cells.[92-95] In turn, Zhang *et al.* showed improved transfection of poly-lysine-pDNA complexes by CLQ co-incubation in HepG2 liver cells *in vitro* as well as in the rat liver *in vivo*.[96] A follow up study revealed that several animals showed 10- to 30-fold enhanced expression while others stayed without effect with the maximal tolerable dose scheme. In addition, 0.6 mg/L appeared to be the cut-off CLQ serum concentration whereupon effects on delivery were observed. In contrast, the improvement in transgene expression could not be linearly correlated to the CLQ serum levels. It was furthermore not possible to reach maximum transgene expression with the *in vivo* applicable CLQ doses, as previously observed *in vitro*. Thus, the *in vivo* applicability of CLQ as a small molecular adjuvant is hampered by its systemic dose-limiting toxicity.[97] Accordingly, the interest in the use of CLQ as a transfection enhancer faded in the following

years. More recently, CLQ was once again applied to enhance siRNA-mediated gene silencing. For instance, Stremersch *et al.* showed that a CLQ treatment post transfection with exosome-like vesicles markedly improved chol-siRNA mediated gene silencing in non-small cell lung cancer cells *in vitro*.[98] Accordingly, CLQ treatment during siRNA-loaded micelle transfection increased gene silencing by approximately 30%. Of note, CLQ did not affect gene silencing by Lipofectamine®. In turn, pretreatment with bafilomycin (a V-ATPase inhibitor) to prevent endosome acidification, completely abolished gene silencing. The authors argued that solely preventing endosome acidification is likely not sufficient to improve NA delivery although they did not question if the uptake was altered upon bafilomycin pretreatment.[99] Notably, a CLQ pretreatment significantly decreased LNP-mediated siRNA delivery.[9] Overall, the adjuvant effect depends on both the carrier and the moment of the adjuvant treatment relative to the transfection. Accordingly, the moment of CLQ treatment post transfection with PEI-coated mesoporous silica NPs determines the extent of the transfection efficiency enhancement. In case of adjuvant treatment 8 hours post transfection, the siRNA-mediated silencing was significantly enhanced whereas a CLQ treatment 36 hours post transfection failed to improve gene silencing. Since this impediment could be countered by the use of nuclease-stabilized siRNA, lysosomal siRNA degradation is potentially an important contributing factor (Figure 2.4).[100] Finally, both pDNA and siRNA delivery by mesoporous silica NPs was enhanced upon introduction of CLQ into the carrier.[101] Thus, despite the dose-limiting systemic toxicity of CLQ, this approach may improve the *in vivo* applicability of CLQ.

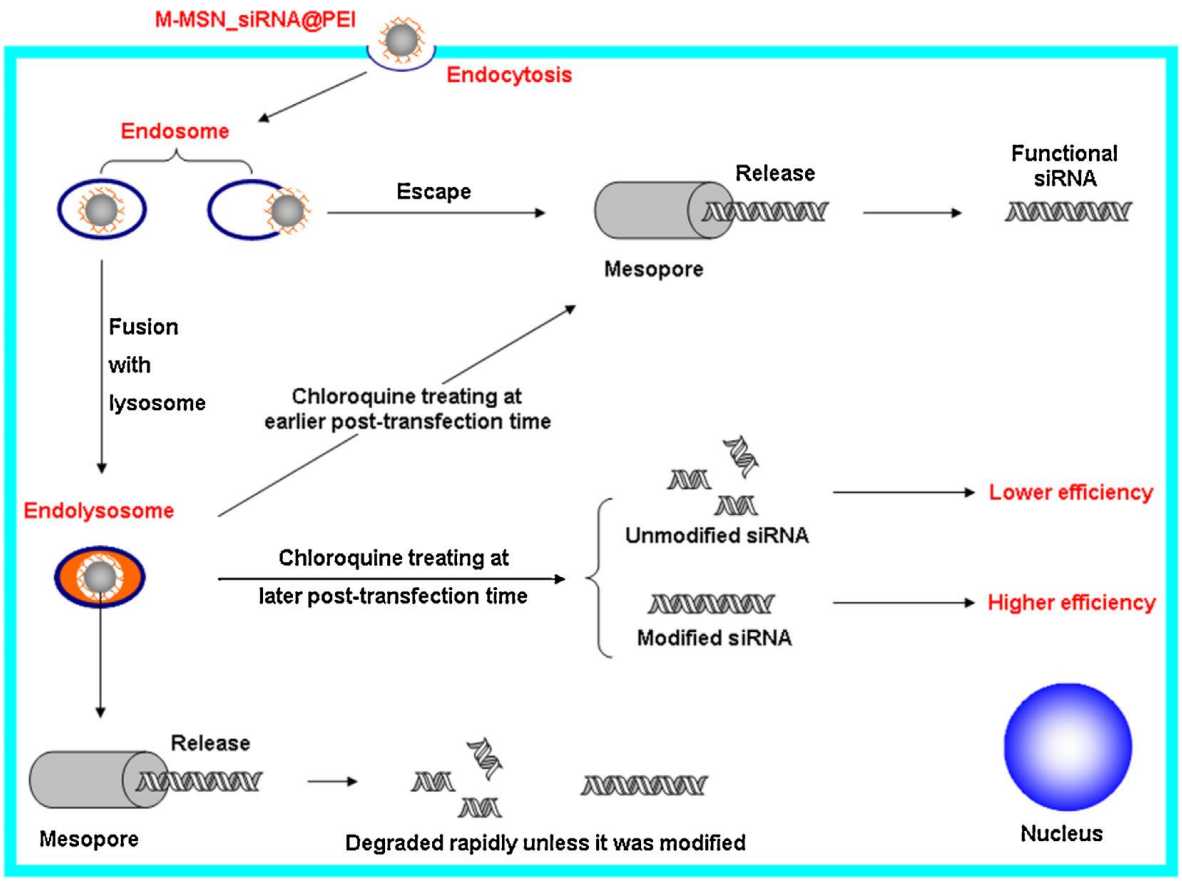

Figure 2.4. Mesoporous silica NPs coated with PEI (MSN_siRNAPEI) enter the cell through endocytosis. Upon timely endosomal escape functional siRNA reaches the cytosol. When CLQ is added early post transfection, escape of functional siRNA is enhanced. When CLQ is added 36 hours post transfection, siRNA is degraded in the lysosomes prior to release. Applying nuclease-stabilized siRNA circumvents this. Hence, even when added 36 hours post transfection, CLQ can induce release of the internalized nuclease-stabilized siRNA. This figure is reproduced from Wang et al.[100] ©Elsevier 2013.

8.2. Dexamethasone and other steroids

Already in 1994 it was believed that dexamethasone could improve the therapeutic potential of NA due to its anti-inflammatory and immune suppressive action.[14] Indeed, dexamethasone pretreatment enhanced luciferase expression in hepatocytes both *in vitro* and *in vivo* independent of the applied promoter sequence on the plasmid. Additionally, histological sections of treated rat livers showed reduced inflammation and an increased number of luciferase expressing hepatocytes.[14] Moreover, an i.p. dexamethasone injection reduced the secretion of tumor necrosis factor α and interleukin-1β in mouse lungs after i.v. injection of lipid-protamine-pDNA complexes and the level of transgene expression was inversely correlated to the cytokine levels.[102] A dexamethasone pretreatment can furthermore improve the *in vivo* therapeutic window of siRNA-loaded LNP in mice by suppressing pro-inflammatory gene expression, cytokine secretion and mitogen-activated

protein kinase phosphorylation without negatively affecting siRNA-mediated gene silencing.[103] Overall, the anti-inflammatory effect enhances the therapeutic efficiency of different NA regardless of applied the carrier or cargo. [104, 105]

Further *in vitro* studies revealed an additional aspect of the mechanism by which dexamethasone enhances transgene expression. For one, the adjuvant effect of dexamethasone could be abolished by pretreatment with a steroid receptor agonist (RU38486), implicating the necessity of glucocorticoid receptor (GR) binding.[104, 105] In addition, Kelly *et al.* observed increased plasmid translocation to the nucleus, which could be explained in terms of dexamethasone-mediated GR activation.[105] This leads to rapid translocation of the receptor-ligand complex to the nucleus and subsequent nuclear pore dilation, facilitating nuclear entry of the pDNA.[106]

Hence, this concept of facilitating shuttling to the nucleus was further explored by either conjugating dexamethasone to pDNA or the incorporation into a nanocarrier. For instance, Rebuffat *et al.* directly coupled dexamethasone to pDNA to enhance nuclear accumulation (Figure 2.5). However, the presence of dexamethasone sterically hindered the transcription initiation of nuclear pDNA.[107] In turn, Gruneich *et al*. successfully incorporated a dexamethasone-spermine conjugate into a liposomal formulation. Compared to Lipofectamine®, this construct induced transgene expression more efficiently combined with less inflammation *in vitro* and *in vivo*.[108] The delivery potential of PAMAM dendrimers could also be improved by dexamethasone conjugation.[109] In addition, conjugation of dexamethasone to PEI even outperformed dexamethasone pretreatment.[110] Of note, similar results could be obtained *in vitro* and *in vivo* by dexamethasone inclusion into a PEI-based vector, underscoring the general nature of the adjuvant effect.[111, 112] However, the therapeutic applicability of this strategy is somewhat limited by the tumor-promoting nature of dexamethasone and corticosteroids in general.[110]

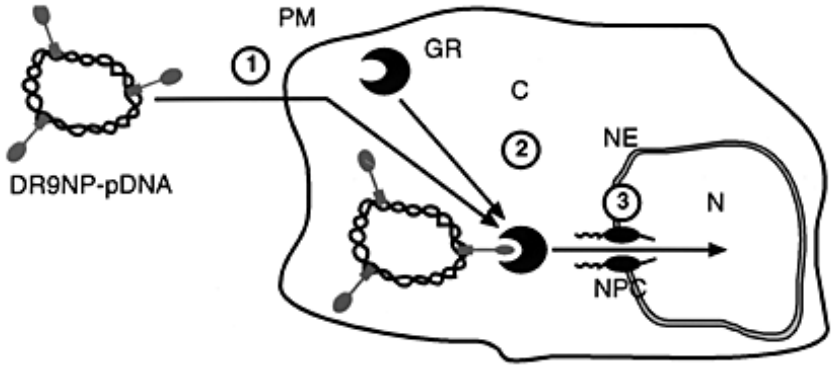

Figure 2.5. (1) Dexamethasone-pDNA conjugates are internalized over the plasma membrane (PM). (2) Dexamethasone facilitates the interaction of the pDNA-dexamethasone conjugate with the glucocorticoid receptor (GR). (3) This complex is transferred to the nucleus, where the GR facilitates dilation of the nuclear pore complex (NPC) to allow pDNA to cross the nuclear envelope (NE). This figure is reproduced from Rebuffat et al.[107] ©Nature Publishing group 2001.

Besides dexamethasone, other steroids are able to activate the GR and consequently improve transgene expression. Indeed, when cortisol is mixed with a plasmid prior to complexation with PEI, reporter gene expression is doubled. Cortisone, which is not able to activate the GR, did not influence the transfection efficiency, confirming the requirement of GR activation for improved translocation to the nucleus.[113] Furthermore, the presence of methylprednisolone during lipofection enhanced transgene expression up to 100-fold. Of note, even greater expression levels were achieved when methylprednisolone was included in the lipoplex.[114] In addition, methylprednisolone tripled luciferase expression in mice muscles, although the expression could not be prolonged compared to the control group.[104] Finally, estradiol increased both the number of transfected cells and the extent of reporter gene expression when applied during Lipofectamine® transfection.[115, 116] Besides improving cellular uptake, estradiol increased transgene translocation to the nucleus through an estrogen receptor-independent mechanism.[114, 116] Similar to methylprednisolone, estradiol inclusion into a lipoplex improved transgene expression to the greatest extent in both bronchial epithelial cells *in vitro* and in nasal and lung epithelium in mice. However, the *in vivo* efficiency was not as high as anticipated based on *in vitro* results, indicating that additional barriers need to be overcome.

9. CONCLUSION AND PERSPECTIVES

In conclusion, we provided a general overview of small molecular adjuvants that can be applied to enhance the NA delivery and/or transfection efficiency, thereby ultimately improving their therapeutic potential. The use of low molecular weight adjuvants provides an exciting alternative to conventional NA delivery approaches, which mainly focus on carrier design. Of note, the discussed small molecular adjuvants form a heterogeneous group and exert their effect by affecting specific aspects of NA delivery. For one, several compounds alter the biodistribution of a nanocarrier through active targeting or enhance tissue penetration. Other adjuvants have the ability to modulate intracellular trafficking or improve endosomal escape, which all prevent lysosomal sequestration and degradation of the carrier and cargo. Finally, some molecules mitigate the innate immune response or enhance the transfection efficiency directly by enhancing transgene expression or influencing cell cycle progression. For most categories of NA transfection enhancers, both *in vitro* and *in vivo* studies highlighted their adjuvant potential. Earlier reports mostly document on molecules capable of improving pDNA transfection, while more recent studies describe low molecular weight adjuvants improving the effect of additional NA therapeutics (Table 2.1).

The pleiotropic molecules CLQ and dexamethasone could generally improve NA transfection efficiencies. In contrast, most identified adjuvants aiming to avoid lysosomal sequestration only positively influenced the transfection efficiency under specific circumstances. Here, the beneficial effect strongly depended on the moment of small molecule treatment relative to the transfection, the applied carrier as well as the NA cargo and the cell model. In addition, the beneficial effect of microtubule (de)stabilizing agents depended on the uptake, trafficking and escape mechanism of the nanocarrier.

Overall, a better understanding of cellular internalization pathways, endosomal escape and intracellular trafficking will aid in rationally combining small molecular adjuvants with the desired NA and/or nanocarrier. Indeed, potentially thousands of proteins are involved in the abovementioned processes and could be targeted with the proper (combination of) adjuvants. In addition more research should be performed on the impact of reducing the innate immune response.

The applicability of the proposed adjuvant strategies requires *in vivo* evaluation in terms of efficacy and safety. Despite the fact that various adjuvants were able to enhance NA delivery *in vivo,* the *in vivo* transfection efficiencies were often lower than expected based on the *in vitro* data. This indicates that the more complex *in vivo* environment poses additional barriers to those mimicked *in vitro*. An integrated approach combining several small molecules that improve delivery at various levels, could potentially more firmly boost the *in vivo* therapeutic potential of NA. In the best possible scenario, a combination of small molecules would synergistically improve the transfection efficiency. Furthermore, the safety of the proposed approaches needs to be addressed, as for instance the use of CLQ is limited by its systemic toxicity. In this regard, the tissue specificity of the delivery strategy and its general impact should be taken into account. In turn, the inclusion of the proposed adjuvants into a nanocarrier alongside the NA or the use of NA-conjugates could pose a solution to potential toxicity questions.

Overall, this review highlights the potential of small molecules to improve NA transfections. It is clear that the use of low molecular weight adjuvants is a promising strategy to improve the therapeutic potential of NA, which will be further explored in the near future.

Table 2.1. Small molecules adjuvants that improve NA delivery grouped according to their mechanism of action.

	Mechanism of improved delivery	Small molecular adjuvant	Moment of adjuvant treatment	*In vitro*	*In vivo*	Carrier/NA	Ref
Small molecules improve NA uptake							
Tumor penetration	Fibrinolytic agent	Losartan	pre	X	X	Doxil LPS	[20]
	Tumor priming	Paclitaxel	pre	X	X	LNP:siRNA	[23-25]
Active targeting	Target asialoglycoprotein receptor	GalNAc	conjugate	X	X	LNP:siRNA	[33]
	Target sigma receptor	Haloperidol	in carrier	X		LNP:DNA	[37]
		Anisamide	in carrier	X	X	LNP:siRNA	[39, 40]
				X		siRNA conjugate	[41]
	Bind Na/K ATPase pump	Cardiac glycosides	in carrier	X		LNP:siRNA	[43]
Stimulate cellular internalization	Stimulate endocytosis	Glycerol	post	X		LNP:DNA	[13]
	ATP produced by metabilization needed for energy-dependent NA uptake	Hexoses (glucose & fructose)	co	X	X	ASO	[44]
Direct interaction with the NA or carrier	Shield siRNA charge Improved cell association	Guanabenz	co	X		Chol-siRNA	[18]
	Reduce size LNP	Hit compounds	pre	X	X	LNP	[16]
Small molecules improve endosomal escape							
	Create pores in late endosomal membrane	Amphotericin B	in carrier	X		Micelle:siRNA	[46]

	Interaction with endosomal membrane	Plant glycoside (SO1681)	Co post in carrier	X		peptide-based carrier, LNP pDNA, mcDNA, siRNA	47
	Block retrograde trafficking from endosomes to Golgi apparatus	Retro-1	post	X	X	SSO ASO	48
	Potential mechanisms: (i) destabilize membrane (ii) defect vesicle formation (iii) increase the rate or extent of tubulation and budding of the carrier-containing vesciles	Hit compounds	post	X	X	SSO ASO chol-siRNA	17
	Different mechanism for hits: (i) hinder acidification/maturation (ii) interfere with trafficking (iii) destabilize endosomal membrane	Hit compounds	co	X		Chol-siRNA LNP:siRNA	16
Small molecules interfere with intracellular trafficking							
	Microtubule depolymerization → Prevent degradation in lysosomes	Colchicine	pre	X		LPS:DNA	54
					X	LPS:DNA	51
		Vinblastine Vincristine Nocodazole Podophyllotoxin	pre	X		LPS:DNA	55
		Taxol	pre	X		LPS:DNA	50
		Nocodazole	pre	X		LPS:DNA	50, 52, 53

	Improved pDNA trafficking over stabilized microtubules	Taxol	co	X		Electroporation pDNA	[56]
	Microtubule stabilization → prevent vesicle fusion	PTX	pre	X		LPS:DNA	[55]
			co	X		polyplex	[24, 25, 59]
	HDAC6 inhibitor → Stabilizes microtubuli by acetylation	NCT-10b	co	X		Electroporation microinjection pDNA	[57]
		Tubacin	co	X		Polyplex:DNA	[58]
	Protein kinase A inhibitor	H89	pre	X		Branched PEI:DNA	[60]
	NPC1 inhibitor (prevent recycling)	NP3.47	co	X		LNP:siRNA	[61]
Small molecules boost transgene expression							
	HDAC inhibitor → (i) prevent of histon deacetylation (ii) acetylation (activation) of transcription factors (iii) influence the expression of genes that regulate the expression of transgenes	Depsipeptide	co		X	LPS:DNA	[67]
			co		X	PEI:DNA	[38]
			post	X		LPS:DNA	[65]
			post	X		CaP:DNA	[65]
		Trichostatin A	post	X		LPS:DNA	[65]
			post	X		Lipofectamine® FuGENE	[70]
			post	X		PEI:DNA	[64]
			post	X		CaP:DNA	[65]
			post	X		electroporation	[56]
		Valproic acid	post	X		PEI:DNA	[64]
			post	X		LPS:DNA	[69]

		Sodium butyrate	post	X		PEI:DNA	[64]
			post	X		electroporation	[56]
		CHAP 31	post	X		LPS:DNA CaP:DNA	[65]
		MS-275	post	X		PEI-DNA	[64]
		Entinostat	co post	X		PEI-DNA	[62]
	DNMT inhibitor	5A2dC		X	X	Gene gun	[73]
		Azacytidine RG-108 Procainamide Hydralazine		X		PEI:DNA	[64]
	Initiate transcription	HMBA Diazepam Hypoxanthine 6-thioguanine	post	X		LPS-DNA	[63, 74]
	Activate protein kinase C	PMA	post	X		PLS-DNA	[63, 74]
Alternative mechanisms to improve the transfection efficiency							
	Reduce innate immune response	BAY11	co post	X		RNAiMAX:mRNA	[81]
	PLK1 inhibition	HMN-214 BI 2536	co	X		PEI:pDNA 1,4C-1,4bis:pDNA	[84]

	Reduce degradation by endo-lysosomal DNAse	DMI-2	co	X		Protein-A-poly-lysine complex lipofection	83
	CDK1 inhibitor	RO-3306	pre	X		PEI:pDNA	68
	Enhance exon skipping	Dantrolene	post	X	X	ASO	85
Small molecule as nanocarrier							
	More compact complex Shielding of siRNA charge	Guanidine groups linked to a biphenyl system	in carrier	X		SMoC:siRNA	89
Pleiotropic adjuvants							
	Intercalate NA → (i) improve release from carrier (ii) prevent degradation (iii) prevent recognition by TLR9 Prevent acidification → (i) prevent endo-lysosome fusion (ii) prevent degradation (iii) prevent TLR9 activation	Chloroquine	pre	X		LPS:pDNA	13
			co	X		Polylysine-molossin:pDNA	92-95
			co		X	Polylysine-molossin:pDNA	96, 97
			post	X		Exosome:siRNA chol-siRNA	98
			post	X		Micelle:siRNA	99
			post	X		MSN-PEI:siRNA	100
			in carrier	X		MSN:siRNA:CLQ	101
Steroids	(i) Reduce innate immune response (ii) Bind glucocorticoid receptor → - facilitate transport to nucleus - dilate nuclear pore	Dexamethasone	pre co		X	pDNA	14
			post	X		LPS:pDNA	14
			pre		X	lipid-protamine:pDNA	102

			pre co post	X		LNP:pDNA Ca/P:pDNA	104
			pre	X		Lipofectamine:pDNA	105
			in carrier	X		Dexa-pDNA conjugate	107
			in carrier	X	X	LPS-dexa:pDNA	108
			in carrier	X		PAMAM-dexa:pDNA	109
			in carrier	X		PEI-dexa:pDNA	110
			in carrier		X	PEI-dexa:pDNA	111
			in carrier	X	X	Au-PEI:pDNA:PEI-dexa	112
		Cortisol	pre	X		Lipofectamine:pDNA	105
			in carrier	X		PEI:dexa-pDNA	113
		Methylprednisolone	co	X		LNP:pDNA	114
			in carrier	X		LNP:pDNA-methylprednisolon	114
			pre		X	pDNA	104
	Improve uptake Improve nuclear translocation	Estradiol	co	X		Lipofectamine:pDNA	115, 116
			co	X		LNP:pDNA	114

REFERENCES

1. Yin, H.; Kanasty, R. L.; Eltoukhy, A. A.; Vegas, A. J.; Dorkin, J. R.; Anderson, D. G. *Nat Rev Genet* **2014,** 15, (8), 541-55.
2. Bauman, J.; Jearawiriyapaisarn, N.; Kole, R. *Oligonucleotides* **2009,** 19, (1), 1-13.
3. Juliano, R. L. *Nucleic Acids Res* **2016,** 44, (14), 6518-48.
4. Sridharan, K.; Gogtay, N. J. *Br J Clin Pharmacol* **2016,** 82, (3), 659-72.
5. Blanco, E.; Shen, H.; Ferrari, M. *Nat Biotechnol* **2015,** 33, (9), 941-51.
6. Deleavey, G. F.; Damha, M. J. *Chem Biol* **2012,** 19, (8), 937-54.
7. Dahlman, J. E.; Abudayyeh, O. O.; Joung, J.; Gootenberg, J. S.; Zhang, F.; Konermann, S. *Nat Biotechnol* **2015,** 33, (11), 1159-61.
8. Ramishetti, S.; Kedmi, R.; Goldsmith, M.; Leonard, F.; Sprague, A. G.; Godin, B.; Gozin, M.; Cullis, P. R.; Dykxhoorn, D. M.; Peer, D. *ACS nano* **2015,** 9, (7), 6706-16.
9. Wittrup, A.; Ai, A.; Liu, X.; Hamar, P.; Trifonova, R.; Charisse, K.; Manoharan, M.; Kirchhausen, T.; Lieberman, J. *Nat Biotechnol* **2015,** 33, (8), 870-6.
10. Martens, T. F.; Remaut, K.; Demeester, J.; De Smedt, S. C.; Braeckmans, K. *Nano Today* **2014,** 9, (3), 344-364.
11. Wilhelm, S.; Tavares, A. J.; Dai, Q.; Ohta, S.; Audet, J.; Dvorak, H. F.; Chan, W. C. W. *Nat Rev Mater* **2016,** 1, (5).
12. Ma, D. *Nanoscale* **2014,** 6, (12), 6415-25.
13. Fraley, R.; Straubinger, R. M.; Rule, G.; Springer, E. L.; Papahadjopoulos, D. *Biochemistry* **1981,** 20, (24), 6978-87.
14. Malone, R. W.; Hickman, M. A.; Lehmann-Bruinsma, K.; Sih, T. R.; Walzem, R.; Carlson, D. M.; Powell, J. S. *J Biol Chem* **1994,** 269, (47), 29903-7.
15. Li, J.; Wang, Y.; Zhu, Y.; Oupicky, D. *J Control Release* **2013,** 172, (2), 589-600.
16. Gilleron, J.; Paramasivam, P.; Zeigerer, A.; Querbes, W.; Marsico, G.; Andree, C.; Seifert, S.; Amaya, P.; Stoter, M.; Koteliansky, V.; Waldmann, H.; Fitzgerald, K.; Kalaidzidis, Y.; Akinc, A.; Maier, M. A.; Manoharan, M.; Bickle, M.; Zerial, M. *Nucleic Acids Res* **2015,** 43, (16), 7984-8001.
17. Yang, B.; Ming, X.; Cao, C.; Laing, B.; Yuan, A.; Porter, M. A.; Hull-Ryde, E. A.; Maddry, J.; Suto, M.; Janzen, W. P.; Juliano, R. L. *Nucleic Acids Res* **2015,** 43, (4), 1987-96.
18. Osborn, M. F.; Alterman, J. F.; Nikan, M.; Cao, H.; Didiot, M. C.; Hassler, M. R.; Coles, A. H.; Khvorova, A. *Nucleic Acids Res* **2015,** 43, (18), 8664-72.
19. Lu, D.; Wientjes, M. G.; Lu, Z.; Au, J. L. *J Pharmacol Exp Ther* **2007,** 322, (1), 80-8.
20. Diop-Frimpong, B.; Chauhan, V. P.; Krane, S.; Boucher, Y.; Jain, R. K. *Proc Natl Acad Sci U S A* **2011,** 108, (7), 2909-14.
21. Cabral, H.; Matsumoto, Y.; Mizuno, K.; Chen, Q.; Murakami, M.; Kimura, M.; Terada, Y.; Kano, M. R.; Miyazono, K.; Uesaka, M.; Nishiyama, N.; Kataoka, K. *Nat Nanotechnol* **2011,** 6, (12), 815-23.
22. Jang, S. H.; Wientjes, M. G.; Au, J. L. S. *Journal of Pharmacology and Experimental Therapeutics* **2001,** 296, (3), 1035-1042.
23. Wong, H. L.; Shen, Z.; Lu, Z.; Wientjes, M. G.; Au, J. L. *Mol Pharm* **2011,** 8, (3), 833-40.
24. Wang, J.; Lu, Z.; Yeung, B. Z.; Wientjes, M. G.; Cole, D. J.; Au, J. L. *J Control Release* **2014,** 178, 79-85.
25. Wang, J.; Lu, Z.; Wang, J.; Cui, M.; Yeung, B. Z.; Cole, D. J.; Wientjes, M. G.; Au, J. L. *J Control Release* **2015,** 216, 103-10.
26. Xue, H. Y.; Tran, N.; Wong, H. L. *Eur J Pharm Biopharm* **2016**.
27. Wittrup, A.; Lieberman, J. *Nat Rev Genet* **2015,** 16, (9), 543-52.
28. Grabbe, S.; Haas, H.; Diken, M.; Kranz, L. M.; Langguth, P.; Sahin, U. *Nanomedicine (Lond)* **2016,** 11, (20), 2723-2734.

29. Kranz, L. M.; Diken, M.; Haas, H.; Kreiter, S.; Loquai, C.; Reuter, K. C.; Meng, M.; Fritz, D.; Vascotto, F.; Hefesha, H.; Grunwitz, C.; Vormehr, M.; Husemann, Y.; Selmi, A.; Kuhn, A. N.; Buck, J.; Derhovanessian, E.; Rae, R.; Attig, S.; Diekmann, J.; Jabulowsky, R. A.; Heesch, S.; Hassel, J.; Langguth, P.; Grabbe, S.; Huber, C.; Tureci, O.; Sahin, U. *Nature* **2016,** 534, (7607), 396-401.
30. Zhi, D.; Zhao, Y.; Cui, S.; Chen, H.; Zhang, S. *Acta Biomater* **2016,** 36, 21-41.
31. Winkler, J. *Ther Deliv* **2013,** 4, (7), 791-809.
32. Zwicke, G. L.; Mansoori, G. A.; Jeffery, C. J. *Nano Rev* **2012,** 3.
33. Akinc, A.; Querbes, W.; De, S.; Qin, J.; Frank-Kamenetsky, M.; Jayaprakash, K. N.; Jayaraman, M.; Rajeev, K. G.; Cantley, W. L.; Dorkin, J. R.; Butler, J. S.; Qin, L.; Racie, T.; Sprague, A.; Fava, E.; Zeigerer, A.; Hope, M. J.; Zerial, M.; Sah, D. W.; Fitzgerald, K.; Tracy, M. A.; Manoharan, M.; Koteliansky, V.; Fougerolles, A.; Maier, M. A. *Mol Ther* **2010,** 18, (7), 1357-64.
34. Bobbin, M. L.; Rossi, J. J. *Annu Rev Pharmacol* **2016,** 56, 103-122.
35. Reuters Alnylam Pharma says discontinues revusiran development. http://www.reuters.com/article/idUSFWN1CB0ML (23/11/2016),
36. Kanasty, R.; Dorkin, J. R.; Vegas, A.; Anderson, D. *Nat Mater* **2013,** 12, (11), 967-77.
37. Mukherjee, A.; Prasad, T. K.; Rao, N. M.; Banerjee, R. *J Biol Chem* **2005,** 280, (16), 15619-27.
38. Liu, Y.; Liggitt, D.; Fong, S.; Debs, R. J. *Gene Ther* **2006,** 13, (24), 1724-30.
39. Li, S. D.; Chono, S.; Huang, L. *J Control Release* **2008,** 126, (1), 77-84.
40. Li, S. D.; Chono, S.; Huang, L. *Mol Ther* **2008,** 16, (5), 942-6.
41. Nakagawa, O.; Ming, X.; Huang, L.; Juliano, R. L. *J Am Chem Soc* **2010,** 132, (26), 8848-9.
42. Dasargyri, A.; Kumin, C. D.; Leroux, J. C. *Adv Mater* **2016**.
43. Tam, Y. Y.; Chen, S.; Zaifman, J.; Tam, Y. K.; Lin, P. J.; Ansell, S.; Roberge, M.; Ciufolini, M. A.; Cullis, P. R. *Nanomedicine* **2013,** 9, (5), 665-74.
44. Han, G.; Gu, B.; Cao, L.; Gao, X.; Wang, Q.; Seow, Y.; Zhang, N.; Wood, M. J.; Yin, H. *Nat Commun* **2016,** 7, 10981.
45. Sahay, G.; Querbes, W.; Alabi, C.; Eltoukhy, A.; Sarkar, S.; Zurenko, C.; Karagiannis, E.; Love, K.; Chen, D.; Zoncu, R.; Buganim, Y.; Schroeder, A.; Langer, R.; Anderson, D. G. *Nat Biotechnol* **2013,** 31, (7), 653-8.
46. Yu, H.; Zou, Y.; Wang, Y.; Huang, X.; Huang, G.; Sumer, B. D.; Boothman, D. A.; Gao, J. *ACS Nano* **2011,** 5, (11), 9246-55.
47. Weng, A.; Manunta, M. D.; Thakur, M.; Gilabert-Oriol, R.; Tagalakis, A. D.; Eddaoudi, A.; Munye, M. M.; Vink, C. A.; Wiesner, B.; Eichhorst, J.; Melzig, M. F.; Hart, S. L. *J Control Release* **2015,** 206, 75-90.
48. Ming, X.; Carver, K.; Fisher, M.; Noel, R.; Cintrat, J. C.; Gillet, D.; Barbier, J.; Cao, C.; Bauman, J.; Juliano, R. L. *Nucleic Acids Res* **2013,** 41, (6), 3673-87.
49. Lukacs, G. L.; Haggie, P.; Seksek, O.; Lechardeur, D.; Freedman, N.; Verkman, A. S. *J Biol Chem* **2000,** 275, (3), 1625-9.
50. Hasegawa, S.; Hirashima, N.; Nakanishi, M. *Gene Ther* **2001,** 8, (21), 1669-73.
51. Chowdhury, N. R.; Hays, R. M.; Bommineni, V. R.; Franki, N.; Chowdhury, J. R.; Wu, C. H.; Wu, G. Y. *J Biol Chem* **1996,** 271, (4), 2341-6.
52. Cardarelli, F.; Digiacomo, L.; Marchini, C.; Amici, A.; Salomone, F.; Fiume, G.; Rossetta, A.; Gratton, E.; Pozzi, D.; Caracciolo, G. *Sci Rep* **2016,** 6, 25879.
53. Lindberg, J.; Fernandez, M. A.; Ropp, J. D.; Hamm-Alvarez, S. F. *Pharm Res* **2001,** 18, (2), 246-9.
54. Nair, R. R.; Rodgers, J. R.; Schwarz, L. A. *Mol Ther* **2002,** 5, (4), 455-62.
55. Wang, L.; MacDonald, R. C. *Mol Ther* **2004,** 9, (5), 729-37.
56. Vaughan, E. E.; Dean, D. A. *Mol Ther* **2006,** 13, (2), 422-8.
57. Vaughan, E. E.; Geiger, R. C.; Miller, A. M.; Loh-Marley, P. L.; Suzuki, T.; Miyata, N.; Dean, D. A. *Mol Ther* **2008,** 16, (11), 1841-7.
58. Barua, S.; Rege, K. *Biomaterials* **2010,** 31, (22), 5894-902.
59. Drake, D. M.; Pack, D. W. *J Pharm Sci* **2008,** 97, (4), 1399-413.

60. Rehman, Z. U.; Hoekstra, D.; Zuhorn, I. S. *J Control Release* **2011,** 156, (1), 76-84.
61. Wang, H.; Tam, Y. Y.; Chen, S.; Zaifman, J.; van der Meel, R.; Ciufolini, M. A.; Cullis, P. R. *Mol Ther* **2016**.
62. Elmer, J. J.; Christensen, M. D.; Barua, S.; Lehrman, J.; Haynes, K. A.; Rege, K. *Biotechnol Bioeng* **2016,** 113, (6), 1345-56.
63. Ishiguro, K.; Sartorelli, A. C. *Eur J Biochem* **2004,** 271, (12), 2379-90.
64. Backliwal, G.; Hildinger, M.; Kuettel, I.; Delegrange, F.; Hacker, D. L.; Wurm, F. M. *Biotechnol Bioeng* **2008,** 101, (1), 182-9.
65. Yasukawa, K.; Sawamura, D.; Goto, M.; Nakamura, H.; Shimizu, H. *Br J Dermatol* **2007,** 157, (4), 662-9.
66. Mehta, A. K.; Majumdar, S. S.; Alam, P.; Gulati, N.; Brahmachari, V. *Gene* **2009,** 428, (1-2), 20-4.
67. Yamano, T.; Ura, K.; Morishita, R.; Nakajima, H.; Monden, M.; Kaneda, Y. *Mol Ther* **2000,** 1, (6), 574-80.
68. Zhou, X.; Liu, X.; Zhao, B.; Liu, X.; Zhu, D.; Qiu, N.; Zhou, Q.; Piao, Y.; Zhou, Z.; Tang, J.; Shen, Y. *J Control Release* **2016,** 234, 90-7.
69. Nan, X.; Hyndman, L.; Agbi, N.; Porteous, D. J.; Boyd, A. C. *Biochem Biophys Res Commun* **2004,** 324, (1), 348-54.
70. Kim, Y. E.; Park, J. A.; Park, S. K.; Kang, H. B.; Kwon, H. J.; Lee, Y. *Dev Reprod* **2013,** 17, (4), 379-87.
71. Wulhfard, S.; Baldi, L.; Hacker, D. L.; Wurm, F. *J Biotechnol* **2010,** 148, (2-3), 128-32.
72. Choi, K. H.; Basma, H.; Singh, J.; Cheng, P. W. *Glycoconj J* **2005,** 22, (1-2), 63-9.
73. Lu, D.; Hoory, T.; Monie, A.; Wu, A.; Wang, M. C.; Hung, C. F. *Vaccine* **2009,** 27, (32), 4363-9.
74. Ishiguro, K.; Sartorelli, A. C. *Leukemia Res* **2008,** 32, (1), 89-96.
75. Devoldere, J.; Dewitte, H.; De Smedt, S. C.; Remaut, K. *Drug Discov Today* **2016,** 21, (1), 11-25.
76. Muruve, D. A.; Petrilli, V.; Zaiss, A. K.; White, L. R.; Clark, S. A.; Ross, P. J.; Parks, R. J.; Tschopp, J. *Nature* **2008,** 452, (7183), 103-7.
77. Robbins, M.; Judge, A.; MacLachlan, I. *Oligonucleotides* **2009,** 19, (2), 89-102.
78. Courreges, M. C.; Kantake, N.; Goetz, D. J.; Schwartz, F. L.; McCall, K. D. *Molecules* **2012,** 17, (10), 12365-77.
79. Clark, K.; Plater, L.; Peggie, M.; Cohen, P. *J Biol Chem* **2009,** 284, (21), 14136-46.
80. Gupta, A.; Rath, P. C. *Biomed Res Int* **2014,** 2014, 817024.
81. Awe, J. P.; Crespo, A. V.; Li, Y.; Kiledjian, M.; Byrne, J. A. *Stem Cell Res Ther* **2013,** 4, (1), 15.
82. Howell, D. P.; Krieser, R. J.; Eastman, A.; Barry, M. A. *Mol Ther* **2003,** 8, (6), 957-63.
83. Ross, G. F.; Bruno, M. D.; Uyeda, M.; Suzuki, K.; Nagao, K.; Whitsett, J. A.; Korfhagen, T. R. *Gene Ther* **1998,** 5, (9), 1244-50.
84. Christensen, M. D.; Elmer, J. J.; Eaton, S.; Gonzalez-Malerva, L.; LaBaer, J.; Rege, K. *J Control Release* **2015,** 204, 20-9.
85. Kendall, G. C.; Mokhonova, E. I.; Moran, M.; Sejbuk, N. E.; Wang, D. W.; Silva, O.; Wang, R. T.; Martinez, L.; Lu, Q. L.; Damoiseaux, R.; Spencer, M. J.; Nelson, S. F.; Miceli, M. C. *Sci Transl Med* **2012,** 4, (164), 164ra160.
86. Gooding, M.; Adigbli, D.; Edith Chan, A. W.; Melander, R. J.; MacRobert, A. J.; Selwood, D. L. *Chem Biol Drug Des* **2014,** 84, (1), 24-35.
87. Choi, K. Y.; Silvestre, O. F.; Huang, X.; Min, K. H.; Howard, G. P.; Hida, N.; Jin, A. J.; Carvajal, N.; Lee, S. W.; Hong, J. I.; Chen, X. *ACS Nano* **2014,** 8, (5), 4559-70.
88. Zhao, Y.; Wang, W.; Guo, S.; Wang, Y.; Miao, L.; Xiong, Y.; Huang, L. *Nat Commun* **2016,** 7, 11822.
89. Gooding, M.; Tudzarova, S.; Worthington, R. J.; Kingsbury, S. R.; Rebstock, A. S.; Dube, H.; Simone, M. I.; Visintin, C.; Lagos, D.; Quesada, J. M.; Laman, H.; Boshoff, C.; Williams, G. H.; Stoeber, K.; Selwood, D. L. *Chem Biol Drug Des* **2012,** 79, (1), 9-21.

90. Cheng, J.; Zeidan, R.; Mishra, S.; Liu, A.; Pun, S. H.; Kulkarni, R. P.; Jensen, G. S.; Bellocq, N. C.; Davis, M. E. *J Med Chem* **2006,** 49, (22), 6522-31.
91. Kuznik, A.; Bencina, M.; Svajger, U.; Jeras, M.; Rozman, B.; Jerala, R. *J Immunol* **2011,** 186, (8), 4794-804.
92. Shewring, L.; Collins, L.; Lightman, S. L.; Hart, S.; Gustafsson, K.; Fabre, J. W. *Transplantation* **1997,** 64, (5), 763-9.
93. Li, J. M.; Collins, L.; Zhang, X.; Gustafsson, K.; Fabre, J. W. *Transplantation* **2000,** 70, (11), 1616-24.
94. Collins, L.; Asuni, A. A.; Anderton, B. H.; Fabre, J. W. *J Neurosci Methods* **2003,** 125, (1-2), 113-20.
95. Collins, L.; Fabre, J. W. *J Gene Med* **2004,** 6, (2), 185-94.
96. Zhang, X.; Collins, L.; Sawyer, G. J.; Dong, X.; Qiu, Y.; Fabre, J. W. *Hum Gene Ther* **2001,** 12, (18), 2179-90.
97. Zhang, X.; Sawyer, G. J.; Dong, X.; Qiu, Y.; Collins, L.; Fabre, J. W. *J Gene Med* **2003,** 5, (3), 209-18.
98. Stremersch, S.; Vandenbroucke, R. E.; Van Wonterghem, E.; Hendrix, A.; De Smedt, S. C.; Raemdonck, K. *J Control Release* **2016,** 232, 51-61.
99. Yu, H.; Xu, Z.; Chen, X.; Xu, L.; Yin, Q.; Zhang, Z.; Li, Y. *Macromol Biosci* **2014,** 14, (1), 100-9.
100. Wang, M.; Li, X.; Ma, Y.; Gu, H. *Int J Pharm* **2013,** 448, (1), 51-7.
101. Bhattarai, S. R.; Muthuswamy, E.; Wani, A.; Brichacek, M.; Castaneda, A. L.; Brock, S. L.; Oupicky, D. *Pharm Res* **2010,** 27, (12), 2556-68.
102. Tan, Y.; Li, S.; Pitt, B. R.; Huang, L. *Hum Gene Ther* **1999,** 10, (13), 2153-61.
103. Abrams, M. T.; Koser, M. L.; Seitzer, J.; Williams, S. C.; DiPietro, M. A.; Wang, W.; Shaw, A. W.; Mao, X.; Jadhav, V.; Davide, J. P.; Burke, P. A.; Sachs, A. B.; Stirdivant, S. M.; Sepp-Lorenzino, L. *Mol Ther* **2010,** 18, (1), 171-80.
104. Braun, S.; Jenny, C.; Thioudellet, C.; Perraud, F.; Claudepierre, M. C.; Langle-Rouault, F.; Ali-Hadji, D.; Schughart, K.; Pavirani, A. *FEBS Lett* **1999,** 454, (3), 277-82.
105. Kelly, A. M.; Plautz, S. A.; Zempleni, J.; Pannier, A. K. *Mol Ther* **2016,** 24, (2), 331-41.
106. Shahin, V.; Albermann, L.; Schillers, H.; Kastrup, L.; Schafer, C.; Ludwig, Y.; Stock, C.; Oberleithner, H. *J Cell Physiol* **2005,** 202, (2), 591-601.
107. Rebuffat, A.; Bernasconi, A.; Ceppi, M.; Wehrli, H.; Verca, S. B.; Ibrahim, M.; Frey, B. M.; Frey, F. J.; Rusconi, S. *Nat Biotechnol* **2001,** 19, (12), 1155-61.
108. Gruneich, J. A.; Price, A.; Zhu, J.; Diamond, S. L. *Gene Ther* **2004,** 11, (8), 668-74.
109. Choi, J. S.; Ko, K. S.; Park, J. S.; Kim, Y. H.; Kim, S. W.; Lee, M. *Int J Pharm* **2006,** 320, (1-2), 171-8.
110. Kim, J. Y.; Ryu, J. H.; Hyun, H.; Kim, H. A.; Choi, J. S.; Yun Lee, D.; Rhim, T.; Park, J. H.; Lee, M. *J Drug Target* **2012,** 20, (8), 667-77.
111. Kim, H.; Kim, H. A.; Bae, Y. M.; Choi, J. S.; Lee, M. *J Gene Med* **2009,** 11, (6), 515-22.
112. Chen, Z.; Zhang, L.; He, Y.; Li, Y. *ACS Appl Mater Interfaces* **2014,** 6, (16), 14196-206.
113. Bernasconi, A. G.; Rebuffat, A. G.; Lovati, E.; Frey, B. M.; Frey, F. J.; Galli, I. *FEBS Lett* **1997,** 419, (1), 103-6.
114. Wiseman, J. W.; Goddard, C. A.; Colledge, W. H. *Gene Ther* **2001,** 8, (20), 1562-71.
115. Jain, P. T.; Gewirtz, D. A. *J Mol Med (Berl)* **1998,** 76, (10), 709-14.
116. Jain, P. T.; Seth, P.; Gewirtz, D. A. *Biochim Biophys Acta* **1999,** 1451, (2-3), 224-32.

CHAPTER 3

The repurposing of cationic amphiphilic drugs to improve the cytosolic delivery of siRNA.

An adapted version of this manuscript is submitted as:

Freya Joris[1], Chiara Bastiancich[2], Lynn De Backer[1], Thijs Van de Vyver[1], Stefaan C. De Smedt[1,], Koen Raemdonck[1]. Cationic amphiphilic drugs induce lysosomal siRNA escape in nanogel transfected cells: towards simple adjuvants of siRNA-mediated gene silencing. *Nano Letters February 2017.*

[1]Lab of General Biochemistry and Physical Pharmacy, Faculty of Pharmaceutical Sciences, Ghent University, Ottergemsesteenweg 460, B-9000 Ghent, Belgium.

[2]Louvain Drug Research Institute (LDRI), Advanced Drug Delivery and Biomaterials, UCL, Avenue E. Mounier B1 73.12, B-1200 Brussels, Belgium.

Table of contents

ABSTRACT

The great therapeutic potential of RNAi has since long been recognized, yet its clinical translation lags behind. Among other limiting factors, the efficient delivery of RNAi-triggers into the cytosol remains a major bottleneck. When an RNAi-effector, such as small interfering (si)RNA, is enclosed in a nanocarrier, uptake generally occurs through endocytosis whereupon the bulk of the cargo remains inactive within the endo-lysosomal compartment. Thus, current suboptimal delivery strategies require optimization in terms of efficiency. We hypothesized that the sequential addition of small molecules following transfection could substantially ameliorate the silencing potential of siRNA-loaded dextran nanogels. We show that carvedilol, desloratadine, nortriptyline and salmeterol, all FDA-approved cationic amphiphilic drugs (CAD), can be repurposed to this end. The four CADs improved gene silencing in a concentration dependent fashion with almost complete silencing at the highest concentration tested. This is the result of the reduced lysosomal stability induced by lysosomal swelling, as the CAD-mediated inhibition of acid sphingomyelinase causes sphingomyelin, cholesterol and phospholipid accumulation. Consequently, the lysosomal membrane is destabilized followed by limited membrane permeabilization. This in turn allows siRNA release into the cytosol and subsequent gene silencing. Of note, the lysosomes could be applied as a depot for prolonged and triggered siRNA release by multiple CAD treatments and this method was proven to enhance the effect of a therapeutic siRNA.

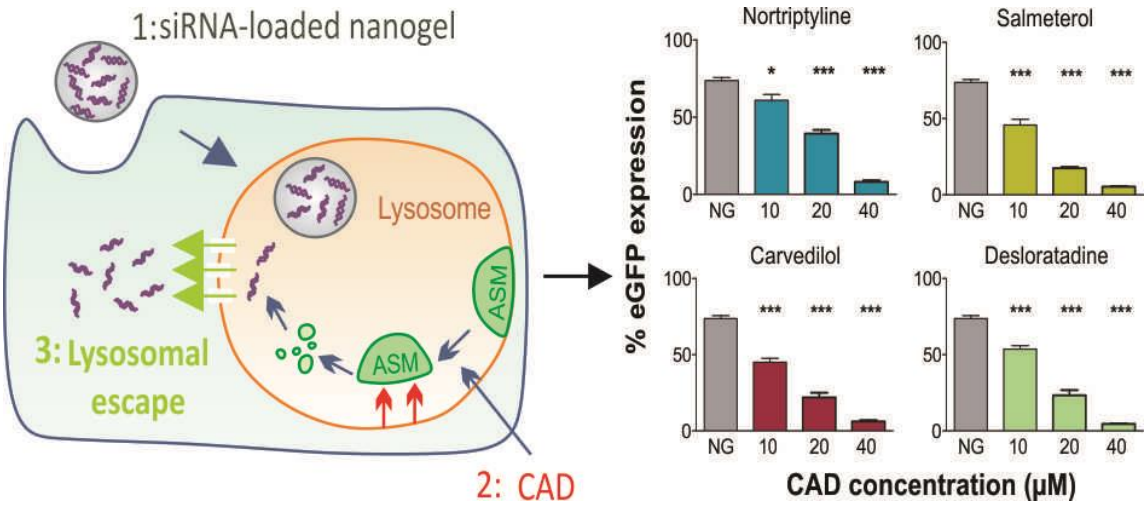

1. INTRODUCTION

The cytosolic delivery of RNA interference (RNAi)-effectors, such as small interfering (si)RNA, triggers the RNAi pathway to efficiently and specifically induce posttranscriptional gene silencing.[1, 2] In theory any gene of interest can be targeted, making siRNAs promising therapeutic candidates for a myriad of genetic disorders and cancer.[3, 4]

Since their negative charge and relatively high molecular weight hinder passive diffusion over the cell membrane, siRNA is generally enclosed in a nanocarrier to ensure cellular uptake.[5] Such carriers are internalized by cells *via* one or more endocytic pathways and consequently confined to the early endosomes. Next, the nanocarriers are progressively trafficked to the late endosomes and finally lysosomes, where both the carrier and its cargo face degradation. However, as cytosolic siRNA delivery is a prerequisite to trigger the RNAi pathway and reduce gene expression, lysosomal entrapment is generally regarded as a non-functional dead end for siRNA therapeutics.[5] To avoid lysosomal degradation, current cell delivery methods aim to stimulate endosomal escape prior to fusion of the endosomes with the lysosomes.[6, 7] Unfortunately, the rapid trafficking towards the lysosomes strongly limits the time-window to induce release.[8] In addition, current escape strategies target early or late endosomes since the induction of severe lysosomal membrane damage is believed to trigger cell death.[6, 9] Despite extensive efforts, state-of-the-art cytosolic delivery strategies largely fail to deliver, as the bulk of the internalized siRNA dose remains entrapped in the lysosomes.[10, 11]

Opposed to the current paradigm, we propose to exploit the lysosomes for timely cytosolic siRNA delivery by repurposing cationic amphiphilic drugs (CADs). CADs are pharmacologically diverse compounds that preferentially accumulate in lysosomes given their amphiphilic and weak basic properties.[12] Here, protonated CADs insert in lysosomal membranes with their hydrophobic segment, causing the detachment of the membrane-associated acid sphingomyelinase (ASM) and its subsequent degradation in the lysosomal lumen (Figure 3.1).[13] Thus, many CADs are known as functional inhibitors of ASM (FIASMAs).[12, 14] Active ASM catalyzes the hydrolysis of sphingomyelin (SM) to ceramide, thereby playing an important role in the maintenance of the lipid homeostasis and lysosomal membrane integrity. Indeed, SM accumulation upon ASM inhibition is associated with reduced

membrane stability and induction of lysosomal membrane permeabilization (LMP) in cancer cells (Figure 3.1).[13, 15, 16]

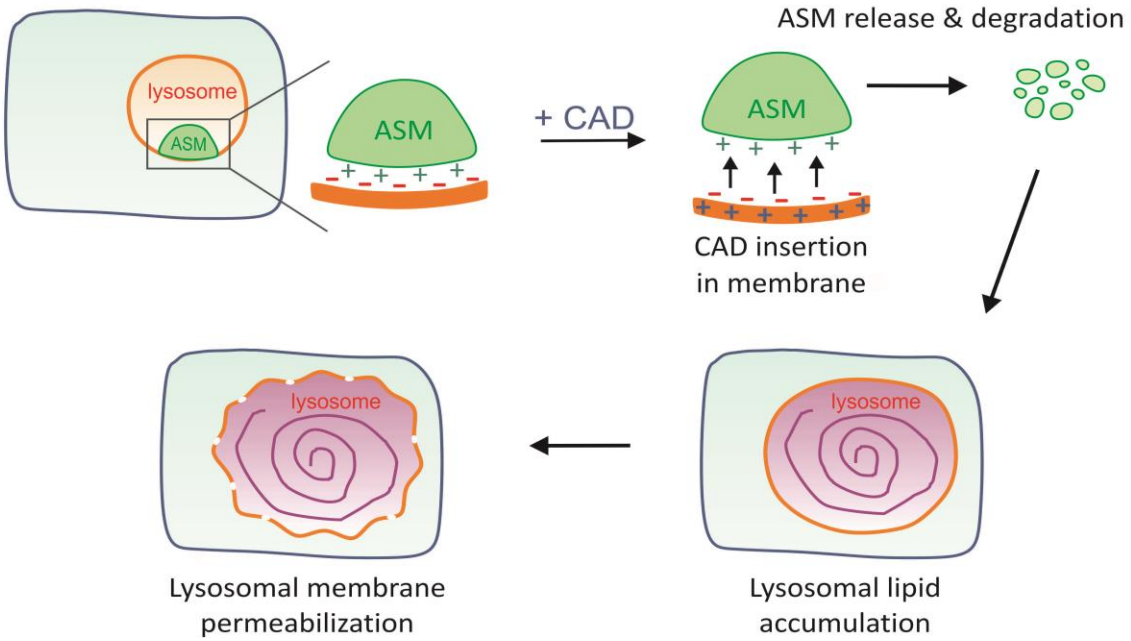

Figure 3.1. Acid sphingomyelinase (ASM) is a membrane bound enzyme present in the lysosomes that contributes to lipid homeostasis. Cationic amphiphilic drugs (CADs) insert in the lysosomal membranes and cause electrostatic repulsion of ASM, thereby inducing ASM release into the lysosomal lumen followed by degradation. As a result, lipids accumulate in the lysosomes, leading to lysosomal swelling and membrane permeabilization.[13, 17]

To evaluate this hypothesis we selected four structurally diverse, FDA-approved CADs with a distinct pharmacological activity, namely carvedilol (a β-blocker), desloratadine (an antihistamine), nortriptyline (an antidepressant) and salmeterol (a β2-agonist) (Figure 3.2). All compounds have an estimated logP > 3 and pKa > 7.4 and can thus be classified as lysosomotropic drugs, CADs and FIASMAs.[12, 14] As a model nanomedicine, we applied siRNA-loaded cationic dextran nanogels (siNGs) that have demonstrated high uptake and gene silencing efficiency in cancer cells.[18, 19] To unambiguously assess the adjuvant effect, the CADs were applied sequentially to a suboptimal siNG transfection.

	CARVEDILOL	DESLORATADINE	NORTRIPTYLINE	SALMETEROL
Drug class	β-blocker	Antihistamine	Antidepressant	β2-agonist
logP	3.42	3.97	4.51	3.82
pKa	8.74	9.73	10.10	10.12

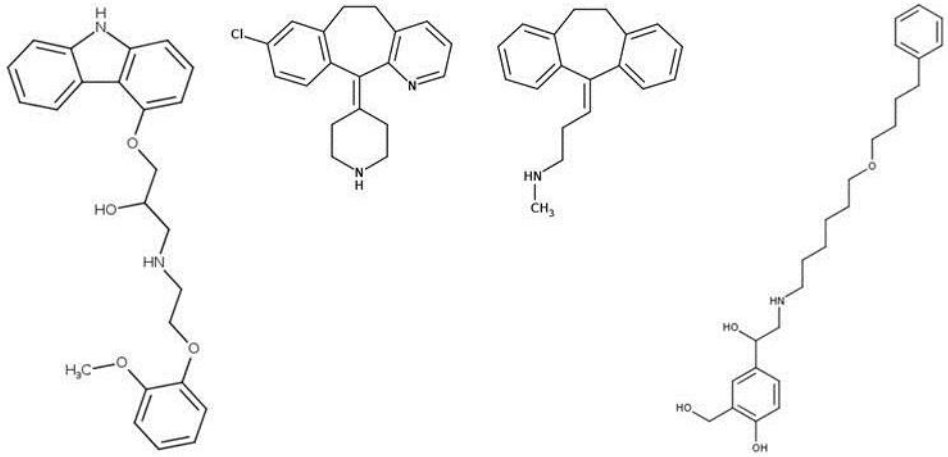

Figure 3.2. The drug class, logP, pKa values and molecular structure of carvedilol, desloratadine, nortriptyline and salmeterol.[20]

2. MATERIALS AND METHODS

2.1. siRNA duplexes

The 21 nucleotide siRNA duplex targetting the enhanced green fluorescent protein (eGFP; sieGFP) and the control siRNA duplex (siCTRL) were purchased from Eurogentec (Belgium). For uptake experiments, the siCTRL duplex was labeled with a Cy5 dye at the 5´ end of the sense strand (Eurogentec, Belgium). In addition, nuclease-stabilized versions of the siEGFP and siCTRL duplexes (Dharmacon, USA) were applied in experiments regarding triggered siRNA release. The siGLO green transfection indicator (Dharmacon, USA) was furthermore used. Finally, custom-designed siRNA with the siSTABLE modification targeting polo-like kinase 1 (siPLK1) was obtained from Dharmacon (USA). The sequences and modifications of the applied siRNA duplexes are summarized in Table 3.1.

Table 3.1. Applied siRNA sequences and duplex modifications.

siRNA	Modification	Manufacturer	Sequence[a]	
			Sense strand (5' -> 3')	Antisense strand (5' -> 3')
siCTRL[b]	/	Eurogentec	UGCGCUACGAUCGACGAUGtt	CAUCGUCGAUCGUAGCGCAtt
siCTRL[b]	Cy5-labelled[c]	Eurogentec	UGCGCUACGAUCGACGAUGtt	CAUCGUCGAUCGUAGCGCAtt
siCTRL[b]	Stabilized[d]	Dharmacon	UAGCGACUAAACACAUCAAUU	UUGAUGUGUUUAGUCGCUAUU
sieGFP[e]	/	Eurogentec	CAAGCUGACCCUGAAGUUCtt	GAACUUCAGGGUCAGCUUGtt
sieGFP[e]	Stabilized[d]	Dharmacon	CAAGCUGACCCUGAAGUUCUU	GAACUUCAGGGUCAGCUUGUU
siGLO	FAM-labelled[f]	Dharmacon	Not provided	Not provided
siPLK1[g]	Stabilized[d]	Dharmacon	CAACCAAAGUCGAAUAUGAUU	UCAUAUUCGACUUUGGUUGUU

[a] Capital and lower case letters respectively represent ribonucleotides and 2'-deoxyribonucleotides; [b] negative control scrambled duplex; [c] the siCTRL duplex was labeled with a Cy5 dye at the 5´ end of the sense strand; [d] siSTABLE RNA strand modification by Dharmacon for use in nuclease-rich environments; [e] siRNA duplex targeting enhanced green fluorescent protein; [f] Fluorescent siCTRL duplex modified to translocate to the nucleus upon successful transfection; [g] siRNA duplex targetting polo-like kinase 1.

2.2. NG complexation

The cationic dextran nanogels (NGs) were prepared *via* an inverse mini-emulsion photopolymerization method.[18, 19] Before the NGs were loaded with siRNA, a 2 mg/mL dispersion of a lyophilized stock was prepared in ice-cooled nuclease free water and sonicated briefly (amplitude 10%). Subsequently, equal volumes of appropriate NG and siRNA dilutions in N-2-hydroxyethylpiperazine-N'-2-ethanesulfonic acid (HEPES) buffer

(pH 7.4, 20 mM) were mixed to a final volume of 100 µL and were allowed to complexate for 15 minutes at room temperature. The same volume of HEPES buffer was added to this dispersion, followed by Opti-MEM® (Invitrogen, Belgium) to a final volume of 1 mL. 300 µL of this dispersion was applied per well during transfection. Hence, three technical replicates were performed for each condition. This complexation procedure was applied for all cell-based experiments and resulted in a 30 µg/mL NG dispersion loaded with 2 nM siRNA (= 0.06 pmol siRNA/µg NGs or 0.6 pmol siRNA/well).

2.3. Cell lines and cell culture conditions

All experiments were performed on the non-small cell lung carcinoma cell line H1299 of which both the wild type (H1299-WT) and the eGFP-expressing variant (H1299-eGFP) were applied. Complete cell medium was prepared by supplementing RPMI 1640 culture medium with 10% fetal bovine serum (FBS, Hyclone™, Thermo Fisher Scientific, Belgium), 2 mM L-Glutamine and 100 U/mL penicillin/streptomycin. The cell lines were cultured in a humidified atmosphere containing 5% CO_2 at 37 °C and culture medium was renewed every other day unless the 80% confluence level was reached. In this case, the cells were split using 0.25% trypsin-EDTA. All products were purchased from Invitrogen (Belgium) unless specifically mentioned otherwise.

2.4. siNG transfection and sequential adjuvant treatment

Cells were transfected with 300µL of the 30 µg/mL NG dispersion loaded with 2 nM siRNA per well during four hours at 37 °C in a humidified atmosphere containing 5% CO_2. Subsequently, the siNG dispersion in Opti-MEM was removed, the cells were washed once with phosphate buffered saline (PBS, Invitrogen, Belgium) and received fresh cell medium. In case of CAD treatment, cell medium containing 10, 20 or 40 µM carvedilol, desloratadine (DL), nortriptyline (NT) or salmeterol was applied. Furthermore, 5 µM NT and DL were tested alone as well as in the following combinations: 5 µM + 5 µM, 10 µM + 10 µM and 20 µM + 20 µM. Furthermore, dextromethorphan was tested in the following concentration range: 10, 20, 40, 80, 120, 160 and 200 µM. In additional experiments, we applied cell medium containing 10, 20 or 40 µM chloroquine, 30 µM U18666A or 300 µM 2-hydroxy oleic acid, the latter either alone or in combination with 10 µM DL. Figure 3.3 shows the molecular structure, logP and pKa values of the additionally applied adjuvants. All small molecules

were obtained from Sigma-Aldrich (Belgium) and the stock solutions were prepared in sterile-filtered BioPerformance Certified dimethyl sulfoxide (DMSO, Sigma-Aldrich, Belgium). The final DMSO concentration brought onto the cells did not exceed 0.16 vol% and this condition was additionally tested for potential off-target effects.

	DEXTROMETORPHAN	CHLOROQUINE	U18666A	2-HYDROXY OLEIC ACID
Drug class	Antitussive	Antimalarial agent	Inhibitor cholesterol synthesis (NPD inducer)	Activator SM synthethase
logP	3.6	4.63	4.51	3.82
pKa	9.85	10.10	10.10	10.12

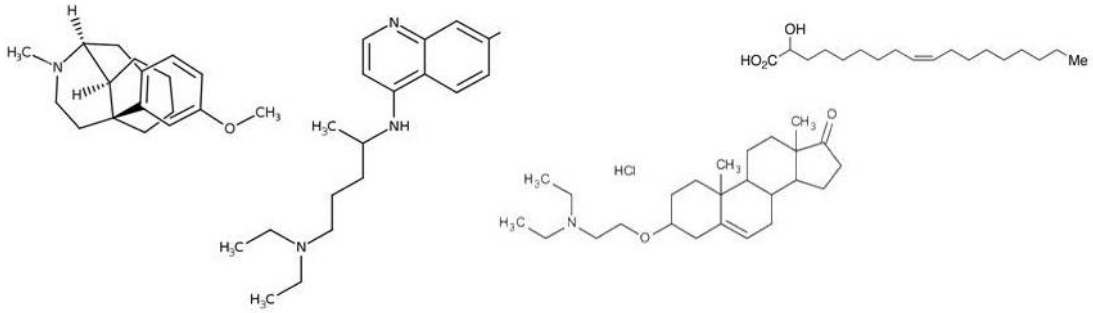

Figure 3.3. The drug category, logP, pKa values and molecular structure of dextrometorphan, chloroquine, U18666A and 2-hydroxy oleic acid.[20]

All adjuvant treatments were performed in complete cell medium and lasted 20 hours, unless specifically mentioned otherwise. Afterwards, the small molecule-containing cell medium was removed and cells were kept in 1 mL fresh cell medium for an additional 24 hours until analysis. In a final set of experiments regarding the triggered siRNA release from the lysosomal compartment, the DL incubation time was reduced to 2 hours without further changes to the protocol timeline. This treatment time was also applied in the experiment where cells were exposed daily or every other day to DL over a period of 6 days.

2.5. Measuring the siNG transfection efficiency

For silencing experiments, H1299-eGFP cells were seeded in 24 well plates at a density of 35000 cells/well and were allowed to settle overnight. Subsequently, the cells were transfected with 0.6 pmol siRNA/well (300 µL siNG dispersion) and treated with 0.5 mL cell medium containing a small molecular adjuvant. Note that for every sieGFP or siPLK1 condition an siCTRL sample was included to account for potential off target effects.

SiNG-mediated eGFP silencing was determined by flow cytometry 48h after the transfection. Sample preparation consisted of washing the cells with PBS, followed by detachment with 0.25% trypsin-EDTA. The cells were collected, centrifuged 5 minutes at 300g, resuspended in 300 µL flow buffer and kept on ice until analysis. For each sample the forward and side scatter as well as the green fluorescent signal were measured for at least 15000 cells. The samples were excited with the 488 laser line and the signal was detected with the 530/30 filter using the FACSCalibur™ flow cytometer (BD Biosciences, Belgium) and BD CellQuest™ acquisition software. Finally, data analysis was performed using the FlowJo software (Tree Star Inc.) and the calculated percentage eGFP expression is presented as the mean ± standard error of the mean (SEM) for four biological replicates.

When probing the evolution of the eGFP signal over an extended period of time, the eGFP signal was measured daily. Hereto, treated cells were passaged every other day and reseeded in new 24 well plates during sample preparation for the flow cytometry measurements.

The silencing potential of siPLK1-NGs was established through evaluating the cell viability. Hereto, we applied the CellTiter GLO® assay (Promega, Belgium). Before initiating the assay, the culture plates and reconstituted assay buffer were placed at room temperature for 30 minutes. Next, the culture medium was replaced by 250 µL fresh cell medium and an equal volume of assay buffer was added. To induce complete cell lysis, the plates were shaken during 2 minutes and the signal was allowed to stabilize for 10 minutes. 100 µL from each well was subsequently transferred to an opaque 96-well plate, which was measured with a GloMax® 96 Microplate Luminometer (Promega, Belgium). Three biological replicates were performed and data are expressed as the mean cell viability (%) ± SEM.

2.6. Cell viability

The H1299-eGFP cells were seeded, transfected and treated with the CADs similar to the silencing experiments. Please note that we only applied siCTRL-loaded NGs in this set of experiments. Again, the CellTiter GLO assay was performed as described above in three biological replicates (data are expressed as the mean ± SEM).

2.7. Release of FITC-dextrans and oligonucleotides

H1299-WT cells were seeded at 105000 cells/dish in 35mm diameter glass bottom microscopy dishes (Greiner Bio-One GmbH, Germany) and were allowed to settle overnight. To visualize the FITC-dextran (FD) release,cells were exposed to 1 mL of a 1 mg/mL dispersion of 10 kDa FD (Sigma-Aldrich, Belgium) in complete cell medium during 1 hour at 37 °C in a humidified atmosphere containing 5% CO_2. To assess oligonucleotide (ON) escape, the NGs were first loaded with 100 nM Alexa Fluor 647-labelled ON (Eurogentec, Belgium) according to the procedure described for siRNA complexation and 900 µL of the ON-NG dispersion was added to each dish. Of note, these oligonucleotides transfer to the nucleus upon release into the cytosol.[21] Following four hours of ON-NG transfection or 1h incubation with FD, the cells were washed with PBS and received 1.5 mL fresh cell medium with or without 10, 20 or 40 µM DL. After an additional incubation period of 20 hours, the cell medium was removed and nuclei were labeled with Hoechst (Molecular Probes™, Belgium) in cell medium during 15 minutes at 37 °C. Finally, the Hoechst solution was removed, fresh cell medium was added and cells were kept at 37 °C in a humidified atmosphere containing 5% CO_2 until imaging.

The samples were imaged using a laser scanning confocal microscope (LSCM, C1si, Nikon) and a 60x oil immersion Plan Apo objective (Nikon, Belgium). The 408, 488 and 633 laser lines were applied to respectively excite the Hoechst labeled nuclei, the FD and ON. During data analysis with ImageJ, both the total cell number and amount of cells with a diffuse FD labeling or ON-positive nuclei were counted. Data are represented as the percentage of cells with a diffuse FD signal for minimum 225 cells per condition in 10 images and the percentage of cells with ON-positive nuclei for at least 180 cells in 10 images.

2.8. Lysosome detection using flow cytometry

H1299-eGFP cells were seeded, transfected and treated with the CADs as described for the cell viability experiments. Following 20 hours of CAD treatment, the lysosomes were labeled with the LysoTracker® Deep Red (LDR) probe (Molecular Probes™, Belgium) through incubation with 1 mL 75 nM LDR in cell medium for 30 minutes at 37 °C. Further sample preparations were carried out as previously described for the silencing experiments. Using the FACSCalibur™ flow cytometer and BD CellQuest™ acquisition software, the LDR signal was detected with the 661/61 filter following excitation with the 635 laser line for at least

15000 cells per sample. Experiments were performed in biological triplicate and fold changes in LDR signal intensity are expressed as the mean ± SEM.

2.9. Visualizing lysosomes with confocal microscopy

H1299-WT cells were seeded as specified for the FD release experiment and transfected with siNGs followed by a 20-hour DL treatment. After removal of the DL-containing cell medium, cells were washed with PBS and incubated with 75 nM LysoTracker® Red DND-99 (Molecular Probes™, Belgium) in cell medium during 30 minutes at 37 °C. Next, the dye was removed, cells were washed with PBS and fixed with 4% paraformaldehyde (PFA) during 15 minutes at room temperature. Finally, the cells were washed twice with PBS, covered with Vectashield antifade mounting medium containing DAPI (Vector Laboratories, USA) and stored at 4 °C until imaging. A LSCM and 100x oil immersion Plan Apo objective (Nikon, Belgium) objective were applied for imaging. The 408 and 561 laser lines respectively excited the DAPI-labeled cores and LysoTracker® Red DND-99-stained lysosomes. The LysoTracker® Red DND-99 signal intensity and area were determined using the ImageJ in at least 115 cells from minimum 11 images.

2.10. Phospholipidosis detection with LipidTOX™ red

H1299-WT cells were seeded and allowed to settle overnight as detailed previously. Next, the cells were incubated with a mixture of a 1/1000 dilution of the LipidTOX™ red phospholipidosis detection reagent (Thermo Fisher Scientific, USA) and the desired CAD in complete cell medium. Upon 20h incubation, the cells were fixed with 4% PFA and stored at 4° covered in Vectashield antifade mounting medium containing DAPI. Imaging occurred with a LSCM and a 100x oil immersion objective. DAPI and the LipidTOX™ red phospholipidosis dye were respectively excited with the 406 and 561 laser lines.

2.11. Cholesterol detection with filipin

Following H1299-WT cell seeding, transfection and DL treatment, the cells were washed once with PBS and fixed with 3% PFA during 1 hour. After washing the samples with PBS, the remnant PFA was quenched with a 1.5 mg/mL glycine solution in PBS during 10 minutes. Next, a 0.1 mg/mL filipin solution in PBS containing 10% FBS was applied for 2 hours. Afterwards, the cells were washed once with PBS containing FBS, once with PBS and finally stored at 4 °C in Vectashield without DAPI (Vector Laboratories, USA). All steps of this

labeling procedure were executed at room temperature. The samples were imaged with a LSCM and a 100x oil immersion objective following excitation with the 406 laser line.

2.12. Sphingomyelin detection with lysenin

Cell seeding, transfection and DL treatment of the H1299-WT cells occurred similar to the previous microscopy experiments. The subsequent staining procedure was carried out at room temperature. Following one wash step with PBS, the cells were fixed with 4% PFA during 15 minutes. The fixative was removed, the cells washed twice with PBS and permeabilized with 0.5% Tween 20 for 15 minutes. Next, the cells were washed twice with blocking buffer (BB, 2 wt% bovine serum albumin (Amresco, USA) in PBS) and kept in BB during 30 minutes. Upon removal, the cells were incubated 2 hours with a 1 µg/mL lysenin (Sigma-Aldrich, Belgium) solution in BB. The cells were subsequently washed twice with PBS before 1 hour incubation with the lysenin rabbit anti-human antiserum (1:500 in BB, Peptanova, Germany). Before and after the subsequent 1-hour incubation period with the secondary goat anti-rabbit AF 647 antibody (1:500 in BB, Molecular Probes™, Belgium), cells were washed with BB. Finally the cells were washed with PBS and stored at 4 °C covered with Vectashield containing DAPI. Using the 408 and 633 laser lines the nuclei and sphingomyelin were excited respectively and detected with a LSCM and a 60x oil immersion objective.

2.13. Transfection with siGLO green transfection indicator

H1299-WT cells were seeded as described previously. For this experiment, NGs were complexated with 100 nM green fluorescent siRNA (siGLO, Dharmacon, USA). Following transfection and 40 µM DL treatment, the cells were fixed with 4% PFA and stored in Vectashield containing DAPI. The samples were imaged with a LSCM and a 100x oil immersion objective following excitation with the 406 and 488 nm laser line to visualize the DAPI and siGLO signal, respectively.

2.14. Statistical analysis

Statistical analysis was performed using the 6th version of the GraphPad Prism software. One-way ANOVA combined with the post-hoc Dunnett test was applied to compare multiple conditions, whereas the student *t*-test was used for direct comparison of 2 conditions.

3. RESULTS

3.1. CAD treatment enhances siRNA-mediated gene silencing

First, we evaluated if an adjuvant treatment with carvedilol (CD), desloratadine (DL) nortriptyline (NT) or salmeterol (ST) enhanced the gene silencing potential of suboptimal siRNA-loaded dextran nanogels (siNGs, 2 nM siRNA) in a non-small cell lung cancer cell line (H1299) that stably expresses the enhanced green fluorescent protein (eGFP).

In line with earlier observations, the suboptimal siRNA-loaded nanogels (siNGs) were efficiently internalized by the H1299 cells (Figure 3.4A) and induced ~25% eGFP silencing under the given experimental conditions (Figure 3.4C).[18, 19] Notably, the sequential treatment by each compound markedly improved the siNG silencing potential in a similar concentration dependent fashion (Figure 3.4C, Figure 3.4D). Compared to the siNGs alone, 10 µM CAD induced a significant increase in eGFP silencing and almost complete gene silencing was obtained with 40 µM. It was verified that the solvent, DMSO, did not influence the siNG-mediated gene silencing (Figure 3.4B). When a combination of CADs was applied, additive effects on gene silencing were observed and no significant variations were detected between the combination of DL and NT or double the concentration of each compound separately (Figure 3.5A). In turn, not all CADs were active in the same dose range. For instance, 10-fold higher concentrations of dextromethorphan were required to obtain a similar adjuvant effect (Figure 3.5C). Our adjuvant approach was furthermore compared to the gold standard for siRNA transfections, ie. Lipofectamine® RNAiMAX lipoplexes. When the latter was applied according to the manufacturers guidelines (5 pmol siRNA per well) maximal gene silencing was obtained (Figure 3.5B). However, when the lipoplexes were diluted to obtain a similar siRNA concentration per well as with the suboptimal siNGs (0.6 pmol siRNA/well or 2nM siRNA) ˜55% gene silencing was obtained, compared to >90% silencing for the siNG-CAD combination (Figure 3.5B). Note that, as compared to Lipofectamine® RNAiMAX, the same level of knockdown can be achieved with a 10-fold lower dose of siRNA by the sequential addition of a CAD to siNG-transfected cells. Finally, sequential addition of the endosomal escape enhancer chloroquine (CLQ) improved siNG-mediated silencing to a similar extent as the first four CADs tested (Figure 3.5D). However,

the use of CLQ as a delivery enhancer is limited by its systemic toxicity, while other CADs, for instance antihistamines, may provide a safer alternative.[22]

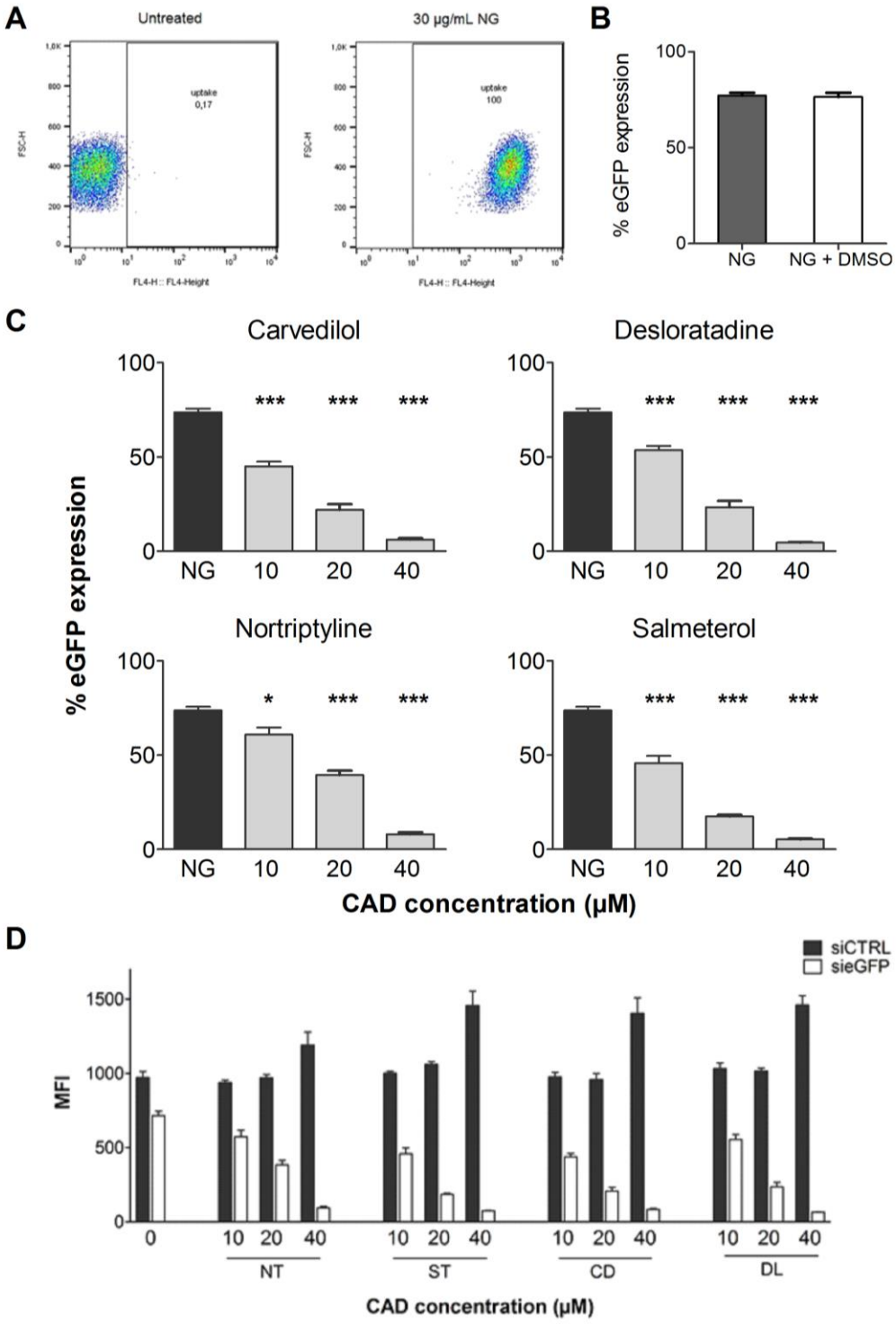

Figure 3.4. (A) Representative scatter plots showing the forward scatter (FSC) and the intensity of the fluorescent Cy5-labeled siRNA measured at 661 nm ± 16 (FL4) from untreated H1299-eGFP cells and cells exposed to 30 µg/mL siNGs. The scatter plots unambiguously indicate that all cells avidly internalize the siRNA-loaded NGs when a concentration of 30 µl/mL siNGs is applied. (B) % eGFP expression following transfection with siNGs alone (gray) or siNG transfection and sequential

exposure to the highest DMSO concentration applied in all CAD experiments (white). Thus, the solvent does not influence the sieGFP-NG mediated gene silencing in H1299-eGFP cells. (C) Transfection of H1299-eGFP cells with suboptimal siNGs resulted in ˜75% eGFP expression. Sequential carvedilol, desloratadine, nortriptyline or salmeterol addition caused significant additional silencing of the stably expressed eGFP in a concentration dependent manner. (D) The mean fluorescence intensity (MFI) for the H1299-eGFP cells transfected with siCTRL-loaded NGs (black) and siEGFP-NGs (white) followed by adjuvant treatment with 10, 20 or 40 µM nortriptyline (NT), salmeterol (ST), carvedilol (CD) or desloratadine (DL). This graph is a representative graph for four independent experiments. Data are represented as mean ± the standard error of the mean (SEM) for minimum three independent biological replicates. Statistical significance, with respect to NG transfection alone, is indicated when appropriate (p<0.05, ** p<0.01, *** p<0.005).*

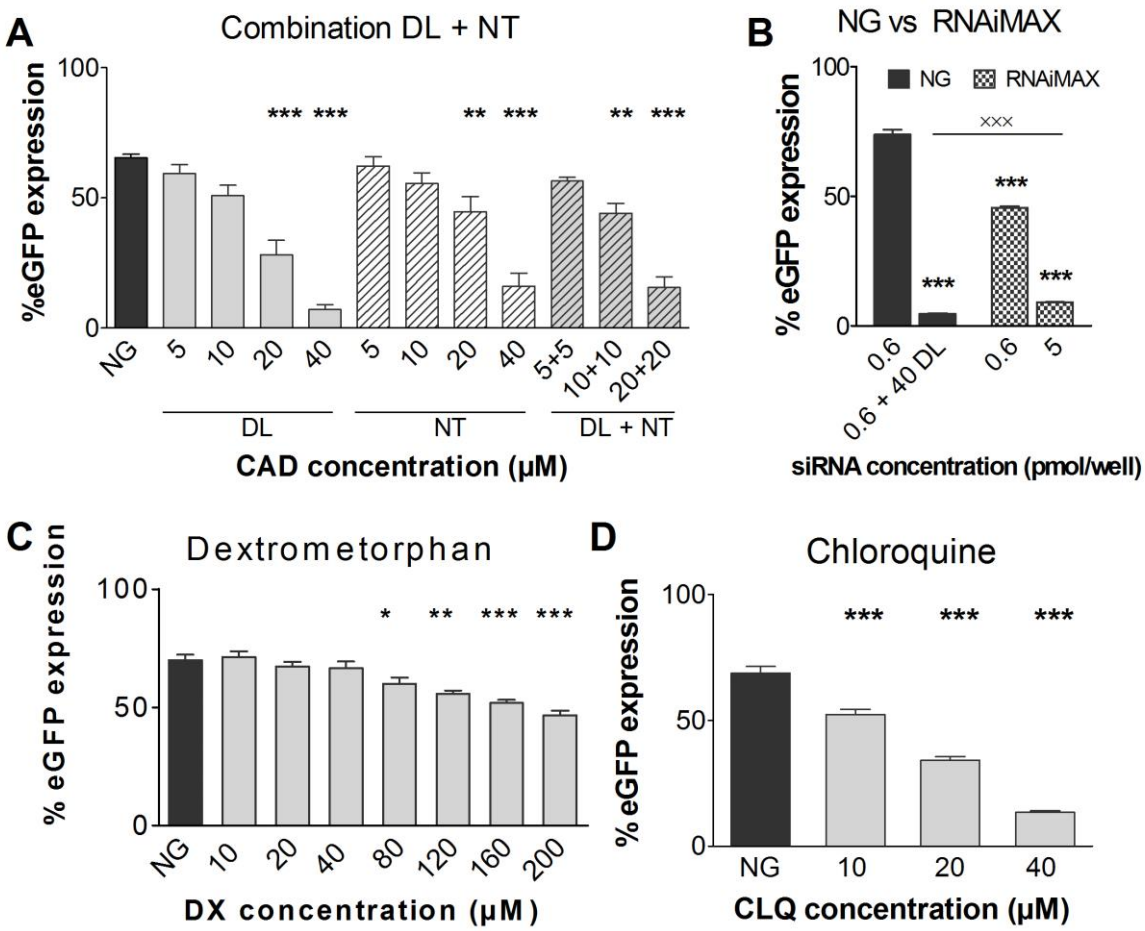

Figure 3.5. (A) Combinations of desloratadine (DL) and nortriptyline (NT) evoked additive effects on eGFP silencing. (B) Comparison of eGFP knockdown between siNGs and lipofectamine RNAiMAX. (C) Dextrometorphan (DX) does not influence gene silencing in the same dose range. (D) Endosomal escape enhancer chloroquine (CLQ) improves gene silencing to a similar extent as the initial molecules tested. Data are represented as mean ± the standard error of the mean (SEM) for minimum three independent biological replicates. Statistical significance, with respect to NG transfection, is indicated when appropriate (p<0.05, ** p<0.01, *** p<0.005). Statistical significance between NG + 40 DL and RNAiMAX is indicated by ^{xxx} (p<0.005). (NG = siNG transfection without sequential adjuvant treatment, CAD = cationic amphiphilic drug)*

3.2. CAD treatment affects cell viability to a minor extent

Next, we evaluated the impact of the CAD treatment alone or sequential to the siNG transfection on cell viability. Figure 3.6A, which shows the viability of H1299-eGFP cells (%) following CAD treatment, indicates that the CADs were fairly well tolerated in the applied concentration range with CD and DL being the least and most biocompatible, respectively. The NG transfection reduced the cell viability to ˜80% (Figure 3.6B), which is an acceptable toxicity level. None of the CADs induced significant additional cytotoxicity at a concentration of 10 µM (Figure 3.6B). For both ST and CD, significant additional cytotoxicity was detected starting from 20 µM, while this was only the case for 40 µM NT or DL. Of note, only for ST and CD did the cytotoxicity observed at 40 µM exceed the sum of the effects from each separate component. Again, DL was best tolerated with ˜60% viability.

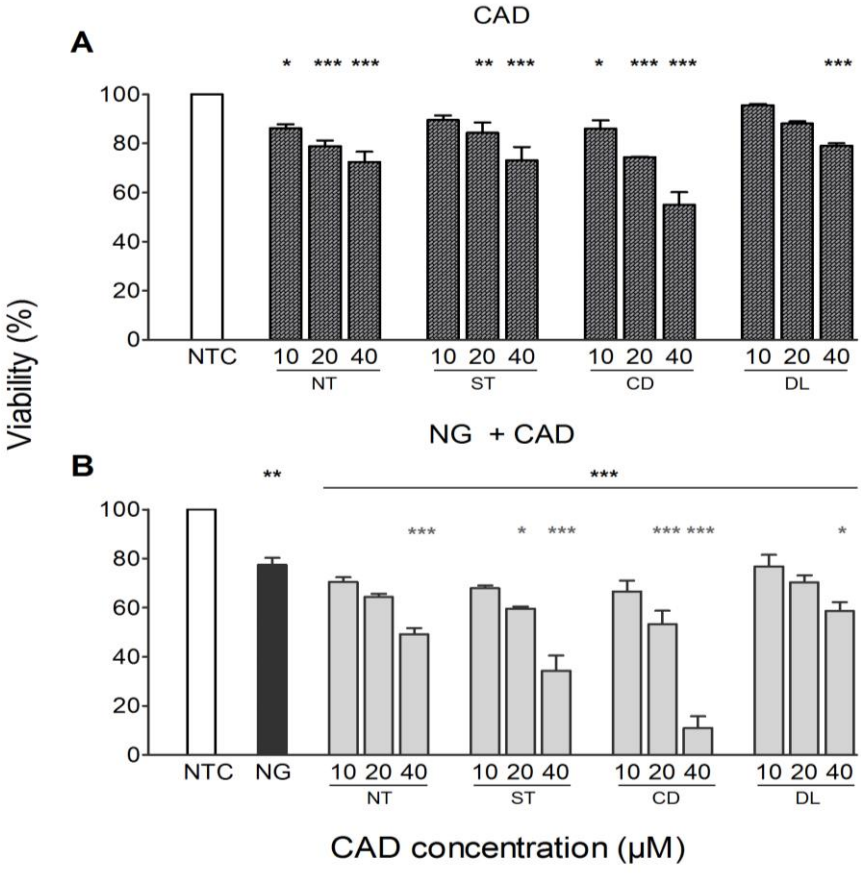

Figure 3.6. Cell viability of H1299-eGFP cells following CAD treatment alone (A) or sequential NG transfection and 20 hours CAD addition (B). Data reflect the mean ± SEM (n = 3) and statistical significance is indicated when appropriate (p<0.05, ** p<0.01, *** p<0.005). In (B) the black * represent significant variations relative to the untreated control (NTC), whereas the grey * resemble significant differences with respect to the cells transfected with siCTRL-NGs. (NTC = not treated control, NG = nanogels, CAD = cationic amphiphilic drug, NT = nortriptyline, ST = salmeterol, CD = carvedilol, DL = desloratadine*)

3.3. Desloratadine improves the cytosolic delivery of macromolecules

Based on current literature[13], we hypothesized that the sequential CAD treatment improved the siNG silencing potential by facilitating the siRNA transfer to the cytosol, through the induction of lysosomal membrane permeabilization (LMP). To visualize LMP as a function of CAD treatment, the H1299-WT cells were first incubated with FITC-labeled dextrans (FD, 10 kDa), being a fluid-phase marker to label the endo-lysosomes. Upon leakage of FD to the cytosol due to LMP, the affected cells show a diffusely stained cytosol in contrast to the typical punctate pattern indicative of endo-lysosomal sequestration.[23] As expected, the punctate pattern was observed in the bulk of the untreated cells (Figure 3.7). Upon DL adjuvant treatment, we observed a concentration dependent increase in the percentage of cells with a diffuse FD labeling, reaching up to ~26% with 40 µM DL.

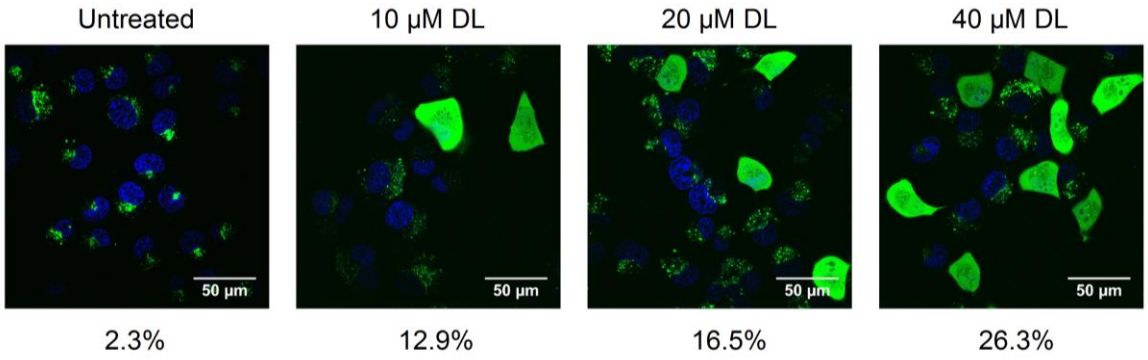

Figure 3.7. Representative confocal images from the intracellular FITC-dextran distribution in untreated H1299-WT cells or cells incubated with 10, 20 or 40 µM desloratadine (DL) following FITC-dextran uptake via endocytosis. The values below the images correspond to the percentage of cells with a diffuse FITC-dextran labeling. The scale bar corresponds to 50 µM.

Subsequently, we confirmed the improved release for our model carrier by applying NGs loaded with Cy5-labeled oligonucleotides (ON), which translocate to the nucleus upon escape.[21] ON were detected in the nuclei of ~1% of the transfected cells. In contrast, ~30% of the cells showcased positive nuclei following a 40 µM DL treatment (data not shown). Although the percentage of positive cells correlates well for both methods, it was lower than anticipated based on the silencing results. This may be explained by the fact that upon release of a limited amount of FD or ON, the labels are diluted in the cytosol or nuclei, respectively, with the fluorescence falling well below the detection limit of a standard fluorescent confocal microscope.[11]

3.4. The lysosomal compartment is affected by CAD treatment

Since CADs were suggested to induce lysosomal siRNA release, we examined the impact of the CAD treatment on the lysosomal compartment of siNG-transfected cells by labeling the endo-lysosomes with LysoTracker® Deep Red (LDR) and quantification through flow cytometry. Figure 3.8A shows that all four CADs alone evoked a similar significant concentration-dependent signal increase compared to the untreated cells. In addition, siNGs transfection alone caused a significant two-fold raise with respect to the untreated control (Figure 3.8B). Importantly, upon sequential CAD treatment, the LDR signal was additionally significantly elevated for all CADs in nearly all concentrations tested.

These observations could visually be confirmed by confocal microscopy following labeling of the endo-lysosomes with LysoTracker® Red. siNG endocytosis explained the two-fold increase in endo-lysosomal volume for NG-transfected cells, as we witnessed an elevation in the number of labeled organelles without notable alterations in their appearance (Figure 3.8C). In turn, the additional LDR signal increase upon sequential CAD treatment coincided with a marked enlargement of the labeled vesicles, which was confirmed by quantification of the LysoTacker® Red signal area (Figure 3.8D).

This CAD-induced lysosomal swelling in turn increased the cellular granularity, which was corroborated by the augmented side scatter (SSC) signal. Upon NG transfection, a minor shift towards higher SSC values could be noted and this trend continued with mounting CAD concentrations (Figure 3.8F). Indeed, for 40 µM DL a clear shift of the cell population, which resulted in a 1.8-fold increase in the mean SSC signal (Figure 3.8E). Similar trends were obtained for NT, ST and CD (Figure 3.9A). The combination of CADs resulted in additive SSC increases and no significant variations were detected between the single compounds and the combination of half of their doses (Figure 3.9B). In line with the concentration-dependent effect of dextromethorphan on siNG-induced gene silencing (Figure 3.5C), only doses above 80 µM significantly augmented the SSC signal (Figure 3.9C), although the effect was less prominent compared to the other molecules tested.

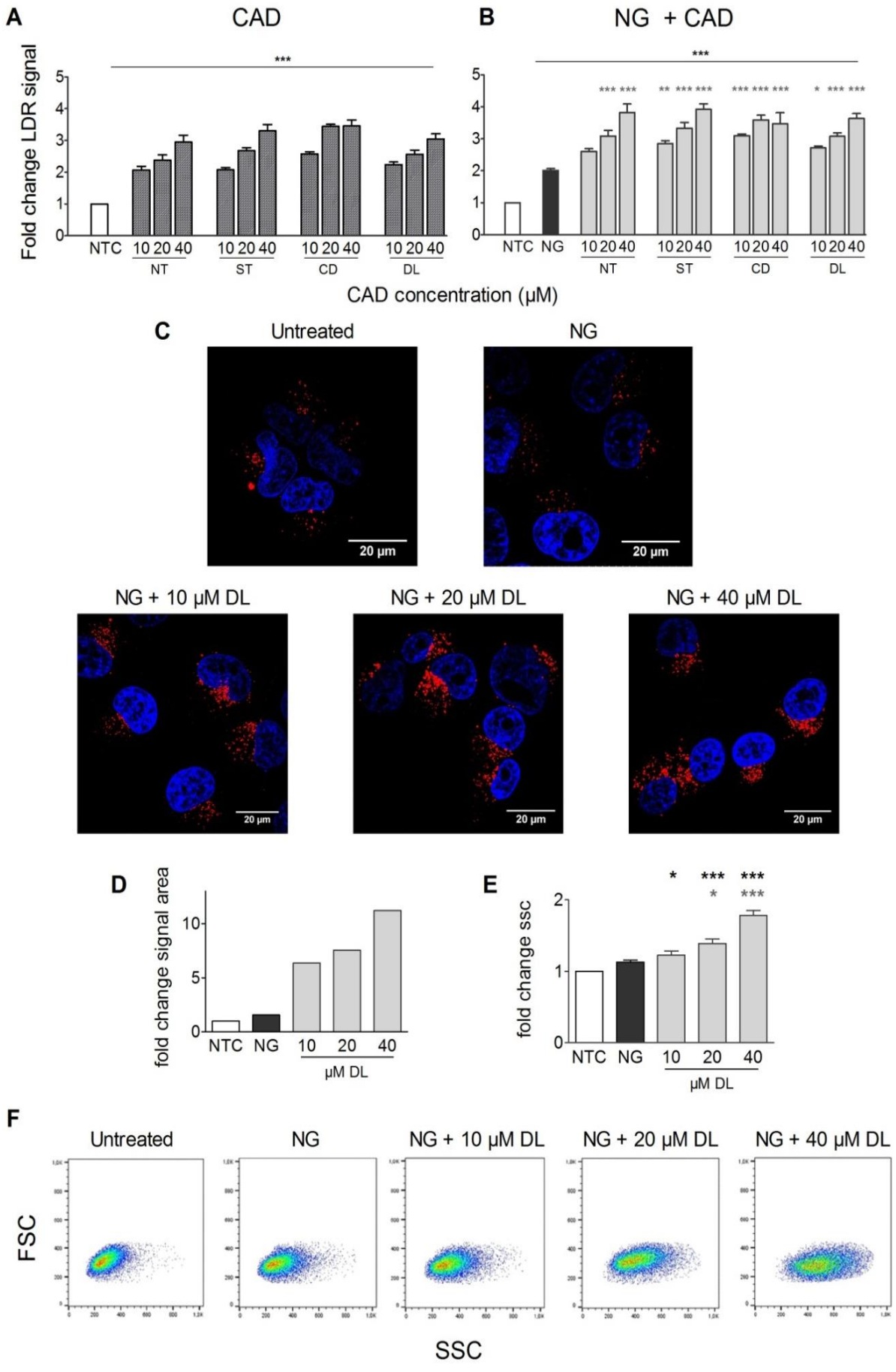
A
CAD
B
NG + CAD
Fold change LDR signal
NTC
10 20 40
NT
ST
CD
DL
CAD concentration (μM)
C
Untreated
NG
20 μm
NG + 10 μM DL
NG + 20 μM DL
NG + 40 μM DL
D
fold change signal area
μM DL
E
fold change ssc
F
FSC
SSC

Figure 3.8. (A) and (B) Fold change in LDR signal measured via flow cytometry for H1299-eGFP cells treated only with the CADs (A) or the combination of siNGs and CADs (B). (C) Representative confocal images showing the endo-lysosomal compartment (red) following LysoTracker® red labeling for untreated H1299-WT cells, NG-transfected cells or cells transfected with siNGs followed by 10, 20 or 40 µM DL treatment. The scale bar corresponds to 20 µm. (D) Fold increase in signal area relative to the untreated control quantified from the confocal images for transfected cells with and without DL. (E) Fold change in side scatter induced by NG transfection or sequential treatment with DL. (F) Representative scatter plots for untreated cells, NG-transfected cells or cells transfected with siNGs followed by 10, 20 or 40 µM DL treatment. Data are represented as the mean ± SEM (n = 3) and statistical significance is indicated when appropriate, in black when referring to the untreated control and in gray when compared to NG transfected cells (p<0.05, ** p<0.001, *** p<0.005). (NTC = not treated control, LDR = LysoTracker® Deep Red, CAD = cationic amphiphilic drug, NG = nanogels, NT = nortriptyline, ST = salmeterol, CD = carvedilol, DL = desloratadine; FSC = forward scatter, SSC = side scatter)*

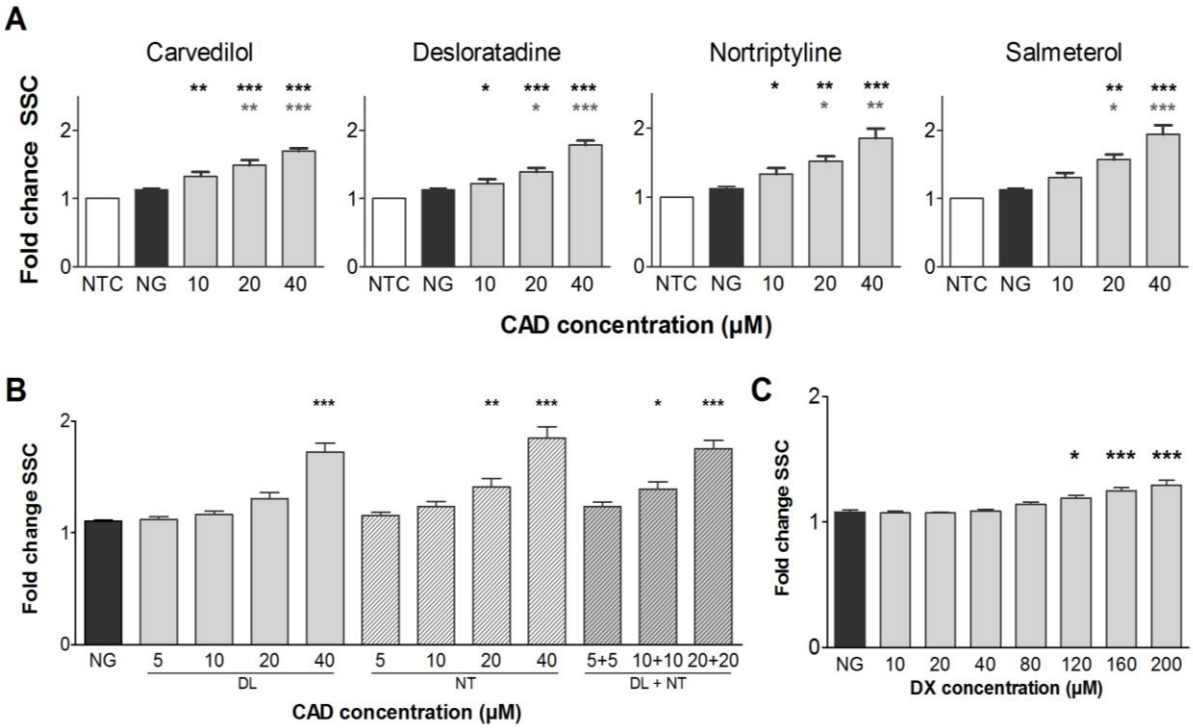

Figure 3.9. (A) Fold increase in side scatter (SSC) signal with respect to the untreated control H1299-eGFP cells by NG transfection alone or with additional CAD treatment. (B) Fold change increase of the SSC signal upon siNG transfection of H1299-eGFP cells whether or not followed by treatment with 10, 20 or 40 µM DL or NT or their combination. (C) Fold change of the SSC signal as a consequence of siNG transfection of H1299-eGFP cells in combination with dextromethorphan treatment (10, 20, 40, 80, 120, 160 or 200 µM). Data are represented as the mean ± SEM (n = 3) and statistical significance is indicated when appropriate in black with reference to the untreated cells and in gray with respect to the NG-transfected cells (p<0.05, ** p<0.001, *** p<0.005). (NTC = not treated control, NG = nanogels, DL = desloratadine, NT = nortriptyline, DX = dextrometorphan)*

3.5. CADs induce a lysosomal storage disease-like phenotype

Since CADs are known lysosomotropic agents and phospholipidosis (PLD) inducers, we subsequently explored whether the enlargement of the lysosomal compartment could be attributed to phospholipid accumulation. Labeling CAD-treated cells with the PLD detection reagent LipidTox Red (Figure 3.10A), revealed that DL treatment induced PLD in a concentration dependent fashion. The lipids accumulated in vesicular structures, which enlarged and became more numerous as a function of the DL concentration. Furthermore, only higher doses of dextromethorphan (≥ 80 µM) clearly induced vesicular phospholipid accumulation, corroborating earlier observations.

Such lipid accumulation is a general phenotypical feature of lysosomal lipid storage disorders.[24] However, in this case we did not experimentally verify whether the lipids effectively accumulated in lysosomal structures. Further experiments applying phospholipid and lysosomal markers following detection by confocal microscopy or transmission electron microscopy could offer more definite proof of the lysosomal lipid accumulation.

Interestingly, several groups applied CADs to induce a Niemann-Pick disease (NPD) phenotype.[25] NPD is a lysosomal storage disorder caused by either a depletion of the cholesterol transport protein NPC1 (NPD type C) or a genetic defect in the acid sphingomyelinase enzyme (ASM, NPD type A). Both NPD type A and C present a similar phenotype that is characterized by enlarged lysosomes due to the accumulation of cholesterol and sphingolipids, including sphingomyelin (SM).[26, 27] To experimentally confirm whether the induction of a NPD phenotype enhances siRNA-mediated gene silencing, we first compared the CAD adjuvant effect to that of U18666A, a structurally different (Figure 3.3) and often applied small molecular inducer of the NPD phenotype. Compared to siNG-transfected cells sequentially treated with 40 µM DL, the cellular granularity was augmented to an even greater extent by 30 µM U18666A (Figure 3.10C). Moreover, U18666A clearly improved siNG-mediated gene silencing (Figure 3.10B), albeit to a lesser extent than 40 µM DL.

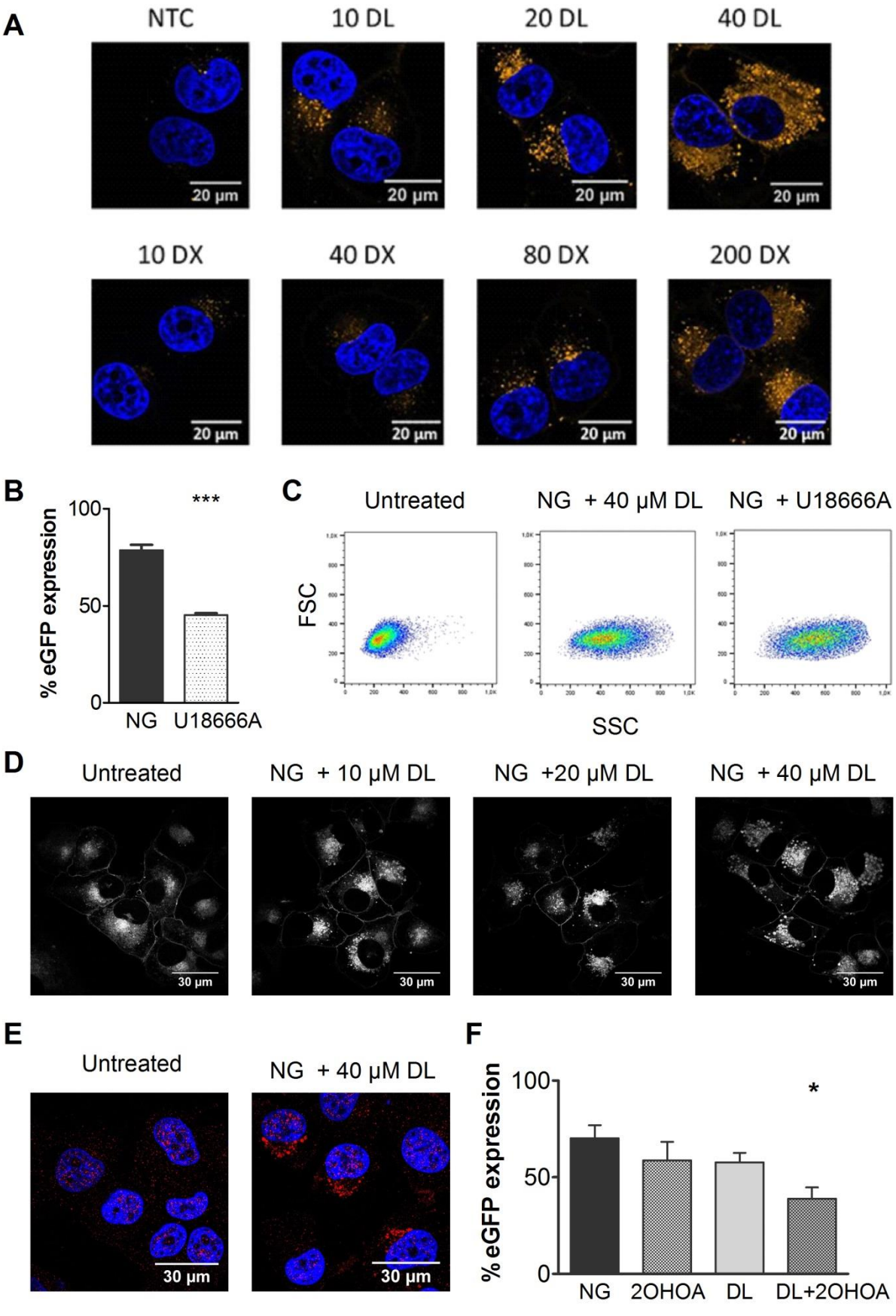
A
NTC
10 DL
20 DL
40 DL
10 DX
40 DX
80 DX
200 DX
20 µm
B
% eGFP expression
100
50
0
***
NG
U18666A
C
Untreated
NG + 40 µM DL
NG + U18666A
FSC
SSC
D
Untreated
NG + 10 µM DL
NG +20 µM DL
NG + 40 µM DL
30 µm
E
Untreated
NG + 40 µM DL
30 µm
F
% eGFP expression
100
50
0
*
NG
2OHOA
DL
DL+2OHOA

*Figure 3.10. (A) Representative confocal images from the phospholipid distribution in H1299-WT cells visualized with LipidTox Red PLD detection reagent in untreated cells and cells treated with 10 or 40 µM DL or 10, 40, 80 or 200 µM DX. The scale bar corresponds to 30 µm. (B) The eGFP silencing induced by adjuvant treatment with 30 µM U18666A compared to siNG transfection alone. (C) Representative scatter plots from untreated cells and siNG-transfected cells receiving sequential treatment with 40 µM DL or 30 µM U18666A. (D) Representative confocal images from the intracellular cholesterol distribution in untreated H1299-WT cells or transfected cells treated with 10, 20 or 40 µM DL. The scale bar corresponds to 30 µm. (E) Representative confocal images showing the intracellular sphingomyelin distribution in untreated H1299-WT cells or transfected cells additionally treated with 10, 20 and 40 µM DL. The scale bar corresponds to 30 µm. (F) The % eGFP expression in H1299-eGFP cells following transfection with the siNGs alone or in combination with 300 µM 2OHOA, 10 µM DL or the combination of both. Data are represented as the mean ± SEM (n = 3) and statistical significance is indicated when appropriate (*** p<0.005) (NG = nanogels, DL = desloratadine, FSC = forward scatter, SSC = side scatter, 2OHOA = 2-hydroxy oleic acid)*

Next, we imaged the cellular cholesterol distribution following siNG transfection and sequential CAD treatment (Figure 3.10D). In the untreated cells, the cholesterol appears to be mainly diffusely present in the cell membrane as well as in the perinuclear region. Upon DL treatment, cholesterol is redistributed to vesicular structures, which enlarge in a concentration dependent fashion. This observation correlates well with our results on endo-lysosomal swelling (Figure 3.8C) and phospholipid accumulation (Figure 3.10A), although co-labeling experiments should be performed to confirm this hypothesis. In addition, we observed similar alterations in the SM distribution upon CAD treatment (Figure 3.10E, supporting the notion that the CADs negatively influence the ASM activity and cause SM accumulation. To confirm that interference with the SM metabolism contributed to the enhanced siNG-mediated gene silencing, we combined 10 µM DL and 300 µM 2-hydroxy oleic acid (2OHOA), a known activator of the SM synthetase. The additive effect of 2-OHOA on the siRNA-mediated gene silencing indeed suggests an involvement of the SM homeostasis in the improved cytosolic siRNA delivery (Figure 3.10F). More definite proof could be provided by performing ASM-activity studies prior to and post CAD exposure.[12]

3.6. The impact of the DL incubation time and multiple DL treatments

All experiments described above involved a 20-hour CAD treatment. Since a 20-hour DL incubation period reduced the cell viability to ˜60%, we evaluated whether a reduction of the exposure time from 20 to 2 hours could reduce the toxicity levels in order to obtain a more applicable strategy to improve siRNA release *in vivo*. Figure 3.11A shows that both a 2h and 20h incubation improved siNG-mediated gene silencing to a similar extent. Of note, the SSC signal was significantly lower in cells exposed 2h to DL (Figure 3.11B), which suggests that the induced PLD phenotype is only transiently present. Interestingly, a 2h DL incubation period did not cause any additional cytotoxicity compared to the siNGs alone (Figure 3.11C). Thus, the more rapid recovery from the PLD state appears to have a positive effect on cell viability.

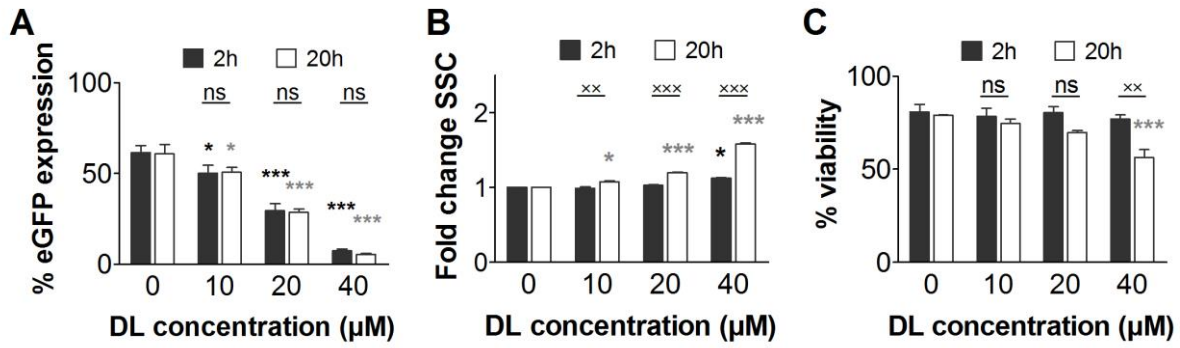

*Figure 3.11. (A) The percentage eGFP expression in H1299-eGFP cells following transfection with the siNGs alone or in combination with a 2h or 20h DL treatment. (B) Fold change in SSC induced by siNG transfection or sequential treatment with siNGs and 2h or 20h DL. (C) Percentage viable cells following siNG transfection whether or not combined with 2h or 20h DL. Data are represented as mean ± SEM (n = 3) and statistical significance is indicated when appropriate by black * when referring to the untreated control and gray * when compared to NG transfected cells (* p<0.05, ** p<0.001, *** p<0.005). Finally, statistical significance between the 2h and 20h condition is indicated by the black ^{x} (^{xx} p<0.01, ^{xxx} p<0.005).*

Next, we investigated whether DL treatment influenced the kinetics of the siNG-mediated gene silencing. Since the compounds are dissolved in DMSO, we first ensured that the presence of DMSO did not alter the siNG-induced eGFP silencing over time (Figure 3.12A). A DL concentration dependent improvement of initial gene silencing (Figure 3.12B) was obtained in correspondence to previous results (Figure 3.4C). From day 2 onwards, the relative eGFP expression steadily increased and at day 7 expression levels reached 100% in all conditions.

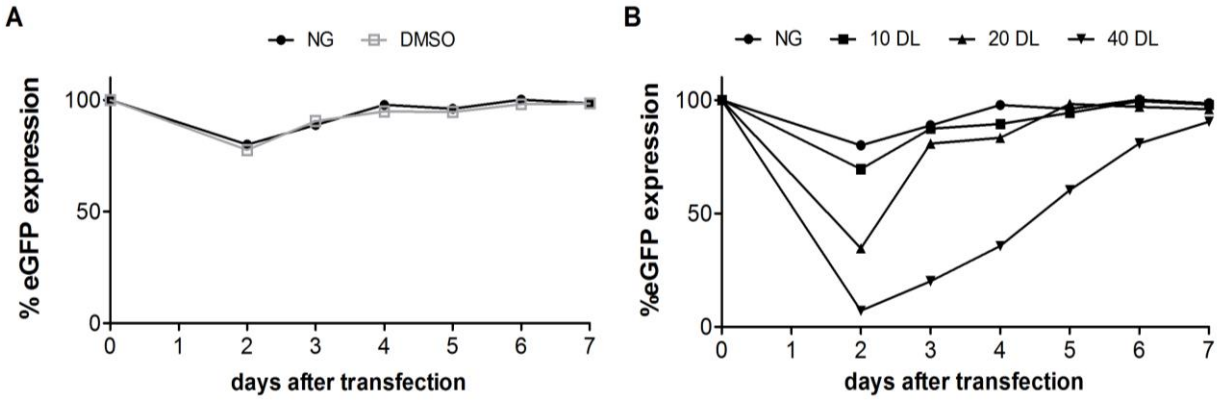

Figure 3.12. (A) Kinetics of the eGFP knockdown in H1299-eGFP cells transfected with siNGs (black) and a single time exposed to 0.16% DMSO in cell medium (gray). This graph shows that the presence of DSMO does not influence the siNG-mediated eGFP silencing. (B) Kinetics of eGFP knockdown in cells transfected with siNGs (circle) and treated with 10 (square), 20 (upwards triangle) or 40 µM (downwards triangle) DL.

Interestingly, confocal images of cells transfected with NGs encapsulating labeled siRNA (siGLO green transfection indicator) revealed enlarged siGLO-NG containing vesicles in DL treated cells (Figure 3.13A), indicating that not all internalized and presumably lysosomally accumulated siRNA is released upon a single adjuvant treatment. The effective lysosomal accumulation is assumed based upon previous co-localization studies from our group[18], but would ideally be experimentally confirmed. Based on the siGLO data, we investigated if multiple DL treatments could induce additional siRNA release at later time points. Since we applied nuclease-stabilized siRNA for this experiment to avoid siRNA degradation, we first confirmed the comparable silencing potential of both siRNA molecules (Figure 3.13B). Most interestingly, we observed that upon multiple 2h DL treatments additional siRNA could be released. Of note, additional cell viability experiments are required to estimate the safety of this approach. In any case, the additional exposure to DL allowed us to maintain minimal eGFP expression levels up to four days post transfection, after which eGFP expression levels gradually augmented to reach basal levels at day 9 following similar kinetics compared to a single DL addition (Figure 3.13C). In comparison, the expression levels reached 100% at day 3 post transfection in case of a suboptimal siNG transfection alone. Despite the retained PLD phenotype by DL treatments after day 4 (Figure 3.13D), the adjuvant treatments failed to provide further prolongation of the maximal gene silencing.

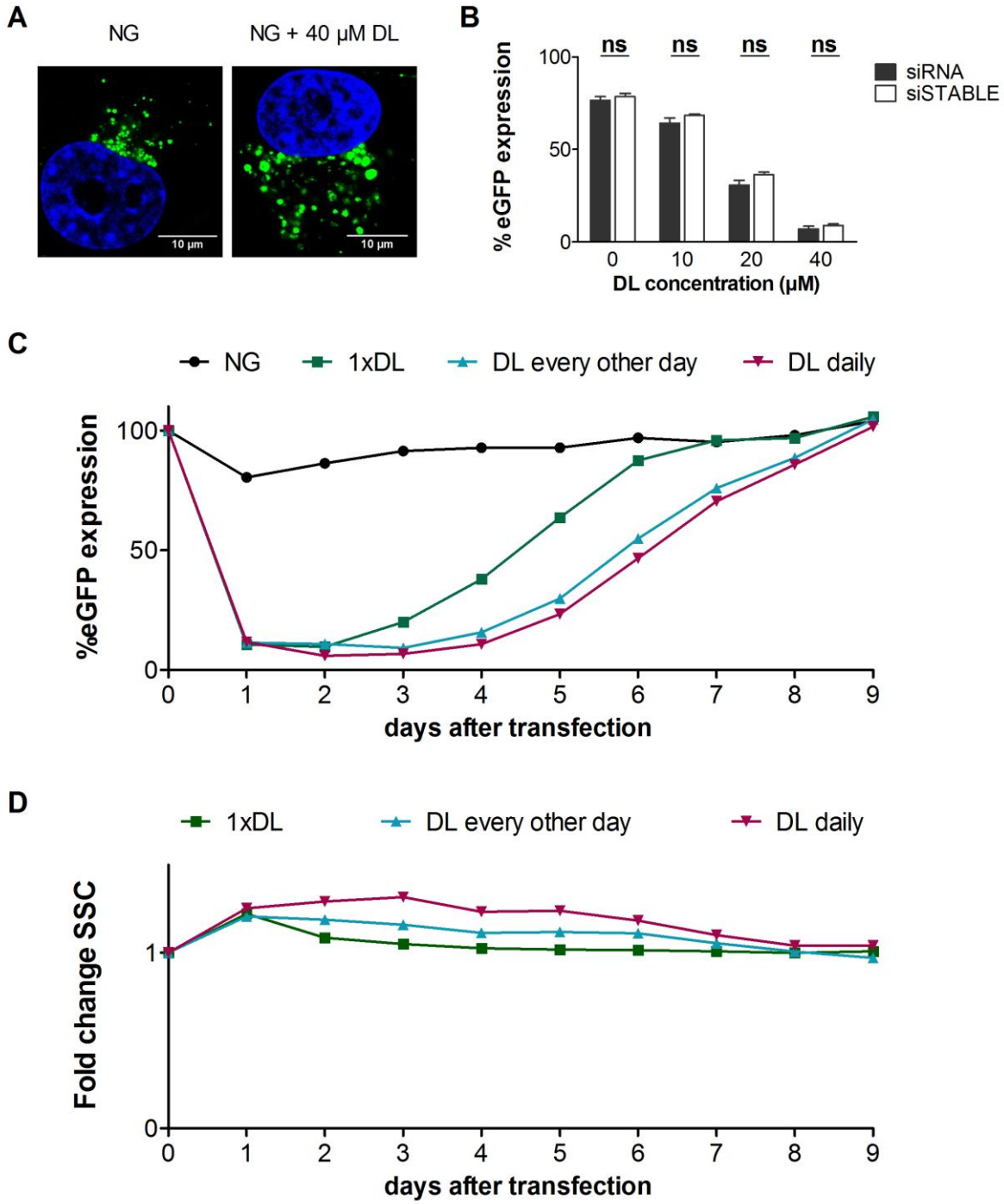

Figure 3.13. (A) Cellular distribution of the siGLO signal in H1299-WT cells transfected with siGLO-NGs alone or subjected to the sequential 40 µM DL treatment. (B) % eGFP expression following NG-mediated siRNA delivery of unmodified siRNA (black) and stabilized siRNA (white) in combination with 10, 20 or 40 µM DL in H1299-eGFP cells. Data are represented as the mean ±SEM (n=3) and the statistical significance is indicated when appropriate. (C) Kinetics of eGFP knowckdown in cells transfected with siNGs (black line) and treated once with 40 µM DL (green line), daily (pink line) or every other day (blue line) until day six post transfection. (D) The evolution of the side scatter signal in H1299-eGFP cells transfected with siNGs followed by a single DL treatment (green) or repeated exposure, namely daily (pink) or every other day (blue) until day 6 after transfection. (NG = nanogels, DL = desloratadine, SSC = side scatter)

3.7. DL improves therapeutic siRNA delivery

Finally, we applied our adjuvant strategy to improve delivery of a therapeutic siRNA targeting polo-like kinase 1 (PLK1). Reducing PLK1 expression halts the cell cycle and induces apoptosis in certain cancer cells, such as the applied H1299 cell line.[28, 29] Hence, reducing PLK1 expression is currently avidly investigated as a potential anti-cancer strategy.

NGs loaded with control siRNA reduced the cell viability to approximately 80% in any condition tested (Figure 3.14A), corroborating previous experiments (Figure 3.6B). Thus, an increase in siRNA dose or DL treatment(s) did not additionally affect cell viability. NGs loaded with 1 and 10 nM siPLK1 did not affect cell viability, while 100 nM siPLK1 reduced the cell viability to ˜60% (Figure 3.14B). The DL adjuvant treatment enhanced siPLK1-mediated cytotoxicity for all siPLK1 doses tested. (Figure 3.14B) Once again, repeating the adjuvant incubation (2h, 40 μM DL) further reduced cell viability (Figure 3.14C). The most extensive adjuvant effect was observed for 10 nM siPLK1 where a maximal effect on cell viability was obtained with a single DL treatment (Figure 7A). For both 10 and 100 nM siPLK1 a second DL treatment did not further reduce the cell viability (Figure 3.14D).

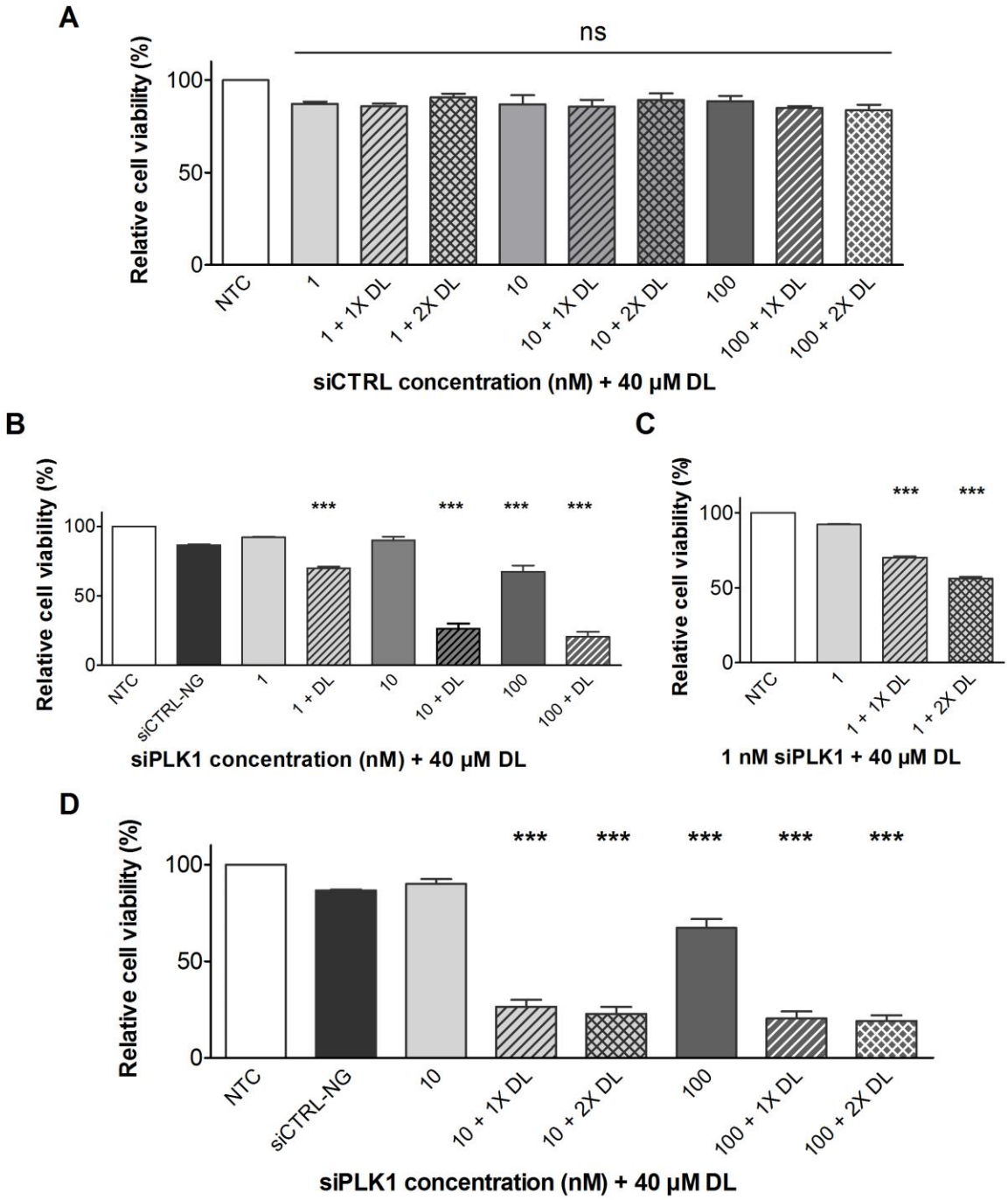

*Figure 3.14. (A) H1299-eGFP cell viability measured upon transfection with siCTRL-NGs as control during the siPLK1 transfection. No significant variations in cell viability could be detected between the various treatment groups. (B) Percentage viable H1299-eGFP cells following transfection with siPLK1-loaded NGs whether or not subjected to a sequential 40 µM DL treatment. (C) % viable cells of cells solely transfected with 1 nM siPLK1-NGs or subjected to one or two 40 µM DL treatments. (D) Relative H1299-eGFP cell viability indicative of PLK1 silencing for cells transfected with 10 or 100 nM siPLK1 and treated not, once or twice with 40 µM DL. A second DL treatment could not further improve the siPLK1 effect. Data are presented as the mean ± SEM (n = 3) and statistical significance is indicated when appropriate (*** p<0.005). (NTC = untreated control, siCTRL-NG =siCTRL-loaded nanogels, DL = desloratadine)*

4. DISCUSSION

The successful application of siRNA therapeutics faces multiple delivery challenges. Formulation into nanoparticles is often proposed to guide the siRNA across extra- and intracellular barriers. However, endocytic uptake of nanomedicines by target cells typically leads to endo-lysosomal sequestration, explaining the poor cytosolic siRNA delivery efficiency of available nanomedicines.[6, 7] In order to avoid lysosomal degradation of the nanocarrier and its cargo, the general consensus states that endosomal escape should occur as soon as possible upon internalization. However, the time frame in which release strategies can be of benefit is rather narrow, as nanocarriers can be trafficked to the lysosomes within the hour after internalization.[8] Moreover, it is believed that membrane-destabilizing agents should ideally avoid acting on lysosomes, as lysosomal membrane permeabilization (LMP) is considered a hallmark of lysosomal cell death.[9] The data presented in this work argue against this leading paradigm, as we propose to target the lysosomes to enhance cytosolic siRNA delivery.

We applied cationic dextran nanogels (NGs) as a model nanocarrier given their siRNA delivery potential in various cell types, endo-lysosomal entrapment following internalization and progressive lysosomal accumulation.[18] CADs were selected as adjuvants given their potential to destabilize the lysosomal compartment through their reported FIASMA activity and ability to induce PLD.[13] We selected four model CADs to evaluate their adjuvant effect on siRNA delivery, namely carvedilol, desloratadine (DL), nortriptyline and salmeterol. Although the four selected molecules differed in drug class and molecular structure, all compounds markedly improved the siNG silencing potential to a similar extent [20] Moreover, the additive effect on gene silencing is in line with the reported additive ASM inhibition.[12] However, not all CADs were active in a similar dose range, for instance 10-fold higher dextrometorphan doses were required to obtain an adjuvant effect. This may be attributed to variations in the molecular structure with the basic amine not being spatially separated from the hydrophobic ring structure, therefore potentially being less available to functionally inhibit ASM.[20, 26]

Throughout the literature, several CADs are applied to induce a Niemann-Pick disease (NPD) phenotype.[30-32] NPD is a lysosomal storage disorder either caused by a lack of functional ASM (type A) or a deficient Niemann-Pick C1 cholesterol transporter (type C). Overall NPD

type A and C show similar phenotypes, characterized by enlarged and less stable lysosomes, which are more prone to LMP.[26, 27] In corroboration, the NPC1 inhibitor U18666A, which is avidly applied to evoke a NPD phenotype, ameliorated siRNA-mediated gene silencing similar to the CADs. In corroboration, Sahay *et al*. showed that gene silencing was enhanced in NPC1$^{-/-}$ cells and upon NPC1 inhibition by NP3.47, which was explained by increased chances of siRNA escape through inhibited exocytosis of the carrier.[8, 33] Likewise, CADs potentially reduced the siNG recycling since FIASMAs are reported to inhibit vesicle fusion[27], although this was not experimentally verified. Overall, this data set suggests that the induction of a NPD phenotype may positively affect siRNA delivery. In our case, the FIASMAs are suggested to induce (endo-)lysosomal swelling due to the accumulation of phospholipids, cholesterol and sphingomyelin. This is in turn reported to destabilize the lysosomal membrane, thereby causing LMP, which may in turn facilitate siRNA release. However, additional experiments are required to provide a more stringent confirmation of the suggested mechanism of improved cytosolic siRNA delivery. For one, to probe the ASM activity in function of the CAD concentration will allow confirmation of the FIASMA effect.[12] The effect of CADs in a cathepsins knock out model would allow to estimate the importance of ASM degradation for the observed improved release. A confirmation of lysosomal lipid accumulation can be provided by labeling both the lysosomes (LAMP-1) and the phospholipids in a single experiment. Indeed, as Lysotracker probes will label acidic organelles, we currently cannot refute the possibility that some of the release is also linked to late endosomes. Finally, the extent of LMP could be estimated by evaluating the release of differentially sized dextrans or quantification of the cytosolic cathepsin concentration.[23]

Similar to previous reports[10, 11], we noted that not all internalized siRNA is released upon a single DL treatment. Hence, we evaluated whether we could induce additional siRNA release with multiple CAD treatments. The NGs are an ideal carrier for this purpose given their biodegradability but relative stability at acidic pH, implying slow siRNA release from the NGs in the lysosomal compartment where the NGs progressively accumulate following transfection.[19] Of note, a potential influence of the CADs on intracellular trafficking may slightly alter the intracellular distribution and requires experimental confirmation. Strikingly, up to day 3 post transfection we could induce additional siRNA release, highlighting the potential of the lysosomes as a depot for triggered and prolonged siRNA release. Starting

from day 4, additional DL treatments remained without effect. This may be attributed to the consequent cell divisions that may have diluted the siNG-containing lysosomes to such an extent that minor additional siRNA release could no longer extend the maximal gene silencing.

An optimal endosomal escape strategy should merge efficiency and safety. Maximal gene silencing was obtained with siNGs encapsulating 2 nM siRNA combined with the highest CAD concentration tested, whereas siRNA doses exceeding 50 nM would otherwise be required. Such a dose sparing strategy could strongly reduce the risk of siRNA-related adverse effects. In addition, any negative impact on cell viability could be avoided for DL by reducing the exposure time. Interestingly, the side scatter signal accordingly decreased, indicative of the reversible nature of the PLD phenotype.[14, 34] In corroboration, the occurrence of drug-induced PLD is only rarely correlated to organ toxicity *in vivo*.[35] The limited cytotoxicity furthermore implies that improved cytosolic siRNA release did not coincide with severe LMP, which typically evokes cell death through excessive leakage of lysosomal cathepsins.[9, 36] In contrast, Petersen *et al.* witnessed cancer cell death through severe LMP induction by siramesine.[13] Such strong LMP inducers might be suitable delivery adjuvants when applied at lower doses. The suggested 'minor' LMP allowing improved siRNA release furthermore suggests that small pores are created in the lysosomal membrane, which solely allow uncomplexed siRNA to transfer to the cytosol. Similarly, Wittrup *et al.* reported that free siRNA escapes the endosomal compartment rather than the entire lipoplex.[10] This hypothesis may be confirmed by evaluating the release of differentially sized dextrans.[23]

Finally, to confirm the enhanced delivery in a therapeutic setting, siRNA targeting polo-like kinase 1 (PLK1) was delivered in the H1299 non-small cell lung cancer cell model, which is particularly sensitive to PLK1 suppression due to its p53 deficiency.[37, 38] DL markedly boosted NG-mediated siPLK-1 delivery, resulting in significantly greater cytotoxicity. This approach requires further confirmation in a relevant *in vivo* model. However, systemically administered NGs show limited stability and are rapidly cleared from the circulation.[39] Their intratumoral administration to a murine xenograft model may furthermore not be advisable given the limited predictive power towards the clinical outcome in human tumors.[40] Hence, the *in vivo* evaluation of the small molecule adjuvant approach will require the

administration of appropriate siRNA delivery vehicles in more complex tumor models that more closely represent the human tumor pathophysiology.

In this work we aimed to repurpose CADs with an acceptable clinical safety profile to boost cytosolic siRNA delivery. In this context, CAD antihistamines were recently repurposed as adjuvants to enhance the efficacy of anti-cancer drugs, evidenced by reduced mortality in patients using antihistamines while receiving chemotherapy.[41] Importantly, it can be rationalized that this CAD adjuvant approach may enhance siRNA delivery to cancer cells *in vivo*. For one, cancer cell lysosomes are generally less stable, show an altered membrane composition and lower ASM activity.[13, 16, 42] In addition, CADs were recently reported to induce LMP in cancer cells *in vivo*.[13, 16] Moreover, sufficiently high concentrations may be reached in tissues given the extremely high distribution volumes of CADs. This may especially be true for cancer cells since CADs are suggested to preferentially accumulate at the more acidic tumor sites.[41] Physiologically based pharmacokinetic modeling could furthermore provide information on *in vivo* ADME processes and will allow us to estimate whether the CADs will accumulate in sufficiently high concentrations to allow improved release and in which tissues the effect will preferentially occur. Overall, to use of a benchmark therapy as a positive control in *both in vitro* and *in vivo* experiments would allow to better estimate the potential therapeutic value of the proposed approach.

5. CONCLUSION

In conclusion, we demonstrated that cationic amphiphilic drugs (CADs) can be repurposed to stimulate cytosolic delivery of siRNA in cancer cells. Indeed CADs induced the accumulation of phospholipids, cholesterol and sphingomyelin, which is assumed to result in the enlargement of the endo-lysosomal compartment and the induction of minor lysosomal membrane permeabilization (LMP) followed by enhanced siRNA release. Importantly, our results suggest that this acquired lysosomal storage disorder-phenotype is responsible for the improved siRNA delivery when CADs were sequentially applied to siNG transfected cancer cells. Most importantly, further CAD treatments could be applied to induce additional siRNA release of the accumulated siRNA, which was not released by the initial CAD treatment. Overall, we believe this is a highly interesting approach, which requires further investigation in terms of the applicable small molecular adjuvants, nanocarriers and nucleic acid cargos.

ACKNOWLEDGEMENTS

FJ is a doctoral fellow of the Agency for Innovation by Science and Technology in Flanders (IWT). CB acknowledges the Education, Audiovisual and Culture Executive Agency (EACEA) of the European Commission in the field of the NanoFar Erasmus Mundus Joint Programme. LDB is a postdoctoral researcher of the Special Research Fund of Ghent University. TVDV is a doctoral fellow of the Research Foundation-Flanders (FWO). KR also acknowledges the FWO for a postdoctoral Research Grant

REFERENCES

1. Fire, A.; Xu, S.; Montgomery, M. K.; Kostas, S. A.; Driver, S. E.; Mello, C. C. *Nature* **1998,** 391, (6669), 806-11.
2. Morris, K. V.; Chan, S. W.; Jacobsen, S. E.; Looney, D. J. *Science* **2004,** 305, (5688), 1289-92.
3. Davidson, B. L.; McCray, P. B., Jr. *Nat Rev Genet* **2011,** 12, (5), 329-40.
4. Wittrup, A.; Lieberman, J. *Nat Rev Genet* **2015,** 16, (9), 543-52.
5. Yin, H.; Kanasty, R. L.; Eltoukhy, A. A.; Vegas, A. J.; Dorkin, J. R.; Anderson, D. G. *Nat Rev Genet* **2014,** 15, (8), 541-55.
6. Martens, T. F.; Remaut, K.; Demeester, J.; De Smedt, S. C.; Braeckmans, K. *Nano Today* **2014,** 9, (3), 344-364.
7. Ma, D. *Nanoscale* **2014,** 6, (12), 6415-25.
8. Sahay, G.; Querbes, W.; Alabi, C.; Eltoukhy, A.; Sarkar, S.; Zurenko, C.; Karagiannis, E.; Love, K.; Chen, D.; Zoncu, R.; Buganim, Y.; Schroeder, A.; Langer, R.; Anderson, D. G. *Nat Biotechnol* **2013,** 31, (7), 653-8.
9. Aits, S.; Jaattela, M. *J Cell Sci* **2013,** 126, (Pt 9), 1905-12.
10. Wittrup, A.; Ai, A.; Liu, X.; Hamar, P.; Trifonova, R.; Charisse, K.; Manoharan, M.; Kirchhausen, T.; Lieberman, J. *Nat Biotechnol* **2015,** 33, (8), 870-6.
11. Gilleron, J.; Querbes, W.; Zeigerer, A.; Borodovsky, A.; Marsico, G.; Schubert, U.; Manygoats, K.; Seifert, S.; Andree, C.; Stoter, M.; Epstein-Barash, H.; Zhang, L. G.; Koteliansky, V.; Fitzgerald, K.; Fava, E.; Bickle, M.; Kalaidzidis, Y.; Akinc, A.; Maier, M.; Zerial, M. *Nature Biotechnology* **2013,** 31, (7), 638-U102.
12. Kornhuber, J.; Muehlbacher, M.; Trapp, S.; Pechmann, S.; Friedl, A.; Reichel, M.; Muhle, C.; Terfloth, L.; Groemer, T. W.; Spitzer, G. M.; Liedl, K. R.; Gulbins, E.; Tripal, P. *PLoS One* **2011,** 6, (8), e23852.
13. Petersen, N. H.; Olsen, O. D.; Groth-Pedersen, L.; Ellegaard, A. M.; Bilgin, M.; Redmer, S.; Ostenfeld, M. S.; Ulanet, D.; Dovmark, T. H.; Lonborg, A.; Vindelov, S. D.; Hanahan, D.; Arenz, C.; Ejsing, C. S.; Kirkegaard, T.; Rohde, M.; Nylandsted, J.; Jaattela, M. *Cancer Cell* **2013,** 24, (3), 379-93.
14. Kornhuber, J.; Tripal, P.; Gulbins, E.; Muehlbacher, M. *Handb Exp Pharmacol* **2013**, (215), 169-86.
15. Saftig, P.; Sandhoff, K. *Nature* **2013,** 502, (7471), 312-313.
16. Gulbins, E.; Kolesnick, R. N. *Cancer Cell* **2013,** 24, (3), 279-281.
17. Gulbins, E.; Palmada, M.; Reichel, M.; Luth, A.; Bohmer, C.; Amato, D.; Muller, C. P.; Tischbirek, C. H.; Groemer, T. W.; Tabatabai, G.; Becker, K. A.; Tripal, P.; Staedtler, S.; Ackermann, T. F.; van Brederode, J.; Alzheimer, C.; Weller, M.; Lang, U. E.; Kleuser, B.; Grassme, H.; Kornhuber, J. *Nat Med* **2013,** 19, (7), 934-8.
18. De Backer, L.; Braeckmans, K.; Demeester, J.; De Smedt, S. C.; Raemdonck, K. *Nanomedicine (Lond)* **2013,** 8, (10), 1625-38.
19. Raemdonck, K.; Naeye, B.; Buyens, K.; Vandenbroucke, R. E.; Hogset, A.; Demeester, J.; De Smedt, S. C. *Adv Funct Mater* **2009,** 19, (9), 1406-1415.
20. Wishart, D. S.; Knox, C.; Guo, A. C.; Shrivastava, S.; Hassanali, M.; Stothard, P.; Chang, Z.; Woolsey, J. *Nucleic Acids Res* **2006,** 34, (Database issue), D668-72.
21. Rehman, Z. U.; Hoekstra, D.; Zuhorn, I. S. *Acs Nano* **2013,** 7, (5), 3767-3777.
22. Zhang, X.; Sawyer, G. J.; Dong, X.; Qiu, Y.; Collins, L.; Fabre, J. W. *J Gene Med* **2003,** 5, (3), 209-18.
23. Aits, S.; Jaattela, M.; Nylandsted, J. *Method Cell Biol* **2015,** 126, 261-285.
24. te Vruchte, D.; Speak, A. O.; Wallom, K. L.; Al Eisa, N.; Smith, D. A.; Hendriksz, C. J.; Simmons, L.; Lachmann, R. H.; Cousins, A.; Hartung, R.; Mengel, E.; Runz, H.; Beck, M.; Amraoui, Y.; Imrie, J.; Jacklin, E.; Riddick, K.; Yanjanin, N. M.; Wassif, C. A.; Rolfs, A.; Rimmele, F.; Wright, N.; Taylor, C.; Ramaswami, U.; Cox, T. M.; Hastings, C.; Jiang, X. T.; Sidhu, R.; Ory, D. S.; Arias,

B.; Jeyakumar, M.; Sillence, D. J.; Wraith, J. E.; Porter, F. D.; Cortina-Borja, M.; Platt, F. M. *J Clin Invest* **2014,** 124, (3), 1320-1328.
25. Shoemaker, C. J.; Schornberg, K. L.; Delos, S. E.; Scully, C.; Pajouhesh, H.; Olinger, G. G.; Johansen, L. M.; White, J. M. *Plos One* **2013,** 8, (2).
26. Funk, R. S.; Krise, J. P. *Mol Pharm* **2012,** 9, (5), 1384-95.
27. Kirkegaard, T.; Roth, A. G.; Petersen, N. H.; Mahalka, A. K.; Olsen, O. D.; Moilanen, I.; Zylicz, A.; Knudsen, J.; Sandhoff, K.; Arenz, C.; Kinnunen, P. K.; Nylandsted, J.; Jaattela, M. *Nature* **2010,** 463, (7280), 549-53.
28. Kawata, E.; Ashihara, E.; Kimura, S.; Takenaka, K.; Sato, K.; Tanaka, R.; Yokota, A.; Kamitsuji, Y.; Takeuchi, M.; Kuroda, J.; Tanaka, F.; Yoshikawa, T.; Maekawa, T. *Molecular Cancer Therapeutics* **2008,** 7, (9), 2904-2912.
29. McCarroll, J. A.; Dwarte, T.; Baigude, H.; Dang, J.; Yang, L.; Erlich, R. B.; Kimpton, K.; Teo, J.; Sagnella, S. M.; Akerfeldt, M. C.; Liu, J.; Phillips, P. A.; Rana, T. M.; Kavallaris, M. *Oncotarget* **2015,** 6, (14), 12020-12034.
30. Cenedella, R. J. *Lipids* **2009,** 44, (6), 477-87.
31. Roff, C. F.; Goldin, E.; Comly, M. E.; Cooney, A.; Brown, A.; Vanier, M. T.; Miller, S. P.; Brady, R. O.; Pentchev, P. G. *Dev Neurosci* **1991,** 13, (4-5), 315-9.
32. Yoshikawa, H. *Brain Dev* **1991,** 13, (2), 115-20.
33. Wang, H.; Tam, Y. Y.; Chen, S.; Zaifman, J.; van der Meel, R.; Ciufolini, M. A.; Cullis, P. R. *Mol Ther* **2016**.
34. Reiners, J. J., Jr.; Kleinman, M.; Kessel, D.; Mathieu, P. A.; Caruso, J. A. *Free Radic Biol Med* **2011,** 50, (2), 281-94.
35. Mesens, N.; Desmidt, M.; Verheyen, G. R.; Starckx, S.; Damsch, S.; De Vries, R.; Verhemeldonck, M.; Van Gompel, J.; Lampo, A.; Lammens, L. *Toxicol Pathol* **2012,** 40, (3), 491-503.
36. Berndtsson, M.; Beaujouin, M.; Rickardson, L.; Havelka, A. M.; Larsson, R.; Westman, J.; Liaudet-Coopman, E.; Linder, S. *Int J Cancer* **2009,** 124, (6), 1463-9.
37. Guan, R.; Tapang, P.; Leverson, J. D.; Albert, D.; Giranda, V. L.; Luo, Y. *Cancer Res* **2005,** 65, (7), 2698-704.
38. Liu, X.; Lei, M.; Erikson, R. L. *Mol Cell Biol* **2006,** 26, (6), 2093-108.
39. Naeye, B.; Deschout, H.; Roding, M.; Rudemo, M.; Delanghe, J.; Devreese, K.; Demeester, J.; Braeckmans, K.; De Smedt, S. C.; Raemdonck, K. *Biomaterials* **2011,** 32, (34), 9120-7.
40. Gould, S. E.; Junttila, M. R.; de Sauvage, F. J. *Nat Med* **2015,** 21, (5), 431-9.
41. Ellegaard, A. M.; Dehlendorff, C.; Vind, A. C.; Anand, A.; Cederkvist, L.; Petersen, N. H. T.; Nylandsted, J.; Stenvang, J.; Mellemgaard, A.; Osterlind, K.; Friis, S.; Jaattela, M. *Ebiomedicine* **2016,** 9, 130-139.
42. Boya, P.; Kroemer, G. *Oncogene* **2008,** 27, (50), 6434-51.

CHAPTER 4

Exploring the broader applicability of a low molecular weight adjuvant approach to improve nucleic acid delivery to the cytosol.

This chapter contains unpublished data.

Freya Joris, Stefaan C. De Smedt, Koen Raemdonck.

Lab of General Biochemistry and Physical Pharmacy, Faculty of Pharmaceutical Sciences, Ghent University, B9000 Ghent, Belgium.

Table of contents

ABSTRACT

Research efforts in the past few decades revealed the enormous therapeutic potential of distinct nucleic acids (NA). Unfortunately, many NA therapeutics are yet to transfer to the clinic, as efficient delivery to their intracellular target site remains a major stumbling block. In **Chapter 3** we showed that cationic amphiphilic drugs (CADs) improve the siRNA-mediated gene silencing in nanogel (NG) transfected cells, which coincided with a transient phospholipidosis (PLD) phenotype. It was suggested that the accumulated phospholipids caused transient lysosomal membrane destabilization and minor lysosomal membrane permeabilization (LMP), thereby allowing enhanced siRNA release to the cytosol. Here we explore the broader applicability of this method in terms of the applied transfection method, NA cargo and small molecular adjuvant. Tobramycin induced PLD but was unable to improve siRNA delivery whereas the therapeutic range of disulfiram was too narrow. Moreover, CADs could not significantly improve mRNA delivery. A sequential CAD treatment was equally unable to strongly enhance the delivery potential of various liposomal formulations, a cholesterol-siRNA conjugate or RNAiMAX. We were able to introduce a CAD as a liposomal building block, but it failed to contribute to the delivery potential of the formulation. Hence, the proposed adjuvant strategy may not be very broadly applicable. However, these data revealed key factors requiring further investigation to allow future rational combinations of small molecular adjuvants, NA and nanocarriers

1. INTRODUCTION

In **Chapter 3** we investigated the potential of cationic amphiphilic drugs (CADs) to improve the gene silencing potential of siRNA-loaded dextran nanogels (siNGs). This improved silencing potential was suggested to be attributed to the inhibition of acid sphingomyelinase (ASM) by the CADs, although this was not experimentally verified. Indeed, the reported lysosomotropic nature of the CADs would ensure lysosomal accumulation and allow functional inhibition of ASM (FIASMA).[1, 2] This suggested interaction was corroborated by the accumulation of sphingomyelin, cholesterol and other phospholipids. We subsequently hypothesized that this lipid imbalance destabilized the lysosomal membrane[3, 4], thereby improving siRNA release to the cytosol. Again, this lysosomal siRNA release could be assumed based on the provided data set but remains to be experimentally confirmed. In any case, we obtain promising results on the potential adjuvant effects of CADs on the therapeutic potential of nucleic acids (NA). Here, we set out to establish the broader applicability of this adjuvant approach in terms of the applied small molecular adjuvant, NA cargo and nanocarrier.

The adjuvant potential of the CADs coincided with a phospholipidosis (PLD) phenotype. Based on this observation we investigated if small molecules without CAD-properties and FIASMA activity, but known to induce PLD could equally improve siRNA delivery. Hereto, we selected tobramycin (TM), which is reported to induce PLD in the kidney upon systemic administration.[5] Results in **Chapter 3** additionally suggested that the siRNA could escape to the cytosol through the destabilization and permeabilization of the lysosomal membrane due to the phospholipid accumulation. Hence, evaluated whether disulfiram (DSF) was able to boost the silencing potential of siNGs. DSF was selected since it has no CAD properties or FIASMA activity but is suggested to destabilize the lysosomes, leading to lysosomal cell death in cancer cells.[6, 7] Thus, we investigated if the FIASMA activity of the CADs is essential for their adjuvant effect.

Besides siRNA, multiple distinct therapeutic NA are being investigated, such as plasmid DNA, messenger RNA (mRNA), antisense oligonucleotides (ASO), splice switching oligonucleotides (SSO) and microRNA. Each NA drug has specific therapeutic applications, according to its mode of action. In contrast, most NA face the same delivery challenges, as they require nanocarriers to protect them from nucleases, to improve their *in vivo* biodistribution and to

ensure transport over the cell membrane. In addition, the NA need to escape the endo-lysosomal compartment in an efficient way to reach their intracellular target site.[8, 9] Therefore we evaluated if our CAD adjuvant approach could similarly improve the delivery of other NA therapeutics, besides siRNA. To contrast the relatively small siRNA duplexes (˜21 base pairs), we selected mRNA, being long single stranded NA (˜1000 bases) that may arrange in secondary structures due to self-complementarity. The delivery of mRNA is mainly pursued in the context of protein replacement therapies or as a vaccination strategy for the treatment of infectious diseases or for cancer immunotherapy.[9] In protein replacement therapies, mRNA outperforms pDNA since mRNA is translated in the cytosol and does not require translocation to the nucleus. This implies that mRNA transfections are not associated with the risk of genomic integration.[10] The efficiency of mRNA is in turn limited by the transient nature of its effect and its immunogenic properties, leading to mRNA degradation and further reduction of the therapeutic protein expression levels.[11] However, this immunogenic potential is considered advantageous in the context of the abovementioned vaccination strategies.[11] Similar to siRNA delivery, mRNA delivery is severely hampered by entrapment in the endo-lysosomes. Hence, to apply the lysosomes as a depot for mRNA release (Figure 3.13C) could be a major advantage to tackle the transient nature of the mRNA effect and gain control over therapeutic protein levels.

The nanogels (NG) applied in **Chapter 3** are polymeric nanocarriers. A second prominent group comprises lipid-based nanocarriers (**Chapter 1**). Such lipid nanoparticles (LNP) generally consist of amphiphilic lipids, which arrange in micellar or lamellar structures in a hydrophilic milieu. Cationic lipids are additionally included to ensure NA complexation, whereas neutral helper lipids may enhance the LNP rigidity (e.g. cholesterol) or improve the endosomal escape efficiency (e.g. 1,2-dioleoyl-*sn*-glycero-3-phosphoethanolamine, DOPE). The LNPs are believed to promote NA endosomal escape through fusion events with the endo-lysosomal membrane. Although fusogenic lipids may stimulate fusion events, a large fraction of the internalized NA dose fails to reach its intracellular target site and remains entrapped in the late endo-lysosomal compartment.[12, 13] Thus, we assessed whether a sequential CAD treatment could improve the siRNA delivery potential of several lipid-based formulations. Furthermore, we evaluated if a CAD could be included as a liposomal building block to improve siRNA delivery.

2. MATERIALS & METHODS

2.1. Nucleic acids

We applied the scrambled control siRNA (siCTRL), eGFP-targeting siRNA (sieGFP), nuclease-stabilized and Cy-5-labeled duplexes as described in **Chapter 3** (Table 3.1). Furthermore, cells were transfected with nuclease-stabilized siRNA covalently linked to cholesterol (Dharmacon, USA) (Table 4.1). In a final set of experiments, eGFP-expressing mRNA was applied. The latter was produced by *in vitro* transcription from the T7 promoter-containing pGEM4Z-GFP-64A plasmid, which was purified and linearized using respectively the QIAquick PCR purification kit (Qiagen, The Netherlands) and Spe I restriction enzymes (Promega, The Netherlands). The linearized plasmid subsequently served as a template for the *in vitro* transcription reaction carried out with the T7 mMessage mMachine kit (Ambion, Belgium), which additionally capped and polyadenylated the mRNA. The obtained mRNA was purified with the RNeasy Mini Kit (Qiagen, Netherlands) and the mRNA concentration and purity were determined by respectively measuring the absorbance at 260 nm and the 260/280 nm absorbance ratio with the NanoDrop 2000c spectrophotometer (Thermo Scientific, USA).

Table 4.1. Applied siRNA sequences and duplex modifications.

siRNA	Modification	Manufacturer	Sequence[a]	
			Sense strand (5' -> 3')	Antisense strand (5' -> 3')
chol-siCTRL	Cholesteryl[a] / Stabilized[b]	Dharmacon	Not provided	Not provided
chol-sieGFP	Cholesteryl[a] / Stabilized[b]	Dharmacon	CAAGCUGACCCUGAAGUUCUU	GAACUUCAGGGUCAGCUUGUU

[a] 5' end of the sense strand modified with a cholesteryl-tetraethyleneglycol linker; [b] siSTABLE RNA strand modification by Dharmacon for use in nuclease-rich environments.

2.2. NG synthesis and complexation

Cationic dextran nanogel (NG) synthesis occurred through an inverse mini-emulsion photopolymerization method.[14, 15] Actual complexation to siRNA-loaded NGs (siNGs) occurred according to the procedure described in **Chapter 3** (section 2.2). In case of complexation with mRNA, 100 µL of a 0.6 mg/mL NG dispersion was added to 100 µL of an appropriate mRNA dilution. Following 15 minutes of complexation at room temperature, 800 µL Opti-MEM was added and 300 µL of the dispersion was brought onto the cells. The mRNA concentrations per well were 0.1; 0.25 and 0.5 µg mRNA.

2.3. Liposome preparation and complexation

Various liposomes (LPS) were prepared *via* the lipid film hydration method. All lipids were obtained from Avanti Polar Lipids (USA) as solutions in chloroform. First, we prepared (2,3-dioleoyloxy-propyl)-trimethylammonium (DOTAP)–cholesterol LPS by mixing appropriate volumes of the lipid solutions in a round bottom flask to obtain a 1:1 mass ratio. Through rotary evaporation under vacuum at 40°C, a lipid film was created and subsequently hydrated using 1 mL HEPES buffer (pH 7.4, 20 mM). The obtained mixture was vortexed and sonicated 1 minute at 10% amplitude to obtain a monodisperse 2 mg/mL LPS dispersion. A similar protocol was applied to prepare DOTAP-DOPE (1,2-dioleoyl-*sn*-glycero-3-phosphoethanolamine) LPS in a 1:1 molar ratio. Finally, we prepared DOPE-nortriptyline (NT) LPS with a 1:1 mass ratio. Hereto, a 1 mg DOPE lipid film was hydrated with a 1 mg/mL NT solution in HEPES buffer to prepare a 2 mg/mL LPS dispersion.

The LPS were complexed with siRNA immediately before the transfection. Hereto, appropriate dilutions of the LPS in HEPES buffer were added to a propper siRNA dilution. This mixture was allowed to complex at room temperature for 30 minutes prior to further dilution in Opti-MEM and transfection. In case of DOTAP-chol LPS, cells were transfected with a 5 or 10 µg/mL LPS dispersion respectively carrying 2.5 and 5 nM siRNA. 10 and 20 µg/mL DOPE-NT LPS were applied to transfect the cells with 12.5 and 25 nM siRNA, respectively. Finally DOTAP-DOPE LPS were complexated with siRNA at a charge ratio equal to 8 and the applied siRNA concentrations per well were 0.1; 0.5; 1; 5 and 10 nM.

2.4. Complexation of commercial carriers

Both Lipofectamine® MessengerMAX and RNAiMAX (Invitrogen, Belgium) were applied according to the manufacturers guidelines. Equal volumes mRNA or siRNA dilutions and MessengerMAX or RNAiMAX dispersions, respectively, were mixed and allowed to complexate during 5 minutes at room temperature. Subsequently, the obtained lipoplexes (LPX) were added to the appointed wells, whereupon transfection occurred in Opti-MEM. According to the guidelines, 0.5 µg mRNA and 5 pmol siRNA were applied per well to obtain optimal protein expression and gene silencing, respectively. To mimic the siRNA concentration applied for a suboptimal siNG transfection, the RNAiMAX LPX were additionally diluted, to allow a more straightforward comparison of both transfection methods (Table 4.2).

Table 4.2. Applied siRNA concentration in terms of nM siRNA/30 µg/mL NGs or pmol siRNA/well.

nM siRNA/30 µg/mL NGs	pmol siRNA/well
2	0.6
16.7	5

2.5. Dynamic Light Scattering and zeta-potential

A Zetasizer Nano ZS (Malvern), equipped with Dispersion Technology Software, was applied to perform dynamic light scattering and ζ-potential measurements to determine the hydrodynamic size and surface charge of the nanocarriers before and after complexation. Appropriate dilutions of the carrier or complexes were prepared in HEPES buffer (20 mM, pH 7.4) right before the measurement.

2.6. Gel retention assay

The The capacity of the NGs to complex mRNA was evaluated through a gel retention assay using a 1.5% agarose (Invitrogen, Belgium) gel containing gelred (1/1000, Biotium, USA) for mRNA visualization. The gel was prepared in TBE buffer (10.8 g/L Tris base, 5.5 g/L boric acid, 0.74 g/L Na2EDTA.2H2O). Next, increasing amounts of mRNA were allowed to complex with a fixed NG concentration. Subsequently, a gel loading solution (Ambion, Belgium) was added to each sample prior to transfer to the gel well. Finally, electrophoresis was performed at 100 V during 40 minutes, followed by UV transillumination and gel photography.

2.7. Cell culture

SiRNA- mediated gene silencing was evaluated in the H1299-eGFP cell line whereas the wild type variant (H1299-WT) was applied for microscopy experiments and to investigate mRNA expression. Both cell lines were cultured as described in **Chapter 3** (Section 2.3). Cells were seeded in 24 well plates at a density of 35000 cells/well for uptake and gene silencing or protein expression experiments. For the phospholipidosis detection with confocal microscopy, we seeded the H1299-WT cells in glass bottom 35 mm diameter microscopy dishes (Greiner Bio-One GmbH, Germany) at 105000 cells per dish.

2.8. Transfection and adjuvant treatment

The transfection protocol described in **Chapter 3** (section 2.4) was applied for all carrier and nucleic acid combinations, whereupon an adjuvant treatment was executed according to experimental needs. In case of desloratadine (DL), 0.5 mL cell medium containing 10, 20 or 40 µM was applied. 40 µM chloroquine (CLQ) and nortriptyline (NT) were respectively tested in combination with chol-siRNA and mRNA-NGs or messengerMAX. Tobramycin (TM) was tested as an adjuvant to siNG delivery in the following concentrations: 100 and 500 µM, 1, 2, 3 and 4 mM. In a similar setup disulfiram (DSF) was added either alone (5, 10, 25 or 50 µM) or in combination with $ZnCl_2$: 5 and 10 µM DSF were combined with 5 µM $ZnCl_2$, and 25 and 50 µM DSF were combined with 10 µM $ZnCl_2$. Finally, we tested the combination of 25µM DSF with 20 µM DL and 10 µM $ZnCl_2$. All small molecules (Figure 4.1) were obtained from Sigma-Aldrich (Belgium) and the stock solutions were prepared in sterile-filtered BioPerformance Certified dimethyl sulfoxide (DMSO, Sigma-Aldrich, Belgium), except for $ZnCl_2$, which was dissolved in sterile water. Most adjuvant treatments lasted 20 hours, except for the combination of mRNA-NGs and DOTAP-DOPE LPS with NT and DL, respectively, where a 2-hour incubation time was applied.

	TOBRAMYCIN	DISULFIRAM	DESLORATADINE	CHLOROQUINE	NORTRIPTYLINE
Drug class	Antibiotic	Alcohol deterrent	Antihistamine	Antimalarial	Antidepressant
logP	-5.8	3.88	3.97	4.63	4.51
pKa	9.83	/	9.73	10.10	10.10

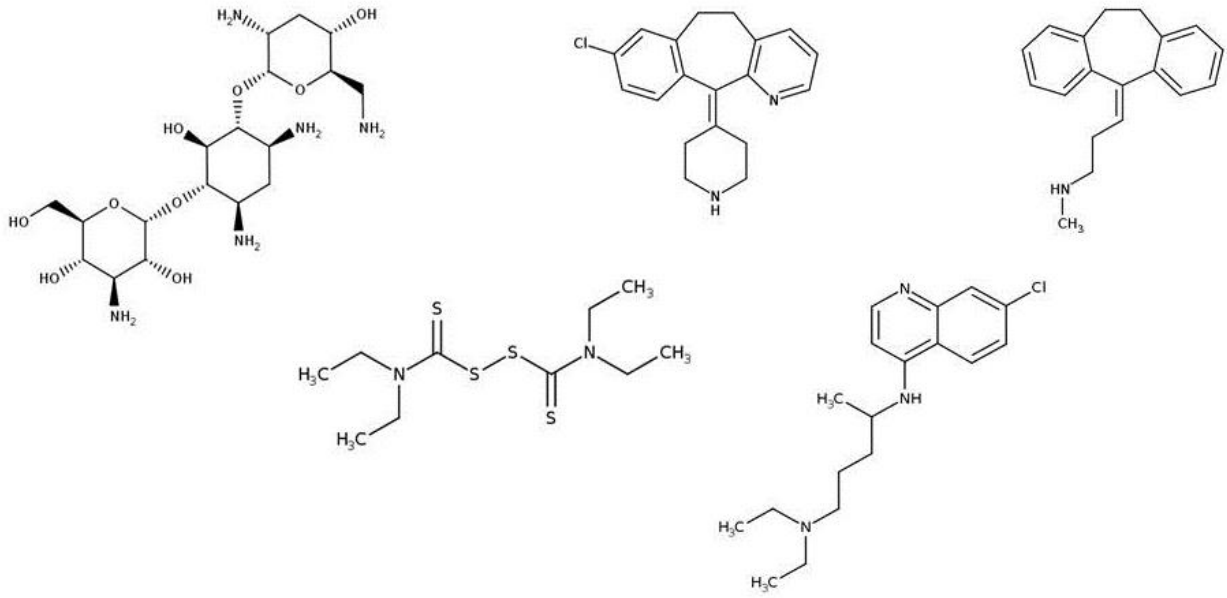

Figure 4.1. The drug class, logP, pKa and molecular structures of tobramycin, disulfiram, desloratadine, chloroquine and nortriptyline.[15]

2.9. Quantifying nanocarrier uptake

To allow fluorescent detection of nanocarrier uptake, 10% of the siCTRL duplex was replaced by Cy5-labeled siCTRL. Subsequent to 4 hours of transfection, the cells were washed with PBS containing 0.1 mg/mL dextran sulphate sodium salt (Sigma-Aldrich, Belgium) to remove the surface-bound siRNA and allow detection of the effectively internalized siNGs. Next, the cells were detached using 0.25% trypsin-EDTA, collected in flow tubes and centrifuged 5 minutes at 300g. Finally, the cell pellet was suspended in 300 µL FACS buffer and samples were kept on ice until analysis. The latter occurred with a FACSCalibur™ flow cytometer (BD Biosciences, Belgium) and BD CellQuest™ acquisition software, collecting 10000 events per sample. The Cy5-labelled siRNA was exited using the red laser line and the fluorescent signal was detected with the 661 nm ± 16 filter. Finally, data analysis was performed using the FlowJo software (Tree Star Inc.), where both the percentage of cells showing carrier uptake as well as their mean fluorescent intensity (MFI) were determined.

2.10. Evaluation of the transfection efficiency

SiRNA-mediated gene silencing and mRNA (eGFP) expression were both evaluated using the FACSCalibur™ flow cytometer as described in **Chapter 3** (section 2.5). Through data analysis we determined the percentage eGFP expression in case of siRNA-mediated gene silencing or both the percentage of cells expressing eGFP and their MFI following mRNA transfection.

2.11. Phospholipidosis detection

To allow labeling of the phospholipids in the H1299-WT cells, the latter were co-exposed to the small molecular adjuvant and a 1/1000 dilution of the LipidTOX™ red phospholipidosis detection reagent (Thermo Fisher Scientific, USA) in complete cell medium. The samples were fixed, covered in Vectashield antifade mounting medium containing DAPI (Vector Laboratories, USA) and imaged as detailed in **Chapter 3** (section 2.10).

2.12. Statistics

Size and ζ-potential data are represented as the mean ± the standard deviation (SD) of three measurements. Flow cytometry results are represented as the mean ± the standard error to the mean (SEM). Statistical analysis was performed with the 6th version of the GraphPad Prism software using one-way ANOVA combined with the post-hoc Dunnett test to compare multiple groups.

3. RESULTS

3.1. Distinct small molecular adjuvants do not equally improve siRNA delivery

3.1.1. Tobramycin

By sequentially applying tobramycin (TM), a phospholipidosis (PLD)-inducer but no a cationic amphiphilic drug (CAD), we assessed whether the induction of a PLD phenotype is sufficient to improve siRNA-mediated gene silencing. Figure 4.2A shows that TM had no effect on the siRNA-mediated gene silencing by siRNA-loaded NGs (siNGs) in H1299-eGFP cells. Even the highest TM concentrations, known to induce PLD, remained without an adjuvant effect. In contrast, TM concentrations >1 mM significantly elevated the side scatter (SSC) signal with respect to the siNG-transfected cells (Figure 4.2B), indicative of increased cell granularity. The extent of the augmentation could however not be compared to the prominent increase observed upon CAD treatment (Figure 3.9A). Figure 4.2C reveals the accumulation of phospholipids for the highest dose tested. Opposed to earlier observations in CAD-treated cells (Figure 3.10A), were the accumulated phospholipids to a large extent located in the plasma membrane and the vesicular structures did not appear as enlarged or numerous.

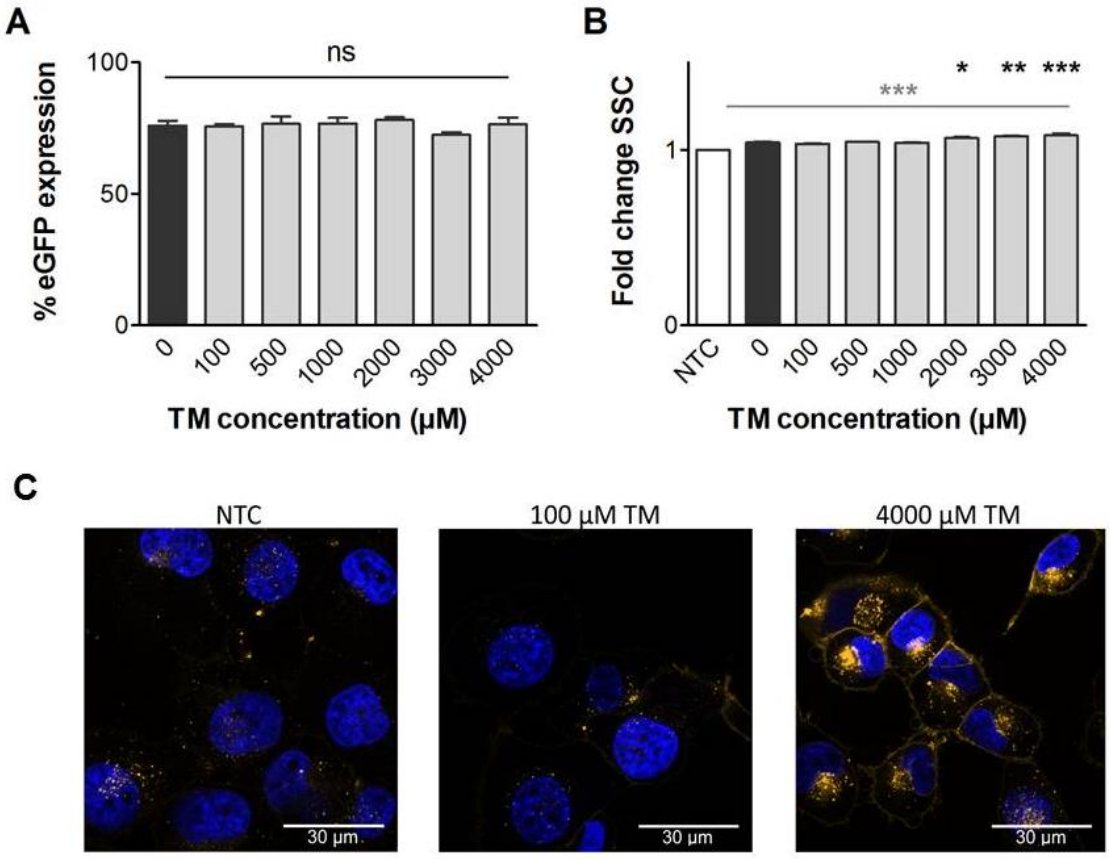

*Figure 4.2. (A) % eGFP expression in H1299-eGFP cells following siNG transfection alone or combined with a 20h tobramycin (TM) adjuvant treatment. (B) Fold change in the side scatter (SSC) signal upon siNG transfection whether or not combined with TM. Data are represented as the mean ± SEM for 3 technical replicates. Statistical significance is represented with reference to the untreated control (NTC) by the grey * or with respect to the siNG transfected cells by the black *. (ns = not significant, * p < 0.05, ** p < 0.01, *** p < 0.005). (C) Representative confocal images of the phospholipid distribution visualized with the LipidTOX™ Red phospholipidosis detection reagent for untreated cells and cells treated 20 hours with 100 or 4000 µM TM. The scale bar corresponds to 30 µm.*

3.1.2. Disulfiram

Next, we evaluated whether disulfiram (DSF) could potentiate siRNA delivery in cancer cells. Figure 4.3A shows that a 20h DSF treatment significantly improved siRNA-mediated gene silencing for all DSF concentrations tested. However, the extent of the effect was limited, with ˜45% eGFP expression remaining at 50 µM DSF, versus almost complete eGFP silencing with 40 µM desloratadine (DL) (Figure 3.4C). The reduced eGFP expression at 50 µM DSF was furthermore accompanied by cell stress, as suggested by the increased mean fluorescent intensity (MFI) in the cells transfected with a control siRNA duplex (siCTRL) (Figure 4.3B). Concurrently, only the highest DSF dose induced a significant increase in the SSC signal with respect to the siNG transfected cells (Figure 4.3C).

DSF is show to induce apoptosis in cancer cells due to its ionophore activity.[7] This DSF-induced apoptosis coincides with cytosolic cathepsin presense, wherefore DFS is suggested to induce lysosomal cell death.[6] The propensity of DSF to evoke cancer cell death is indeed correlated to the Zn^{2+} concentration in the extracellular milieu, as an increased number of apoptotic cells were detected when supplementing the cell culture medium with 20 µM Zn^{2+}.[7] Since our objective is to destabilize the lysosomes to allow siRNA release without evoking severe cell stress, we applied the combination of 5 or 10 µM DSF with 5 µM $ZnCl_2$. However, no significant differences were detected in gene silencing as a function of $ZnCl_2$ supplementation (Figure 4.3D). Next, we combined higher DSF doses (25 or 50 µM) with 10 µM $ZnCl_2$. Figure 4.3E shows the MFI of H1299-eGFP cells transfected with siCTRL (black) or eGFP-targeting siRNA (sieGFP, white) for the different adjuvant combinations. For 25 µM DSF, the MFI in the sieGFP sample additionally decreased upon co-incubation with 10 µM $ZnCl_2$, indicative of enhanced silencing. This coincided with cell stress, as evidenced by the increased MFI in the concurrent siCTRL sample. Both siCTRL and sieGFP transfected cells

treated with the combination of 50 µM DSF and 10 µM $ZnCl_2$ in turn showed a pronounced drop in eGFP expession levels, indicative of severe cell stress and cell death.

Finally, we evaluated the combination of DSF and desloratadine (DL). Given the different mechanism through which LMP is induced, an additive or even synergistic destabilising effect on the lysosomal membrane was anticipated. However, similar eGFP expression levels were observed in the 20 µM DL and 25 µM DSF + 20 µM DL sample (Figure 4.3F), implying that supplementing DL with DSF was not of added value. In contrast, when 10 µM $ZnCl_2$ was additionally applied, a strong cytotoxic response was noted similar to the combination of 50 µM DSF and 10 µM $ZnCl_2$.

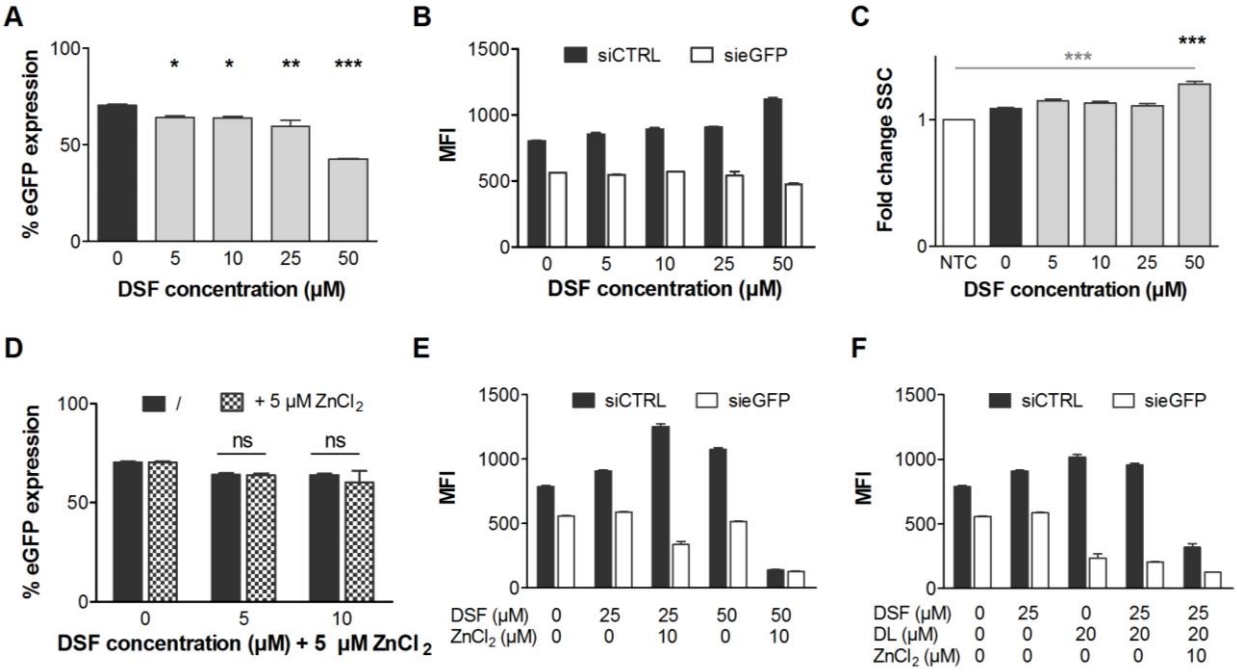

*Figure 4.3. (A) % eGFP expression in H1299 cells upon siNG transfection whether or not combined with mounting disulfiram (DSF) concentrations for 20 hours. (B) Representative plot of the mean eGFP fluorescence intensities (MFI) of cells treated with NGs loaded with siCTRL (black bars) or siEGFP (white bars) as a function of the DSF concentration. (C) Fold change in the side scatter (SSC) signal as a function of the applied DSF concentration additive to siNG transfection. The fold change was calculated relative to the untreated control (NTC). (D) % eGFP expression for cells transfected with siNGs followed by exposure to to DSF alone (black bars) or DSF in combination with 5 µM $ZnCl_2$ (blocked bars). (E) A representative MFI plot for siNG transfected cells with siCTRL (black) or sieGFP (white) followed by 25 or 50 µM DSF alone or in combination with 10 µM $ZnCl_2$. (F) A representative MFI plot for siCTRL-NGs (black) or siEGFP-NGs (white) transfected cells exposed to different combinations of 25 µM DSF, 20 µM desloratadine (DL) and 10 µM $ZnCl_2$. (A), (C) and (D) Data are represented as the mean ± SEM for 3 technical replicates in a single biological replicate. Statistical significance is represented by grey * with reference to the untreated control (NTC) or by black * with respect to the siNG transfected cells. (ns not significant, * $p < 0.05$, ** $p < 0.01$, *** $p < 0.005$).*

3.2. The therapeutic potential of mRNA is not strongly enhanced by CADs

Next, we evaluated whether CADs could improve the therapeutic effect of larger mRNA molecules (˜ 1000 bases, as determined with agarose gel electrophoresis) upon mRNA-NG transfection. First, we showed that the NGs completely complexed the mRNA in all evaluated ratios (Figure 4.4A). The size and ζ-potential furthermore remained unaltered upon complexation (Table 4.3).

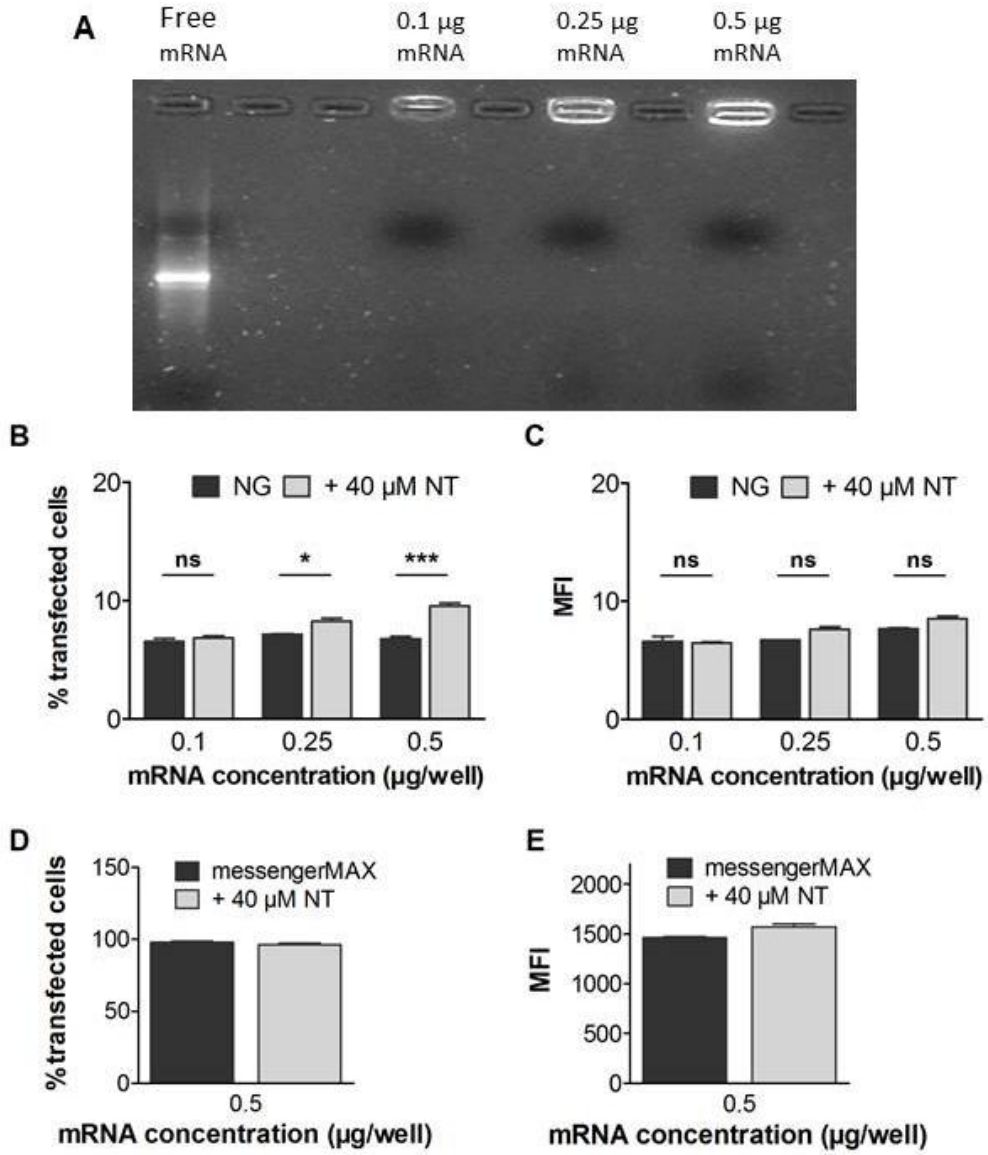

*Figure 4.4. (A) NGs completely complex 0.1, 0.25 and 0.5 µg mRNA as evaluated with an agarose gel retention assay. (B) and (C) The transfection efficiency in terms of the percentage of transfected H1299 cells (B) and the eGFP mean fluorescent intensity (MFI) of the transfected cells (C) for mRNA-NG transfected cells alone (black bars) or combined with a 20h 40 µM nortriptyline (NT) treatment (grey bars). (D) and (E) The transfection efficiency in terms of the percentage of transfected cells (D) and the eGFP MFI (E) of cells transfected with messengerMAX (black bars) with or without 40 µM NT (grey bars). The data are represented as the mean ± SEM for 3 technical replicates. Statistical significance is indicated when appropriate. (ns = not significant, * p < 0.05, *** p < 0.005).*

Table 4.3. The hydrodynamic size (nm) and surface charge (mV) of NGs in HEPES buffer before and after complexation with mRNA.

	Size (nm)	PDI	ζ-potential (mV)
NG	196.2 ± 1.2	0.133	23.2 ± 0.1
NG + 0.1 µg mRNA	196.7 ± 0.8	0.167	22.7 ± 0.8
NG + 0.25 µg mRNA	195.5 ± 0.7	0.133	22.3 ± 0.7
NG + 0.5 µg mRNA	195.7 ± 2.4	0.171	22.9 ± 0.6

Subsequently, we evaluated the transfection efficiency of the mRNA-NGs in terms of the number of transfected cells as well as the eGFP expression levels (Figure 4.4B and 4.4C). Overall, a low number of cells was successfully transfected by the mRNA-NGs, as values no higher than ˜ 6% were obtained for each mRNA concentration. An adjuvant treatment with 40 µM nortriptyline (NT) induced a significant, though only minor augmentation of the percentage of transfected cells (up to ˜ 10%). Concurrently, protein expression remained low and was not significantly elevated by 40 µM NT.

The mRNA-NG transfection was additionally compared to the commercial gold standard for mRNA transfections, i.e. messengerMAX™. When the latter was applied according to the manufacturers' guidelines, the entire cell population was successfully transfected and high protein expression levels were observed (Figure 4.4D and 4.4E). A NT adjuvant treatment did neither alter the percentage of transfected cells nor the eGFP expression levels.

3.3. Lipid-based transfection methods are less prone to the CAD adjuvant effect

3.3.1. Cholesterol-siRNA

One strategy to circumvent the necessity of a carrier for the systemic administration of siRNA is the use of cholesterol-siRNA (chol-siRNA) conjugates. Here, cholesterol facilitates siRNA transport across the cell membrane and protects the siRNA against nuclease-mediated degradation.[17, 18] Figure 4.5A shows that the intrinsic silencing potential of the chol-siRNA was low, with less than 10% eGFP silencing at 100 nM chol-siRNA. The application of 40 µM desloratadine (DL) or chloroquine (CLQ) had little impact on the transfection efficiency (Figure 4.5A), despite the clear increase of the SSC signal (Figure 4.5B), indicating succesful induction of the lysosomal storage disorder phenotype.

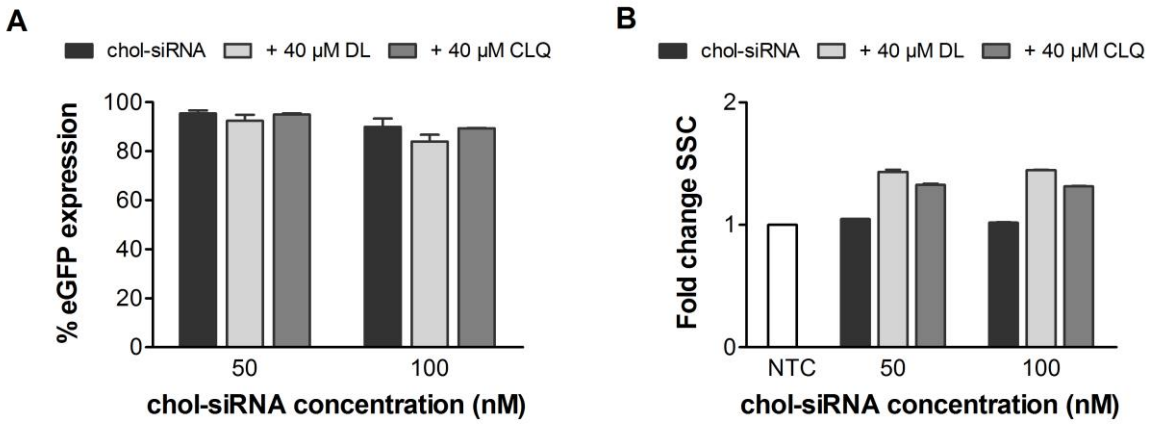

Figure 4.5. The percentage eGFP expression (A) and fold change in side scatter (SSC) signal relative to the untreated control (B) upon transfection with 50 or 100 nM chol-siRNA alone (black bars) or in combination with 40 µM desloratadine (DL, light grey bars) or chloroquine (CLQ, dark grey bars). Data are represented as the mean ± SEM for 3 technical replicates. (NTC = untreated control)

3.3.2. DOTAP-cholesterol liposomes

Next, we evaluated the potency of CADs to boost DOTAP-cholesterol liposome (LPS)-mediated siRNA delivery. At the applied charge ratio, all siRNA is complexed by the LPS.[19] DLS measurements furthermore revealed desirable lipoplex characteristics, namely a hydrodynamic size of ~100 nm and a positive surface charge to stimulate internalization through interaction with the negatively charged cell surface (Table 4.4).

Table 4.4. The hydrodynamic size (nm) and surface charge (mV) of DOTAP-chol LPS in HEPES buffer before and after siRNA complexation.

	Size (nm)	PDI	ζ-potential (mV)
DOTAP-chol	119.8 ± 1.0	0.295	58.5 ± 0.9
DOTAP-chol + siRNA	116.8 ± 0.1	0.293	57.9 ± 2.9

Similar to experiments by Dakwar *et al.*, the transfection efficiency of the DOTAP-chol LPS was evaluated in both Opti-MEM and serum containing cell medium (i.e. full medium).[20] Figure 4.6A and 4.6E indicate that the entire cell population internalized the DOTAP-chol LPS irrespective of the applied transfection medium. However, the extent of LPS uptake increased for the higher LPS concentration upon transfection in full medium, whereas the uptake did not vary between both LPS concentrations in Opti-MEM (Figure 4.6B and 4.6F).

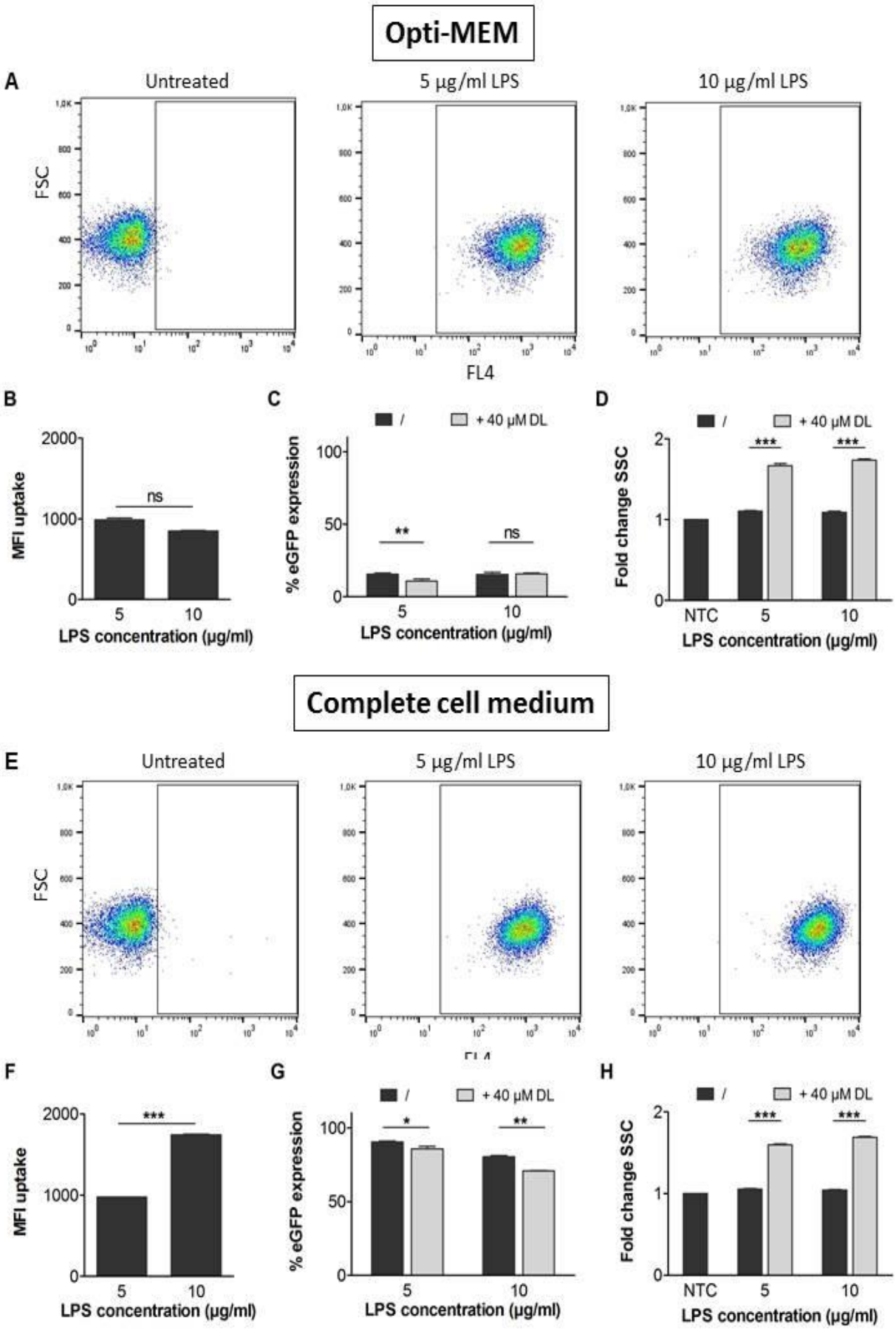
Opti-MEM
A
Untreated
5 µg/ml LPS
10 µg/ml LPS
FSC
FL4
B
MFI uptake
ns
LPS concentration (µg/ml)
C
/
+ 40 µM DL
% eGFP expression
**
ns
LPS concentration (µg/ml)
D
/
+ 40 µM DL
Fold change SSC
***
***
NTC
LPS concentration (µg/ml)
Complete cell medium
E
Untreated
5 µg/ml LPS
10 µg/ml LPS
FSC
F
MFI uptake
***
LPS concentration (µg/ml)
G
/
+ 40 µM DL
% eGFP expression
*
**
LPS concentration (µg/ml)
H
/
+ 40 µM DL
Fold change SSC
***
***
NTC
LPS concentration (µg/ml)

*Figure 4.6. (A) and (E) Representative of scatter plots showing the forward scatter (FSC) as a function of the FL4 signal indicating LPS uptake in the entire cell population in Opti-MEM (A) and serum containing cell medium (E). (B) & (F) Mean fluorescent intensity (MFI) of the Cy5-labeled siRNA upon LPS uptake as a function of the LPS concentration (µg/mL) for cells transfected in Opti-MEM (B) or complete cell medium (F). (C) & (G) % remnant eGFP expression as a function of the LPS concentration upon transfection with LPS alone (black bars) or combined with 40 µM desloratadine (DL) (grey bars) with the transfection performed in Opti-MEM (C) or complete cell medium (G). (D) & (H) Fold chance in the side scatter (SSC) signal relative to the untreated control as a function of the LPS concentration with (grey bars) or without (black bars) 40 µM desloratadine (DL) adjuvant treatment with the transfection performed in Opti-MEM (D) or full medium (H). Data are represented as the mean ± SEM for 3 technical repeats and statistical significance is indicated when appropriate. (ns = not significant, * p < 0.05, ** p < 0.01, *** p < 0.005)*

Following transfection in Opti-MEM, nearly maximal eGFP gene silencing was obtained for 5 and 10 µg LPS/mL, repsectively carrying 2.5 and 5 nM siRNA (Figure 4.6C). Interestingly, despite similar or even improved uptake of the highest LPS dose in full medium, the transfection efficiency was significantly lower with only ˜10% and ˜15% eGFP silencing for respectively 5 µg and 10 µg LPS/mL (Figure 4.6G). 40 µM DL caused a slight, though significant additional reduction in eGFP expression for 5 µg LPS/mL in Opti-MEM (Figure 4.6C), while this effect was not observed for the highest LPS concentration in Opti-MEM, despite the clear increase in the SSC signal (Figure 4.6C and 4.6D). However, the near optimal results of the LPS transfection alone did not allow much room for improvement. Here, the suboptimal transfection in full medium was significantly enhanced (Figure 4.6G), concurrent to the increased SSC signal (Figure 4.6H).

To exclude potential effects of lysosomal siRNA degradation following LPS-mediated delivery, this set of experiments was repeated for DOTAP-chol LPS loaded with nuclease-stabilized siRNA (siSTABLE). The LPS showed similar uptake behavior in Opti-MEM and full medium irrespective of the applied siRNA (data not shown). The transfection of siSTABLE-LPS was slightly less efficient compared to LPS encapsulating unmodified siRNA in both transfection media (Figure 4.7). Overall the adjuvant treatment had no or only a minor effect on the transfection efficiency. Overall, the slight improvement in siRNA delivery obtained for the DOTAP-chol LPS as a result of DL treatment is by no means comparable to the vast effect observed for the siNGs.

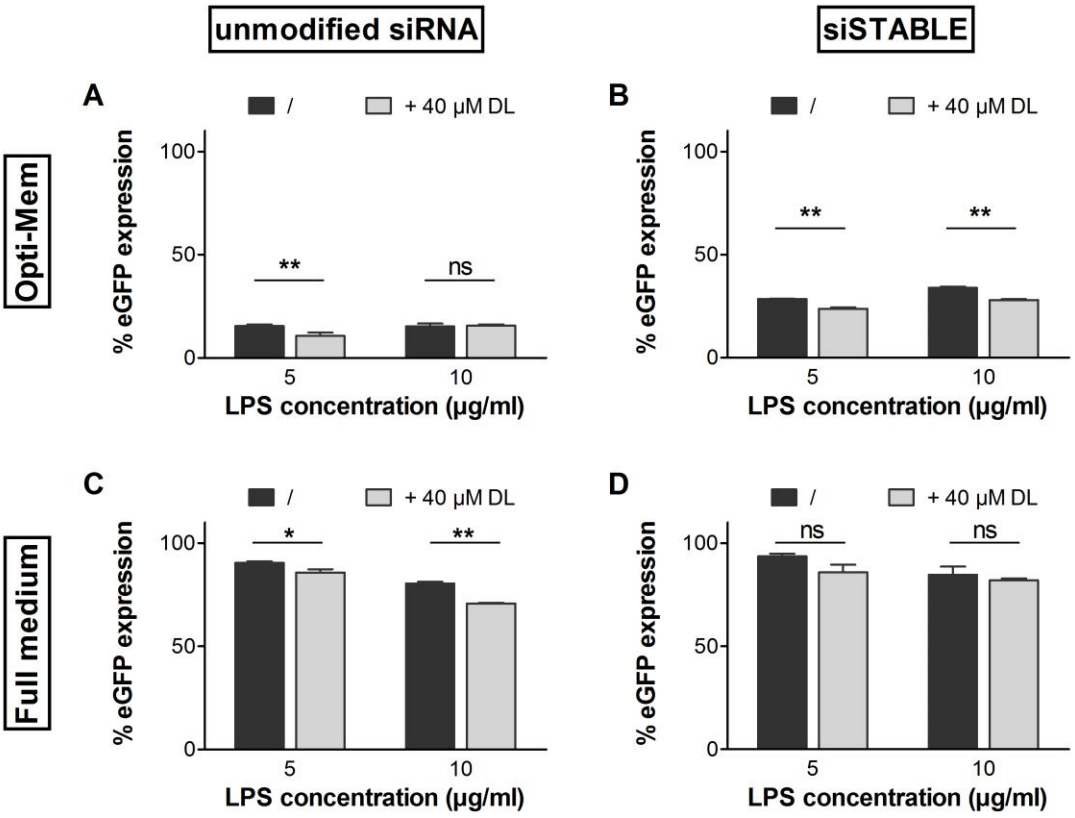

*Figure 4.7. % GFP expression as a function of the LPS concentration following DOTAP-cholesterol LPS transfection in Opti-MEM (A) and (B) or full medium (C) and (D) with LPS loaded with unmodified siRNA (A) & (C) or siSTABLE (B) & (D). Graphs show the transfection efficiency of the LPS alone (black bars) or combined with 40 µM desloratadine (DL, grey bars). Data are represented as the mean ± SEM for 3 technical replicates and statistical significance is indicated when appropriate. (ns = not significant, * p < 0.05, ** p < 0.01)*

3.3.3. DOTAP-DOPE liposomes

Besides DOTAP-chol LPS, we evaluated DOTAP-DOPE LPS, in which the fusogenic helper lipid DOPE replaces the stabilizing cholesterol. Again, previous data from our group demonstrated that the LPS show complete siRNA complexation at a charge ratio (+/-) of 8.[21] DLS measurements indicate that complexes a hydrodynamic size of ˜100 nm and a strong positive surface charge of ˜60 mV were obtained.

Figure 4.8A and 4.8B respectively show the LPS uptake in terms of the percentage of positive cells and the silencing potential of DOTAP-DOPE LPS as a function of the siRNA concentration. 1 nM siRNA was selected for further testing, given its uptake in nearly 100% of the cells and its suboptimal silencing potential (˜20%). When we subsquently combined the DOTAP-DOPE LPS with a 10, 20 or 40 µM DL, no significant improvement of the eGFP silencing potential could be detected (Figure 4.8C).

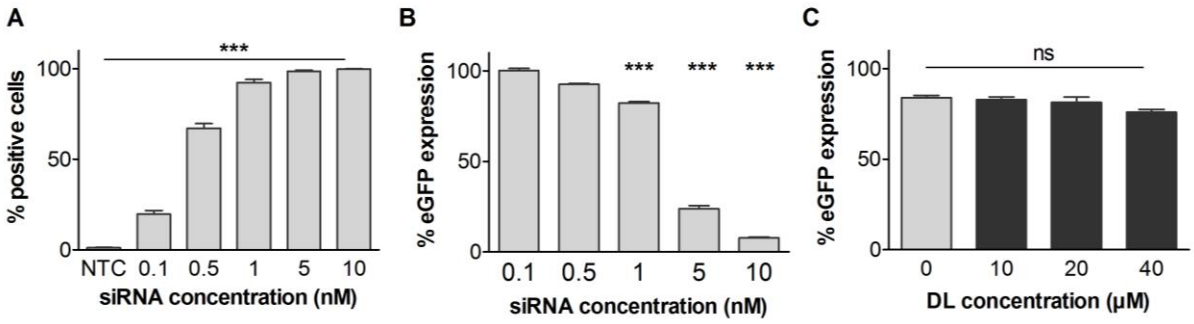

*Figure 4.8. (A) Uptake of siRNA-loaded DOTAP-DOPE LPS in terms of the percentage of positive cells. (B) The transfection efficiency of DOTAP-DOPE LPS as a function of the applied siRNA concentration. (C) The influence of 20 hours adjuvant treatment with 10, 20 or 40 μM desloratadine (DL) on the transfection efficiency of suboptimal siRNA-loaded DOTAP-DOPE LPS. Data are represented as the mean ± SEM for 3 technical replicates and statistical significance is indicated when appropriate. (ns not significant, *** $p < 0.005$)*

3.3.4. DOPE-nortriptyline liposomes

A potential disadvantage of the proposed CAD adjuvant strategy is the need for relatively high CAD doses. Hence, we explored the potential of introducing a CAD adjuvant as a building block of the nanocarrier by combining NT and DOPE. Interestingly, DLS data indicate liposome formation (Table 4.5), although the inclusion of NT into the LPS was not further verified.

Table 4.5. The hydrodynamic size (nm) and surface charge (mV) of DOPE-NT LPS in HEPES buffer before and after siRNA complexation.

	Size (nm)	PDI	ζ-potential (mV)
DOPE-NT	105.5 ± 0.1	0.269	30.9 ± 0.8
DOPE-NT + siRNA	112.9 ± 1.0	0.184	30.7 ± 0.5

The The transfection efficiency of the DOPE-NT LPS was compared to the DOTAP-DOPE LPS. Both LPS were internalized by the entire cell population (Figure 4.9A), although the corresponding MFI was significantly higher for the DOTAP-DOPE LPS (Figure 4.9B). The DOPE-NT LPS evoked a concentration-dependent eGFP silencing, albeit to a lesser extent than the DOTAP-DOPE LPS (Figure 4.9C). However, the succesfull transfection by the DOPE-NT LPS was not accompanied by an elevation of the SSC signal as witnessed with free NT (Figure 4.9D, Figure 3.9A).

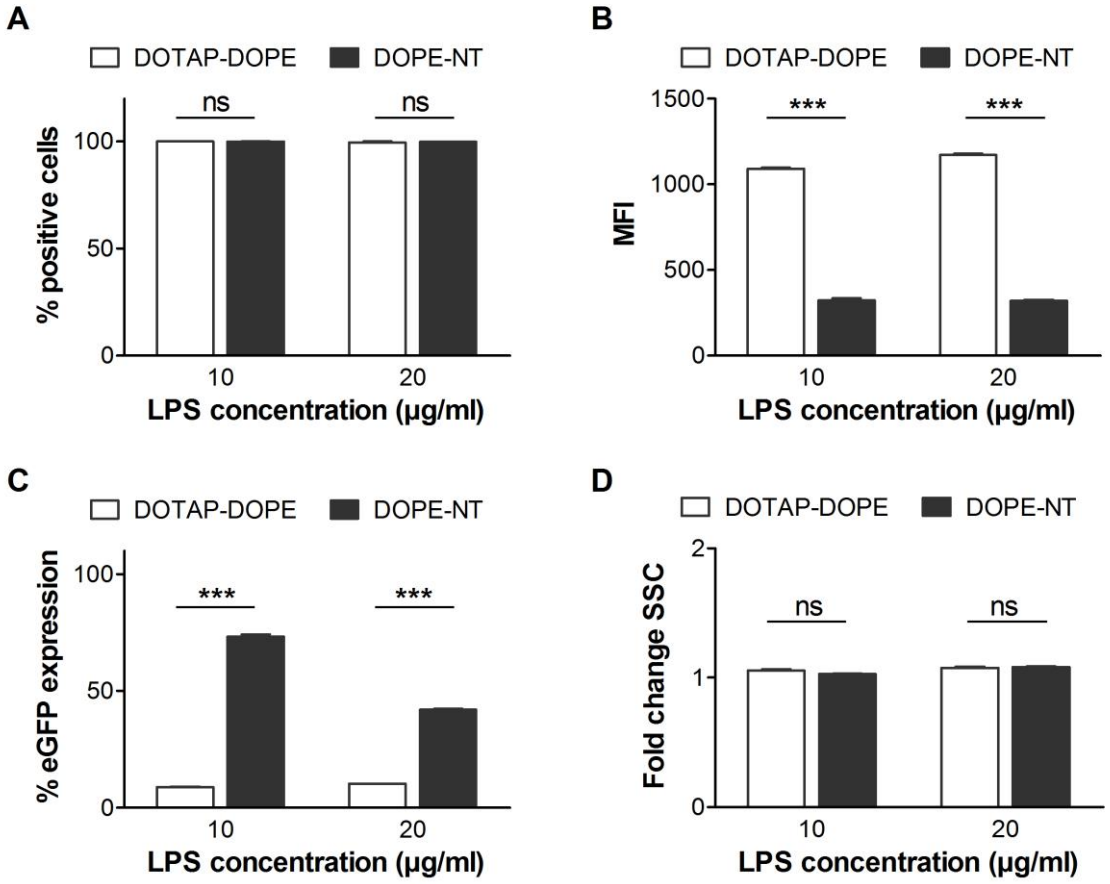

*Figure 4.9. (A) and (B) Uptake of DOTAP-DOPE (white bars) and DOPE-NT (black bars) LPS in terms of the percentage of positive cells (A) and the mean fluorescent intensity (MFI) of the positive cells (B). (C) The transfection efficiency in terms of the percentage eGFP expression in H1299-eGFP cells transfected with DOTAP-DOPE (white bars) and DOPE-NT (black bars) LPS, as a function of the applied LPS concentration. (D) The fold change of the side scatter (SSC) signal relative to the untreated control for cells transfected with DOTAP-DOPE (white bars) or DOPE-NT (black bars) LPS. Data are represented as the mean ± SEM for 3 technical replicates and statistical significance between DOTAP-DOPE or DOPE-NT LPS is indicated when appropriate. (ns = not significant, *** $p < 0.005$)*

3.3.5. Commercial lipofection reagent RNAiMAX

Finally, we evaluated the combination of DL and the commercial lipid-based carrier RNAiMAX, which is considered the gold standard for siRNA transfections. Two siRNA doses were applied, namely 0.6 and 5 pmol siRNA/well. Figure 4.10 shows nearly complete gene silencing at the highest dose tested whereas 0.6 pmol siRNA/well only reached up to ˜55% gene silencing. Similar to the results obtained with messengerMAX, 40 µM DL did not significantly improve the silencing potential of the lipoplexes.

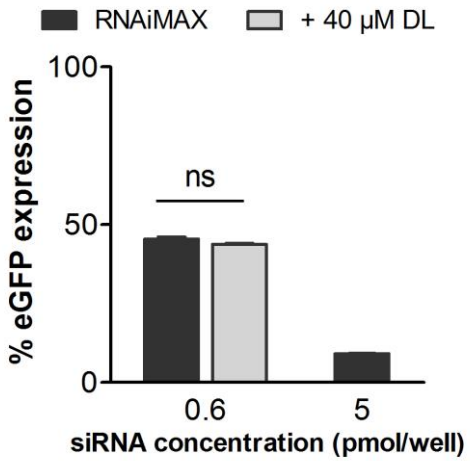

Figure 4.10. Percentage eGFP expression upon transfection with RNAiMAX as a function of the siRNA concentration per well for cells solely transfected with RNAiMAX (black bars) or combined with a 2-hour 40 µM desloratadine (DL) treatment (grey bar). Data are represented as the mean ± SEM for 3 technical replicates and statistical significance between RNAiMAX with and without adjuvant treatment is indicated when appropriate. (ns = not significant)

4. DISCUSSION

In **Chapter 3** we established that a sequential treatment with a cationic amphiphilic drug (CAD) improves siRNA-mediated gene silencing in NG transfected cells. Additionally, we showed that CADs induce a phospholipidosis (PLD) phenotype, with the accumulation of phospholipids, sphingomyelin and cholesterol, which is believed to destabilize the lysosomal membrane thereby allowing siRNA transfer the cytosol. Here, we evaluated the wider applicability of this method in terms of the small molecular adjuvant, the nucleic acid cargo and the nanocarrier. It must be noted that all experiments were performed in a single biological replicate with the graphs showing the mean ± the standard error to the mean of three technical replicates. Hence, data interpretation should occur with caution and the trends should ideally be confirmed by additional biological replicates.

4.1. Distinct small molecular adjuvants do not equally improve siRNA delivery

First, we evaluated tobramycin (TM) given its reported potential to induce phospholipidosis (PLD) in renal tubular cells *in vivo* without being a cationic amphiphilic drug (CAD). [5, 22] Despite the fact that TM contains various basic amines, with the strongest base being characterized by a pKa value of 9.83, TM cannot be classified as a CAD given its strong hydrophilic nature (logP = -5.8).[16] Consequently, TM cannot be considered to functionally inhibit acid sphingomyelinase (ASM, FIASMA), but induces PLD by binding phospholipids in the acidic environment of the late endosomes/lysosomes thereby preventing degradation by lysosomal phospholipases.[5, 23]

The induction of PLD with high TM doses could be visualized upon LipidTOX^{TM} red labeling (Figure 4.2C), in accordance to previous reports.[24] The high TM doses required to evoke this phenotype could be explained in terms of the less favorable physicochemical properties for cellular uptake through passive diffusion. Despite the induction of PLD, no concurrent improvement in siRNA-mediated gene silencing could be detected (Figure 4.2A). Of note, the deviating cellular distribution of the accumulated phospholipids could explain the differences in the extent of SSC increase for TM (Figure 4.2B) and DL (Figure 3.8A) and may potentially clarify the lack of adjuvant effect for TM.

These results suggest that accumulation of specific lipids is likely required to improve the potential of the siNGs. However, in order to draw a firm conclusion on the general

applicability of non-CAD PLD-inducers as small molecular adjuvants, additional compounds require evaluation. In any case would the adjuvant application of an antibiotic like TM be less advisable given the issue of antibiotic resistance. TM furthermore induces tissue specific PLD in renal tubular cells *in vivo*, which limits the general applicability, but may reduce off-target adverse events.[5]

Subsequently, we evaluated the adjuvant potential of the alcohol deterrent disulfiram (DSF). DSF is characterized by a high logP value (3.88), but does not contain a protonatable amine group.[16] Hence, it is neither a lysosomotropic compound nor a FIASMA.[2, 16] Interestingly, recent literature showed that DSF causes apoptosis combined with elevated cytosolic cathepsin levels, which strongly suggest the induction of lysosomal cell death through lysosomal membrane permeabilization (LMP). DSF indeed induced apoptotic cell death in many, but not all, cell and xenograft models tested and this effect is tightly connected to the availability of Zn^{2+}- or Cu^{2+}-ions.[6, 7, 25] By its ionophore activity, DSF transports these bivalent ions into the cell, leading to a sudden increase of the cellular Zn^{2+} or Cu^{2+} concentration. As a protective measure, the DSF-ion complexes are rapidly shuttled to the lysosomal compartment. Consequently, the proteasome is inhibited, which is suggested to affect the lysosomal function, thereby allowing cathepsin release and apoptosis induction.[26] In addition, the lysosomes are no longer confined to the perinuclear region.[6, 25] Overall, the DSF-mediated augmentation of the lysosomal Zn^{2+} or Cu^{2+} concentration is assumed to cause lysosomal dysfunction, potentially leading to LMP.[7, 26] Here, we evaluated whether this lysosome destabilizating capacity could be applied to our advantage to improve siRNA delivery in cancer cells.

Although DSF an sich significantly improved siRNA-mediated gene silencing (Figure 4.3A), the extent of the effect could not be compared to that of the initially evaluated FIASMAs (Figure 3.2). Since the DSF activity is related to the extracellular Zn^{2+} concentration, we combined both components. Where 5 µM Zn^{2+} failed to potentiate the effect of DSF (Figure 4.3D), 10 µM Zn^{2+} enhanced the adjuvant effect of 25 µM DSF (Figure 4.3E). In contrast, a strong cytotoxic response was noted with the combination of 50 µM DSF and 10 µM Zn^{2+} (Figure 4.3E). Although the effect on the lysosomal compartment was not experimentally explored, we hypothesize that this combinated perturber the lysosomes to such an extent that the potential adjuvant effect was overruled by cytotoxicity. Lysosomal cell death is of course a

desirable outcome in the light of an anti-cancer therapy. Hence, the strong cytotoxicity observed for the combination of DSF, DL and Zn^{2+} (Figure 4.3F) is a highly interesting observation since the cytotoxic effect of DSF could be potentiated by the relatively safe DL. Taken together, we can assume that not all lysosome perturbing compounds will be equally applicable as delivery enhancers given the disparity between efectuating siRNA release and inducing cytotoxicity.

4.2. The therapeutic potential of mRNA is not strongly enhanced by CADs

Secondly, we investigated whether mRNA expression could be by a sequential CAD treatment. To vary a single factor at a time, we applied the NGs as a delivery vehicle for the eGFP-encoding mRNA. Although the number of negative charges for mRNA largely exceeds that of siRNA (˜1000 for the applied mRNA molecules versus ˜42 for an siRNA duplex) the NG complexation capacity was not exceeded by the notably lower mRNA doses, which explains the observed complete complexation (Figure 4.4A).[14] However, only limited eGFP expression levels were obtained (Figure 4.4B and C) with the mRNA dose recommended for optimal transfection with messengerMAX (0.5 µg mRNA/well) with or without a sequential CAD treatment. Hence, we hypothesized that the mRNA may be less easily released from the NGs and/or the endosomes. Since it is assumed that only the free NA cargo transfers to the cytosol, the enhanced NA-carrier interaction may in turn explain the limited potentiating effect of the sequential CAD treatment. A second possible explanation for the limited transfection efficiency is that the mRNA molecule may be too large to cross the endo-lysosomal membrane. In corroboration, CADs were not able to significantly enhance mRNA expression upon transfection with messengerMAX.

These data suggest that our approach may not allow improved transfection of larger NA, leaving many questions unanswered on the level of the NA cargo. To firmly establish the adjuvant potential, we should evaluate the impact of NA dissociation from the carrier and the potential to improve the delivery of NA with distinct sizes and configurations.

4.3. Lipid-based transfection methods are less prone to the CAD adjuvant effect

In **Chapter 3** we applied a polymeric nanocarrier to achieve siRNA transfection. Here, we evaluated if our proposed CAD adjuvant method can be applied to additional transfection methods, such as siRNA-cholesterol conjugates, lipid nanoparticles and a commercial lipid-based transfection reagent.

4.3.1. Cholesterol-siRNA conjugate

A cholesterol-siRNA conjugate (chol-siRNA) was the first construct to successfully induce hepatic gene silencing *in vivo* following i.v. injection.[17] The efficacy was attributed to the increased half-life and the enhanced internalization at the target site compared to naked siRNA. Indeed, the cholesterol moiety protects the siRNA duplex against nucleases and ensures the connection to lipoprotein particles in the blood stream. This in turn improves the chol-siRNA biodistribution by avoiding rapid renal clearance and stimulating chol-siRNA uptake in the liver through endocytosis upon recognition by the lipoprotein receptor.[13, 27]

Our group previously observed good uptake and gene silencing by a chol-siRNA conjugate in the H1299-eGFP cells.[28] However, we were not able to confirm these results (Figure 4.5A). Most importantly, the suboptimal silencing could not be improved by DL or chloroquine (CLQ) (Figure 4.5A) despite the induction of a PLD phenotype (Figure 4.5B). Besides low chol-siRNA uptake, the lack of the adjuvant effect may be explained in terms of a different uptake pathway for chol-siRNA compared to the siNGs. Indeed, binding to lipoprotein particles is a prerequisite for the receptor-mediated endocytosis observed *in vivo*, but is unlikely to occur upon transfection in Opti-MEM. Consequently, chol-siRNA may not be predominantly trafficked to the endo-lysosomal compartment [29], although this was not experimentally verified in our setup. In contrast, both Ming *et al.* and Gilleron *et al.* were able to improve the silencing potential of chol-siRNA by effectuating release from the late endosomal compartment, which suggests at least partial endo-lysosomal chol-siRNA entrapment.[30, 31] The induction of a Niemann-Pick disease (NPD) phenotype may in turn not be an ideal strategy to improve chol-siRNA delivery since cholesterol shuttling by the Niemann-Pick C1 (NPC1) protein is inhibited in NPD cells[32, 33], thereby potentially reducing the chances of chol-siRNA escape.

4.3.2. Liposomes and commercial transfection reagents

Overall, LNP are most frequently applied as drug delivery vehicles and have advanced furthest in their clinical development[8, 34], which is of interest towards the translation of our adjuvant approach. Hence, we evaluated if DL could enhance the gene silencing potential by relatively simple siRNA-loaded DOTAP-DOPE and DOTAP-cholesterol liposomes (LPS) to establish whether our adjuvant approach is applicable to lipid-based nanocarriers.

In case of the DOTAP-cholesterol LPS, a sequential 40 µM DL treatment had no significant or only a very limited effect regardless of the transfection medium, despite the induction of a PLD phenotype (Figure 4.6H). This could not be attributed to siRNA degradation (Figure 4.7). Likewise, no significant improvement of suboptimal DOTAP-DOPE LPS could be achieved (Figure 4.9).

Many reports indicate that LPS are internalized through endocytosis, followed by intracellular trafficking to the lysosomal compartment. For liposomal formulations, endosomal escape is believed to occur *via* fusion of the LPS with the endo-lysosomal membrane[35, 36], which can be stimulated by the application of fusogenic lipids like DOPE.[37, 38] However, even for the most effective carriers only a small fraction of the internalized NA dose reaches the cytosol, while the majority of the LPS and their NA cargo are progressively sequestered in the lysosomes.[13] PLD induction by DL was not able to induce additional siRNA release in our setup, which may be attributed to differences in siRNA release from the LPS. As of today, relatively little is known regarding nanocarrier degradation and/or NA decomplexation in the endo-lysosomes. Since de Duve stated the lysosomes to be the cell's recycling bins[39], it is generally assumed that carriers and cargo reaching this organelle undergo degradation. Free nucleic acids are indeed rapidly degraded in the lysosomes and NA inclusion in a lipid- or polymer-based carrier clearly reduced and delayed NA hydrolysis[40], suggesting slow and incomplete NA detachment from the carrier. Since this release is in all probability imperative to our adjuvant strategy, it can be rationalized that the adjuvants fail to potentiate the siRNA-loaded LPS due to slower siRNA release from the carrier. Lipid-based carriers are suggested to be degraded by phospholipases, which show substrate preference for phosphatidylcholine and -ethanolamine groups.[41] However, the cationic surface charge and multilamellar configuration of the LPS do not favor degradation[42], thereby potentially delaying NA release. Such factors may additionally explain why CADs were not able to

significantly enhance the transfection potential of commercial lipid-based transfection reagents (Figure 4.4E and 4.10). Hence, future experiments should be set up to study the carrier degradation. It should also be confirmed that CADs do not negatively affect LPS degradation by a secondary inhibition of the lysosomal phospholipases.

Finally, we evaluated if a CAD as a liposomal building block could improve the therapeutic potential of the formulation. If so, this would allow using lower CAD doses and would potentially minimize off-target effects of the free drug. DLS results indicated successful LPS formation for the combination of DOPE and NT. This implies that NT was inserted in the lipid-bilayer, as the conical lipid DOPE is not able to form lamellar structures by itself. However, the extent of NT inclusion in the bilayer and the core of the LPS warrants further research. Compared to the DOTAP-DOPE LPS, uptake for the DOPE-NT LPS was lower in terms of the mean fluorescent signal of the positive cells. This may be explained by the stronger positive charge of the DOTAP-DOPE LPS, which may allow enhanced interaction with the negative cell membrane. However, since the fluorescent signal stems from the Cy5-labeled siRNA, the differences likely stem from variations in siRNA complexation. The latter was not experimentally determined for the DOPE-NT LPS. We obtained suboptimal silencing results with the DOPE-NT LPS. Of note, the induced silencing was not accompanied by an increased SSC signal. Hence, siRNA release is in all probability rather a consequence of the fusogenic properties of DOPE than the FIASMA activity of NT. The absence of an increased SSC signal suggests that an insufficient amount of NT is released from the bilayer or the hydrophilic core to induce the PLD phenotype.

5. CONCLUSION

Despite the great potential of a CAD adjuvant treatment to enhance siRNA-mediated gene silencing upon siNG transfection as show in **Chapter 3**, similar results could not be obtained with alternate small molecular adjuvants, nucleic acid cargos, nanocarriers or transfection reagents. It is anticipated that the cellular internalization, intracellular trafficking and lysosomal degradation of the carrier and/or NA decomplexation are of major importance to whether a CAD adjuvant approach will have a potentiating effect. Elucidation of these events may provide an explanation to why an adjuvant approach may or may not be successful and will allow a more rational combination of adjuvants, NA and carriers in the future.

AKNOWLDGEMENTS

J. Devoldere is acknowledged for providing the eGFP expressing mRNA. We furthermore thank G. Dakwar for the advice on liposome preparation. G. Nuyten is acknowledged for the experimental aid on the tobramycin experiments.

REFERENCES

1. Kornhuber, J.; Muehlbacher, M.; Trapp, S.; Pechmann, S.; Friedl, A.; Reichel, M.; Muhle, C.; Terfloth, L.; Groemer, T. W.; Spitzer, G. M.; Liedl, K. R.; Gulbins, E.; Tripal, P. *PLoS One* **2011,** 6, (8), e23852.
2. Kornhuber, J.; Tripal, P.; Gulbins, E.; Muehlbacher, M. *Handb Exp Pharmacol* **2013**, (215), 169-86.
3. Petersen, N. H.; Olsen, O. D.; Groth-Pedersen, L.; Ellegaard, A. M.; Bilgin, M.; Redmer, S.; Ostenfeld, M. S.; Ulanet, D.; Dovmark, T. H.; Lonborg, A.; Vindelov, S. D.; Hanahan, D.; Arenz, C.; Ejsing, C. S.; Kirkegaard, T.; Rohde, M.; Nylandsted, J.; Jaattela, M. *Cancer Cell* **2013,** 24, (3), 379-93.
4. Gulbins, E.; Kolesnick, R. N. *Cancer Cell* **2013,** 24, (3), 279-281.
5. De Broe, M. E.; Paulus, G. J.; Verpooten, G. A.; Roels, F.; Buyssens, N.; Wedeen, R.; Van Hoof, F.; Tulkens, P. M. *Kidney Int* **1984,** 25, (4), 643-52.
6. Chen, D.; Cui, Q. C.; Yang, H.; Dou, Q. P. *Cancer Res* **2006,** 66, (21), 10425-33.
7. Wiggins, H. L.; Wymant, J. M.; Solfa, F.; Hiscox, S. E.; Taylor, K. M.; Westwell, A. D.; Jones, A. T. *Biochem Pharmacol* **2015,** 93, (3), 332-42.
8. Juliano, R. L. *Nucleic Acids Res* **2016,** 44, (14), 6518-48.
9. McIvor, R. S. *Molecular Therapy* **2011,** 19, (5), 822-823.
10. Weissman, D. *Expert Rev Vaccines* **2015,** 14, (2), 265-281.
11. Devoldere, J.; Dewitte, H.; De Smedt, S. C.; Remaut, K. *Drug Discov Today* **2016,** 21, (1), 11-25.
12. Gilleron, J.; Querbes, W.; Zeigerer, A.; Borodovsky, A.; Marsico, G.; Schubert, U.; Manygoats, K.; Seifert, S.; Andree, C.; Stoter, M.; Epstein-Barash, H.; Zhang, L. G.; Koteliansky, V.; Fitzgerald, K.; Fava, E.; Bickle, M.; Kalaidzidis, Y.; Akinc, A.; Maier, M.; Zerial, M. *Nature Biotechnology* **2013,** 31, (7), 638-U102.
13. Wittrup, A.; Ai, A.; Liu, X.; Hamar, P.; Trifonova, R.; Charisse, K.; Manoharan, M.; Kirchhausen, T.; Lieberman, J. *Nat Biotechnol* **2015,** 33, (8), 870-6.
14. De Backer, L.; Braeckmans, K.; Demeester, J.; De Smedt, S. C.; Raemdonck, K. *Nanomedicine (Lond)* **2013,** 8, (10), 1625-38.
15. Raemdonck, K.; Naeye, B.; Buyens, K.; Vandenbroucke, R. E.; Hogset, A.; Demeester, J.; De Smedt, S. C. *Adv Funct Mater* **2009,** 19, (9), 1406-1415.
16. Wishart, D. S.; Knox, C.; Guo, A. C.; Shrivastava, S.; Hassanali, M.; Stothard, P.; Chang, Z.; Woolsey, J. *Nucleic Acids Res* **2006,** 34, (Database issue), D668-72.
17. Soutschek, J.; Akinc, A.; Bramlage, B.; Charisse, K.; Constien, R.; Donoghue, M.; Elbashir, S.; Geick, A.; Hadwiger, P.; Harborth, J.; John, M.; Kesavan, V.; Lavine, G.; Pandey, R. K.; Racie, T.; Rajeev, K. G.; Rohl, I.; Toudjarska, I.; Wang, G.; Wuschko, S.; Bumcrot, D.; Koteliansky, V.; Limmer, S.; Manoharan, M.; Vornlocher, H. P. *Nature* **2004,** 432, (7014), 173-8.
18. Lorenz, C.; Hadwiger, P.; John, M.; Vornlocher, H. P.; Unverzagt, C. *Bioorg Med Chem Lett* **2004,** 14, (19), 4975-7.
19. Dakwar, G. R.; Ghazaryan, A.; Braeckmans, K.; Ceelen, W.; Mailänder, V.; De Smedt, S. C.; Remaut, K. *Article in preparation*.
20. Dakwar, G. R. G., A.; Braeckmans, K.; Ceelen, W.; Mailänder, V.; De Smedt, S. C.; Remaut, K. *Article in preparation*.
21. Dakwar, G. R.; Zagato, E.; Delanghe, J.; Hobel, S.; Aigner, A.; Denys, H.; Braeckmans, K.; Ceelen, W.; De Smedt, S. C.; Remaut, K. *Acta Biomater* **2014,** 10, (7), 2965-75.
22. Goracci, L.; Ceccarelli, M.; Bonelli, D.; Cruciani, G. *J Chem Inf Model* **2013,** 53, (6), 1436-1446.
23. Carlier, M. B.; Laurent, G.; Claes, P. J.; Vanderhaeghe, H. J.; Tulkens, P. M. *Antimicrob Agents Chemother* **1983,** 23, (3), 440-9.
24. Nioi, P.; Pardo, I. D.; Snyder, R. D. *Drug Chem Toxicol* **2008,** 31, (4), 515-28.
25. Lovborg, H.; Oberg, F.; Rickardson, L.; Gullbo, J.; Nygren, P.; Larsson, R. *Int J Cancer* **2006,** 118, (6), 1577-80.

26. Berndtsson, M.; Beaujouin, M.; Rickardson, L.; Havelka, A. M.; Larsson, R.; Westman, J.; Liaudet-Coopman, E.; Linder, S. *Int J Cancer* **2009,** 124, (6), 1463-9.
27. Juliano, R. L.; Ming, X.; Nakagawa, O. *Acc Chem Res* **2012,** 45, (7), 1067-76.
28. Stremersch, S.; Vandenbroucke, R. E.; Van Wonterghem, E.; Hendrix, A.; De Smedt, S. C.; Raemdonck, K. *J Control Release* **2016,** 232, 51-61.
29. Yang, S. D.; Chen, Y. F.; Ahmadie, R.; Ho, E. A. *J Control Release* **2013,** 167, (1), 29-39.
30. Ming, X.; Carver, K.; Fisher, M.; Noel, R.; Cintrat, J. C.; Gillet, D.; Barbier, J.; Cao, C.; Bauman, J.; Juliano, R. L. *Nucleic Acids Res* **2013,** 41, (6), 3673-87.
31. Gilleron, J.; Paramasivam, P.; Zeigerer, A.; Querbes, W.; Marsico, G.; Andree, C.; Seifert, S.; Amaya, P.; Stoter, M.; Koteliansky, V.; Waldmann, H.; Fitzgerald, K.; Kalaidzidis, Y.; Akinc, A.; Maier, M. A.; Manoharan, M.; Bickle, M.; Zerial, M. *Nucleic Acids Res* **2015,** 43, (16), 7984-8001.
32. Sahay, G.; Querbes, W.; Alabi, C.; Eltoukhy, A.; Sarkar, S.; Zurenko, C.; Karagiannis, E.; Love, K.; Chen, D.; Zoncu, R.; Buganim, Y.; Schroeder, A.; Langer, R.; Anderson, D. G. *Nat Biotechnol* **2013,** 31, (7), 653-8.
33. Eltoukhy, A. A.; Sahay, G.; Cunningham, J. M.; Anderson, D. G. *Acs Nano* **2014,** 8, (8), 7905-7913.
34. Whitehead, K. A.; Langer, R.; Anderson, D. G. *Nat Rev Drug Discov* **2009,** 8, (2), 129-38.
35. Martens, T. F.; Remaut, K.; Demeester, J.; De Smedt, S. C.; Braeckmans, K. *Nano Today* **2014,** 9, (3), 344-364.
36. Felgner, J. H.; Kumar, R.; Sridhar, C. N.; Wheeler, C. J.; Tsai, Y. J.; Border, R.; Ramsey, P.; Martin, M.; Felgner, P. L. *J Biol Chem* **1994,** 269, (4), 2550-61.
37. Gao, X.; Huang, L. *Gene Ther* **1995,** 2, (10), 710-22.
38. Dominska, M.; Dykxhoorn, D. M. *J Cell Sci* **2010,** 123, (Pt 8), 1183-9.
39. De Duve, C.; Wattiaux, R. *Annu Rev Physiol* **1966,** 28, 435-92.
40. Laurent, N.; Coninck, S. W. D.; Mihaylova, E.; Leontieva, E.; Warnier-Pirotte, M. T.; Wattiaux, R.; Jadot, M. *Febs Letters* **1999,** 443, (1), 61-65.
41. Schulze, H.; Kolter, T.; Sandhoff, K. *Bba-Mol Cell Res* **2009,** 1793, (4), 674-683.
42. Glukhova, A.; Hinkovska-Galcheva, V.; Kelly, R.; Abe, A.; Shayman, J. A.; Tesmer, J. J. G. *Nature Communications* **2015,** 6.

PART II

***In vitro* approaches to probe the toxicity of inorganic nanoparticles.**

CHAPTER 5

Assessing nanoparticle toxicity with cell-based assays: influence of cell culture parameters and optimized models for bridging the *in vitro-in vivo* gap.

An adapted manuscript of this chapter is published as:

Freya Joris[†], Bella B. Manshian[∫], Karen Peynshaert[†], Stefaan C. De Smedt[†,§], Kevin Braeckmans[†,‡], Stefaan J. Soenen[†,‡]. Assessing nanoparticle toxicity with cell-based assays: Influence of cell culture parameters and optimized models for bridging the *in vitro-in vivo* gap. *Chemical Society Reviews 2013*.

[†]Lab of General Biochemistry and Physical Pharmacy, Faculty of Pharmaceutical Sciences, Ghent University, B9000 Ghent, Belgium.

[∫]DNA Damage Research Group, School of Medicine, Swansea University, SA2 8PP Swansea, UK.

[§]Ghent Research Group on Nanomedicine, Ghent University, B9000 Ghent, Belgium.

[‡]Centre for Nano- and Biophotonics, Ghent University, B9000 Ghent, Belgium.

Table of contents

ABSTRACT

The number of newly engineered nanomaterials is vastly increasing along with their applications. Despite the fact that a lot of interest and effort are being put into the development of nano-based biomedical applications, the level of translational clinical output remains limited due to uncertainty on the toxicological profiles of the nanoparticles (NPs). As NPs used in biomedicines are likely to directly interact with cells and biomolecules, it is imperative to rule out any adverse effect before they can be safely applied. The initial nanosafety screening is preferably performed *in vitro*, but extrapolation to the *in vivo* outcome remains challenging. In addition, generated *in vitro* and *in vivo* data are often conflicting, which consolidates the *in vitro-in vivo* gap and impedes the formulation of unambiguous conclusions on NP toxicity. Consequently, more consistent and relevant *in vitro* and *in vivo* data need to be acquired in order to bridge this gap. This is in turn in conflict with the incentive to reduce the number of animals used for *in vivo* toxicity testing. Therefore the need for more reliable *in vitro* models with a higher predictive power, mimicking the *in vivo* environment more closely, becomes more prominent. In this review we will discuss the current paradigm and routine methods for nanosafety evaluations, and give an overview of adjustments that can be made to the cultivation systems in order to optimise current *in vitro* models. We will also describe various novel model systems and highlight future prospects.

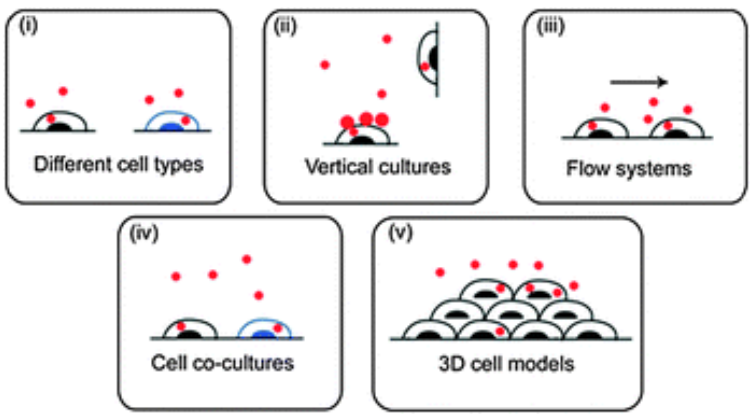

1. INTRODUCTION

Since the 1980's the field of nanotechnology has increasingly gained importance, leading to a large number of applications since the 1990's. Today, inorganic nanoparticles (NPs) are applied in various technological applications and consumer goods. For example, zinc oxide (ZnO)NPs are used in sunscreens and toothpastes and silver (Ag)NPs can be found in food packages, deodorants and are applied as a preservative in cosmetics.[1-3] Given the ever increasing use of NPs and the high interest of exploiting the exceptional features of NPs in biomedical applications, it is expected that both intentional and unintentional exposure will become more frequent.[4, 5] Consequently, the increasing implementation of nanotechnology in our daily lives is joined with raising concerns on potential adverse effects towards human health.[6] It is therefore recommended that the safety of these products, towards consumers and workers at the production site, is carefully evaluated before the introduction to the market.[4, 5, 7] However, there are currently only very limited regulations on the use and the safety criteria for nanomaterials in industrial applications or consumer goods. Major obstacles on the route to an appropriate legislation are the broad nature of nanotechnology, the incredible pace at which the field keeps advancing and the enormous variety in types of nanomaterials, each with different physicochemical properties and specific applications.[7] This legislation should cover all aspects of nanotechnology without any material or application being left out, which is, from a practical point of view, extremely hard to obtain. In order to try and overcome this predicament, the European Commission has launched a recommendation on a definition of nanomaterials in 2011 that states that a nanomaterial is: "A natural, incidental or manufactured material containing particles, in an unbound state or as an aggregate or as an agglomerate and where, for 50% or more of the particles in the number size distribution, one or more external dimensions is in the size range from 1 - 100 nm. In specific cases and where warranted by concerns for the environment, health, safety or competitiveness the number size distribution threshold of 50 % may be replaced by a threshold between 1 and 50 %."[8] As every definition has its limitations and introduces technical challenges, regulatory bodies have not yet come to a global agreement on the correct definition, but the most used criterion is the size limitation.[9-11] Nanotechnology is subsequently defined as the manipulation and application of particles and systems with at least one dimension below 100 nm.[10] For nanomedicine purposes these technologies are used to develop applications for diagnosis,[12, 13] imaging,[14, 15] treatment [16, 17] and prevention

of diseases.[18-20] A recent novelty in nanomedicine is the concept of theranostics, where particles combine diagnostic and therapeutic features in a single construct.[21, 22] For example, Kirui *et al*. created immunotargeted gold-coated iron oxide (IO)NPs to visualize colorectal tumors by magnetic resonance imaging followed by treatment with hyperthermia.[23]

It is on the one hand due to the minute dimensions of the NPs that they exhibit many unique properties (e.g. IONPs are superparamagnetic[24] and gold (Au)NPs have a localized surface plasmon resonance[25]) because of which they can be implemented in novel innovative applications.[26] These dimensions are on the other hand often the cause of adverse health effects through the higher surface area to volume ratio and enhanced surface reactivity.[27, 28] The fact that both the great potential and the high risk lie in the miniature dimensions of the NPs is referred to as the nanomaterial-paradox and underscores the importance of a thorough toxicological analysis.[9] Even though nanotechnology has been evolving since the 1980's, it was only in 2004 that Donaldson *et al.* mentioned the importance of nanotoxicology - as a subcategory of toxicology - to enable the further development of safe and sustainable nanotechnology.[29] Nanotoxicology is referred to as the study on interactions between NPs and biological systems with an emphasis on establishing a relationship, if any, between the physicochemical properties of the NP and the toxicological responses.[30] It is crucial that nanotoxicology is regarded as a distinct category of toxicology since standard toxicity assays, initially developed for the evaluation of chemical substances, are often inadequate for nanotoxicity assessment. This can be attributed to the different mechanisms leading to nanocytotoxicity, the specific behavior of the NPs in culture media and the possible interference of NPs with various toxicity assays.[9, 31-33] Therefore the classical toxicity-testing paradigm needs to be optimized to be applicable for nanosafety evaluation. The experimental design is, besides the assays, also subject to optimization, as it is clear from literature that it has the potential to influence the uptake and/or the observed toxicological effects.[34-37]

This chapter provides an overview of current methods used for nanosafety evaluations and factors related to the cell model that are likely to influence the outcome of the experiments. Furthermore we will propose adjustments that can be made to the cultivation system in order to minimize artifacts and resemble the *in vivo* situation more closely, as illustrated by recent findings from literature.

2. NANOTOXICOLOGY

2.1. Common mechanisms of nanocytotoxicity

As mentioned above, nanotoxicology should be regarded as a specific subcategory of toxicology since the general toxicology paradigm cannot completely cover NP-induced cytotoxicity.[29] Of note, generally higher levels of toxicity are observed for NPs in comparison to their bulk material,[20, 30] which is attributed to the higher surface area to volume ratio, possible surface reactivity and susceptibility to NP degradation and ion leaching.[27, 38] In addition, most chemicals induce cell damage through interactions with specific biomolecules, whereas a single NP may cause cytotoxicity *via* a combination of adverse events.

A true general paradigm on how NPs evoke cell injury remains to be elucidated. However, it can be stated that cytotoxicity can be elucidated *via* 4 distinct categories of events: (i) effects related to induction of reactive oxygen species (ROS), (ii) effects due to direct interactions of the NPs with biomolecules, (iii) effects from leached ions and (iv) effects related to the protein corona.

Nel *et al.* have put ROS induction forward as one of the main mechanisms through which inorganic NPs induce cytotoxicity, as this effect has been observed in a multitude of *in vivo* and *in vitro* studies.[39-43] It is proposed that ROS can be induced either through intrinsic ROS generating properties of the NP or cell-mediated ROS generation. In the latter category, NPs can interfere with the anti-oxidative defense mechanism by reducing the activity of the anti-oxidative defense enzymes.[44] Furthermore NPs can activate several signaling pathways through interaction with cell surface receptors.[45] Hereby stress-dependent signaling pathways are activated, which alter gene expression of the anti-oxidant response element, leading to ROS overproduction.[46] In addition, NPs can cause increased ROS production in the mitochondria through interference with the respiratory chain.[46, 47] Finally, several NPs are capable of activating NADPH oxidase, thereby inducing ROS production.[48, 49] In the first category (intrinsic ROS generating properties), NPs are intrinsically capable of generating ROS through the presence of reactive surface groups or surface bound radicals.[27] In addition, transition metals present on the surface or leached from the NP in the acidic environment of the endo-lysosomes can generate ROS *via* Fenton chemistry.[27, 45] Overall, ROS induction can

be a consequence of a single or a combination of the abovementioned events. Furthermore, Nel *et al.* proposed a tired response of the cells to elevated ROS levels, which has been confirmed in *in vitro* and *in vivo* studies for different NPs. In general limited ROS levels induce an anti-oxidative response, medium ROS levels evoke a proliferative and inflammatory response and persistently high levels of oxidative stress induce apoptotic and necrotic signaling pathways.[27]

The induction of ROS can have a multitude of downstream effects. Indeed, ROS is known to induce general cell damage, as it can interact with DNA, proteins, lipids and organelles.[27] First, oxidative DNA damage influences gene expression or can induce mutagenesis or apoptosis in case of insufficient repair mechanisms.[50] Secondly, proteins can be activated or inactivated as a consequence of ROS presence.[51] ROS can furthermore cause actin stress fiber formation and therefore alter the cell's morphology, motility and adhesion.[52, 53] Persistent ROS induction will trigger a stress response leading to the production of cytokines and the induction of an inflammatory response. If ROS is not neutralized in a timely fashion, a feed-forward loop keep stimulating both ROS and cytokine production leading to immunotoxicity.[27]

Due to lipid peroxidation, membranes can be damaged, which in turn leads to malfunctioning organelles. Indeed, the mitochondria, endoplasmatic reticulum (ER) and lysosomes are reported to suffer from ROS.[54] This secondary ROS damage can in turn lead to downstream effects such as altered signaling and a perturbed calcium homeostasis.[54] In addition, both ER stress and lysosomal destabilization can induce autophagy and an inflammatory response.[55]

Of note, this ROS paradigm does not account for all NPs: cerium oxide (CeO_2)NPs, for example, were found not to induce ROS but on the contrary even showed a protective effect against ROS damage *in vivo* as well as *in vitro.*[56, 57] Furthermore, Harris *et al.* could not detect increased ROS levels upon IONP exposure in a high content screening (HCS).[58] In addition, IONPs were shown to exhibit an intrinsic peroxidase-like activity in a cell free environment as well as in mesenchymal stem cells, where they even promoted cell proliferation.[59, 60] Of note, only unimpaired IONPs displayed this peroxidase-like activity. Importantly, when IONPs are trafficked to the lysosomes upon endocytosis, the acidic and degrading environment

induces ion leaching. Upon saturation of the cell's iron homeostasis, excess iron ions subsequently cause increased ROS production through Fenton chemistry.[61] This feature underscores the complexity of NP-cell interactions and highlights the importance of the intracellular localization of the NPs.

The second main mechanism through which NPs induce adverse effects is by interacting directly with biomolecules, such as DNA, proteins and lipids, which in turn leads to downstream effects. Notably, most ROS-related events may also occur through direct NP-biomolecule interactions. For instance, NPs can alter gene expression *via* interactions with signal transduction pathways, interference with epigenetic gene regulation or the transcriptional or translational machinery through their perinuclear localisation.[50, 51, 62] In addition, very small NPs with a diameter below 5 nm may directly interact with DNA to alter its expression.[63] Studies furthermore show that NPs can interact with components of the cytoskeleton thereby potentially altering cell morphology as well as signal transduction.[64-66] In addition, NPs were shown to interfere with receptor-ligand interactions and signalling pathways.[67, 68] Comparable to ROS-induced damage; NPs are capable of damaging membranes and organelles such as the mitochondria and lysosomes. This may in turn evoke autophagy or an inflammatory response.[51, 69] Of note, some NPs were also shown to induce an immune response through interaction with the Toll Like Receptor 4.[70] Finally, NPs are also capable of directly evoking ER stress, which in turn leads to autophagy, increased calcium levels and potentially inflammation or apoptosis.[69, 71]

The third general element causing NPs to induce toxicity is their susceptibility to degradation. Depending on the uptake mechanisms and subsequent trafficking many NPs end up in the acidic and degrading environment of the lysosomes.[45, 72] This environment can cause degradation or even dissolution of the NP, resulting in the leaching of free ions or an increase in reactive surface groups.[45] The following impact on cell wellbeing depends on the chemical composition of the NP. For cadmium (Cd)-containing quantum dots (QDs), for example, the leaching of highly toxic Cd^{2+}-ions is considered to be the main cause of any observed toxicity.[73, 74] It has been shown for several NPs that the induced toxicity is more severe for the nanoparticulate form than its ionic counterpart. This is called the "Trojan Horse effect" as it can likely be contributed to a more efficient uptake of the NP through

endocytosis compared to the free ionic form, which consequently leads to elevated intracellular ionic concentrations.[51]

Finally, it is known that NPs avidly bind serum proteins to their surface, creating a protein corona.[75] The nature of this corona depends on the NPs physicochemical properties and the composition of the microenvironment (e.g. cell culture media) surrounding the NPs.[30, 76] The binding of serum proteins to the NP surface is an important determinant in how the cells 'see' the NPs and therefore influences NP uptake and toxicity.[77-79] Additionally, proteins incorporated in this corona can undergo conformational changes and because of which the cell may recognize them as an antigen and initiate an immune response.[20, 29] An immune response can furthermore be triggered by direct interactions of NPs with immune cells, complement activation and facilitation of antigen-specific hypersensitivity reaction through interactions with T lymphocytes or the release of chemokines and cytokines. Here, the mechanism of immunotoxicity appears to be both cell- and NP-dependent.[80]

Overall, in the current nanotoxicity paradigm ROS induction has been proposed as the main toxic effect, which can lead to a plethora of downstream effects. Yet this section highlights the need for a multiparametric nanosafety evaluation at sublethal NP doses to thoroughly investigate the effect on cell homeostasis. The uptake mechanism and ultimate intracellular location of the NPs must also be taken into account as these parameters co-determine the extent and mechanism of the NP-induced injury.

2.2. Routine methods for nanotoxicity testing

In the NP development process nanosafety is primarily evaluated *in vitro.*[81, 82] It is essential to note that, prior to any toxicity testing, the NPs must be thoroughly characterized with respect to the purity and physicochemical properties. NP characterization should be performed both on the dry and wet state, with the latter ideally being a relevant medium such as the cell culture medium or a biological fluid.[82, 83] NP characterization will not be elaborately discussed here, but further information can be found *via* alternative literature.[83-86] This section summarizes the main methodological principles of *in vitro* nanosafety evaluation as well as the most important shortcomings.

2.2.1. Routine *in vitro* methods

In vitro assays are mainly the first to be conducted in a toxicological evaluation.[87] Most *in vitro* studies are conducted in classical 2D monocultures of cancer or long-lived cell lines although the use of stem cells or primary cells is steadily increasing. The selection of a relevant cell type generally depends on the expected *in vivo* target organ and application of the NP and/or the expected exposure.[88] In a vast majority of the studies the cells are exposed to the NP dispersion during a single incubation period, which mostly ranges from 3 up to 48 hours.[87, 89, 90] The induced toxicity is subsequently evaluated using mainly biochemical assays, including enzymatic assays and enzyme-linked immunoassays with a fluorometric or spectrophotometric read-out. Such assays remain popular given their relatively short duration, the uncomplicated detection principle and straightforward data processing.[91] Furthermore, the possibility of up scaling and automation of the execution, detection and data processing makes these assays highly convenient in regard to a high throughput approach.[91, 92] Another popular method is to stain specific cellular components with fluorescently labeled antibodies or molecular probes.[45, 87, 93] This approach allows detection *via* a plate reader or flow cytometry or is combined with microscopy-based analysis. The latter is an important tool for the evaluation of morphological features like cell spreading and organelle behavior, but will also increasingly be applied in high content screening (HCS) approaches to evaluate cellular processes.[94, 95]

Finally specialized techniques are used to evaluate specific parameters. For example, ion leaching can be detected in cell-free conditions using specialized buffers and the intactness of stem cell functionality can be evaluated by observing the efficiency of cellular differentiation induced by specific protocols.[45, 96]

2.2.2. Issues with routine *in vitro* methods

Up until now, many conflicting data have been generated as shown in reviews on the toxicity of a specific NP or the correlation between the NPs physicochemical properties and the evoked effects.[28, 97-99] This led to an increasing awareness that the routine *in vitro* testing paradigm may not be as appropriate for nanosafety assessments as initially assumed.[100, 101] Nel *et al.* first raised this thought in 2006, emphasizing on the necessity to optimize several elements of the testing paradigm.[27] We believe that the major issues with the current *in vitro* methods are (i) the (mostly) incomplete NP characterization, (ii) the lack of consensus

on the dose metric, (iii) the possibility of NPs interfering with the assays, (iv) the shortcomings inherent to the most used classical 2D monocultures and (v) the lack of standardization and guidelines on how to perform an *in vitro* nanosafety evaluation.[11, 100-103] Thus, classic assays may be appropriate for nanotoxicity elements but factors such as the preparation of the NP dispersion and the inclusion of additional controls to avoid the effect of assay interference should be optimized.

a. NP characterisation

A first shortcoming to the current nanotoxicity testing strategy paradigm is the often incomplete characterization of the NPs. Thorough NP characterization is imperative, as different physicochemical properties could potentially influence the outcome of nanosafety studies. In this regard, a consensus should be reached on which parameters to characterize as well as on the methods that should be applied. Combined efforts from multiple groups, overviewed by the European Commission, lead to the identification of NP parameters that should be characterized as well as to guidelines on appropriate methods. With regard to the latter, it is recognized that additional efforts are needed since some methods are only applicable to a subset of NPs, novel methods are required to asses certain parameters and several methods still require standardization.[104] Furthermore, it is proposed to obtain information on the physical characteristics (size distribution, shape and aspect ratio, agglomeration/aggregation and porosity), the chemical properties (chemical composition and crystallinity), the NP surface properties (charge, photocatalysis and surface reactivity) and parameters relevant for fate and exposure (zeta potential, dustiness and water solubility/dispersibility/dissolution kinetics).[105]

Importantly, NPs should be characterized both in dry and wet state. In addition, it is crucial to characterize the NPs in the applied exposure medium since cell media applied for *in vitro* studies often contain high salt and protein concentrations, which can respectively induce NP aggregation and form a protein corona on the NP surface. Both factors can in turn have an impact on NP size, charge and colloidal stability. [106] Hence, info on NP properties in the applied medium is essential for correct data interpretation.

A final hurdle is the difficulty to retrieve reliable conclusions on the effect of a single physicochemical parameter on nanosafety. This originates from the fact that altering one parameter, for example surface charge, without affecting any other (hydrodynamic size, colloidal stability, nature of the coating…) is not an easy task.[103] In addition, when changing a single parameter, scientist should take into account how this parameter may change when the NP is dispersed in the applied culture medium.

b. NP concentration

Besides the NPs physicochemical parameters, NP concentration is an additional element that requires optimization. Here, a consensus is needed on methods to determine the concentration as well as the dose metric [107, 108109, 110]since currently various studies apply different dose metrics, which reduces the inter-study comparability.[107, 108] Most often, NP concentration is expressed in terms of mass/volume. This option requires the least thorough characterization to determine the NP concentration and is considered the most straightforward. However, it is not always the most relevant metric, as smaller NPs often evoke a stronger toxic response in comparison to their larger counterparts at similar mass/volume doses.[37, 103] Logically, the number of NPs present is much higher for smaller NPs than for their larger counterpart at similar mass doses. In addition, this dose metric does not allow easy comparison of the effects induced by NPs consisting of materials with different densities.

Wittmaack considers particle number/volume to be the best dose metric.[109] Other groups believe that the concentration should be expressed in terms of surface area/volume since both particle size and number are contained in this metric.[110, 111] Of note, these metrics are not influenced by differences in particle density, which is the case for the mass/volume metric. Thus, it was suggested that if authors should prefer to use the NP mass/volume ratio to express the concentration, it should be combined with the NP number/volume concentration to provide sufficient information in order to enable interpretation of the toxicity data between different studies.[40, 107, 112]

The applicability of the surface area/volume unit has been demonstrated by Rushton *et al.* who found a significant correlation between the *in vitro* oxidative response and the inflammatory response *in vivo* for nine different NPs with distinct physicochemical

properties when the concentration was expressed in surface area/volume.[113] When the same group applied this method to a previous data set, in which no *in vitro-in vivo* correlation could be observed, a clear correlation was now established.[113, 114]

c. Assay interference

A third major issue is the potential of NPs to interfere with classical biochemical assays.[101, 115] NPs with optical properties can, for instance, alter the outcome of an assay based on a spectrophotometric or fluorometric read-out.[32] Such read-outs can furthermore be altered by changes in the fluorescence or absorbance characteristics of the indicator due to direct interaction with the NPs.[116, 117] Additionally, NPs may interact with enzymes or substrates because of their high absorbance capacity and/or catalytic activity and change their structure and/or function.[101, 102, 115] Kroll *et al.* looked into the interference of 24 well-characterised NPs with four frequently used *in vitro* assays and observed concentration-, NP- and assay-dependent interferences.[31] More recently, Ong *et al.* showed that NP interference could not be predicted based on NP-assay component interactions and our current understanding of NP behaviour.[115] Consequently it is imperative to validate the assays for each specific type of NP by assuring that the measured toxicity, or the lack thereof, is indeed caused by the NP and is not merely a consequence of assay interference.[115, 118, 119] Therefore appropriate controls should be introduced: besides a negative (no treatment) and positive (maximum effect) control, the positive control should be tested in combination with the NPs. Test reagents should also be incubated with the NPs to rule out any possible interaction with its components.[64] Furthermore, every single parameter should ideally be evaluated with multiple assays, which supply complementary information and have a different assay- and detection principle, to validate the obtained results.[120]

Finally, strategies to determine cellular uptake levels and intracellular localization are correlated to the type of NP tested and may therefore differ for different types of NPs. However, adapting a NP to enable detection by a specific technique may not be the most suitable approach, as linking a fluorescent probe to the particle may influence the formation of the protein corona or the NP-biomolecule interactions and therefore alter its behaviour and toxicological profile.[82]

d. Shortcomings to classical 2D monocultures

Regarding the cell models applied for nanosafety testing, the most frequently applied monocultures are static models with a reduced level of complexity in contrast to the complex and dynamic *in vivo* environment and therefore show several important shortcomings.[30, 121] Importantly, the cell model determines in which state ((un)differentiated, (un)polarized) the cells are exposed to the NPs as well as the contact time, which can in turn influence the nanosafety profile.

For most *in vitro* assessments a single cell type is selected to represent the desired target organ in an attempt to predict an *in vivo* effect.[37] Hereto, most often the parenchymal cell type is selected, which can in turn be represented by either a (cancer or long-lived) cell line or primary cells. Of note, this first selection has already been shown to influence the nanosafety profile since several groups have shown that NP-induced effects differ in different cell lines or primary cells representing the same tissue.[122-124] Variations between culturing methods and extensive *in vitro* culturing can furthermore affect the phenotype and potentially influence the cell-NP interactions, but such factors are often overlooked during data interpretation. An important example is the use of antibiotics in culture media to prevent bacterial contamination since their presence has been reported to alter the cell biochemistry.[125]

Since organs consist of multiple differentiated cell types, all with their specific function, modeling the *in vivo* response by using a single cell type is furthermore nearly impossible.[126] Hence, the impact of intercellular communication between different cell types cannot be taken into account in such simplified models, which is believed to be a major factor contributing to the large discrepancies between *in vitro* and *in vivo* data (Section 5).

Next, most studies apply monolayer cultures or cell suspensions for their nanosafety assessment. However, these 2D cultures generally fail to reproduce cell polarization, differentiation and specific architecture as observed at the organ level (Section 6). In addition, the extracellular matrix (ECM) produced by cells in a monolayer is less dense and incomplete in comparison to the one found *in vivo.*[127] This ECM is a very important factor as it is a key regulator in homeostasis and phenotype expression and forms a natural barrier with small pores, limiting NP diffusion into the tissue.[128]

Taken together, oversimplified 2D models fail to reconstitute the *in vivo* microenvironment as they offer a reductionist approach with spatial limitations leading to expression of a different cellular phenotype and consequently to the vast *in vitro-in vivo* gap.[129]

e. Standardisation of in vitro nanotoxicology methods

Given the many shortcomings mentioned in the previous sections, we believe that *in vitro* nanosafety assessments would tremendously benefit from a standardization of the entire testing paradigm. Regarding NP characterization, we previously mentioned the need of standardization of both the parameters to be evaluated as well as the methods through which this should be performed. Subsequently a consensus should be reached on how NP dispersions in relevant exposure media should be prepared. Various groups simply disperse the NPs in the culture media and let agglomeration and/or aggregation take its course, whereas others by numerous means try to avoid such events. Hereto, surface modification, addition of surfactants or methods like sonication are applied but were in turn shown to influence the nanosafety profile.[130-132] For instance, altering the duration and intensity of sonication affects the physicochemical properties and dissolution kinetics of copper oxide NPs and subsequently their toxicity profile.[133] In addition, results from a study by Oberdörster *et al.* using surfactant stabilized dispersions have been put to question since the observed toxicity might have been caused by surfactant residuals.[134] We believe that it is better not to alter the dispersion state and to strive for a medium resembling the *in vivo* tissue microenvironment as close as possible to mimic relevant exposure scenarios.[135, 136]

In a next step, attention should be paid to standardization of incubation conditions, as overexposure levels should be avoided. The importance thereof becomes clear when evaluating genotoxicity for example: acute toxicity at overexposure conditions can mistakenly be interpreted for genotoxicity since apoptosis is associated with DNA fragmentation.[137, 138] Therefore, genotoxicity and other effects on cell homeostasis should be evaluated at sublethal doses. In addition, the determination of relevant dose ranges is severely hampered by the lack of exposure data and doses required for specific applications. Therefore, *in vitro* nanotoxicity testing currently focuses on the determination of the No Observed Adverse Effect Level (NOAEL) values instead of evaluating realistic exposure scenarios or dosages.[37] Furthermore, nanosafety should be evaluated of functional NP concentrations, being the intracellular NP concentration needed for a certain application.[139]

With regard to incubation conditions, several treatment regiments should be defined to mimic acute and long-term exposure, as different toxicity profiles have already been obtained for both exposure regiments.[140]

Nanosafety testing should additionally look beyond live/dead scoring in order to develop a more predictive paradigm towards adverse *in vivo* outcomes. Hence, a shift could be observed towards the evaluation of cell function and effects on cellular homeostasis at sublethal NP doses.[141, 142] In this regards, we believe that the interstudy comparability could be increased by a standardization in terms of which assays should be applied as well as at which time points evaluation should be performed. Ideally, several assays would be applied to assess the same parameter to improve the robustness of the assessment.[120] In addition, the selected parameters should be evaluated over an extended time course to obtain information on possible long-term effects of NP exposure.[61, 143]

Finally, we believe that the applied cell models should be standardized. We propose to define a set of cell lines representing different organs for screening purposes, whereas more intricate models should be applied for thorough *in vitro* nanosafety assessments. When applying cell lines, researches should furthermore avoid to evaluate NP-cell interactions in cells showing senescence due to extensive passaging *in vitro*. Besides, the cell phenotype may alter due to extensive in vitro culturing. Hence, cells should be characterized prior to the nanotoxicity study to ensure the quality of the cell model. Finally, cell culture parameters should be standardized as the application of distinct culture media, whether or not containing antibiotics, may alter the phenotype and heavily impact the outcome of nanotoxicity evaluations. Overall, all culture parameters that could potentially influence the outcome (cell seeding density, culture medium composition, etc.) should be defined to counter the generation of conflicting results.

In conclusion, further research regarding method optimization of the entire *in vitro* nanosafety testing paradigm is highly recommended in order to obtain reproducible data that would allow to draw firm conclusions regarding NP toxicity.

2.2.3. Novel methods for toxicity testing

In order to overcome certain shortcomings as well as to meet emerging challenges, several novel methodologies were developed in the last few years, of which an overview is provided in this section.

a. Particokinetics

NP dosimetry poses challenges in terms of the selection of the proper dose metric. In addition, it has been proposed that the dose to which the cells are exposed is not necessarily correctly represented by the initial concentration of the NP dispersion due to events as NP agglomeration and/or aggregation and subsequent sedimentation. To meet this challenge, Teeguarden *et al.* proposed the concept of particokinetics to model the solution dynamics of the NPs.[110] They marked diffusion, sedimentation and aggregation as predominant processes determining the NP dispersion. Additionally, they suggested a distinction between the administered, delivered and cellular dose respectively being the dose added to the cell culture, the dose reaching the cell surface and the dose reaching the interior of the cell (Figure 5.1). The latter is the most interesting for nanosafety studies but is also the most difficult to determine. They proposed to calculate the delivered dose combining the administrated dose and the NPs particokinetics.[110] Recently the initial model was optimized and is now referred to as the *In vitro* Sedimentation, Diffusion and Dosimetry model (ISDD).[144] However, some debate on the applicability of the model remains, as it has been stated that the calculated doses will be underestimated for monodisperse NP suspensions since ISDD does not take convectional forces that develop in most solutions into account.[145] In contrast, Ahmad Khanbeigi *et al.* found measured cellular doses to correlate well with computed delivered doses for several NPs in various exposure conditions, indicating the applicability of the model.[146]

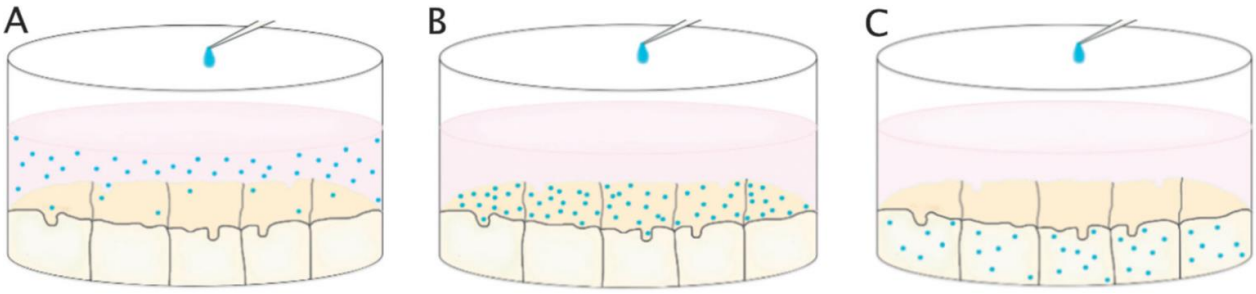

Figure 5.1. Schematic representation of the concept of administered dose (A), delivered dose (B) and cellular dose (C).

b. Label-free methods

One of the major drawbacks of classical toxicity assays is the possible interference of the NPs with either the assay components or the read-out. Hence, label-free methods have been put forward as an alternative to evaluate nanotoxicity *in vitro*. Here, the read-out is based on physical qualities, such as impedance, refractive index and viscoelasticity.[147] Since label-free methods are non-invasive, there is no need to sacrifice the cells to perform the end-point measurement as is the case for biochemical methods. Thus, label-free methods allow continuously monitoring the cellular response and establishing the dynamics of cell-NP interactions.[148, 149] Such techniques typically allow evaluating parameters that are related to cell adhesion, such as cell proliferation, viability, morphology, migration and detachment. In contrast, label-free methods are not able to provide information on the mechanism through which NPs induce adverse events. Several label-free methods were developed over the past few years and are extensively reviewed elsewhere.[147]

A popular example of a label-free method is electro-chemical impedance sensing. Here, cells are cultured on culture plates with integrated microelectrodes, which continuously measure the electrical impedance signal.[150] This method is mainly applied to evaluate acute cytotoxicity but can also provide information on cell morphology.[147] In the last few years, several groups found good correlations between impedance-based acute toxicity measurements and data obtained with classical cell viability assays for different NPs in various cell types, underscoring the broad applicability of this method.[148, 149, 151] In addition, real time cell analyzers can be applied in a high throughput setting,[149, 151] which makes this method a good candidate for initial large scale safety screenings to identify the least acute cytotoxic NPs for a certain application.

c. Multiparametric nanosafety evaluation

Since it was observed that NPs can cause multiple effects *via* different mechanisms, awareness has risen on the necessity to evaluate nanotoxicity *in vitro* by a multiparametric method.[91, 152] Endpoints such as acute toxicity, ROS induction, morphological alterations, genotoxicity and NP degradation have been put forward as important parameters that should be included.[45, 120, 153] Even though no consensus on the optimal design of this multiparametric method has been reached yet, several examples have been proposed recently.[64, 152] We believe that methods to evaluate the effect on cell homeostasis should

preferably be biochemical or microscopy-based assays, as they are easily amendable for a screening approach.[120] Most importantly, positive and negative controls should be included during analysis and toxicity thresholds must be defined to allow appropriate interpretation of the observed effects. In addition, such schemes require the definition of and extrapolation to potential *in vivo* adverse events.

d. Screening approaches

Despite many recent efforts in the field of nanotoxicology, this discipline is not yet able to keep up with the tremendous pace of the development of new nanomaterials. In order to overcome this impediment, several groups have proposed to apply high throughput or high content screening approaches to assess nanosafety.[45, 149, 154] The use of screening techniques is imperative to enable simultaneous testing of multiple doses in different cell types by using various assays in a reasonable amount of time.[120, 153] When combined with a multiparametric approach, high content imaging is a highly promising tool as it allows the extraction and evaluation of multiple parameters simultaneously in thousands of cells for every evaluated condition.[155, 156] Consequently, such techniques can be implemented for NP toxicity fingerprinting as well as to prioritize NPs for *in vivo* evaluations.[154] Finally, several groups also suggest the implementation of omic-techniques to screen for genotoxicity, alterations in protein expression or biomarkers related to cellular pathways.[92, 157]

e. Assessments at single cell level

Most assays and techniques provide a single end point value for the entire cell population. However, it has been shown that NP uptake is often not homogeneous. In contrast, NP uptake can vary quite extensively between different cells in the same population depending on the size of the cell, the cell cycle phase during NP contact and on the NP agglomeration state.[158, 159] The recently developed high content techniques have enabled the analysis of cell-NP interactions at the single cell level, which showed that the evoked responses can be correlated to the intracellular NP dose.[158, 159] For instance, Manshian *et al.* divided the cells into different groups based on the intracellular QD dose and obtained different cellular responses in these groups. Low intracellular doses could be correlated with cytoprotective events, whereas cells with a high QD loading experienced cytotoxicity, which combined lead to a zero net result for the overall population.[159]

f. QSAR and in silico models

Screening approaches will generate a vast amount of data at a high pace, causing the bottleneck of nanotoxicity testing to shift from the assay execution to data processing. Therefore bio-informatics are gaining importance as automated data analysis will be necessary to keep up with the rapidly evolving field of nanotechnology.[160]

A popular subject in bio-informatics is the setup of an *in silico* approach to nanotoxicity with the development of quantitative structure-activity relationships (QSAR) as the ultimate goal. These QSARs will in turn allow the prediction of the toxicity of newly engineered NPs based on their physicochemical properties, enabling an even faster evolution of nanotechnology through a safety-by-design approach.[160] The development of *in silico* models and HCS go hand in hand as on the one hand the development of a reliable *in silico* model requires a large amount of data, which can be provided by HCS and bio-informatic tools are on the other hand indispensable for an efficient processing of HCS data.[160] Recently, Puzyn *et al.* developed a QSAR that predicts the toxicity of metal oxide NPs in *E. Coli* based on the effect of 17 different metal oxide NPs.[161] However, many obstacles still need to be overcome before the implementation of the first QSAR that allows the prediction of the adverse effects of any NP towards human health. Therefore, clear correlations between the NPs physicochemical properties and observed effect must be found, large-scale comparative studies should be performed and the QSARs must be validated, which requires the identification of reference nanomaterials with well-known effects.[45, 91]

3. THE NATURE OF CELL TYPE-DEPENDENT EFFECTS

In vitro studies are mostly performed on cancer cell lines or long-lived cell lines, as these are readily available, relatively inexpensive and easy to cultivate due to their enhanced proliferative capacity. Yet, it is known that cancer cells have a disturbed apoptotic balance and a higher metabolic activity to sustain their high proliferation rate.[162] Overall, cancer cells express an altered phenotype compared to primary cells characterized by a loss of normal cell features, enlarged irregular nuclei, a small cytoplasmic volume and an irregular cell size, shape and arrangement.[163] Long lived cell lines in turn express a phenotype that is not entirely stable, as changes may have been induced intentionally during their immortalization or unintentionally by the long cultivation time and extensive *in vitro* manipulation.[164, 165]

These alterations may include changes in cellular homeostasis, growth potential, biological responses, signal transduction etc. Hence, doubts have been raised on whether these cell lines are a reliable representation of the *in vivo* situation and on their usefulness for general *in vitro* nanosafety evaluations. Subsequently, the use of primary cells or stem cells has been put forward as an alternative since it is assumed that these cells mimic the *in vivo* cellular situation more closely.[165, 166] However, these cells are not always easily obtained and require specific handling, making them a less suitable cell model for screening approaches. In addition, primary cells may in turn suffer from batch-to-batch differences, which could lead to a reduced reproducibility that is not an issue for cell lines. The use of pooled stocks may be a good strategy to overcome these interbatch differences and allows taking interindividual variations into account, which is in turn not possible when applying cell lines. This section summarizes several studies that verified whether various cell types differ in their way of handling administered NPs in terms of NP uptake and cytotoxicity.

3.1. Effect of the cell type on nanoparticle uptake and processing

Most NPs enter the cell through the process of endocytosis. Some exceptions can be found as for phagocytic cells phagocytosis remains the main uptake mechanism.[167] Wang *et al.* furthermore observed QD uptake by passive diffusion in red blood cells.[168] But this must be put into perspective, as red blood cells are not capable of endocytosis.

The uptake mechanism is highly important as it determines the intracellular location of the NPs. NPs entering the cell by passive diffusion will directly interact with the cytosol, while NPs taken up by endo- or phagocytosis are retained in vesicles, which can be distributed throughout the cytoplasm or localized in a specific cellular region.[168, 169]

The uptake kinetics and intracellular location were compared in different cell types since they are important determinants for the final response. For example, the uptake of 1.9 nm diameter AuNPs was found to be higher in human prostate and breast cancer cell lines (DU154 and MDA-MB231) than in a human lung epithelium long-lived cell line (L132).[170] Diaz *et al.* compared the uptake of five different NPs in normal human monocytes, lymphocytes and erythrocytes, mouse macrophages and four human cancer cell lines: a myeloid-monocytic cell line (U937), a T-cell line (Jurkat), a B-cell line (HMY) and a prostatic cancer cell line (PC3). Human monocytes rapidly phagocytized all NPs tested but the mouse

macrophages showed an even higher uptake, which was comparable to the uptake in PC3 cells. The monocytic cell line did not show NP internalization, which is in conflict with results from other studies showing a higher uptake capacity for cancer cell lines.[170-172] As all other cell types tested did not show significant NP uptake, the authors have put the phagocytic machinery in combination with the cell type forward as predominant factors for NP uptake.[173] This is the general belief and is supported by several studies.[174]

Regarding intracellular localization of the same particles in different cell types, widely varying results have been obtained. PEGylated micelles, for example, were shown to have similar distributions in a human lung cancer cell line and long-lived cell line (A549 and MRC-5) and a human kidney epithelium long-lived cell line (293T).[162] However, Barua and Rege observed significant variations in intracellular localization of QDs in three phenotypically closely related human prostate cancer cell lines (Figure 5.2). It was observed that the QDs were trapped in lysosomes scattered throughout the cytoplasm in PC3 cells, localized at a single juxtanuclear location in PC3-PSMA cells and a combination of both was found in PC3-flu cells.[175] They coupled these observations to (i) the loss of polarity in malignant cells influencing the sorting and trafficking potency of the cells, (ii) the slight differences in receptor expression profiles and (iii) a disruption of the microtubule network in PC3 cells impeding further trafficking to the juxtanuclear region.[175]

It is clear that the cell type is an important factor to NP uptake, influencing both the uptake mechanism as well as the extent, with cancer cell lines mostly showing higher uptake levels when compared to uptake in long-lived cell lines and primary cells. Intracellular distribution also appears to be cell type dependent and has even been found to differ substantially between phenotypically closely related cell lines. Therefore these findings underscore the importance of selecting a representative cell type that mimics the *in vivo* situation as closely as possible, as toxicity is logically related to NP uptake, determining the cellular dose and location of the NPs.

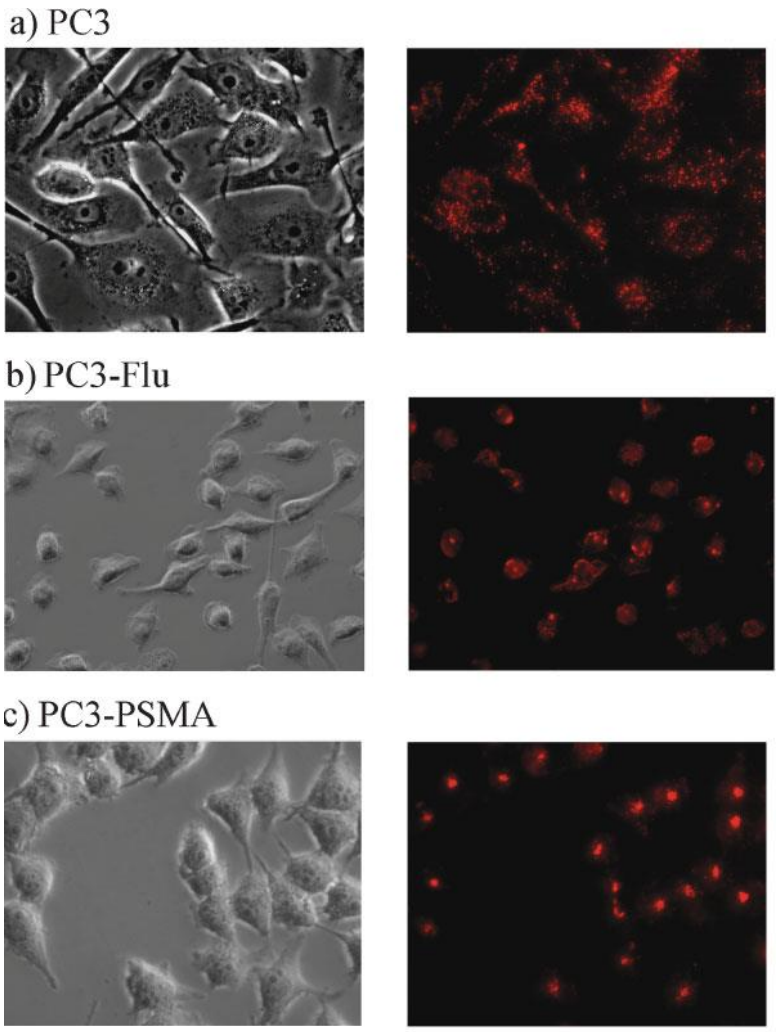

Figure 5.2. The effect of cell phenotype on NP processing as illustrated by the clear differential intracellular localization patterns of QDs in highly similar, but slightly differing human PC3 cells. (a) PC3, (b) PC3-flu, (c) PC3-PSMA. This figure is reproduced with permission from Barua and Rege.[176] © Wiley-VCH 2009.

3.2. Effect of the cell type on NP toxicity

Only recently more awareness was raised on cell type-dependent effects being one of the factors leading to discordant *in vitro* nanotoxicity data. Since the use of cell lines for *in vitro* nanotoxicity assessment has been put to question, several groups compared the effects of NP exposure in cell lines to those in primary or stem cells representing the same tissue. In various cases, the primary cells and stem cells have been found to be less sensitive to NP toxicity than long-lived cancer cell lines.[164, 176] For instance, Hanley *et al.* found two human T-cell lymphoma cell lines (Jurkat and Hut-78) to be respectively 28- and 35-fold more sensitive to ZnONP exposure than human primary T-cells (Figure 5.3A).[177] In contrast, Bregoli *et al.* observed an impaired proliferation in primary human hematopoietic progenitor cells

after antimony oxide NP exposure while the proliferative capacity of none of the seven hematopoietic (cancer and long-lived) cell lines tested was affected.[165] Likewise, three independent groups found normal bronchial epithelial cells to experience more acute toxicity following NP exposure than the A549 cancer cell line or 16HBE immortalized cell line.[122-124] In contrast, Kermanizadeh *et al.* found similar responses to different NPs in both primary human hepatocytes and the hepatoma C3A cell line, indicating that certain cell lines can be applied to model nanosafety.[178] Hence, this body of data warrants the careful selection of a cell model and a case-by-case evaluation of the applicability of a certain cell line.

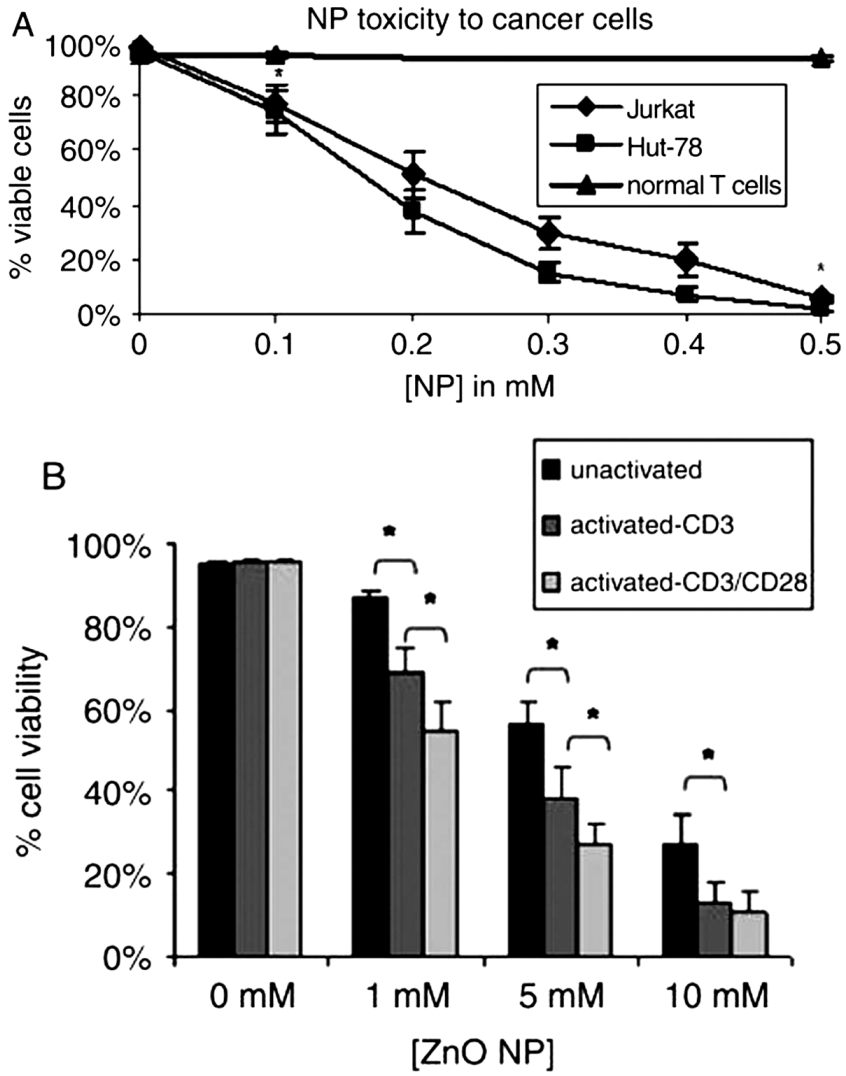

Figure 5.3. The effect of cell phenotype on NP toxicity as illustrated by (A) differential viability after ZnONP exposure of Jurkat and Hut-78 cancer cell lines and normal human T lymphocytes and (B) differential viability after ZnONP exposure for unactivated and activated human T lymphocytes. This figure is reproduced with permission from Hanley et al.[178] © IOP Sciences 2008.

As the focus of *in vitro* toxicity testing is shifting to the use of primary cells, it was put to question whether cellular differentiation has an influence on the induced toxicity. Several studies show a higher sensitivity towards nanotoxicity for differentiated cells, which can be explained by the fact that undifferentiated cells adapt better to new conditions than differentiated cells.[179, 154] Accordingly, Saretzki *et al.* found the stress defence mechanism (antioxidant capacity and DNA repair mechanism) in murine embryonic stem cell to be superior to that of various differentiated murine cells (fibroblasts, hematopoietic progenitor cells and 3T3 fibroblast long-lived cell line).[180]

A number of groups furthermore tried to elucidate the mechanisms causing various cell types to react differently to NP exposure. First of all the physiological cell function appears to be important. For instance, macrophages and monocytes are involved in the clearing of xenobiotics as they can ingest many compounds in high quantities by phagocytosis, which explains the higher uptake levels and susceptibility to nanotoxicity.[173, 174, 181] A second factor is the variation in proliferative capacity of different cell types: rapidly proliferating cells can experience less toxicity due to the fast dilution of the cellular NP contents with every cell division. Indeed, Chang *et al.* found three epithelial cancer cell lines (A549, MKN-28 and HT-29, average doubling time 23h) to be less prone to silica (SiO_2)NP-induced injury than three long-lived fibroblast cell lines (WS1, CCD-966sk and MRC-5, average doubling time 128.4h). This was explained by the higher cell division rate of the former and the associated dilution of cellular NP levels.[182] Additionally, NP uptake depends on the cell cycle phase, being maximal in the G2/M phase. Therefore, rapidly proliferating cells may experience more cytotoxicity due to higher NP uptake levels. This was demonstrated by Hanley *et al.* as activated primary human T lymphocytes showed a higher susceptibility to ZnONP-induced injury in comparison to resting human T lymphocytes due to the preferential targeting of the actively proliferating cells (Figure 5.3B).[177] A final factor is intrinsic variations between cell types such as their natural anti-oxidative capacity. For instance, Mukherjee *et al.* accounted the stronger ROS induction and GSH depletion by AgNPs in HeLa cells compared to the HaCaT cells (a human dermal cancer cell line) to the lower natural antioxidant capacity of the former.[183]

Overall, the response to NP exposure is highly cell type-dependent and the observed differences in sensitivity may largely be explained by variations in cell function influencing NP uptake, metabolic activity, natural antioxidant activity and proliferative capacity. These data underscore the importance of selecting a relevant cell system for NP hazard assessment, which is a balancing act since both primary cells and cell lines show specific advantages and major shortcomings. Therefore, further research is needed in order to determine proper cell models and according cell culture protocols.

4. THE EFFECT OF NP AGGLOMERATION AND SEDIMENTATION

Initially it was assumed that the NP dose to which cells are exposed, is accurately represented by the concentration of the NP dispersion since NPs were believed to be evenly dispersed by Brownian motion.[34] This appeared not to be true, as NPs in dispersion are additionally subject to agglomeration or aggregation and sedimentation.[110, 184] It is important to note the difference between agglomeration and aggregation since both terms are often confused: aggregates are formed by covalent bonds and are therefore not as easy to break as agglomerates, which are held together by van der Waals forces, hydrophobic interactions and/or hydrogen-bonds.[185] The formation of agglomerates originates from the pursuit of a state with a lower free surface energy and is strongly promoted by the hydrophobic nature of most NPs.[173, 185] Thus, agglomeration occurs in media when attractive forces overpower the electrostatic or steric repulsion between NPs.[186] Since both diffusion and sedimentation are influenced by agglomeration, the latter is expected to have a major impact on NP uptake and toxicity.[187] Therefore the concept of dose is more complex and dynamic for NPs and requires the modeling of the NP behavior in dispersion.[110, 144]

Several NP- and medium-related factors have been shown to influence NP agglomeration. Parameters in the first category are the NP surface charge, size and shape. For example nanorods and –fibers agglomerate more easily than spheres and smaller NPs typically aggregate more than their larger counterparts at similar mass doses, which can be explained by the higher number density.[188, 189] Several medium-related parameters like pH, salt composition and ion concentration were also suggested to potentially influence NP agglomeration.[186, 190, 191] Additionally, the presence of proteins has been shown to be a very important factor.[186] Yet, its effect on NP agglomeration is not fully understood as several

groups obtained conflicting data, showing either less or more agglomeration in serum containing media.[192, 193] However, several groups recently showed that mixing the NPs with serum protein prior to the addition to culture medium, stabilizes the final NP dispersion.[184, 194, 195]

It is crucial to take the influence of NP agglomeration on diffusion and sedimentation and subsequently on NP uptake and toxicity into account when evaluating nanosafety. Certainly since agglomerates or aggregates show altered kinetics when compared to their single NP counterparts with the same size.[186] However, evaluating NP agglomeration in the applied cell medium or biological fluid is not an easy task. Dynamic light scattering is a commonly used technique but is limited to samples in simple or diluted media as other light scattering components, such as serum proteins, can interfere with the measurements.[196] To overcome these obstacles, alternative methods have been put forward, such as the use of fluorescence correlation spectroscopy or fluorescent single particle tracking, which allow the accurate and precise determination of the size distribution of fluorescent NPs in undiluted biological fluids.[196, 197] Additionally, UV spectroscopy can be applied to evaluate the dispersion state of NPs with a surface plasmon resonance.[194]

This section provides an overview of studies evaluating the influence of NP sedimentation on uptake and toxicity as well as innovative setups to avoid the effect of sedimentation during *in vitro* nanosafety assessments.

4.1. Effect of nanoparticle agglomeration and sedimentation on NP uptake

Several studies showed that the impact of agglomeration is not straightforward, as aggregates show either enhanced or impeded uptake when compared to single NPs.[188, 189, 192, 194, 195] The higher uptake levels for aggregates can be explained by the fact that they reach the cells more rapidly by sedimentation, while the transport rate of single NPs is limited by diffusion.[189] In contrast, agglomerates have a fractal structure and thus a lower mass density compared to a solid NP of a similar size, which reduces the sedimentation rate and potentially NP uptake.[144] Hence, agglomerates will not necessarily behave as a NP of the same size, further complicating nanosafety assessments.[106] Indeed, Hirsh *et al.* found 65 nm AuNPs to be more rapidly and extensively taken up by HeLa cells than agglomerates at least double their size.[184] In addition, when the agglomerate/aggregate size is similar to, or larger

than the cell itself, uptake is impeded by physical restrictions to the uptake processes.[188, 192] These observations support the assumption that larger aggregates do not enter the cell *via* the same mechanism as single NPs or small agglomerates, as most common endocytosis routes like clathrin- or caveolin-mediated endocytosis are limited to the uptake of materials with dimensions of maximally 120 nm.[192]

From the available (conflicting) data it cannot be concluded whether single NPs or small agglomerates/aggregates are taken up to a greater or lesser extent, but we do hypothesize that following factors are equally important; (i) the extent of agglomeration/aggregation, (ii) the size and density of the NPs/agglomerates/aggregates and (iii) the cellular uptake mechanism. The extent of agglomeration and the size of the agglomerates will not only determine the rate of sedimentation, and hereby the rate of NP transport towards the cells, but also the way in which the cells will handle these materials. Non-specialized cells will typically prefer smaller NPs, while cells capable of ingesting larger materials will take up higher levels of agglomerates. As such, it is clear that agglomeration and sedimentation have an influence on NP uptake that cannot be neglected.

4.2. Effect of nanoparticle agglomeration and sedimentation on NP toxicity

Similar to NP uptake, the influence of agglomeration/aggregation on nanotoxicity is not straightforward. On the one hand, clear correlations have been found between NP concentration, aggregation, precipitation and cell injury for ZnONPs, QDs and carbon nanotubes (CNTs).[36, 195, 198] On the other hand, several studies show reduced cytotoxicity for agglomerated NPs, due to the fact that smaller entities are in general taken up more avidly by non-specialized cells and more easily reach intracellular structures such as the cell nucleus or mitochondria, which are less accessible to larger NPs or agglomerates.[188, 199, 200] Yoon *et al*. further hypothesized that adherent cells might be more affected by NP deposition through sedimentation than cells in suspension and therefore compared aluminum oxide NP and agglomerate toxicity in suspension cells (THP-1) and three adherent cell lines (A549, 293T and J774A-1: a mouse macrophage cancer cell line). Toxicity was observed in the THP-1, A549 and 293T cell lines, but only in the A549 and 293T cell lines was time dependent toxicity witnessed that could be related to sedimentation of the agglomerates, which confirmed their hypothesis.[201] Likewise, Anders *et al.* observed increased and reduced nanotoxicity in suspension and adherent cultures, respectively when

exposed to stable NP dispersions compared to dispersions containing agglomerates.[195] In addition, agglomerate size is an influencing factor, as Sharma *et al.* found smaller IONP agglomerates to induce more severe effects than their larger counterparts at similar cellular mass doses.[106]

These data highlight the influence of NP sedimentation on *in vitro* nanotoxicity studies and indicate that it can result in either underestimated or exaggerated toxicity estimations. Therefore, in order to reduce the *in vitro-in vivo* gap, there is a need for novel models in which the effect of NP sedimentation can be avoided. Such models should provide results that are more relevant to the applied NP dose rather than reaching unrealistically high cell exposure levels due to NP sedimentation.

4.3. New model systems to minimize sedimentation effects

Since sedimentation is not observed *in vivo* and was demonstrated to affect nanotoxicity *in vitro*, several groups have tried to develop novel model systems such as inverted cultures, flow models and microfluidic systems in which the influence of sedimentation can be reduced or completely avoided.

4.3.1. Inverted models

Cho *et al.* developed an inverted cell model in which they evaluated the influence of sedimentation on uptake of Au nanospheres, -cages and -rods in human breast cancer cells (SK-BR-3). This is an elegant and straightforward cell model in which sedimentation itself is not avoided but will not result in increased cellular exposure levels for cells that are cultured in the inverted configuration (cells grown on an insert at the top of the medium, facing downwards). The authors observed much more avid NP internalization in classical cell cultures in comparison to cells cultured in the inverted configuration (Figure 5.4). However, no variations were observed in toxicity: cell viability remained approximately 90% of the control values in all conditions tested, but this may be due to the type of material and the limited concentration range tested. Overall, the differential uptake in upright or inverted configuration depended on the NPs physical properties and was most distinct for NPs with a greater propensity to sediment, underscoring the necessity to avoid the influence of NP sedimentation.[34]

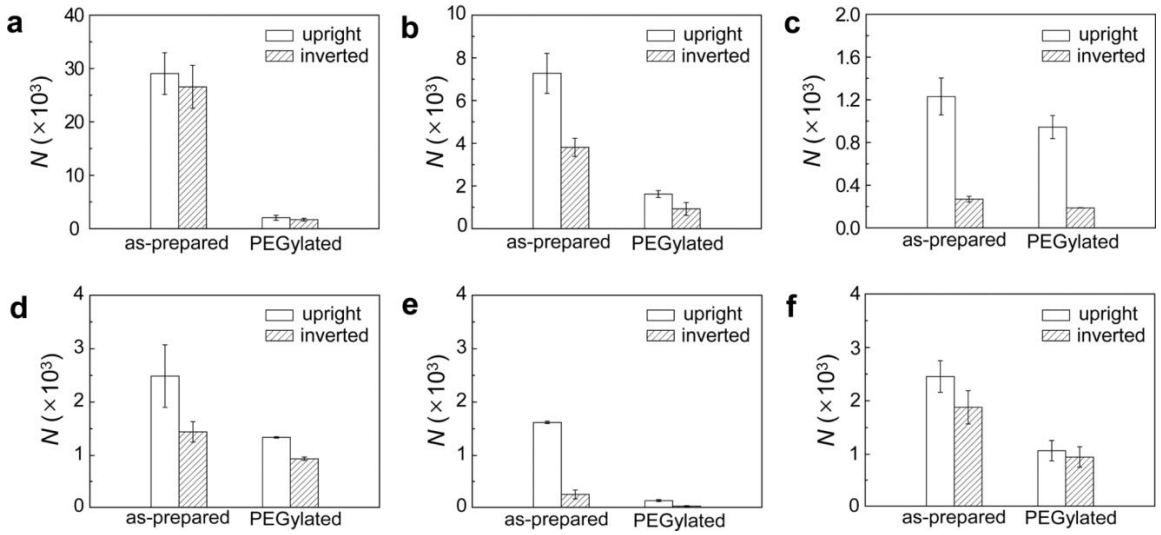

Figure 5.4. The effect of cell culture configurations (normal horizontal (= upright) versus hanging down (= inverted)) on the uptake of various types of NPs. Differential uptake of (a) 15 nm nanospheres (120 pM); (b) 54 nm nanospheres (20 pM); (c) 100 nm nanospheres (2.8 pM); (d) 62 nm nanocages (20 pM); (e) 118 nm nanocages (2.6 pM); and (f) nanorods (20 pM) in the upright and inverted configuration. This figure is reproduced with permission from Cho et al.[34] © Nature Publishing Group 2011.

4.3.2. Flow and microfluidic models

More complicated models are flow or microfluidic systems where gravitational setting is impeded or even completely avoided. The applied flow also assists in acquiring a more homogeneous NP distribution and alters the cell-NP contact time.[36, 121] Additionally, applying a flow implies the continuous renewal of culture medium, which ensures a sustained supply of nutrients and a constant pH.[35] To us, the main advantage is that cells show a more *in vivo*-like behavior as a laminar flow can activate endothelial cells and suppress proliferation, apoptosis and ROS induction.[202] Cellular morphology is also altered as the shear stress (SS) induces elongation of endothelial cells in the direction of the applied flow and formation of actin stress fibers, which cluster around the nucleus to protect the cells from hemodynamic damage.[202-204] Finally, Samuel *et al.* observed membrane blebbing under flow conditions, whereas cells under static conditions showed a smooth and flattened membrane.[204]

Several groups compared NP uptake under flow and static conditions. Samuel *et al.* observed uptake of untargeted NPs in cells from a HUVEC cell line (CRL-1730) under flow conditions but not in the classical static 2D cultures. They also did not find any difference in NP uptake in activated or unactivated CRL-1730 cells.[204] In contrast, most other groups typically found higher uptake levels under static conditions, due to the contribution of NP agglomeration

and sedimentation.[203, 205, 206] In addition, most studies clearly show higher uptake levels for targeted NPs in activated endothelial cells.[203, 204, 205]

Subsequently the influence of the level of applied SS on NP uptake was explored. Most studies found the highest uptake under the lowest SS, as NPs are more likely to sediment on top of the cells under these conditions, which prolongs the cell-NP contact time.[207,208]

As uptake is significantly altered under flow conditions it is expected that the same will be true for nanotoxicity. On the one hand Mahto *et al.* observed significantly higher levels of QD toxicity in 3T3 fibroblasts in static configuration following a 12h exposure time: cells in static condition showed approximately 30% cell viability whereas the percentage of living cells under SS remained as high as 75% and significantly fewer cells were deformed or detached.[35] Kim *et al.* on the other hand found significant levels of toxicity under high SS conditions whereas HUVECs under static conditions or low SS did not show significant toxicity after 2h exposure to unmodified SiO_2NPs. They accounted this difference to the possible activation of the HUVECs under higher SS,[121] while we believe that the shorter incubation time must also be taken into account.

Interestingly the application of shear stress was also shown to alter NP agglomerate size and the polydispersity of the NP dispersion.[209] Finally, Braun *et al.* reported that shear flow alters the protein corona as the protein concentration present on PEG- and tannic acid-coated AuNPs subjected to flow was increased with ˜25% compared to the protein corona present on the same NPs in the same medium under static conditions. This observation was explained by the increased possibility for NP-protein interactions leading to a greater number of proteins adsorbed onto the NP surface.[210]

It is clear from these data that toxicity levels found in classical 2D monocultures are either exaggerated or underestimated in comparison to levels obtained from *in vitro* experiments where (the effect of) sedimentation is avoided. When NP toxicity is evaluated in a flow system an extra level of complexity is added as the induced SS has an impact on the NP dispersion characteristics, the protein corona and cell behavior, which in turn influence NP uptake and toxicity. It is observed that targeted NPs are taken up more avidly under flow conditions, while non-functionalized NPs show higher uptake under static conditions. Nanotoxicity results are on the contrary conflicting so no firm conclusions can be drawn on

this subject yet. However, as toxicity levels measured in these novel model systems significantly differ from those obtained from classical static 2D monocultures, which are believed to be less *in vivo*-like, we believe that flow models should be optimized and that their use should be promoted.

5. THE EFFECT OF CELL COMMUNICATION

Another important shortcoming of the monoculture model is the lack of intercellular communication. This crosstalk between different cell types is known to be vital in sustaining homeostasis and in complicated processes like the processing of xenobiotics, inflammation and immune responses. Such events can consequently hardly be accurately mimicked in simplified monocultures.[211, 212]

Several groups have focused on establishing co-culture models in order to overcome this shortcoming and bridge the *in vitro-in vivo* gap. Multiple types of co-cultures can be set up representing various tissues. Here, two or more cell types are combined and cells can be cultured either in direct contact or be separated by culture inserts. Cells co-cultured on culture inserts show a more differentiated phenotype, develop tight and adherent junctions and are polarized, implying that the cells have an apical and basolateral membrane with a distinct composition.[213, 214] Thus, these models mimic the *in vivo* environment more closely and are therefore assumed to have a higher predictive power. This section provides an overview of studies evaluating NP uptake and toxicity in these novel model systems.

5.1. Effect of intercellular communication on NP uptake

Since it is well known that the majority of the NPs are rapidly taken up by the reticulo-endothelial system after intravenous administration, it was investigated whether the same trend could be observed *in vitro* in co-cultures of epithelial and phagocytic cells. Indeed, the highest and lowest uptake levels were respectively found in the macrophages and epithelial cells.[215] Furthermore, Rothen-Rutishauer *et al*. evaluated uptake of polystyrene beads, AuNPs and TiO_2NPs in a co-culture consisting of A549 cells, human monocyte derived macrophages (MDM) and human monocyte derived dendritic cells (MDDC). They observed preferential uptake of all NPs in the MDMs and the lowest uptake levels in A549 cells (Figure 5.5). Compared to the MDDCs, uptake in MDMs was twice as high, which was explained by

its 2-fold greater phagocytic capacity.[216] Likewise, when exposing mixed cultures of primary neural cells, microglia – the brain's macrophages – were shown to preferentially internalize NPs.[215] As previously mentioned, co-culturing cells can result in more differentiated and polarized cells that show a more barrier-like phenotype, which impedes NP uptake.[213]

Overall, NP uptake is significantly altered in co-cultures with the two main factors determining NP uptake being (i) the level of cellular differentiation and (ii) the combination of cell types and their preferential uptake mechanism, especially when phagocytic cells are included.

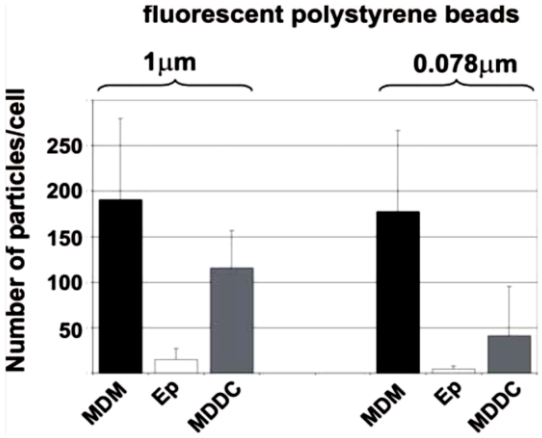

Figure 5.5. Preferential uptake of fluorescent polystyrene beads in human monocyte derived macrophages (MDM) in co-culture with A549 cells (EP) and human monocyte derived dendritic cells (MDDC). This figure is reproduced with permission from Rothen-Rutishauser et al.[217] © Biomed Central 2007.

5.2. Effect of intercellular communication on NP toxicity

Many studies on co-cultures apply models representing alveolar tissue since the lung is expected to be one of the major target organs for NP-induced toxicity following the inhalation of airborne NPs. In this regard, particulate matter (PM_{10}) treatment was shown to cause a co-culture to secrete more cytokines than the sum of the cytokine secretion observed in the corresponding monocultures.[217, 218] This increased cytokine production can in turn render cells more susceptible to NP-induced damage. For instance, Kim *et al.* observed that the NP-induced tumor necrosis factor$_\alpha$ (TNF_α) release by RAW264.7 cells in a RAW264.7/MLE12 (murine alveolar long-lived cell line) co-culture rendered this co-culture more susceptible to NP-induced apoptosis when compared to the respective monocultures.[219]

Another popular co-culture model consists of alveolar epithelial and microvascular endothelial cells to mimic the air-blood-barrier. Culture inserts separate the two cell types and only the epithelial cells (representing the apical membrane) are typically exposed to NPs. Various studies revealed that this type of co-culture is more resilient towards nanotoxicity in terms of acute toxicity but shows an increased inflammatory response.[213, 214, 220] In turn, Ramos-Godinez *et al.* did not find any changes in cytokine release by a A549/HUVEC co-culture due to TiO_2NP exposure. However, HUVECs from the co-culture did show a significant increase in adhesion molecules, a 3 to 4-fold increase in monocyte adhesion and a 2-fold increase in nitric oxide production. These results were comparable to HUVECs directly exposed to NPs, implying that endothelial cells were activated *via* intercellular communication.[221] Recently, this phenomenon was confirmed by Sisler *et al.* who observed actin remodeling, ROS induction and inflammation in HMVEC cells following NP exposure of the co-cultured small airway epithelial cells.[222] Importantly, in none of these studies the NPs were found to cross the culture insert, possibly due to the barrier formed by the epithelial cells or NP agglomeration, confirming that endothelial cells were activated through intercellular communication after NP exposure of the epithelial cells.

The activation status of macrophages in co-culture has also been shown to influence nanotoxicity: non-activated macrophages act as a reservoir, thus performing a protective function, while activated macrophages elicit secondary toxicity in the accompanying cell type *via* cytokine secretion.[223, 224] According to van Berlo *et al.* the protective or aggravating effect towards NP toxicity furthermore depends on the combination of cell types as they found macrophages to protect A549 cells against oxidative DNA damage whereas the neutrophils aggravated the effects.[225]

The complexity of the model can further be increased *via* the introduction of additional cell types. For example, Alfaro-Moreno *et al.* evaluated the effects of PM_{10} in several combinations of cell lines: A549/HMC-1, THP-1/HMC-1, A549/THP-1/HMC-1 and A549/THP-1/HMC-1/EAhy296. They found that all cultures had a distinct cytokine excretion profile with the cytokine production being either amplified or mitigated in co-culture, which was confirmed by Napierska *et al*.[226, 227] This was explained by the differential expression of cell surface receptors depending on the cell type or changes in crosstalk between the cells by adding of an extra cell type.[226] Besides the cytokine excretion, Müller *et al.* also found the

total antioxidant capacity to be modulated in an A549, MDC and MDDC co-culture.[228] Finally, Clift *et al.* investigated the effect of CNT on 16HBE, MDM, MDDC monocultures and their triple culture. They found the TNF_{α} secretion to be highest in both MDM and MDDC monocultures, the interleukin (IL)8 secretion to be less pronounced in the 16HBE monoculture than the triple culture and the effect on ROS production to vary in all four models.[229]

Besides models representing the lung, additional co-culture models were established to mimic various tissues or barriers. For instance, Lui *et al.* combined HUVEC and THP-1 cells and found the NP-exposed co-culture to secrete higher cytokines levels than the monocultures and found the monocytes to activate the HUVECs, concurrent to observations in the lung.[230] In turn, Xu *et al.* modeled the blood brain barrier (BBB) through the combination of primary rat microvascular endothelial cells, pericytes and astrocytes. Upon exposure to AgNPs, they observed an increased blood brain barrier permeability, reduced gap junctions, a reduced anti-oxidative capacity, an inflammatory response and apoptosis.[231] The gastro-intestinal (GI) tract can furthermore be modeled by combining the Caco-2/TC7 and the mucus secreting HT29-MTX colon carcinoma cell lines. The mucus was shown to have a protective effect towards NP-induced damage and the co-culture again responded differently towards AgNP exposure than the corresponding monocultures.[232] Additionally, Walczak *et al.* applied the Caco-2 cell line as a monoculture and in co-cultures combined with HT29-MTX alone or HT29-MTX and M-cells to evaluate NP translocation. The secreted mucus in the Caco-2/HT29-MTX co-culture reduced NP translocation whereas results from the triple and monoculture were quite similar.[233]

In summary, cells respond differently to NP exposure in a mono- or co-culture setup. Apart from some exceptions, co-cultures are generally found to be more resilient to acute toxicity but show a significant increase in cytokine release, indicative of an inflammatory response. Hence, co-culture models allow the study of effects that could not be picked up in monoculture experiments. However, given that the observed effect depends on the applied combination of cell types and can be altered by the addition of an extra cell type, standardization is required. In addition, the predictive power of these models should be confirmed, certainly since Braakhuis *et al.* unexpectedly found the best correlation with *in vivo* data for the 16HBE monoculture rather than the 16HBE/HUVEC/THP-1 triple culture.[234]

6. THE EFFECT OF A 3D ENVIRONMENT

The loss of the specific 3D tissue architecture and cell polarization is a final major shortcoming of monocultures. This can be overcome by applying 3D cultures, where cells show a more *in vivo*-like phenotype as well as ECM production. Additionally, the cell-cell and cell-matrix communication is promoted due to the tighter packing of the cells in a 3D setup. In turn, the enhanced communication influences a number of important cellular functions such as migration, invasion, proliferation, apoptosis and differentiation.[235] Consequently, cells cultured in a 3D setup are able to acquire tissue-like organization and differentiation to levels that have thus far been impossible to reach in a classical 2D setting.[129, 236] Thus, cellular responses to NP exposure in a 3D model are expected to be significantly different from those observed in a monolayer culture.[127]

Furthermore, the cultivation time of cells in 3D models can be prolonged, which enables long(er)-term *in vitro* experiments.[237] Hence, 3D models allow the evaluation of cumulative effects of repeated NP exposure, which is less feasible in 2D cultures since cells do not survive longer cultivation periods, dedifferentiate or rapidly divide causing dilution of the NPs and an associated dilution of possible effects.

A number of 3D systems have been developed of which the multicellular spheroid models, mimicking solid tumours, are most widely used. Another approach is the use of natural or synthetic hydrogels as a scaffold in which cells can be seeded.[238] However, hydrogel-based scaffolds are likely to be less useful for nanosafety studies as thick scaffolds may limit NP diffusion towards the cells. The recent use of 3D models to assess nanosafety is discussed in this section.

6.1. Effect of a 3D environment on NP uptake

Since cells cultured in spheroids are known to produce a more dense and complex ECM, several groups compared NP uptake in a 2D and 3D setting. In comparison to classical 2D monocultures where NPs are taken up by all cells, an uneven distribution and limited penetration is obtained in spheroids.[235, 239, 240] Consequently, NP uptake is generally lower and found to be restricted to the peripheral layers of the spheres.[235, 240] An interesting study by Huang *et al.* compared 2, 6 and 15 nm AuNP uptake in an MCF-7 monolayer, spheroid model and mouse breast tumors *in vivo*. The spheroids and tumors showed similar trends in

tissue penetration as 2 and 6 nm NPs could penetrate the deeper regions of the cell mass, but 15 nm NPs were only found in the periphery. In contrast, all NPs were evenly distributed throughout the monolayer.[241] Thus, NP distribution is generally less homogeneous in 3D cultures and the ECM hampers NP penetration into a 3D matrix. This limits NP uptake to the cells in the peripheral layers of the 3D culture, especially for larger NPs.

6.2. Effect of a 3D environment on NP toxicity

Subsequently, several groups compared NP-induced toxicity in 2D and 3D cultures. In general, the toxicity induced by NP enclosed anti-cancer agents was found to be significantly lower (5- to 20-fold) in spheroid models than in the classical monolayer.[235, 239] Concurrently, various groups confirmed that this paradigm also accounts for inorganic NPs, as for instance CdSe/ZnS QD-, IONP- and SiO_2NP-induced toxicity in HeLa microspheres was radial and lower in the 3D setup.[128, 240, 242]

In one of the first studies using 3D models for nanotoxicity purposes Lee *et al*. evaluated 2.9 nm QD and 3.5 nm AuNP toxicity in HepG2 2D and spheroid cultures and found a substantially lower toxicity in the latter. The number of dead cells was significantly lower in the 3D setup and most dead cells were found in the periphery of the sphere, creating a rugged surface (Figure 5.6). Longer exposure times induced more severe damage to the cells in periphery of the sphere while the interior remained unimpaired. When the same incubation conditions were applied to 2D cultures, they overall observed more cell death (Figure 5.7). The core of the sphere remained unaffected due to the protective effect of the barrier created by the ECM and the dead cells remaining on the exterior of the sphere due to the initial tight packing, thereby temporarily enhancing the efficiency of the barrier.[243] Chia *et al.* obtained similar results upon exposing a colon cell spheroid culture to ZnONPs. However, they noted only a temporary protective effect of the outer layer consisting of the ECM and dead cells.[244] In addition, they observed different modes of ZnONP-induced cell death for cell cultured in a monolayer or a spheroid and the cytokine production by the outer cells of the sphere was shown to induce an inflammatory response in the core cells.[244] In correspondence to many studies, AgNPs, SiO_2NP and ZnONPs induced more severe toxicity in a 2D HepG2 culture. Of note, the outcome in the 3D model depended on the matrix material applied to create the spheroid culture, as for all NPs tested HepG2 cells in Matrigel and collagen experienced the least and most cytotoxicity, respectively.[236] This

warrants the need for further optimization of 3D spheroid models as well as the confirmation of the predictive value towards *in vivo* adverse outcomes.

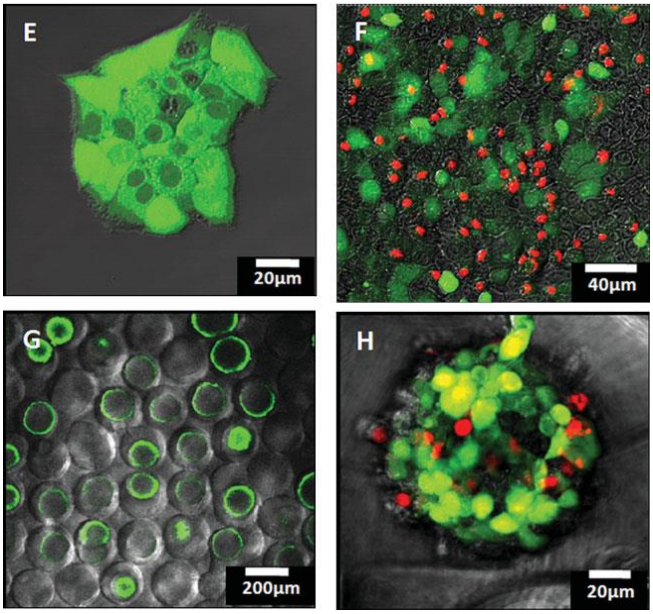

Figure 5.6. The effect of NP toxicity in both a 2D and 3D cellular environment. Confocal images of live/dead (red)-stained normal (E) 2D and (G) 3D spheroid cultures and after QD exposure in (F) 2D and (H) 3D spheroid cultures. This figure is reproduced with permission from Lee et al.[243] © Wiley-VCH 2009.

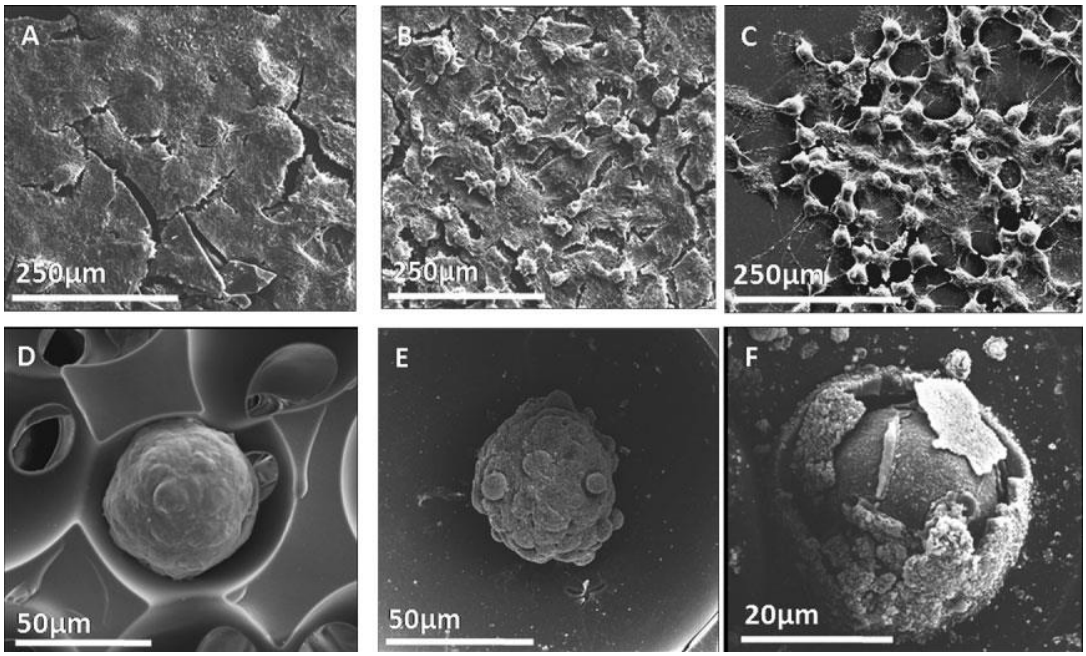

Figure 5.7. Effect of NPs on cell morphology on 2D and 3D cell cultures. SEM images of 2D and 3D spheroid cultures before and after CdTe QD exposure. Typical morphology of (A) 2D and (D) 3D spheroid cultures after 5 days without CdTe QD exposure. Representative morphology of (B) 2D and (E) 3D spheroid cultures after 12 h of CdTe QD treatment. Morphological change of (C) 2D and (F) 3D spheroid cultures after 24 h of CdTe QD exposure. This figure is reproduced with permission from Lee et al.[243] © Wiley-VCH 2009.

In conflict with most observations, Sambale *et al.* did not observe significant differences in ZnONP-evoked cell injury in NIH-3T3 spheroid cultures. Additionally, A549 spheroids were more severely affected than the corresponding monolayer, which was explained by the loose confirmation of the spheroid.[245] Likewise, Yu *et al.* found 5 and 30 nm IONPs to cause more severe toxicity to porcine aortic endothelial cells in a 3D alginate matrix than in a conventional monolayer. However, it must be noted that cells were unable to divide once added to the matrix while cells in 2D culture retained their proliferative capacity. Since toxicity was measured after 72h exposure time, cells in 2D cultures were likely to be exposed to lower IONP doses as the NPs were diluted upon cell division. This protective effect was likely to be impeded in the 3D setup, possibly causing the cells to show higher stress levels and toxicity.[246]

In conclusion, culturing cells in a 3D setup has a major influence on the phenotype and cell function and provides different insights on NP-induced damage, which could not be retrieved from the corresponding monolayer cultures. Importantly, most studies show hampered NP penetration through the ECM barrier and altered cellular uptake. Subsequently, toxicity is generally less pronounced and limited to the outer layers of the sphere. Overall, we believe that the development of 3D models is a recent milestone in bridging the *in vitro-in vivo* gap and that these models are likely to gain importance in the coming years.

7. ALTERNATIVE CELL MODELS

Since the cell model was shown to have a major impact on nanosafety studies, alternative or even more complex cell models were recently applied, of which several examples are discussed in this section.

Susewind *et al.* developed a 3D co-culture model that represents the intestinal mucosa. Hereto the THP-1 and MUTZ-3 (human dendritic cells) cell lines were cultured in a collagen scaffold which remained separated from the Caco-2 cell line *via* a Transwell insert. They observed less acute toxicity and increased IL8 release in the 3D co-culture model than in the corresponding monocultures, which is in line with previously discussed results.[247] In turn, Klein *et al.* seeded A549, THP-1, HMC-1 and EA.hy926 cells on a microporous membrane to

achieve a 3D orientation. Uptake of aerosolized SiO_2NPs at the air-liquid interface was only observed in the THP-1 cells and ROS levels were significantly lower in their model compared to the respective monocultures.[248] Furthermore, the lung can be represented by the commercially available human primary bronchial epithelial 3D MucilAir^{TM} model. CeO_2NP uptake in this model was found to be hindered by the presence of respiratory mucus due to NP aggregation and NP removal by mucociliary clearance. In consequence no CeO_2NP–related toxicity was observed in this model in contrast to A549 and BEAS-2B monocultures.[249] Furthermore, precision cut lung slices were combined with a human macrophage cell line (AMJ2-C11) to allow the evaluation of the role of macrophages on injury at the organ level.[250] Kermanizadeh *et al.* in turn established the applicability of a commercially available 3D liver microtissue model to evaluate nanosafety. This model allows repeated exposure experiments, which were shown to elicit more severe effects than a single NP exposure, with the toxicity not being limited to the outer layer of the model.[178] Finally, Esch et al. applied a body-on-a-chip system to evaluate the potential toxicity of AgNPs. Hereto the GI-tract and liver were mimicked by the Caco-2/HT29-MTX and HepG2/C3A co-cultures respectively and connected in a microfluidic device. They observed that ˜9% of the NPs could pass through the GI barrier as single NPs or small aggregates. The latter in turn induced more severe liver injury than expected based on exposure of the liver co-culture alone.[251]

Overall, more complicated cell models allow evaluation of more intricate events, which cannot be mimicked in an oversimplified monoculture and thereby provide valuable information on NP-mediated adverse events. However, such models are more labor intensive and are therefore currently less applicable for the screening of large sets of NPs. In addition the predictive value of most proposed models should be assessed to identify the *in vitro* models showing the best *in vitro-in vivo* correlation for future use.

8. CONCLUSION & PERSPECTIVES

The present chapter provides an overview of several strategies that have recently been put forward in order to try and optimize cell models for more robust and reliable *in vitro* analysis of NP uptake and toxicity prior to any *in vivo* applications. Where the field of nanotoxicology is advancing fast, it is still lagging behind the rapid developments in the field of nanotechnology. The thorough evaluation of nanomaterial-cell or –tissue interactions is greatly impeded by the numerous types of NPs (each with their specific features) and the heavy impact of even the most miniature changes to a single physicochemical parameter on the NPs interaction with biological entities,

The most used *in vitro* model, namely the classical 2D monoculture, is a very reductionist approach were most complexity of the *in vivo* situation is lost. Therefore, results from *in vitro* studies often did not relate very well to findings obtained in *in vivo* studies. Several groups have therefore made substantial efforts in trying to optimize the current *in vitro* models to mimic the *in vivo* conditions more closely. Inverted cell cultures, flow models, co-cultures, 3D cell cultures or combinations all have specific advantages for NP uptake and toxicity studies when compared to the classical 2D monolayers as described in the various sections above.

Since the field of nanotechnology keeps blooming and the safety of nanomaterials remains questionable as we are all being exposed more and more, it is expected that all these models will gain more importance as more robust rapid screening tools. Based on the data obtained with these models, better predictions on NP safety should be possible as well as a better selection of materials that are more interesting to further *in vivo* evaluation. However, further optimization is needed to fully exploit the benefits of these models. Ideally, these novel models would be adapted to a high content setting as to date they are rather labor intensive. For instance, using co-culture or 3D models combined with flow models in a HCS setting would enable these methods to be used as rapid screening tools. Of note, the predictive power of the proposed models towards *in vivo* adverse outcomes should be evaluated to define the most suitable candidates to be applied in future nanosafety evaluations.

Given the rapid developments in the field of nanotoxicology and the on-going maturation of this niche area into a full scientific discipline, more relevant *in vitro* models such as the ones described in the present review will become increasingly important in various research areas that are linked to the use of nanomaterials in biological settings. Considering that most of these models have only recently been introduced, it is to be expected that more optimized models such as combinations of the ones mentioned will have big impacts on our understanding of how nanosized materials interact with cells and tissues under physiologically relevant conditions.

REFERENCES

1. McIntyre, R. A. *Science progress* **2012,** 95, (Pt 1), 1-22.
2. Bouwmeester, H.; Dekkers, S.; Noordam, M. Y.; Hagens, W. I.; Bulder, A. S.; de Heer, C.; ten Voorde, S. E. C. G.; Wijnhoven, S. W. P.; Marvin, H. J. P.; Sips, A. J. A. M. *Regul Toxicol Pharm* **2009,** 53, (1), 52-62.
3. Thomas, T.; Thomas, K.; Sadrieh, N.; Savage, N.; Adair, P.; Bronaugh, R. *Toxicol Sci* **2006,** 91, (1), 14-19.
4. Schrand, A. M.; Dai, L.; Schlager, J. J.; Hussain, S. M. *Advances in experimental medicine and biology* **2012,** 745, 58-75.
5. Maynard, A. D. *The Annals of occupational hygiene* **2007,** 51, (1), 1-12.
6. Maynard, A. D.; Warheit, D. B.; Philbert, M. A. *Toxicol Sci* **2011,** 120 Suppl 1, S109-29.
7. Som, C.; Nowack, B.; Krug, H. F.; Wick, P. *Accounts of chemical research* **2012**.
8. EU, Commision Recommendation of 18 October 2011 on the definition of nanomaterial. Commision, E., Ed. Official Journal of the European Union: Brussels, 2011; Vol. 2011/696/EU.
9. Donaldson, K. *Nanomedicine (Lond)* **2006,** 1, (2), 229-34.
10. Vincent. M. Hoyt, E. M. *Journal of Chemical Health and Safety* **2008,** 15, (2), 10-15.
11. Arora, S.; Rajwade, J. M.; Paknikar, K. M. *Toxicology and applied pharmacology* **2012,** 258, (2), 151-65.
12. Sillerud, L. O.; Solberg, N. O.; Chamberlain, R.; Orlando, R. A.; Heidrich, J. E.; Brown, D. C.; Brady, C. I.; Vander Jagt, T. A.; Garwood, M.; Vander Jagt, D. L. *Journal of Alzheimer's disease : JAD* **2012**.
13. Zhu, Y.; Chandra, P.; Shim, Y. B. *Analytical chemistry* **2012**.
14. Liu, L.; Ye, Q.; Wu, Y.; Hsieh, W. Y.; Chen, C. L.; Shen, H. H.; Wang, S. J.; Zhang, H.; Hitchens, T. K.; Ho, C. *Nanomedicine : nanotechnology, biology, and medicine* **2012,** 8, (8), 1345-54.
15. Ghosh, D.; Lee, Y.; Thomas, S.; Kohli, A. G.; Yun, D. S.; Belcher, A. M.; Kelly, K. A. *Nature nanotechnology* **2012,** 7, (10), 677-82.
16. Udhrain, A.; Skubitz, K. M.; Northfelt, D. W. *International journal of nanomedicine* **2007,** 2, (3), 345-52.
17. Lee, S. J.; Huh, M. S.; Lee, S. Y.; Min, S.; Lee, S.; Koo, H.; Chu, J. U.; Lee, K. E.; Jeon, H.; Choi, Y.; Choi, K.; Byun, Y.; Jeong, S. Y.; Park, K.; Kim, K.; Kwon, I. C. *Angew Chem Int Ed Engl* **2012,** 51, (29), 7203-7.
18. Poltl-Frank, F.; Zurbriggen, R.; Helg, A.; Stuart, F.; Robinson, J.; Gluck, R.; Pluschke, G. *Clinical and experimental immunology* **1999,** 117, (3), 496-503.
19. Meetoo, D. *Br J Nurs* **2009,** 18, (19), 1201-6.
20. El-Ansary, A.; Al-Daihan, S. *Journal of toxicology* **2009,** 2009, 754810.
21. Duncan, R.; Gaspar, R. *Molecular pharmaceutics* **2011,** 8, (6), 2101-41.
22. Fernandez-Fernandez, A.; Manchanda, R.; McGoron, A. J. *Applied biochemistry and biotechnology* **2011,** 165, (7-8), 1628-51.
23. Kirui, D. K.; Khalidov, I.; Wang, Y.; Batt, C. A. *Nanomedicine : nanotechnology, biology, and medicine* **2012**.
24. Wang, Y. X.; Hussain, S. M.; Krestin, G. P. *European radiology* **2001,** 11, (11), 2319-31.
25. Nguyen, D. T.; Kim, D. J.; Kim, K. S. *Micron* **2011,** 42, (3), 207-27.
26. Yang, J.; Gunn, J.; Dave, S. R.; Zhang, M.; Wang, Y. A.; Gao, X. *The Analyst* **2008,** 133, (2), 154-60.
27. Nel, A.; Xia, T.; Madler, L.; Li, N. *Science* **2006,** 311, (5761), 622-627.
28. Hussain, S. M.; Braydich-Stolle, L. K.; Schrand, A. M.; Murdock, R. C.; Yu, K. O.; Mattie, D. M.; Schlager, J. J.; Terrones, M. *Adv Mater* **2009,** 21, (16), 1549-1559.
29. Donaldson, K.; Stone, V.; Tran, C. L.; Kreyling, W.; Borm, P. J. A. *Occup Environ Med* **2004,** 61, (9), 727-728.
30. Fischer, H. C.; Chan, W. C. W. *Current opinion in biotechnology* **2007,** 18, (6), 565-571.

31. Kroll, A.; Pillukat, M. H.; Hahn, D.; Schnekenburger, J. *Archives of toxicology* **2012,** 86, (7), 1123-1136.
32. Monteiro-Riviere, N. A.; Inman, A. O.; Zhang, L. W. *Toxicology and applied pharmacology* **2009,** 234, (2), 222-35.
33. Magdolenova, Z.; Lorenzo, Y.; Collins, A.; Dusinska, M. *Journal of toxicology and environmental health. Part A* **2012,** 75, (13-15), 800-6.
34. Cho, E. C.; Zhang, Q.; Xia, Y. *Nature nanotechnology* **2011,** 6, (6), 385-91.
35. Mahto, S. K.; Yoon, T. H.; Rhee, S. W. *Biomicrofluidics* **2010,** 4, (3).
36. Kirchner, C.; Liedl, T.; Kudera, S.; Pellegrino, T.; Javier, A. M.; Gaub, H. E.; Stolzle, S.; Fertig, N.; Parak, W. J. *Nano letters* **2005,** 5, (2), 331-338.
37. Johnston, H. J.; Hutchison, G.; Christensen, F. M.; Peters, S.; Hankin, S.; Stone, V. *Crit Rev Toxicol* **2010,** 40, (4), 328-346.
38. Duffin, R.; Tran, L.; Brown, D.; Stone, V.; Donaldson, K. *Inhal Toxicol* **2007,** 19, (10), 849-856.
39. Nel, A.; Xia, T.; Madler, L.; Li, N. *Science* **2006,** 311, (5761), 622-7.
40. Oberdorster, G.; Oberdorster, E.; Oberdorster, J. *Environmental health perspectives* **2005,** 113, (7), 823-39.
41. Park, E. J.; Park, K. *Toxicol Lett* **2009,** 184, (1), 18-25.
42. Chen, B.; Liu, Y.; Song, W. M.; Hayashi, Y.; Ding, X. C.; Li, W. H. *Biomedical and environmental sciences : BES* **2011,** 24, (6), 593-601.
43. Soenen, S. J.; De Cuyper, M.; De Smedt, S. C.; Braeckmans, K. *Methods in enzymology* **2012,** 509, 195-224.
44. Freyre-Fonseca, V.; Delgado-Buenrostro, N. L.; Gutierrez-Cirlos, E. B.; Calderon-Torres, C. M.; Cabellos-Avelar, T.; Sanchez-Perez, Y.; Pinzon, E.; Torres, I.; Molina-Jijon, E.; Zazueta, C.; Pedraza-Chaverri, J.; Garcia-Cuellar, C. M.; Chirino, Y. I. *Toxicol Lett* **2011,** 202, (2), 111-9.
45. Soenen, S. J.; Rivera-Gil, P.; Montenegro, J. M.; Parak, W. J.; De Smedt, S. C.; Braeckmans, K. *Nano today* **2011,** 6, (5), 446-465.
46. Feng, X.; Chen, A.; Zhang, Y.; Wang, J.; Shao, L.; Wei, L. *International journal of nanomedicine* **2015,** 10, 4321-40.
47. Xie, Y.; Liu, D.; Cai, C.; Chen, X.; Zhou, Y.; Wu, L.; Sun, Y.; Dai, H.; Kong, X.; Liu, P. *International journal of nanomedicine* **2016,** 11, 3557-70.
48. Culcasi, M.; Benameur, L.; Mercier, A.; Lucchesi, C.; Rahmouni, H.; Asteian, A.; Casano, G.; Botta, A.; Kovacic, H.; Pietri, S. *Chemico-biological interactions* **2012,** 199, (3), 161-76.
49. Wilhelmi, V.; Fischer, U.; Weighardt, H.; Schulze-Osthoff, K.; Nickel, C.; Stahlmecke, B.; Kuhlbusch, T. A.; Scherbart, A. M.; Esser, C.; Schins, R. P.; Albrecht, C. *PloS one* **2013,** 8, (6), e65704.
50. Singh, N.; Manshian, B.; Jenkins, G. J.; Griffiths, S. M.; Williams, P. M.; Maffeis, T. G.; Wright, C. J.; Doak, S. H. *Biomaterials* **2009,** 30, (23-24), 3891-914.
51. Hussain, S.; Garantziotis, S.; Rodrigues-Lima, F.; Dupret, J. M.; Baeza-Squiban, A.; Boland, S. *Advances in experimental medicine and biology* **2014,** 811, 111-34.
52. Buyukhatipoglu, K.; Clyne, A. M. *Journal of biomedical materials research. Part A* **2011,** 96, (1), 186-95.
53. Naumanen, P.; Lappalainen, P.; Hotulainen, P. *Journal of microscopy* **2008,** 231, (3), 446-54.
54. Brookes, P. S.; Yoon, Y.; Robotham, J. L.; Anders, M. W.; Sheu, S. S. *American journal of physiology. Cell physiology* **2004,** 287, (4), C817-33.
55. Yu, K. N.; Chang, S. H.; Park, S. J.; Lim, J.; Lee, J.; Yoon, T. J.; Kim, J. S.; Cho, M. H. *PloS one* **2015,** 10, (6), e0131208.
56. Niu, J.; Azfer, A.; Rogers, L. M.; Wang, X.; Kolattukudy, P. E. *Cardiovascular research* **2007,** 73, (3), 549-59.
57. Pagliari, F.; Mandoli, C.; Forte, G.; Magnani, E.; Pagliari, S.; Nardone, G.; Licoccia, S.; Minieri, M.; Di Nardo, P.; Traversa, E. *ACS nano* **2012,** 6, (5), 3767-75.

58. Harris, G.; Palosaari, T.; Magdolenova, Z.; Mennecozzi, M.; Gineste, J. M.; Saavedra, L.; Milcamps, A.; Huk, A.; Collins, A. R.; Dusinska, M.; Whelan, M. *Nanotoxicology* **2015,** 9 Suppl 1, 87-94.
59. Gao, L.; Zhuang, J.; Nie, L.; Zhang, J.; Zhang, Y.; Gu, N.; Wang, T.; Feng, J.; Yang, D.; Perrett, S.; Yan, X. *Nature nanotechnology* **2007,** 2, (9), 577-83.
60. Huang, D. M.; Hsiao, J. K.; Chen, Y. C.; Chien, L. Y.; Yao, M.; Chen, Y. K.; Ko, B. S.; Hsu, S. C.; Tai, L. A.; Cheng, H. Y.; Wang, S. W.; Yang, C. S.; Chen, Y. C. *Biomaterials* **2009,** 30, (22), 3645-51.
61. Petters, C.; Thiel, K.; Dringen, R. *Nanotoxicology* **2016,** 10, (3), 332-42.
62. Pisanic, T. R., 2nd; Blackwell, J. D.; Shubayev, V. I.; Finones, R. R.; Jin, S. *Biomaterials* **2007,** 28, (16), 2572-81.
63. Gu, Y. J.; Cheng, J. P.; Lin, C. C.; Lam, Y. W.; Cheng, S. H.; Wong, W. T. *Toxicology and applied pharmacology* **2009,** 237, (2), 196-204.
64. Soenen, S. J.; Manshian, B.; Montenegro, J. M.; Amin, F.; Meermann, B.; Thiron, T.; Cornelissen, M.; Vanhaecke, F.; Doak, S.; Parak, W. J.; De Smedt, S.; Braeckmans, K. *ACS nano* **2012,** 6, (7), 5767-83.
65. Wu, Y. L.; Putcha, N.; Ng, K. W.; Leong, D. T.; Lim, C. T.; Loo, S. C. J.; Chen, X. D. *Accounts of chemical research* **2013,** 46, (3), 782-791.
66. Tay, C. Y.; Cai, P.; Setyawati, M. I.; Fang, W.; Tan, L. P.; Hong, C. H.; Chen, X.; Leong, D. T. *Nano letters* **2014,** 14, (1), 83-8.
67. Pan, Y.; Ding, H.; Qin, L.; Zhao, X.; Cai, J.; Du, B. *Journal of biomedical nanotechnology* **2013,** 9, (10), 1746-56.
68. Comfort, K. K.; Maurer, E. I.; Braydich-Stolle, L. K.; Hussain, S. M. *ACS nano* **2011,** 5, (12), 10000-8.
69. Peynshaert, K.; Manshian, B. B.; Joris, F.; Braeckmans, K.; De Smedt, S. C.; Demeester, J.; Soenen, S. J. *Chemical reviews* **2014,** 114, (15), 7581-609.
70. Qu, G.; Liu, S.; Zhang, S.; Wang, L.; Wang, X.; Sun, B.; Yin, N.; Gao, X.; Xia, T.; Chen, J. J.; Jiang, G. B. *ACS nano* **2013,** 7, (7), 5732-45.
71. Christen, V.; Fent, K. *Chemosphere* **2012,** 87, (4), 423-34.
72. See, V.; Free, P.; Cesbron, Y.; Nativo, P.; Shaheen, U.; Rigden, D. J.; Spiller, D. G.; Fernig, D. G.; White, M. R.; Prior, I. A.; Brust, M.; Lounis, B.; Levy, R. *ACS nano* **2009,** 3, (9), 2461-8.
73. Soenen, S. J.; Demeester, J.; De Smedt, S. C.; Braeckmans, K. *Biomaterials* **2012,** 33, (19), 4882-8.
74. Mahto, S. K.; Park, C.; Yoon, T. H.; Rhee, S. W. *Toxicol in Vitro* **2010,** 24, (4), 1070-1077.
75. Cedervall, T.; Lynch, I.; Lindman, S.; Berggard, T.; Thulin, E.; Nilsson, H.; Dawson, K. A.; Linse, S. *Proceedings of the National Academy of Sciences of the United States of America* **2007,** 104, (7), 2050-5.
76. Maiorano, G.; Sabella, S.; Sorce, B.; Brunetti, V.; Malvindi, M. A.; Cingolani, R.; Pompa, P. P. *ACS nano* **2010,** 4, (12), 7481-91.
77. Lynch, I.; Salvati, A.; Dawson, K. A. *Nature nanotechnology* **2009,** 4, (9), 546-7.
78. Mahmoudi, M.; Laurent, S.; Shokrgozar, M. A.; Hosseinkhani, M. *ACS nano* **2011,** 5, (9), 7263-76.
79. Laurent, S.; Burtea, C.; Thirifays, C.; Hafeli, U. O.; Mahmoudi, M. *PloS one* **2012,** 7, (1), e29997.
80. Dobrovolskaia, M. A.; Shurin, M.; Shvedova, A. A. *Toxicology and applied pharmacology* **2016,** 299, 78-89.
81. Donaldson, K.; Borm, P. J.; Castranova, V.; Gulumian, M. *Particle and fibre toxicology* **2009,** 6, 13.
82. Oberdorster, G.; Maynard, A.; Donaldson, K.; Castranova, V.; Fitzpatrick, J.; Ausman, K.; Carter, J.; Karn, B.; Kreyling, W.; Lai, D.; Olin, S.; Monteiro-Riviere, N.; Warheit, D.; Yang, H. *Particle and fibre toxicology* **2005,** 2, 8.

83. Sayes, C. M.; Warheit, D. B. *Wiley interdisciplinary reviews. Nanomedicine and nanobiotechnology* **2009,** 1, (6), 660-70.
84. Wu, L.; Zhang, J.; Watanabe, W. *Advanced drug delivery reviews* **2011,** 63, (6), 456-69.
85. Jiang, J. K.; Oberdorster, G.; Biswas, P. *J Nanopart Res* **2009,** 11, (1), 77-89.
86. Hassellov, M.; Readman, J. W.; Ranville, J. F.; Tiede, K. *Ecotoxicology* **2008,** 17, (5), 344-61.
87. Hillegass, J. M.; Shukla, A.; Lathrop, S. A.; MacPherson, M. B.; Fukagawa, N. K.; Mossman, B. T. *Wiley interdisciplinary reviews. Nanomedicine and nanobiotechnology* **2010,** 2, (3), 219-31.
88. Jones, C. F.; Grainger, D. W. *Advanced drug delivery reviews* **2009,** 61, (6), 438-56.
89. Kang, S. J.; Kim, B. M.; Lee, Y. J.; Chung, H. W. *Environmental and molecular mutagenesis* **2008,** 49, (5), 399-405.
90. Lin, W.; Huang, Y. W.; Zhou, X. D.; Ma, Y. *Toxicology and applied pharmacology* **2006,** 217, (3), 252-9.
91. Nel, A.; Xia, T.; Meng, H.; Wang, X.; Lin, S.; Ji, Z.; Zhang, H. *Accounts of chemical research* **2012**.
92. Lai, D. Y. *Wiley interdisciplinary reviews. Nanomedicine and nanobiotechnology* **2012,** 4, (1), 1-15.
93. Carol, P.; Sreejith, S.; Ajayaghosh, A. *Chemistry, an Asian journal* **2007,** 2, (3), 338-48.
94. Abraham, V. C.; Taylor, D. L.; Haskins, J. R. *Trends in biotechnology* **2004,** 22, (1), 15-22.
95. Zhou, X.; Cao, X.; Perlman, Z.; Wong, S. T. *Journal of biomedical informatics* **2006,** 39, (2), 115-25.
96. Chung, T. H.; Wu, S. H.; Yao, M.; Lu, C. W.; Lin, Y. S.; Hung, Y.; Mou, C. Y.; Chen, Y. C.; Huang, D. M. *Biomaterials* **2007,** 28, (19), 2959-66.
97. Lewinski, N.; Colvin, V.; Drezek, R. *Small* **2008,** 4, (1), 26-49.
98. Kumar, V.; Kumari, A.; Guleria, P.; Yadav, S. K. *Reviews of environmental contamination and toxicology* **2012,** 215, 39-121.
99. Clift, M. J.; Stone, V. *Theranostics* **2012,** 2, (7), 668-80.
100. Hartung, T.; Sabbioni, E. *Wiley interdisciplinary reviews. Nanomedicine and nanobiotechnology* **2011**.
101. Dhawan, A.; Sharma, V. *Analytical and bioanalytical chemistry* **2010,** 398, (2), 589-605.
102. Kroll, A.; Pillukat, M. H.; Hahn, D.; Schnekenburger, J. *European journal of pharmaceutics and biopharmaceutics : official journal of Arbeitsgemeinschaft fur Pharmazeutische Verfahrenstechnik e.V* **2009,** 72, (2), 370-7.
103. Rivera-Gil, P.; Jimenez De Aberasturi, D.; Wulf, V.; Pelaz, B.; Del Pino, P.; Zhao, Y.; De La Fuente, J. M.; Ruiz De Larramendi, I.; Rojo, T.; Liang, X. J.; Parak, W. J. *Accounts of chemical research* **2012**.
104. OECD, PHYSICAL-CHEMICAL PROPERTIES OF NANOMATERIALS:

    EVALUATION OF METHODS APPLIED IN THE OECD-WPMN TESTING PROGRAMME. In *Series on the Safety of Manufactured Nanomaterials no. 65*, Paris, 2016; Vol. ENV/JM/MONO(2016)7.
105. OECD, PHYSICAL-CHEMICAL PARAMETERS: MEASUREMENTS AND METHODS RELEVANT FOR

    THE REGULATION OF NANOMATERIALS. In *Series on the Safety of Manufactured Nanomaterials no. 63*, Paris, 2016; Vol. ENV/JM/MONO(2016)2.
106. Sharma, G.; Kodali, V.; Gaffrey, M.; Wang, W.; Minard, K. R.; Karin, N. J.; Teeguarden, J. G.; Thrall, B. D. *Nanotoxicology* **2014,** 8, (6), 663-75.
107. Sager, T. M.; Castranova, V. *Particle and fibre toxicology* **2009,** 6.
108. Donaldson, K.; Schinwald, A.; Murphy, F.; Cho, W. S.; Duffin, R.; Tran, L.; Poland, C. *Accounts of chemical research* **2012**.
109. Wittmaack, K. *Environmental health perspectives* **2007,** 115, (2), 187-94.
110. Teeguarden, J. G.; Hinderliter, P. M.; Orr, G.; Thrall, B. D.; Pounds, J. G. *Toxicol Sci* **2007,** 95, (2), 300-312.

111. N. Feliu, B. P., Q. Zhang, P. del Pino, A. Nyström, W. J. Parak. *WIREs Nanomedicine & Nanobiotechnology* **2015**.
112. Monteiller, C.; Tran, L.; MacNee, W.; Faux, S.; Jones, A.; Miller, B.; Donaldson, K. *Occup Environ Med* **2007,** 64, (9), 609-15.
113. Rushton, E. K.; Jiang, J.; Leonard, S. S.; Eberly, S.; Castranova, V.; Biswas, P.; Elder, A.; Han, X.; Gelein, R.; Finkelstein, J.; Oberdorster, G. *Journal of toxicology and environmental health. Part A* **2010,** 73, (5), 445-61.
114. Oberdorster, G. *Journal of internal medicine* **2010,** 267, (1), 89-105.
115. Ong, K. J.; MacCormack, T. J.; Clark, R. J.; Ede, J. D.; Ortega, V. A.; Felix, L. C.; Dang, M. K.; Ma, G.; Fenniri, H.; Veinot, J. G.; Goss, G. G. *PloS one* **2014,** 9, (3), e90650.
116. Ramakrishna, G.; Ghosh, H. N. *J Phys Chem B* **2001,** 105, (29), 7000-7008.
117. Hedderman, T. G.; Keogh, S. M.; Chambers, G.; Byrne, H. J. *J Phys Chem B* **2004,** 108, (49), 18860-18865.
118. Griffiths, S. M.; Singh, N.; Jenkins, G. J.; Williams, P. M.; Orbaek, A. W.; Barron, A. R.; Wright, C. J.; Doak, S. H. *Analytical chemistry* **2011,** 83, (10), 3778-85.
119. Soenen, S. J.; De Cuyper, M. *Nanomedicine (Lond)* **2010,** 5, (8), 1261-75.
120. Damoiseaux, R.; George, S.; Li, M.; Pokhrel, S.; Ji, Z.; France, B.; Xia, T.; Suarez, E.; Rallo, R.; Madler, L.; Cohen, Y.; Hoek, E. M.; Nel, A. *Nanoscale* **2011,** 3, (4), 1345-60.
121. Kim, D.; Lin, Y. S.; Haynes, C. L. *Analytical chemistry* **2011,** 83, (22), 8377-82.
122. Wilkinson, K. E.; Palmberg, L.; Witasp, E.; Kupczyk, M.; Feliu, N.; Gerde, P.; Seisenbaeva, G. A.; Fadeel, B.; Dahlen, S. E.; Kessler, V. G. *ACS nano* **2011,** 5, (7), 5312-5324.
123. Schlinkert, P.; Casals, E.; Boyles, M.; Tischler, U.; Hornig, E.; Tran, N.; Zhao, J. Y.; Himly, M.; Riediker, M.; Oostingh, G. J.; Puntes, V.; Duschl, A. *J Nanobiotechnol* **2015,** 13.
124. Feng, W.; Guo, J.; Huang, H.; Xia, B.; Liu, H.; Li, J.; Lin, S.; Li, T.; Liu, J.; Li, H. *PloS one* **2015,** 10, (4), e0123520.
125. Llobet, L.; Montoya, J.; Lopez-Gallardo, E.; Ruiz-Pesini, E. *Tissue Eng Part C Methods* **2015,** 21, (11), 1143-7.
126. Unger, R. E.; Halstenberg, S.; Sartoris, A.; Kirkpatrick, C. J. *Methods Mol Biol* **2011,** 695, 229-41.
127. Goodman, T. T.; Ng, C. P.; Pun, S. H. *Bioconjugate chemistry* **2008,** 19, (10), 1951-9.
128. Luo, Y.; Wang, C.; Hossain, M.; Qiao, Y.; Ma, L.; An, J.; Su, M. *Analytical chemistry* **2012,** 84, (15), 6731-8.
129. Huh, D.; Hamilton, G. A.; Ingber, D. E. *Trends Cell Biol* **2011,** 21, (12), 745-754.
130. Bagwe, R. P.; Hilliard, L. R.; Tan, W. *Langmuir : the ACS journal of surfaces and colloids* **2006,** 22, (9), 4357-62.
131. Bihari, P.; Vippola, M.; Schultes, S.; Praetner, M.; Khandoga, A. G.; Reichel, C. A.; Coester, C.; Tuomi, T.; Rehberg, M.; Krombach, F. *Particle and fibre toxicology* **2008,** 5, 14.
132. Sun, Y. P.; Li, X. Q.; Zhang, W. X.; Wang, H. P. *Colloid Surface A* **2007,** 308, (1-3), 60-66.
133. Kakinen, A.; Kahru, A.; Nurmsoo, H.; Kubo, A. L.; Bondarenko, O. M. *Toxicol in Vitro* **2016,** 36, 172-179.
134. Zhu, S. Q.; Oberdorster, E.; Haasch, M. L. *Mar Environ Res* **2006,** 62, S5-S9.
135. Porter, D.; Sriram, K.; Wolfarth, M.; Jefferson, A.; Schwegler-Berry, D.; Andrew, M.; Castranova, V. *Nanotoxicology* **2008,** 2, (3), 144-154.
136. Stern, S. T.; McNeil, S. E. *Toxicol Sci* **2008,** 101, (1), 4-21.
137. Gavrieli, Y.; Sherman, Y.; Ben-Sasson, S. A. *The Journal of cell biology* **1992,** 119, (3), 493-501.
138. Krug, H. F.; Wick, P. *Angew Chem Int Ed Engl* **2011**.
139. Soenen, S. J.; Manshian, B.; Doak, S. H.; De Smedt, S. C.; Braeckmans, K. *Acta biomaterialia* **2013,** 9, (11), 9183-93.
140. Aude-Garcia, C.; Villiers, F.; Collin-Faure, V.; Pernet-Gallay, K.; Jouneau, P. H.; Sorieul, S.; Mure, G.; Gerdil, A.; Herlin-Boime, N.; Carriere, M.; Rabilloud, T. *Nanotoxicology* **2016,** 10, (5), 586-96.

141. George, S.; Xia, T.; Rallo, R.; Zhao, Y.; Ji, Z.; Lin, S.; Wang, X.; Zhang, H.; France, B.; Schoenfeld, D.; Damoiseaux, R.; Liu, R.; Lin, S.; Bradley, K. A.; Cohen, Y.; Nel, A. E. *ACS nano* **2011,** 5, (3), 1805-17.
142. Zhang, H.; Wang, X.; Wang, M.; Li, L.; Chang, C. H.; Ji, Z.; Xia, T.; Nel, A. E. *Small* **2015,** 11, (31), 3797-805.
143. Petters, C.; Dringen, R. *Neurochemistry international* **2015,** 81, 1-9.
144. Hinderliter, P. M.; Minard, K. R.; Orr, G.; Chrisler, W. B.; Thrall, B. D.; Pounds, J. G.; Teeguarden, J. G. *Particle and fibre toxicology* **2010,** 7, (1), 36.
145. Lison, D.; Thomassen, L. C.; Rabolli, V.; Gonzalez, L.; Napierska, D.; Seo, J. W.; Kirsch-Volders, M.; Hoet, P.; Kirschhock, C. E.; Martens, J. A. *Toxicol Sci* **2008,** 104, (1), 155-62.
146. Ahmad Khanbeigi, R.; Kumar, A.; Sadouki, F.; Lorenz, C.; Forbes, B.; Dailey, L. A.; Collins, H. *Journal of controlled release : official journal of the Controlled Release Society* **2012,** 162, (2), 259-66.
147. Sperber, M. H., C.; Lemberger, M.M.; Goricnik, B.; Hinterreiter, N.; Lukic, S.; Oberleitner, M.; Stolwijk, J.A.; Wegener, J., Monitoring the Impact of Nanomaterialson Animal Cells by Impedance Analysis: A Noninvasive, Label-Free, and Multimodal Approach. In *Measuring Biological Impacts of Nanomaterials*, Springer International Publishing Switzerland: 2015.
148. Seiffert, J. M.; Baradez, M. O.; Nischwitz, V.; Lekishvili, T.; Goenaga-Infante, H.; Marshall, D. *Chemical research in toxicology* **2012,** 25, (1), 140-52.
149. Cimpan, M. R.; Mordal, T.; Scholermann, J.; Allouni, Z. E.; Pliquett, U.; Cimpan, E. *J Phys Conf Ser* **2013,** 429.
150. Caballero-Díaz, E. V. C. M. *Trends in Analytical Chemistry* **2016**.
151. Otero-Gonzalez, L.; Sierra-Alvarez, R.; Boitano, S.; Field, J. A. *Environmental science & technology* **2012,** 46, (18), 10271-8.
152. George, S.; Pokhrel, S.; Xia, T.; Gilbert, B.; Ji, Z.; Schowalter, M.; Rosenauer, A.; Damoiseaux, R.; Bradley, K. A.; Madler, L.; Nel, A. E. *ACS nano* **2010,** 4, (1), 15-29.
153. Astashkina, A.; Mann, B.; Grainger, D. W. *Pharmacology & therapeutics* **2012,** 134, (1), 82-106.
154. Jan, E.; Byrne, S. J.; Cuddihy, M.; Davies, A. M.; Volkov, Y.; Gun'ko, Y. K.; Kotov, N. A. *ACS nano* **2008,** 2, (5), 928-38.
155. Anguissola, S.; Garry, D.; Salvati, A.; O'Brien, P. J.; Dawson, K. A. *PloS one* **2014,** 9, (9), e108025.
156. Manshian, B. B.; Moyano, D. F.; Corthout, N.; Munck, S.; Himmelreich, U.; Rotello, V. M.; Soenen, S. J. *Biomaterials* **2014,** 35, (37), 9941-50.
157. Schnackenberg, L. K.; Sun, J.; Beger, R. D. *Methods Mol Biol* **2012,** 926, 141-56.
158. Ware, M. J.; Godin, B.; Singh, N.; Majithia, R.; Shamsudeen, S.; Serda, R. E.; Meissner, K. E.; Rees, P.; Summers, H. D. *ACS nano* **2014,** 8, (7), 6693-6700.
159. Manshian, B. B.; Munck, S.; Agostinis, P.; Himmelreich, U.; Soenen, S. J. *Sci Rep-Uk* **2015,** 5.
160. Cohen, Y.; Rallo, R.; Liu, R.; Liu, H. H. *Accounts of chemical research* **2012**.
161. Puzyn, T.; Rasulev, B.; Gajewicz, A.; Hu, X. K.; Dasari, T. P.; Michalkova, A.; Hwang, H. M.; Toropov, A.; Leszczynska, D.; Leszczynski, J. *Nature nanotechnology* **2011,** 6, (3), 175-178.
162. Wang, J.; Fang, X.; Liang, W. *ACS nano* **2012,** 6, (6), 5018-30.
163. Baba, A. C., C. , TUMOR CELL MORPHOLOGY. In *Comparative Oncology*, The Publishing House of the Romanian Academy: Bucharest, 2007.
164. Albrecht, C.; Scherbart, A. M.; van Berlo, D.; Braunbarth, C. M.; Schins, R. P.; Scheel, J. *Toxicol in Vitro* **2009,** 23, (3), 520-30.
165. Bregoli, L.; Chiarini, F.; Gambarelli, A.; Sighinolfi, G.; Gatti, A. M.; Santi, P.; Martelli, A. M.; Cocco, L. *Toxicology* **2009,** 262, (2), 121-9.
166. Lankoff, A.; Sandberg, W. J.; Wegierek-Ciuk, A.; Lisowska, H.; Refsnes, M.; Sartowska, B.; Schwarze, P. E.; Meczynska-Wielgosz, S.; Wojewodzka, M.; Kruszewski, M. *Toxicol Lett* **2012,** 208, (3), 197-213.
167. Zhao, F.; Zhao, Y.; Liu, Y.; Chang, X. L.; Chen, C. Y.; Zhao, Y. L. *Small* **2011,** 7, (10), 1322-1337.

168. Wang, T. T.; Bai, J.; Jiang, X.; Nienhaus, G. U. *ACS nano* **2012,** 6, (2), 1251-1259.
169. Schweiger, C.; Hartmann, R.; Zhang, F.; Parak, W. J.; Kissel, T. H.; Rivera Gil, P. *J Nanobiotechnol* **2012,** 10.
170. Coulter, J. A.; Jain, S.; Butterworth, K. T.; Taggart, L. E.; Dickson, G. R.; McMahon, S. J.; Hyland, W. B.; Muir, M. F.; Trainor, C.; Hounsell, A. R.; O'Sullivan, J. M.; Schettino, G.; Currell, F. J.; Hirst, D. G.; Prise, K. M. *International journal of nanomedicine* **2012,** 7, 2673-85.
171. Lunov, O.; Syrovets, T.; Loos, C.; Beil, J.; Delecher, M.; Tron, K.; Nienhaus, G. U.; Musyanovych, A.; Mailander, V.; Landfester, K.; Simmet, T. *ACS nano* **2011,** 5, (3), 1657-1669.
172. Sur, I.; Cam, D.; Kahraman, M.; Baysal, A.; Culha, M. *Nanotechnology* **2010,** 21, (17), 175104.
173. Diaz, B.; Sanchez-Espinel, C.; Arruebo, M.; Faro, J.; de Miguel, E.; Magadan, S.; Yague, C.; Fernandez-Pacheco, R.; Ibarra, M. R.; Santamaria, J.; Gonzalez-Fernandez, A. *Small* **2008,** 4, (11), 2025-34.
174. Greulich, C.; Diendorf, J.; Gessmann, J.; Simon, T.; Habijan, T.; Eggeler, G.; Schildhauer, T. A.; Epple, M.; Koller, M. *Acta biomaterialia* **2011,** 7, (9), 3505-14.
175. Barua, S.; Rege, K. *Small* **2009,** 5, (3), 370-6.
176. Wang, Y.; Aker, W. G.; Hwang, H. M.; Yedjou, C. G.; Yu, H.; Tchounwou, P. B. *The Science of the total environment* **2011,** 409, (22), 4753-62.
177. Hanley, C.; Layne, J.; Punnoose, A.; Reddy, K. M.; Coombs, I.; Coombs, A.; Feris, K.; Wingett, D. *Nanotechnology* **2008,** 19, (29), 295103.
178. Kermanizadeh, A.; Gaiser, B. K.; Ward, M. B.; Stone, V. *Nanotoxicology* **2013,** 7, (7), 1255-71.
179. Zhang, H.; Xia, T.; Meng, H.; Xue, M.; George, S.; Ji, Z.; Wang, X.; Liu, R.; Wang, M.; France, B.; Rallo, R.; Damoiseaux, R.; Cohen, Y.; Bradley, K. A.; Zink, J. I.; Nel, A. E. *ACS nano* **2011,** 5, (4), 2756-69.
180. Saretzki, G.; Armstrong, L.; Leake, A.; Lako, M.; von Zglinicki, T. *Stem Cells* **2004,** 22, (6), 962-71.
181. Sohaebuddin, S. K.; Thevenot, P. T.; Baker, D.; Eaton, J. W.; Tang, L. P. *Particle and fibre toxicology* **2010,** 7.
182. Chang, J. S.; Chang, K. L.; Hwang, D. F.; Kong, Z. L. *Environmental science & technology* **2007,** 41, (6), 2064-8.
183. Mukherjee, S. G.; O'Claonadh, N.; Casey, A.; Chambers, G. *Toxicol in Vitro* **2012,** 26, (2), 238-51.
184. Hirsch, V.; Kinnear, C.; Rodriguez-Lorenzo, L.; Monnier, C. A.; Rothen-Rutishauser, B.; Balog, S.; Petri-Fink, A. *Nanoscale* **2014,** 6, (13), 7325-31.
185. Gosens, I.; Post, J. A.; de la Fonteyne, L. J. J.; Jansen, E. H. J. M.; Geus, J. W.; Cassee, F. R.; de Jong, W. H. *Particle and fibre toxicology* **2010,** 7.
186. Albanese, A.; Chan, W. C. W. *ACS nano* **2011,** 5, (7), 5478-5489.
187. Vippola, M.; Falck, G. C.; Lindberg, H. K.; Suhonen, S.; Vanhala, E.; Norppa, H.; Savolainen, K.; Tossavainen, A.; Tuomi, T. *Human & experimental toxicology* **2009,** 28, (6-7), 377-85.
188. Brown, S. C.; Kamal, M.; Nasreen, N.; Baumuratov, A.; Sharma, P.; Antony, V. B.; Moudgil, B. M. *Adv Powder Technol* **2007,** 18, (1), 69-79.
189. Limbach, L. K.; Li, Y. C.; Grass, R. N.; Brunner, T. J.; Hintermann, M. A.; Muller, M.; Gunther, D.; Stark, W. J. *Environmental science & technology* **2005,** 39, (23), 9370-9376.
190. Allouni, Z. E.; Cimpan, M. R.; Hol, P. J.; Skodvin, T.; Gjerdet, N. R. *Colloids and surfaces. B, Biointerfaces* **2009,** 68, (1), 83-7.
191. Stebounova, L. V.; Guio, E.; Grassian, V. H. *J Nanopart Res* **2011,** 13, (1), 233-244.
192. Drescher, D.; Orts-Gil, G.; Laube, G.; Natte, K.; Veh, R. W.; Osterle, W.; Kneipp, J. *Analytical and bioanalytical chemistry* **2011,** 400, (5), 1367-1373.
193. Murdock, R. C.; Braydich-Stolle, L.; Schrand, A. M.; Schlager, J. J.; Hussain, S. M. *Toxicol Sci* **2008,** 101, (2), 239-253.
194. Yang, J. A.; Lohse, S. E.; Murphy, C. J. *Small* **2014,** 10, (8), 1642-51.
195. Anders, C. B.; Chess, J. J.; Wingett, D. G.; Punnoose, A. *Nanoscale research letters* **2015,** 10, (1), 448.

196. Braeckmans, K.; Buyens, K.; Bouquet, W.; Vervaet, C.; Joye, P.; De Vos, F.; Plawinski, L.; Doeuvre, L.; Angles-Cano, E.; Sanders, N. N.; Demeester, J.; De Smedt, S. C. *Nano letters* **2010,** 10, (11), 4435-4442.
197. Liedl, T.; Keller, S.; Simmel, F. C.; Radler, J. O.; Parak, W. J. *Small* **2005,** 1, (10), 997-1003.
198. Wick, P.; Manser, P.; Limbach, L. K.; Dettlaff-Weglikowska, U.; Krumeich, F.; Roth, S.; Stark, W. J.; Bruinink, A. *Toxicol Lett* **2007,** 168, (2), 121-31.
199. Zook, J. M.; MacCuspie, R. I.; Locascio, L. E.; Halter, M. D.; Elliott, J. T. *Nanotoxicology* **2011,** 5, (4), 517-530.
200. Bae, E.; Park, H. J.; Lee, J.; Kim, Y.; Yoon, J.; Park, K.; Choi, K.; Yi, J. *Environmental toxicology and chemistry / SETAC* **2010,** 29, (10), 2154-60.
201. Yoon, D.; Woo, D.; Kim, J. H.; Kim, M. K.; Kim, T.; Hwang, E. S.; Baik, S. *J Nanopart Res* **2011,** 13, (6), 2543-2551.
202. Ando, J.; Yamamoto, K. *Antioxidants & redox signaling* **2011,** 15, (5), 1389-403.
203. Bhowmick, T.; Berk, E.; Cui, X.; Muzykantov, V. R.; Muro, S. *Journal of controlled release : official journal of the Controlled Release Society* **2012,** 157, (3), 485-92.
204. Samuel, S. P.; Jain, N.; O'Dowd, F.; Paul, T.; Kashanin, D.; Gerard, V. A.; Gun'ko, Y. K.; Prina-Mello, A.; Volkov, Y. *International journal of nanomedicine* **2012,** 7, 2943-2956.
205. Lin, A.; Sabnis, A.; Kona, S.; Nattama, S.; Patel, H.; Dong, J. F.; Nguyen, K. T. *Journal of Biomedical Materials Research Part A* **2010,** 93A, (3), 833-842.
206. Fede, C.; Fortunati, I.; Weber, V.; Rossetto, N.; Bertasi, F.; Petrelli, L.; Guidolin, D.; Signorini, R.; De Caro, R.; Albertin, G.; Ferrante, C. *Microvasc Res* **2015,** 97, 147-55.
207. Farokhzad, O. C.; Khademhosseini, A.; Yon, S. Y.; Hermann, A.; Cheng, J. J.; Chin, C.; Kiselyuk, A.; Teply, B.; Eng, G.; Langer, R. *Analytical chemistry* **2005,** 77, (17), 5453-5459.
208. Kusunose, J.; Zhang, H.; Gagnon, M. K.; Pan, T.; Simon, S. I.; Ferrara, K. W. *Ann Biomed Eng* **2013,** 41, (1), 89-99.
209. Grabinski, C.; Sharma, M.; Maurer, E.; Sulentic, C.; Mohan Sankaran, R.; Hussain, S. *Nanotoxicology* **2016,** 10, (1), 74-83.
210. Braun, N. J.; DeBrosse, M. C.; Hussain, S. M.; Comfort, K. K. *Mater Sci Eng C Mater Biol Appl* **2016,** 64, 34-42.
211. Savolainen, K.; Alenius, H.; Norppa, H.; Pylkkanen, L.; Tuomi, T.; Kasper, G. *Toxicology* **2010,** 269, (2-3), 92-104.
212. Sayes, C. M.; Reed, K. L.; Subramoney, S.; Abrams, L.; Warheit, D. B. *J Nanopart Res* **2009,** 11, (2), 421-431.
213. Kasper, J.; Hermanns, M. I.; Bantz, C.; Utech, S.; Koshkina, O.; Maskos, M.; Brochhausen, C.; Pohl, C.; Fuchs, S.; Unger, R. E.; James Kirkpatrick, C. *European journal of pharmaceutics and biopharmaceutics : official journal of Arbeitsgemeinschaft fur Pharmazeutische Verfahrenstechnik e.V* **2012**.
214. Kasper, J.; Hermanns, M. I.; Bantz, C.; Maskos, M.; Stauber, R.; Pohl, C.; Unger, R. E.; Kirkpatrick, J. C. *Particle and fibre toxicology* **2011,** 8.
215. Pinkernelle, J.; Calatayud, P.; Goya, G. F.; Fansa, H.; Keilhoff, G. *Bmc Neurosci* **2012,** 13.
216. Rothen-Rutishauser, B.; Muhlfeld, C.; Blank, F.; Musso, C.; Gehr, P. *Particle and fibre toxicology* **2007,** 4, 9.
217. Wottrich, R.; Diabate, S.; Krug, H. F. *International journal of hygiene and environmental health* **2004,** 207, (4), 353-61.
218. Ishii, H.; Hayashi, S.; Hogg, J. C.; Fujii, T.; Goto, Y.; Sakamoto, N.; Mukae, H.; Vincent, R.; van Eeden, S. F. *Resp Res* **2005,** 6.
219. Kim, K. H.; Kim, S. Y.; Chun, B. H.; Lee, Y. K.; Chung, N. *J Korean Soc Appl Bi* **2011,** 54, (1), 30-36.
220. R.;, B.; P.;, M.; M.;, C.; M., G. *BioMed Research International* **2013,** 2013, 8.
221. Ramos-Godinez, M. D.; Gonzalez-Gomez, B. E.; Montiel-Davalos, A.; Lopez-Marure, R.; Alfaro-Moreno, E. *Toxicol in Vitro* **2012,** 27, (2), 774-781.

222. Sisler, J. D.; Pirela, S. V.; Friend, S.; Farcas, M.; Schwegler-Berry, D.; Shvedova, A.; Castranova, V.; Demokritou, P.; Qian, Y. *Nanotoxicology* **2015,** 9, (6), 769-79.
223. Soma, C. E.; Dubernet, C.; Barratt, G.; Benita, S.; Couvreur, P. *Journal of Controlled Release* **2000,** 68, (2), 283-289.
224. Al-Hallak, K. M.; Azarmi, S.; Anwar-Mohamed, A.; Roa, W. H.; Lobenberg, R. *European journal of pharmaceutics and biopharmaceutics : official journal of Arbeitsgemeinschaft fur Pharmazeutische Verfahrenstechnik e.V* **2010,** 76, (1), 112-9.
225. van Berlo, D.; Wessels, A.; Boots, A. W.; Wilhelmi, V.; Scherbart, A. M.; Gerloff, K.; van Schooten, F. J.; Albrecht, C.; Schins, R. P. *Free radical biology & medicine* **2010,** 49, (11), 1685-93.
226. Alfaro-Moreno, E.; Nawrot, T. S.; Vanaudenaerde, B. M.; Hoylaerts, M. F.; Vanoirbeek, J. A.; Nemery, B.; Hoet, P. H. *The European respiratory journal : official journal of the European Society for Clinical Respiratory Physiology* **2008,** 32, (5), 1184-94.
227. Napierska, D.; Thomassen, L. C.; Vanaudenaerde, B.; Luyts, K.; Lison, D.; Martens, J. A.; Nemery, B.; Hoet, P. H. *Toxicol Lett* **2012,** 211, (2), 98-104.
228. Muller, L.; Riediker, M.; Wick, P.; Mohr, M.; Gehr, P.; Rothen-Rutishauser, B. *Journal of the Royal Society, Interface / the Royal Society* **2010,** 7 Suppl 1, S27-40.
229. Clift, M. J.; Endes, C.; Vanhecke, D.; Wick, P.; Gehr, P.; Schins, R. P.; Petri-Fink, A.; Rothen-Rutishauser, B. *Toxicol Sci* **2014,** 137, (1), 55-64.
230. Liu, X.; Sun, J. *International journal of nanomedicine* **2014,** 9, 1261-73.
231. Xu, L.; Dan, M.; Shao, A.; Cheng, X.; Zhang, C.; Yokel, R. A.; Takemura, T.; Hanagata, N.; Niwa, M.; Watanabe, D. *International journal of nanomedicine* **2015,** 10, 6105-18.
232. Georgantzopoulou, A.; Serchi, T.; Cambier, S.; Leclercq, C. C.; Renaut, J.; Shao, J.; Kruszewski, M.; Lentzen, E.; Grysan, P.; Eswara, S.; Audinot, J. N.; Contal, S.; Ziebel, J.; Guignard, C.; Hoffmann, L.; Murk, A. J.; Gutleb, A. C. *Particle and fibre toxicology* **2016,** 13, 9.
233. Walczak, A. P.; Kramer, E.; Hendriksen, P. J.; Tromp, P.; Helsper, J. P.; van der Zande, M.; Rietjens, I. M.; Bouwmeester, H. *Nanotoxicology* **2015,** 9, (4), 453-61.
234. Braakhuis, H. M.; Giannakou, C.; Peijnenburg, W. J. G. M.; Vermeulen, J.; van Loveren, H.; Park, M. V. D. Z. *Nanotoxicology* **2016,** 10, (6), 770-779.
235. Godugu, C.; Patel, A. R.; Desai, U.; Andey, T.; Sams, A.; Singh, M. *PloS one* **2013,** 8, (1), e53708.
236. Dubiak-Szepietowska, M.; Karczmarczyk, A.; Jonsson-Niedziolka, M.; Winckler, T.; Feller, K. H. *Toxicology and applied pharmacology* **2016,** 294, 78-85.
237. Hackenberg, S.; Zimmermann, F. Z.; Scherzed, A.; Friehs, G.; Froelich, K.; Ginzkey, C.; Koehler, C.; Burghartz, M.; Hagen, R.; Kleinsasser, N. *Environmental and molecular mutagenesis* **2011,** 52, (7), 582-9.
238. Nyga, A.; Cheema, U.; Loizidou, M. *Journal of cell communication and signaling* **2011,** 5, (3), 239-48.
239. Mitra, M.; Mohanty, C.; Harilal, A.; Maheswari, U. K.; Sahoo, S. K.; Krishnakumar, S. *Molecular vision* **2012,** 18, 1361-78.
240. Ulusoy, M.; Lavrentieva, A.; Walter, J. G.; Sambale, F.; Green, M.; Stahl, F.; Scheper, T. *Toxicol Res-Uk* **2016,** 5, (1), 126-135.
241. Huang, K.; Ma, H.; Liu, J.; Huo, S.; Kumar, A.; Wei, T.; Zhang, X.; Jin, S.; Gan, Y.; Wang, P. C.; He, S.; Zhang, X.; Liang, X. J. *ACS nano* **2012,** 6, (5), 4483-93.
242. Movia, D.; Prina-Mello, A.; Bazou, D.; Volkov, Y.; Giordani, S. *ACS nano* **2011,** 5, (11), 9278-9290.
243. Lee, J.; Lilly, G. D.; Doty, R. C.; Podsiadlo, P.; Kotov, N. A. *Small* **2009,** 5, (10), 1213-21.
244. Chia, S. L.; Tay, C. Y.; Setyawati, M. I.; Leong, D. T. *Small* **2015,** 11, (6), 702-712.
245. Sambale, F.; Lavrentieva, A.; Stahl, F.; Blume, C.; Stiesch, M.; Kasper, C.; Bahnemann, D.; Scheper, T. *J Biotechnol* **2015,** 205, 120-129.
246. Yu, M.; Huang, S. H.; Yu, K. J.; Clyne, A. M. *Int J Mol Sci* **2012,** 13, (5), 5554-5570.

247. Susewind, J.; Carvalho-Wodarz, C. D.; Repnik, U.; Collnot, E. M.; Schneider-Daum, N.; Griffiths, G. W.; Lehr, C. M. *Nanotoxicology* **2016,** 10, (1), 53-62.
248. Klein, S. G.; Serchi, T.; Hoffmann, L.; Blomeke, B.; Gutleb, A. C. *Particle and fibre toxicology* **2013,** 10.
249. Kuper, C. F.; Grollers-Mulderij, M.; Maarschalkerweerd, T.; Meulendijks, N. M. M.; Reus, A.; van Acker, F.; den Seuken, E. K. Z. V.; Wouters, M. E. L.; Bijlsma, S.; Kooter, I. M. *Toxicol in Vitro* **2015,** 29, (2), 389-397.
250. Hofmann, F.; Blasche, R.; Kasper, M.; Barth, K. *PloS one* **2015,** 10, (1).
251. Esch, M. B.; Mahler, G. J.; Stokor, T.; Shuler, M. L. *Lab Chip* **2014,** 14, (16), 3081-3092.

CHAPTER 6

The impact of the species and cell type on the nanosafety profiles of iron oxide nanoparticles in neural cells.

An adapted manuscript of this chapter is published as:

Freya Joris[▲], Daniel Valdepérez[†], Beatriz Pelaz[†], Stefaan J. Soenen[◊], Bella B. Manshian[◊], Wolfgang J. Parak[†], Stefaan C. De Smedt[▲,1,], Koen Raemdonck[▲,1]. The impact of the species and cell type on the nanosafety profiles of iron oxide nanoparticles in neural cells. *Journal of Nanobiotechnology* 2016.

[▲] Lab of General Biochemistry and Physical Pharmacy, Faculty of Pharmaceutical Sciences, Ghent University, Ottergemsesteenweg 460, B-9000 Ghent, Belgium.

[†] Philipps University of Marburg, Department of Physics, Renthof 7, D-35037 Marburg, Germany.

[◊] Biomedical MRI Unit/MoSAIC, Department of Medicine, KULeuven, Herestraat 49, B-3000 Leuven, Belgium.

Table of contents

ABSTRACT

While nanotechnology is advancing rapidly, nanosafety tends to lag behind since general mechanistic insights into cell-nanoparticle (NP) interactions remain rare. To tackle this issue, standardization of nanosafety assessment is imperative. In this regard, we believe that the cell type selection should not be overlooked since the applicability of cell lines could be questioned given their altered phenotype. Hence, we evaluated the impact of the cell type on *in vitro* nanosafety evaluations in a human and murine neuroblastoma cell line, neural progenitor cell line and in neural stem cells. Acute toxicity was evaluated for gold, silver and iron oxide (IO)NPs, and the latter were additionally subjected to a multiparametric analysis to assess sublethal effects. The stem cells and murine neuroblastoma cell line respectively showed most and least acute cytotoxicity. Using high content imaging, we observed cell type- and species-specific responses to the IONPs on the level of reactive oxygen species production, calcium homeostasis, mitochondrial integrity and cell morphology, indicating that cellular homeostasis is impaired in distinct ways. Our data reveal cell type-specific toxicity profiles and demonstrate that a single cell line or toxicity end point will not provide sufficient information on *in vitro* nanosafety. We propose to identify a set of standard cell lines representing different target organs for screening purposes and to select cell types for detailed nanosafety studies based on the intended application and/or expected exposure.

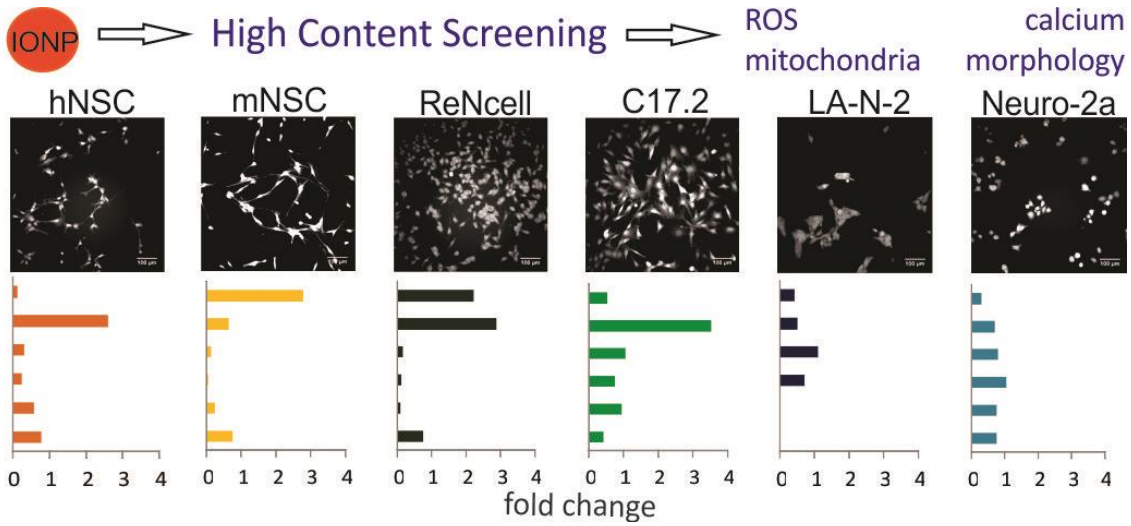

1. INTRODUCTION

In recent years, many inorganic nanoparticles (NPs) have made their way to the market as they are being incorporated into various consumer products.[1] Moreover, their unique properties are being extensively explored for various biomedical applications. For instance, gold NPs (AuNPs) and iron oxide NPs (IONPs) hold great promise as theranostic agents for cancer treatment through hyperthermia combined with tumour detection *via* respectively photoacoustic or magnetic resonance imaging.[2] Additionally, silver NPs (AgNPs) are good candidates for wound dressings and antibacterial coatings of medical devices due to their enhanced antimicrobial properties.[3] However, to date only a few nano-enabled products were successfully translated into the clinic. Besides general targeting issues, this can primarily be attributed to their elusive safety profiles.[4] Despite extensive efforts, a general paradigm on how inorganic NPs are able to affect homeostasis on the level of the cell, organ or organism and to which physicochemical NP properties this can be attributed, is largely lacking.[5]

In general, nanosafety evaluations struggle with two important obstacles. The first is the fast pace at which nanotechnology keeps advancing, leading to the development of a plethora of NPs with distinct physicochemical properties, which should ideally undergo safety evaluation prior to their (biomedical) implementation. The second is the lack of standardization of *in vitro* nanosafety studies, as various groups apply different assays on various cell types. This results in low inter-study comparability and the publication of conflicting data, which complicates the elucidation of general paradigms on NP-cell interactions.[6, 7]

The first hurdle can be overcome by implementing high throughput or high content techniques in order to speed up *in vitro* nanosafety testing.[8, 9] Secondly, much effort is being put into the standardization of various factors of *in vitro* nanosafety studies.[10, 11] In this regard, we believe that the cell type selection should receive equal attention. In most studies a cell line is selected since they are in general more readily accessible, less expensive and easier to cultivate when compared to primary cells.[7, 12] However, cancer cell lines have a disturbed anti-apoptotic balance as well as an altered metabolism to sustain their high proliferation rate.[13] The phenotype expressed by immortalized cells is in turn not entirely stable and might undergo changes due to the extensive *in vitro* manipulation or the initial immortalization.[14] Hence, a shift towards the use of primary or stem cells as well as more

complex cell culture models for *in vitro* nanosafety testing strategies has been recently noted. In contrast, primary cells can suffer from clonal variations and have a limited lifespan *in vitro*, making rational cell type selection a balancing act.[7]

Subsequent to the realization that the cell type could be of substantial importance, several groups have shown that NP-induced effects vary in cell lines retrieved from different tissues or species.[15-18] However, only a few studies compared NP effects in a cancer or immortalized cell line versus primary cells representing the same tissue and species.[19, 20] Unfortunately, available data contrast one another wherefore no unambiguous conclusions could yet be formulated on whether cell lines can generally be applied as a reliable model for *in vitro* nanosafety studies. In addition, many of the abovementioned reports choose to either focus on interspecies variations or cell-type related differences in NP-evoked effects and do not address both factors in a single study.

Here, we present a side-by-side comparison of NP-evoked effects in six related neural cell types thereby evaluating the extent of both species and cell type related variations in NP-induced cytotoxicity. We selected a neuroblastoma cell line, neural progenitor cell line and neural stem cells derived from either humans or mice (Table 6.1) and purposely applied the optimal culture conditions for each cell type. These cell types were selected as potential models to assess the safety of neural stem cells labelling with nanosized contrast agents prior to transplantation in the context of regenerative medicine.[21-23] In turn, the synthesized AuNPs, AgNPs and IONPs with a diameter below 10 nm make them good candidates for the proposed application.[24]

Table 6.1. Cell types applied in this study.

	Stem cells	Progenitor cell line	Cancer cell line
Human	hNSC [25]	ReNcell [26]	LA-N-2 [27]
Mouse	mNSC [25]	C17.2 [28]	Neuro-2a [29]

First, we surveyed the acute toxicity of AuNPs, AgNPs and IONPs in all cell types. Subsequently we selected the IONPs for further evaluation given the minor acute toxicity. Hereto we applied a validated multiparametric approach, using automated imaging, to evaluate the effect of sublethal doses on the production of reactive oxygen species (ROS),

the calcium (Ca^{2+}) homeostasis, mitochondrial health and cell morphology.[30] Importantly, our data reveal distinct and cell type specific toxicity profiles that warrant careful selection of appropriate cell models for future nanosafety studies, taking both species and target tissue into account, and caution misinterpretation of experimental results based on a single cell type and/or toxicity end point.

2. MATERIALS & METHODS

2.1. NP synthesis and characterization

AuNPs, AgNPs and IONPs were synthesized, coated with the polymer poly(isobutylene-*alt*-maleic anhydride) (PMA) grafted with dodecylamine and characterized by the lab of Prof. W.J. Parak. Detailed information on the synthesis and characterization procedures is provided in **Appendix A**.

2.2. Cell culture

The human neural stem cells (hNSCs) required the culture plates to be coated with 10 µg/mL poly-L-ornithin and 6 µg/mL laminin (Sigma, Belgium) in phosphate buffered saline (PBS) prior to use. Complete cell medium consisted of KnockOut™ Dulbecco's modified Eagle's medium (DMEM)/F12 supplemented with StemPro® NSC FSM supplement, basic fibroblast growth factor (FGF) recombinant protein, epidermal growth factor (EGF) recombinant protein, 2 mM L-Glutamine and 2% penicillin/streptomycin (Gibco, Invitrogen, Belgium). Similar as for the hNSCs, culture plates for the murine neural stem cells (mNSCs) were coated with poly-L-ornithin and laminin before use. Complete cell medium was prepared by freshly adding 20 ng/mL FGF, 20 ng/mL EGF and 2 µg/mL heparin (Millipore, Belgium) to Neural Stem Cell Expansion Medium (Millipore, Belgium) containing 2% penicillin/streptomycin. For the ReNcell VM cell line, plates were coated with 20 µg/mL laminin in DMEM/F12 (Invitrogen, Belgium) and cells were cultured in cell medium consisting of ReNcell NSC maintenance medium (Millipore, Belgium) with 2% penicillin/streptomycin. Again, 20 ng/mL FGF and 20 ng/mL EGF were added freshly to complete the cell medium. The C17.2 progenitor cell line did not require culture plates to be coated. By adding 10% fetal bovine serum (FBS, Invitrogen, Belgium), 5% horse serum (Invitrogen, Belgium), 2 mM L-Glutamine and 2% penicillin/streptomycin to DMEM (Invitrogen, Belgium) complete cell medium was prepared. The culture medium for the human neuroblastoma cell line, LA-N-2, was prepared by mixing 43.5% Eagle's minimal essential medium (Sigma, Belgium), 43.5% HAM F12 (Sigma, Belgium), 10% FBS, 2% penicillin/streptomycin and 2 mM L-Glutamine. Finally, for the murine neuroblastoma Neuro-2a cell line complete medium contained 43% DMEM, 42% Opti-MEM (Invitrogen, Belgium), 10% FBS, 2% penicillin/streptomycin and 2 mM glutamine.

For acute toxicity experiments, all cell types were seeded at the density of 25000 cells/well. For further cell experiments we determined appropriated seeding densities in 24-well plates for each cell type individually. In the interest of cell segmentation during data analysis, the optimal seeding density was defined as the density that rendered approximately 80% confluency at the end point of the assay. The volume of cell medium applied for seeding and IONP incubation was adapted to the initial density.

The cells were cultured at 37 °C in a humidified atmosphere completed with 5% CO_2. Cell medium was renewed every other day and cells were split after reaching 80% confluency. Here, the cells were dissociated with 0.05% trypsin–EDTA (Invitrogen, Belgium), after which the cells were centrifuged (4 minutes, 300 g), resuspended in fresh culture medium and seeded at appropriate densities.

2.3. Cytotoxicity

All cell types were seeded at 25000 cells per well in opaque 96-well plates and were allowed to settle overnight. Thereafter the cells were incubated with 2.5, 5, 10, 25, 50 and 100 nM of the AuNPs and AgNPs and 3.5, 7, 14, 35, 70 and 140 nM of the IONPs for 24 hours at 37 °C (5% CO_2). After 24h NP incubation, the CellTiter-GLO® assay (Promega, Belgium) was performed according to the manufacturer's instructions. In short, 100 µL of the assay buffer was added to each well. Plates were shaken during two minutes after which a 10-minute incubation period was respected. Finally, the signal was measured using a GloMax® 96 Microplate Luminometer (Promega, Belgium). Experiments were performed in triplicate and the data are represented as the mean ± the standard error to the mean (SEM).

2.4. High content imaging

For the multiparametric analysis, cells were seeded in 24-well plates and were allowed to attach overnight. Optimal seeding cell densities were identified for each cell type individually. The optimal seeding density was defined as the density that would result in an 80% confluent cell layer in the untreated control at the end point of the assay. In order to preserve the cell density/cell medium volume ratio for all cell types, we varied the latter according to the optimal cell seeding density (Table 6.2).

Table 6.2. Seeding density and incubation volume/well.

	hNSC	mNSC	ReNcell	C17.2	LA-N-2	Neuro-2a
Cell density	35000	17500	17500	15000	50000	15000
Volume (µL)	700	350	350	300	1000	300

For the evaluation of effects on ROS production and $[Ca^{2+}]_c$ 7, 14, 35, 70 and 140 nM IONP dispersions were applied, whereas for the effects on cell morphology and the mitochondria 3.5, 7, 14, 35 and 70 nM were tested as effects on cell function were expected to occur starting from lower NP doses. As the volume of cell medium used for incubation was adjusted according to the cell density, the NP number/volume cell medium/cell number remained equal in all high content experiments. Similar to acute toxicity experiments, the cells were incubated with the IONPs for 24 hours at 37 °C in an atmosphere containing 5% CO_2 after which staining and analysis were performed. This set of data is presented as mean ± SEM from two independent replicates.

2.5. Reactive oxygen species and cytoplasmic calcium levels

To allow detection of reactive oxygen species (ROS) the general ROS marker CellROX® green probe (Molecular Probes, Invitrogen, Belgium) was selected. The latter was combined with the Rhod-2 AM (Molecular Probes, Invitrogen, Belgium), which becomes strongly fluorescent upon interaction with free Ca^{2+} in the cytoplasm.

The IONP containing medium was discarded subsequent to 24 hours exposure and the cells were washed once with PBS with Ca^{2+} (PBS^+, Invitrogen, Belgium). To allow visualization of reactive oxygen species (ROS), the cells were labeled with 5 µM CellROX® green (Molecular Probes, Belgium) in cell medium (250 µL/well). Following a 30 minute incubation period at 37 °C, the probe was removed and cells were washed once with PBS^+. The following 30 minutes cells were stained with a 5 µM Rhod-2 AM (Molecular Probes, Belgium) solution in PBS^+ (250 µL/well). After discarding the Rhod-2 AM and washing the cells with PBS^+, the cells were fixed with 4% paraformaldehyde. Following a 15-minute incubation period at room temperature the fixative was removed, cells were washed once with PBS without Ca^{2+} (PBS^-, Invitrogen, Belgium) and were stored in 500 µL PBS^-/well at 4 °C, protected from light until analysis.

During data acquisition the FITC/FITC excitation/emission (ex/em) filter combination was applied to visualize ROS whereas the Ca^{2+} signal was detected using the Cy3/Cy3 ex/em filters. Using a 20x magnification, a minimum of 5000 cells was imaged in at least 60 fields in two independent wells. The IN Cell Developer Toolbox software (GE Healthcare Life Sciences, Belgium) was applied to develop protocols and analyze the obtained images. The total cell number could be counted in the FITC/FITC images after defining the nuclei. Subsequent to determining the basal ROS levels, induction or reduction of ROS production (respectively cells with a ROS signal above or below background level) could be determined. In the Cy3/Cy3 images the signal area and total cell area were determined to quantify the effect on cytoplasmic free Ca^{2+}. The Ca^{2+} signal area was divided by the total cell area and the values for treated cells were normalized against the untreated control cells.

2.6. Effect on mitochondrial health and cell morphology

The mitochondria were labelled with Mitotracker® CMX-ROS Red (Molecular Probes, Invitrogen, Belgium), which specifically accumulates in the mitochondria based on its membrane potential. To allow evaluation of cell morphology the HCS CellMask™ Blue probe (Molecular Probes, Invitrogen, Belgium) was applied.

Following 24 hours exposure to the IONPs, the IONP containing medium was removed. Cells were washed once with PBS with Ca^{2+} (PBS^{+}, Invitrogen, Belgium) and incubated 30 minutes at 37 °C with 250 µL of a 250 nM Mitotracker® CMX-ROS Red (Molecular Probes, Invitrogen, Belgium) solution in cell medium. Following removal of the dye, the cells were washed once with PBS^{+} and fixed with 4% paraformaldehyde during 15 minutes at room temperature. After discarding the fixative and washing the cells with PBS^{-}, we applied 5 µg/mL HCS CellMask™ Blue (Molecular Probes, Invitrogen, Belgium) in PBS^{-} to label the cell cytoplasm. Subsequent to a 10-minute incubation period at room temperature, the label was removed by aspiration. Finally, the cells were washed with PBS^{-} and stored in 500 µL PBS^{-}/well at 4 °C and protected from light until analysis with the IN Cell Analyser 2000.

The mitochondria were detected with the TexasRed/TexasRed and Dapi/Dapi ex/em filters were used to record the CellMask™ Blue signal. Similar as before, minimum 5000 cells were imaged per condition in 60 fields per well (in two independent wells) using a 20x magnification lens. The obtained images were analyzed with in-house developed protocols

with the IN Cell Developer Toolbox software. Since the HCS CellMask™ Blue preferentially resides in the nucleus, the total cell number could be obtained from the Dapi images by defining and counting the nuclei. Subsequently, cells touching the image borders were excluded from analysis of cell morphology parameters. Next, cells were segmented based on the nuclei, the cytoplasm was recognized based on signal intensity and eventual holes were filled. For each condition, the average cell area was determined and normalized against the untreated control. In addition, the cell circularity was determined for each cell individually. The latter is a value between zero and one, with one representing a perfect sphere. Images in the orange channel provided information on the mitochondria. These organelles were defined based on the signal intensity and the mitochondrial signal area the within the total cell area was determined and normalized against the untreated control.

2.7. Statistics

Acute toxicity data are expressed as mean ± SEM (n=3). IN Cell data are presented as mean values normalized against the untreated control ± SEM (n=2). Statistical analysis was performed using one-way ANOVA combined with post-hoc Dunnett test.

3. RESULTS & DISCUSSION

3.1. Synthesized inorganic NPs display similar physicochemical characteristics

AuNP, AgNP and IONP synthesis was initiated with the aim of obtaining a similar core diameter. All NPs had a mean core diameter around 3.8 nm, as measured by transmission electron microscopy. Subsequently all NPs were coated with poly(isobutylene-*alt*-maleic anhydride) grafted with dodecylamine (PMA), which was selected as it ensures colloidal stability over a wide pH range and a uniform coating of the different core materials.[31] Dynamic light scattering measurements in water showed a hydrodynamic diameter of 9.0 nm, 8.9 nm and 12.3 nm and a negative zeta-potential around -45 mV, -35 mV, and -54 mV for the coated AuNPs, AgNPs and IONPs respectively. All obtained values correspond well to data reported on the characterization of NPs synthesized *via* similar protocols.[32, 33] The NPs were synthesized with the intention of obtaining similar physicochemical properties so that discrepancies in cell responses could be related to variations between the cell types.

3.2. Cytotoxicity depends on both the NP core material and the cell type

In initial cell experiments, we evaluated cell viability following 24 h NP exposure with the CellTiter GLO® assay. In Figure 6.1 a general concentration-dependent decrease in ATP signal can be observed for every evaluated NP–cell type combination. Although the extent of this decrease clearly varies, the onset of this downward trend depended on both the applied NP and the cell type. In all cell types, the most severe effect was observed following AuNP treatment, while the cells were least affected by the IONPs. The toxicity observed for the AgNPs can likely in part be explained in terms of Ag^+-ion leaching.[34] In turn, the severe acute cytotoxicity induced by the AuNPs could possibly be attributed to genotoxicity due to direct interactions between the 3.8 nm diameter AuNPs and DNA.[35] In addition, note that determining NP concentrations is not straightforward, as various methods/models need to be applied for different NP materials (Appendix A). This may affect the comparison of absolute concentrations of NPs of different materials and may additionally explain the severe toxicity observed here for the AuNPs. Given the limited loss of cell viability observed for the IONPs, the latter were selected for further evaluation of sublethal effects.

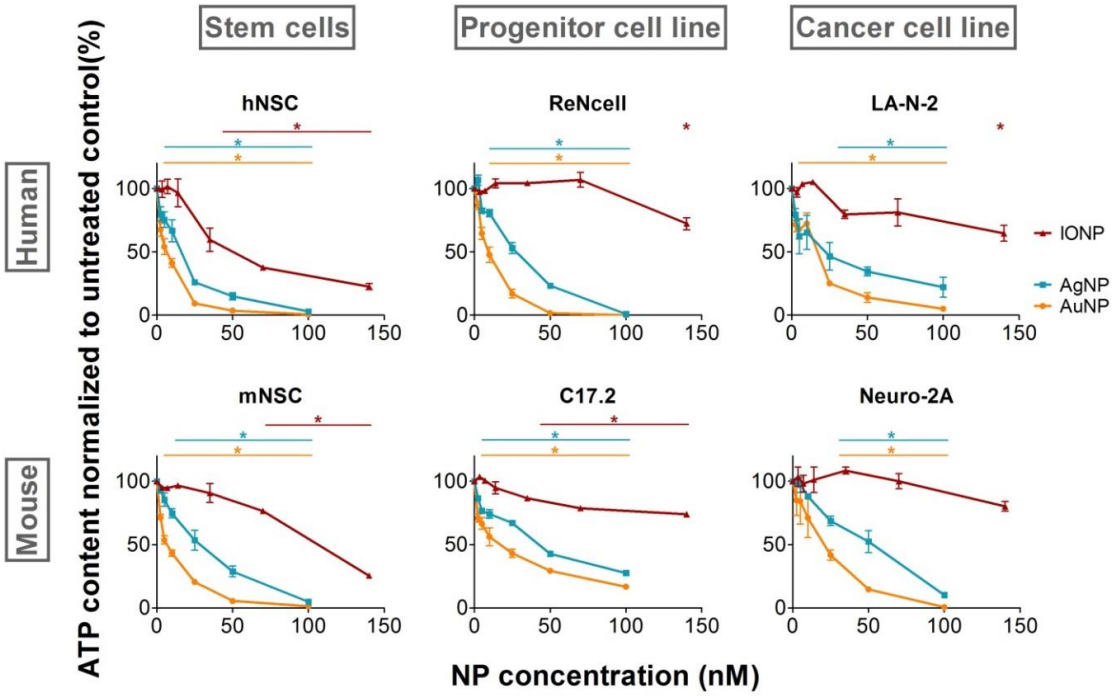

Figure 6.1. A concentration-dependent decrease in ATP content, as measured via the CellTiter GLO® assay, is observed for every NP-cell type combination tested. Results for the AuNPs (yellow), AgNPs (blue) and IONPs (red) are represented as mean ± standard error of the mean (SEM, n=3). Statistical significance is indicated when appropriate for each type of NP in the corresponding color of the graphs (p<0.05, AuNPs (yellow), AgNPs (blue) and IONPs (red)).*

Independent of the core material, the Neuro-2a cells were least susceptible to NP exposure whereas the hNSC, followed by the mNSC, were most sensitive. The susceptibility ranking for the other cell types varied with the NP core material. This greater sensitivity of the NSC, as found under the conditions reported here, is dissimilar to several studies where cell lines were found to be more susceptible to NP-induced acute cell injury.[18, 19] However, our data correlate well with previous work from Bregoli *et al.* who did not observe any toxic effects in several hematopoietic cell lines while primary bone marrow cells were clearly affected.[14] Of note, Wilkinson *et al.* and Schlinkert *et al.* independently found normal bronchial epithelial cells to experience more acute toxicity than the A549 cancer cell line.[36, 37]

3.3. ROS induction is observed in two out of six cell types

Since we found the IONPs to induce the least acute cell damage, it was decided to probe for sublethal effects caused by these NPs using a multiparametric methodology. The evaluation of effects on cell function has become crucial, as it is generally recognized that nanosafety evaluations should go beyond live/dead scoring in order to establish a more predictive paradigm.[15, 38] Subtle changes in cell function might indeed be more predictive towards *in*

vivo adverse outcomes. For instance, NP-promoted reactive oxygen species (ROS) production in pulmonary cells has been linked to acute inflammation in the lung.[39, 40] ROS induction is also stated to be the main mechanism *via* which metallic NPs induce cell stress. Persisting ROS induction can subsequently lead to oxidative stress and damage cellular components such as DNA, proteins and membrane lipids.[6]

Upon IONP treatment, we observed an increased ROS production in two out of six cell types, namely the mNSC and human ReNcells (Figure 6.2). ROS production was significantly reduced in the other four cell types. Notably, for both the reduced or increased ROS levels, the effect was most prominent in the NSC. Again the murine neuroblastoma cell line (Neuro-2a) was least affected in terms of ROS. Given the variable effects, no general statements can be made on whether the human or murine cell types were more severely affected than their counterparts.

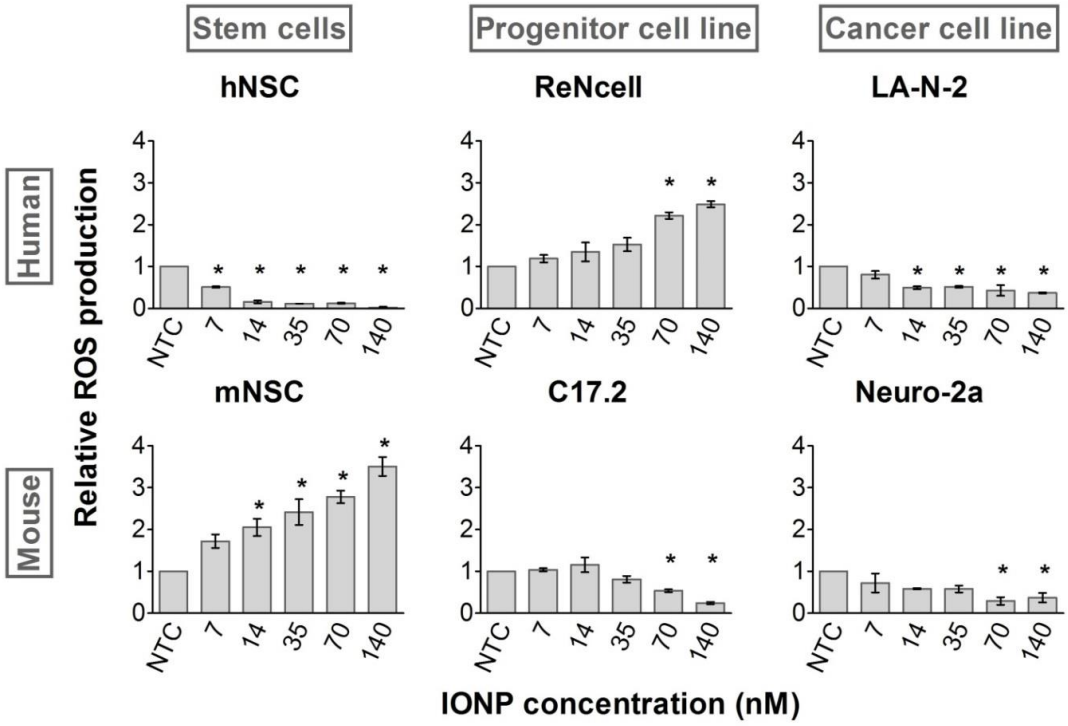

Figure 6.2. Effects on ROS production following IONP exposure visualized with the CellROX® green probe. A significant induction of ROS production was observed in the mNSC and human ReNcells. In the other four cell types a significant reduction was observed. Statistical significance is indicated when appropriate (p<0.05). (NTC = not treated control)*

Although ROS induction by IONPs is often observed,[19, 39, 41] NP-induced cytotoxicity cannot always be attributed to an increased ROS production.[42] Interestingly, Harris *et al*. also witnessed reduced ROS levels in their high content analysis of IONP-induced effects on a

mammalian fibroblast cell line.[6] Additionally, IONPs can exhibit an intrinsic peroxidase-like activity in mesenchymal stem cells and thus reduce the cellular ROS content, especially of H_2O_2.[43, 44] As this effect was only witnessed when IONPs remained intact, IONP biocompatibility is presumably to a large extent affected by the intracellular location and the way the cell processes the IONPs. In confirmation, Sabella *et al.* found greater cell perturbation by metallic NPs when they were trafficked to the acidic lysosomes in comparison to the same NPs present in the cytosol, due to the enhanced degradation in the acidic compartments.[45] Indeed, this degradation will be accountable for an increased amount of free iron ions, which may in turn enhance ROS production *via* for instance Fenton chemistry.[6, 46] A final factor that could clarify our observation is the intrinsically different anti-oxidative capacity of the various cell types.[15, 17] Thus, the cell itself likely determines NP biocompatibility to a large extent.

3.4. IONP exposure perturbs cellular calcium homeostasis

Subsequently, we evaluated the effect of IONP exposure on Ca^{2+} homeostasis. The intracellular free Ca^{2+} concentration ($[Ca^{2+}]_c$) is a valuable toxicity marker since Ca^{2+} is involved in a plethora of processes such as cell proliferation, mitochondrial function and gene expression.[47, 48] Ca^{2+} is furthermore of ultimate importance for proper cell function in neural cells, as it is required for neurotransmitter release and cellular excitability.[8, 49] Additionally, Ca^{2+} is since long known to be an important regulator of cell death, where a significant increase in $[Ca^{2+}]_c$ is noted.[47] A mild reduction can on the contrary be correlated with an impaired cell function due to enhanced intracellular Ca^{2+} storage or efflux in an effort to retain cell homeostasis, while cell lysis is correlated to a more severe decrease.[48, 50]

On the one hand, a significant concentration-dependent increase in $[Ca^{2+}]_c$ was observed in the hNSC, ReNcells, and C17.2 cells (Figure 6.3). The effect was more severe in the progenitor cell lines compared to the hNSC and the ReNcells showed the highest $[Ca^{2+}]_c$. On the other hand, a decline of the $[Ca^{2+}]_c$ was detected in the mNSC, LA-N-2 and Neuro-2a cells. In contrast to previous parameters, the Neuro-2a cells showed more severe effects in terms of the perturbation of the calcium homeostasis. Again, no unambiguous conclusions could be drawn on whether human or murine cell types are more sensitive towards NP exposure.

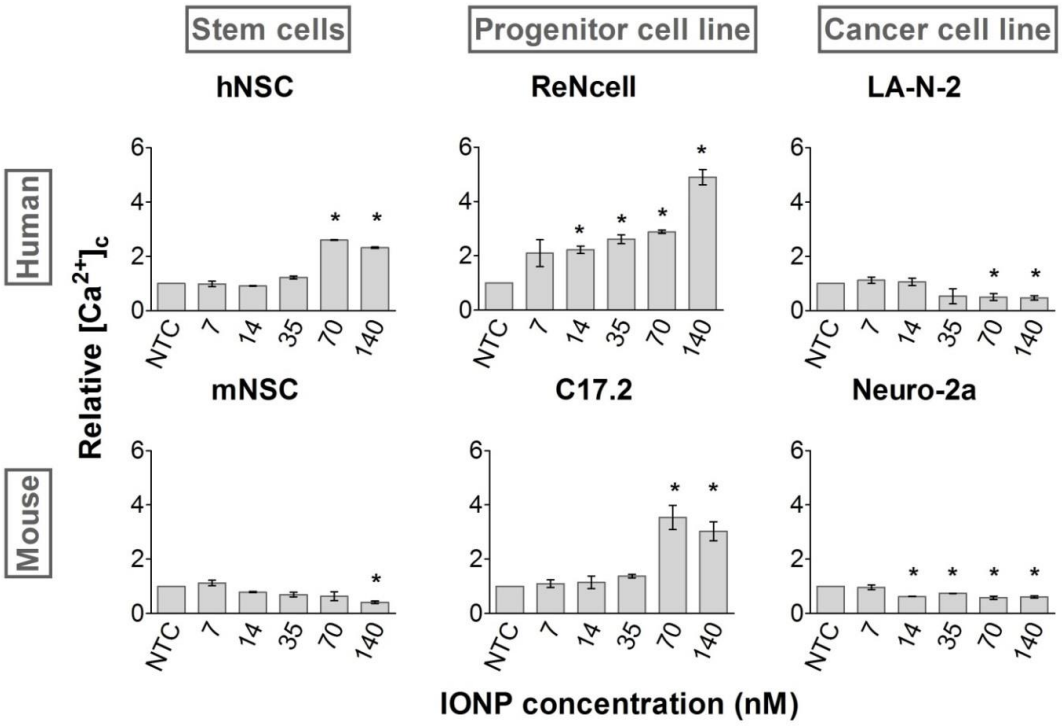

Figure 6.3. Effect on $[Ca^{2+}]_c$ as determined following labelling with Rhod-2 AM. A significant increase in $[Ca^{2+}]_c$ was observed in the hNSC and both progenitor cell lines whereas a significant reduction was observed in the remaining three cell types ($p<0.05$). Statistical significance is indicated when appropriate ($p<0.05$). (NTC = not treated control)*

Multiple studies investigating the influence of NP exposure on the Ca^{2+} homeostasis also found $[Ca^{2+}]_c$ to be augmented.[51] Since this response could be interpreted as a cell death signal, this outcome could be correlated to the initially observed acute toxicity (Figure 6.1).[47, 52] Although we would have expected to observe a greater increase in $[Ca^{2+}]_c$ in the hNSC when compared to the ReNcells based on the acute toxicity data, the opposite was true. In line with the observed decline in $[Ca^{2+}]_c$ in three out of six cell types, Haase *et al.* documented diminished Ca^{2+} responses at cytotoxic NP doses in mNSC.[3] This observation could on the one hand be explained in terms of cell lysis. On the other hand, stressed cells can maintain their Ca^{2+} homeostasis by elevating Ca^{2+} efflux *via* the plasma membrane Ca^{2+} ATPase pump.[50] We hypothesized that this occurred in the neuroblastoma cell lines where ATP levels were to a minor extent reduced and thus still allowed sufficient pump function.

In general, two groups could be distinguished based on the elevation or diminution of $[Ca^{2+}]_c$. Even though similar trends were retrieved in each group, it is clear that the extent of the perturbation of cellular Ca^{2+} homeostasis varied with the cell type. Since Ca^{2+} homeostasis is significantly altered upon cell transformation or immortalization in favour of

cell proliferation,[53] it was not surprising that NP exposure variably altered the $[Ca^{2+}]_c$. Notably, cell type specific toxicity profiles started to emerge as various combinations of the thus far evaluated effects were obtained.

3.5. Mitochondria are affected by IONP loading

Next, the effect of IONP exposure on mitochondrial homeostasis was evaluated. The mitochondria are interesting organelles as they are the cell's main energy suppliers, involved in programmed cell death, an important source of ROS and to a large extent regulated by Ca^{2+}.[52, 54] This Ca^{2+}-mediated regulation is furthermore influenced by external stimuli: in combination with a stress inducer Ca^{2+} promotes ROS production and possibly cell death, whereas under physiological conditions Ca^{2+} stimulates the oxidative respiration in the mitochondria and thus ATP production.[52] Interestingly, the importance of oxidative respiration for overall cellular ATP production varies with the cell type: both cancer cells and stem cells rather rely on cytosolic glycosylation for their ATP production.[54, 55] Hence, it is conceivable that mitochondria will not only be differentially affected, but also that the impact of mitochondrial perturbation on overall cell homeostasis will vary in the different cell types.

To visualize the mitochondria, we selected a probe that specifically labels the organelles based on their membrane potential ($\Delta\Psi_m$). Loss of this potential, as a result of mitochondrial membrane permeabilization, will render the organelle undetectable and has been associated with cytochrome C release and cell death initiation.[52, 56] During data analysis, such events could be detected as a reduction of the relative mitochondrial area. Figure 6.4 shows that all cell types, except the Neuro-2a cells, showed significant mitochondrial damage. Accordingly, the loss of $\Delta\Psi_m$ following NP exposure has already been described in multiple studies for several NPs in cell types from various lineages and species.[8, 9, 42] In the NSC all IONP doses caused a decreased signal area, though the effect was only significant starting from 7 nM. In contrast, the affected cell lines (ReNcell, C17.2 and LA-N-2) were significantly affected by all IONP doses. The effects were most outspoken in the ReNcells, closely followed by the hNSC and mNSC. The mitochondria in the C17.2 and LA-N-2 cell lines were perturbed to a lesser extent. Notably, the human cell types were more severely affected than the murine counterpart. In addition, the neuroblastoma cell lines were most resilient on the mitochondrial level. In correspondence, Heerdt *et al.* have previously found

mitochondria in transformed cells to be less sensitive to perturbation due to an intrinsically lower mitochondrial activity and higher $\Delta\Psi_m$.[57]

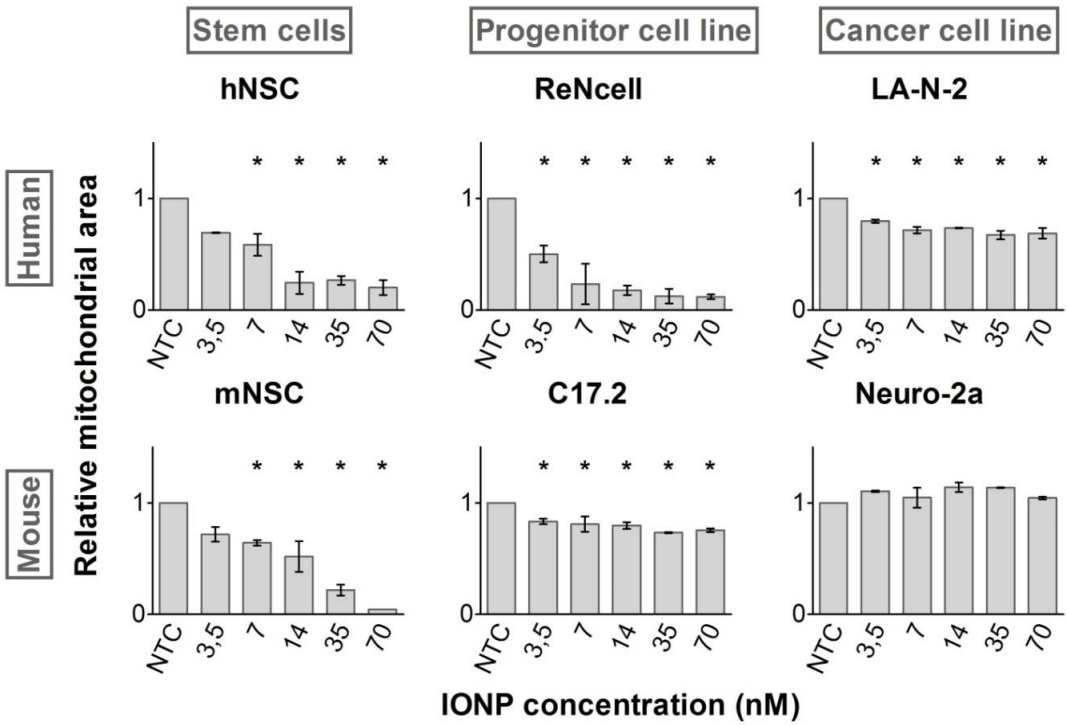

Figure 6.4. Effects on the mitochondria labelled with Mitotracker® CMX-ROS in terms of the relative signal area representing the size of the mitochondrial compartment relative to the total cell area. Except for the Neuro-2a cell line, all cell types showed a significant decrease in mitochondrial area. Statistical significance is indicated when appropriate (p<0.05). (NTC = not treated control)*

3.6. IONP loading affects cell morphology

Lastly, we examined alterations in cell morphology following IONP exposure. Cell morphology is a convenient parameter, especially for neural cells given their intricate architecture.[8] Moreover, numerous NPs have been shown to alter cell morphology as a secondary effect of ROS induction or *via* direct interactions with elements of the cytoskeleton.[58, 59] In addition to the changes in the morphological appearance, certain cell functions that require signalling *via* these components can subsequently be impaired.[59, 60] Thus, subtle effects on cell morphology can indirectly herald perturbation of cell function whereas severe morphological alterations, *i.e.* cell rounding and shrinking, can be interpreted in terms of cell death.[47]

After staining the entire cell cytoplasm, the impact of IONP exposure on cell morphology was quantified *via* two parameters: cell area and cell circularity. The latter is applied as a measure of cell spreading and is a value between zero and one, where one represents a perfect sphere. Although the extent of neurite outgrowth is often applied to evaluate the morphology of neural cells,[61] this parameter was not selected for this work, as several cell types are not capable of forming neurites.

While only a significantly decreased cell area was noted for the C17.2 cell line, both a reduced cell area and an increase in circularity were observed in the NSC, ReNcells and Neuro-2a cells (Figure 6.5). Thus, the cells became both smaller and more spherical in a concentration-dependent fashion, which was most outspoken in the ReNcells. Such loss of specific morphological features and cell shrinking has already been described in numerous studies for multiple NPs and cell types.[3, 8, 22, 42] Since it is known that cell transformation or immortalization affects cell morphology, it is not surprising that morphology was also differentially affected in the various cell types. For instance the mNSCs were more strongly affected in terms of morphology whereas only minor effects were observed in the C17.2 or Neuro-2a cell line (Figure 6.6). Since stem cells have a more intricate architecture in comparison to most cell lines, it was not surprising that the morphology of the former was impaired more extensively. Finally, as the LA-N-2 cells tend to grow in clusters we evaluated effects on cell morphology in terms of the total cluster area and number of cells per cluster, which both showed a similar concentration-dependent decrease starting from 3.5 nM IONPs. Since the decrease in cluster area was slightly more severe than the number of cells per cluster, we concluded that the cell area also decreased with every dose tested.

Overall, we observed similar effects on cell morphology (cell rounding and shrinking) in the various cell types in contrast to previously evaluated parameters. However, the exact trends and extent of the responses clearly differed. Importantly, these variations could not unequivocally be linked to one or a specific combination of responses observed for the other toxicity parameters investigated in this study, underscoring the cell type specific nature of the recorded toxicity profiles.

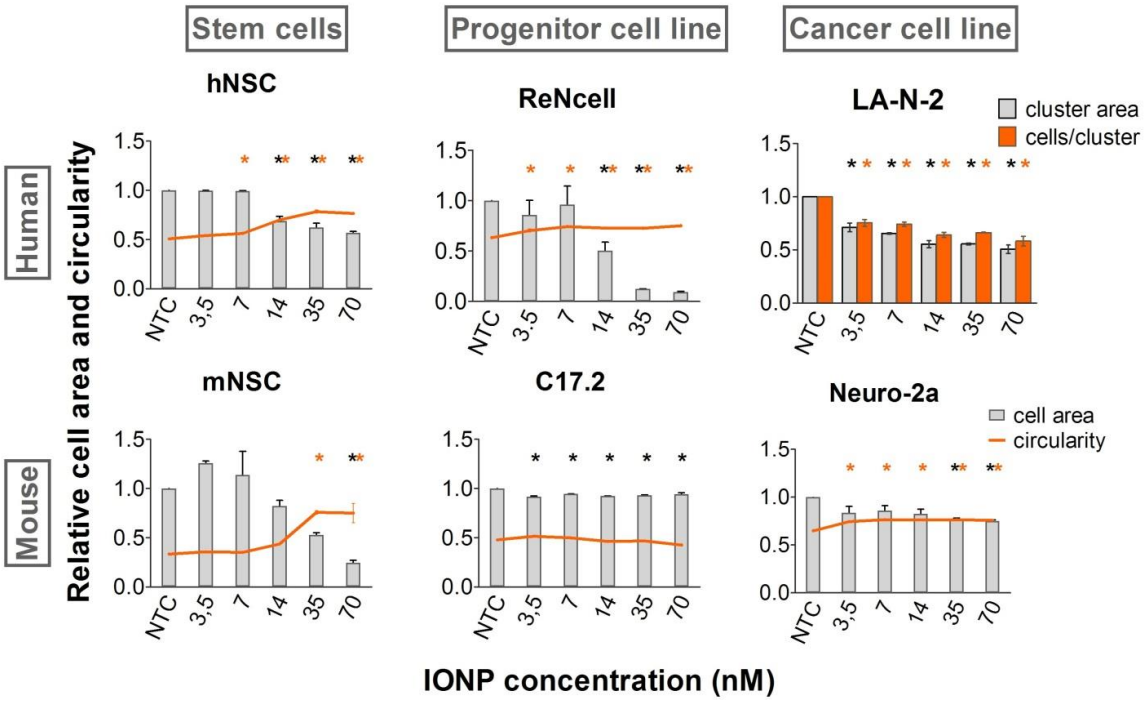

Figure 6.5. IONP-induced alterations in cell area (grey bars) and cell circularity (orange lines) visualized after labelling of the cytoplasm with the CellMask™ Blue probe for the NSC, progenitor cell lines and murine neuroblastoma cell line. Cell circularity is a measure of cell spreading and is a value between zero and one, where one represents a perfect sphere. LA-N-2 cell morphology was analysed in terms of cluster area (grey bars) and number of cells per cluster (orange bars). A decreased cell area and increased cell circularity were detected in the NSC, ReNcell and Neuro-2a cell line. For the C17.2 cells only a diminution in cell area was detected. In the LA-N-2 cell line a reduction in cells per cluster and cluster size were observed. Statistical significance is indicated when appropriate (p<0.05), in black for the cell area and orange in case of the cell circularity (respectively cluster area and cells per cluster in case of the LA-N-2 cell line). (NTC = not treated control)*

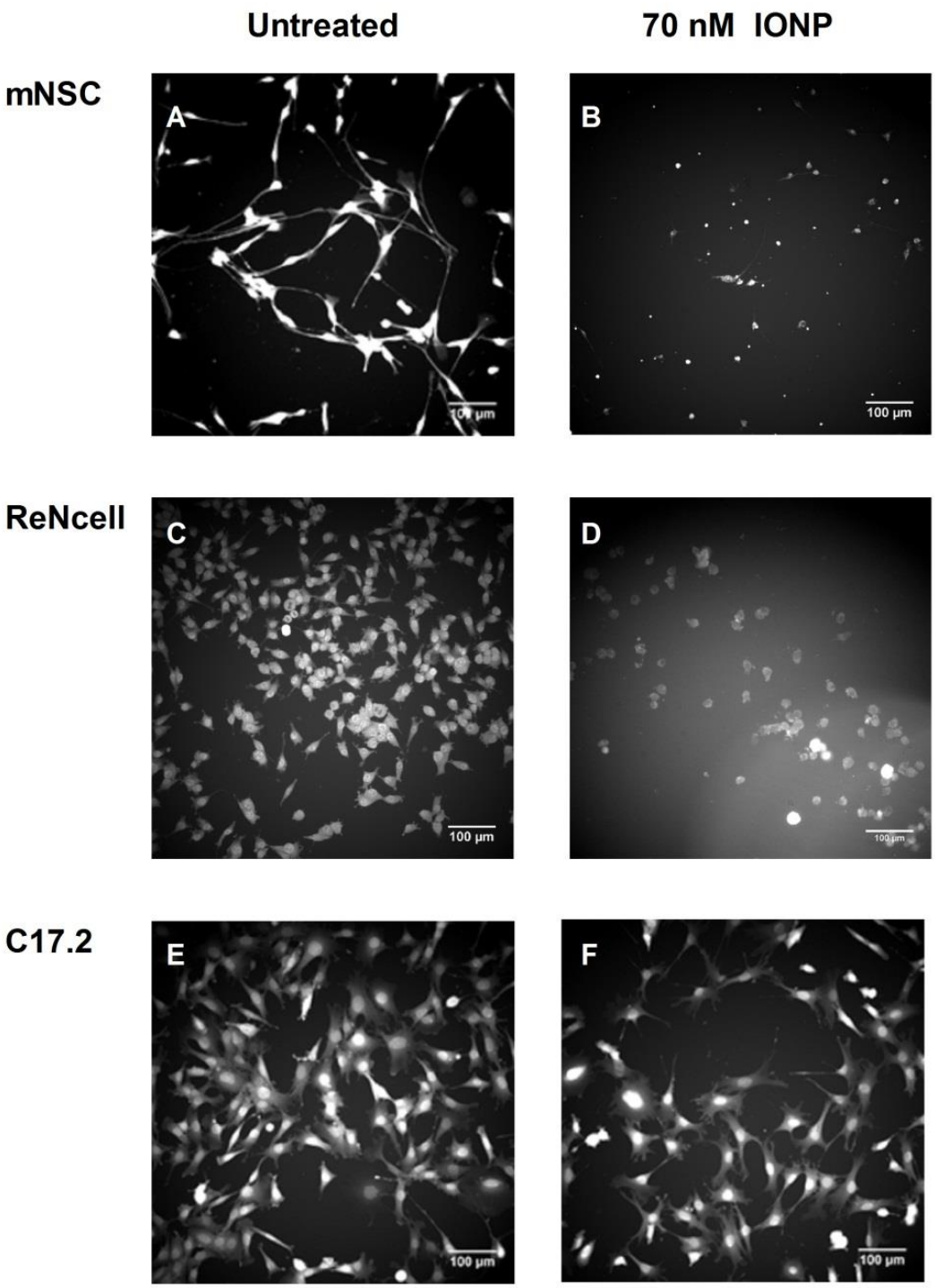

Figure 6.6. Representative images of untreated mNSCs (A), ReNcells (C) and C17.2 cells (E) as well the morphological alterations induced by exposure to 70 nM IONP (B, D & F). The mNSCs are clearly affected in terms of both cell area and circularity. The altered circularity in the ReNcells is less outspoken as initial morphology is less complex. Finally IONP treatment only caused a reduction in the cell area in the C17.2 cell line.

3.7. Multiparametric analysis reveals cell type-specific toxicity profiles

In general, our data set reveals that each cell type reacted in a specific way to IONP exposure in terms of both extent and nature of the responses (Table 6.3). This could not have been deduced from the acute toxicity assessment (Figure 6.1) but became increasingly clear with every additionally evaluated parameter. Furthermore, the obtained profiles would likely become increasingly complex with the addition of supplementary end points such as the influence on autophagy, induction of endoplasmic reticulum stress or genotoxicity. Note that it was not the primary objective of this study to unravel the underlying toxicity mechanisms. Additional experiments should therefore be performed, for instance on the type of cell death or gene expression. Instead, the aim was to clearly show the impact of both the species and the cell type, under its optimal cell culture conditions on the nanotoxicity profile within one single study. We show that for 3 different, though related neural cell types (stem cells, immortalized cells and cancer cells) the effects in the human cells were often more outspoken than the murine alternative. In addition, we found the NSC from each species to be more sensitive to IONP exposure than the cell lines.

Table 6.3. Cell type-specific nanotoxicity profiles induced by 24h exposure to 70 nM IONPs.

	ROS	Ca^{2+}	Mitochondria	Cell morphology	
				Area	Circularity
hNSC	↓	↑	↓	↓	↑
mNSC	↑	↓	↓	↓	↑
ReNcell	↑	↑	↓	↓	↑
C17.2	↓	↑	↓	↓	=
LA-N-2	↓	↓	↓	(*)	(*)
Neuro-2a	↓	↓	=	↓	↑

The observed variations in cell responses can be explained in several possible ways. One may argue that variations in NP uptake in the various cell types will be an important factor. In this regard, dose heterogeneity at single cell level due to variations in NP uptake in the same population will also lead to response heterogeneity.[62] In addition, NP uptake is related to the colloidal stability in the applied cell culture media. Although we did not evaluate the

abovementioned parameters in detail, it was previously shown that PMA-coated NPs show good stability in biological media and that they are taken up well by various cell types.[30, 63] Besides the extent of NP uptake, we believe that the cellular response is strongly related to the intracellular NP processing. This will in part depend on the uptake pathway since the latter will co-determine the intracellular trafficking route and the ultimate intracellular location. Indeed, as previously mentioned when NPs are present in the acidic and degrading environment of the endo-lysosomes, stronger cytotoxicity is observed than when the NPs reside in the cytosol.[45] In addition, the variations in intrinsic cell properties, such as the anti-oxidative capacity, metabolic rate (e.g. Ca^{2+} homeostasis) and mitochondrial activity, are to a large extent accountable for the revealed divergent toxicity profiles. Combined, these elements advocate an *in vitro* toxicity profiling that takes intrinsic cell properties and variations in the studied cell population into account. Indeed, to understand the intrinsic cellular capacity to traffic and handle exogenous materials could be of key importance to anticipate NP-evoked effects.

Furthermore, our data indicate that it is imperative to apply multiparametric methods that look beyond live/dead scoring. Notably, even when only minor variations could be detected in the cell viability, as for instance for the Neuro-2a and ReNcells, cellular homeostasis was distinctly altered. In addition, minor cell viability alterations for the ReNcells did not imply that the cell homeostasis was not impaired. Accordingly, Ge *et al.* found IONPs to evoke important effects on cell function without affecting cell viability.[64] Also, toxicity endpoints included in nanosafety screens should be carefully selected, as some are more sensitive or indicative of the induced damage. An example of the latter is the use of cell area and circularity as parameters to describe alterations in cell morphology. Although effects on cell circularity occurred sooner, the impact on cell area was more outspoken and illustrative for the extent of the actual damage in cell types without a complex architecture. Finally, the safety of the coating should be investigated in further detail to determine its possible contribution to some of the observed effects.

Notably, we found that none of the cell types included in this work would be a suitable substitute for any other tested. In contrast, other groups did succeed in identifying a cell line alternative for primary cells based on similar cellular responses to NP exposure.[12] In such cases the use of those cell lines should be encouraged. However, the generalized use of cell

lines should be approached with caution, especially when performing a detailed toxicity profiling to elucidate the mechanisms *via* which NPs alter cell homeostasis. Indeed, cell lines are not always ideal candidates for the analysis of cell function and may not be representative in terms of discrete cell perturbation.[19] Thus, it would be fitting to select a cell type based on the expected exposure and/or intended application of the NPs. We also propose to cautiously apply non-human cell types since we, as well as several other groups, have observed notable interspecies variations.[15, 16]

For screening purposes the selection of a proper cell type is a balancing act. Indeed, primary cells can suffer from several drawbacks like an often limited availability, specific cultivation requirements, a limited life-span, and possible inter-batch and –individual variations, which possibly limit the throughput.[7, 12] Hence, cell lines are still the preferred candidates when performing a large-scale screening of numerous NPs. For this reason and because it is highly unlikely that one single cell type will emerge as a universal model, we strongly believe that the definition of a set of standard cell lines would constitute a definite asset in standardizing nanosafety assessments. The selected cell types would preferably be known to mimic responses observed in primary cells and would ideally be thoroughly characterized in terms of their intrinsic properties in order to enhance our understanding of the NP-induced effects. The standard cell lines should provide models for relevant target organs or tissues and the cell line selection for screening should be based on the expect exposure or application.

4. CONCLUSION

In this work, we investigated the effect of both species and cell type related variations on NP-evoked responses in six related neural cell types *via* a multiparametric approach. Interestingly, the observed impact on cellular health varied widely in each cell type in terms of both the nature and extent of the analyzed effects and cell type-specific nanotoxicity profiles were obtained. Hence, conclusions on the safety of a NP should preferably not be based on the evaluation of a single toxicity end point in a single cell type. We propose to rationally select a cell model based on the envisioned (biomedical) application and/or exposure scenario, especially when performing an extensive *in vitro* toxicity assessment with the aim of unveiling mechanisms *via* which the NPs inflict cell injury. Finally, with regard to standardization of *in vitro* nanosafety evaluations, we strongly believe that for the safety screening of large sets of nanomaterials the selection of a set of standard cell types, representing relevant target tissues, from which a cell line could be selected for a specific nanosafety study would contribute to the generation of more consistent nanosafety data.

ACKNOWLEDGEMENTS

We thank Shareen Doak from the DNA damage group, Institute of Life Sciences, Swansea University, UK for the use of the IN Cell Analyzer 2000. Additionally we wish to thank Sebastian Munck and Nicky Corthout from the VIB Centre for Biology of Disease, Belgium for the technical guidance in the use of the IN Cell Analyzer 2000 and IN Cell Developer Toolbox software. We would also like to thank Tianqiang Wang for support in nanoparticle characterization and Karsten Kantner for the ICP measurements. Parts of this work were supported by DFG Germany (GRK 1782 to WJP) and by the European Commission (grant FutureNanoNeeds to WJP). BP acknowledges the Alexander von Humboldt Foundation for a postdoctoral fellowship.

REFERENCES

1. Stark, W. J.; Stoessel, P. R.; Wohlleben, W.; Hafner, A. *Chem Soc Rev* **2015,** 44, (16), 5793-805.
2. Lim, E. K.; Kim, T.; Paik, S.; Haam, S.; Huh, Y. M.; Lee, K. *Chemical reviews* **2015,** 115, (1), 327-94.
3. Haase, A.; Rott, S.; Mantion, A.; Graf, P.; Plendl, J.; Thunemann, A. F.; Meier, W. P.; Taubert, A.; Luch, A.; Reiser, G. *Toxicol Sci* **2012,** 126, (2), 457-68.
4. Min, Y.; Caster, J. M.; Eblan, M. J.; Wang, A. Z. *Chemical reviews* **2015,** 115, (19), 11147-90.
5. Rivera-Gil, P.; De Aberasturi, D. J.; Wulf, V.; Pelaz, B.; Del Pino, P.; Zhao, Y. Y.; De La Fuente, J. M.; De Larramendi, I. R.; Rojo, T.; Liang, X. J.; Parak, W. J. *Accounts of chemical research* **2013,** 46, (3), 743-749.
6. Nel, A.; Xia, T.; Madler, L.; Li, N. *Science* **2006,** 311, (5761), 622-7.
7. Joris, F.; Manshian, B. B.; Peynshaert, K.; De Smedt, S. C.; Braeckmans, K.; Soenen, S. J. *Chemical Society reviews* **2013,** 42, (21), 8339-59.
8. Jan, E.; Byrne, S. J.; Cuddihy, M.; Davies, A. M.; Volkov, Y.; Gun'ko, Y. K.; Kotov, N. A. *ACS nano* **2008,** 2, (5), 928-38.
9. George, S.; Pokhrel, S.; Xia, T.; Gilbert, B.; Ji, Z.; Schowalter, M.; Rosenauer, A.; Damoiseaux, R.; Bradley, K. A.; Madler, L.; Nel, A. E. *ACS nano* **2010,** 4, (1), 15-29.
10. Ong, K. J.; MacCormack, T. J.; Clark, R. J.; Ede, J. D.; Ortega, V. A.; Felix, L. C.; Dang, M. K.; Ma, G.; Fenniri, H.; Veinot, J. G.; Goss, G. G. *PloS one* **2014,** 9, (3), e90650.
11. N. Feliu, B. P., Q. Zhang, P. del Pino, A. Nyström, W. J. Parak. *WIREs Nanomedicine & Nanobiotechnology* **2015**.
12. Kermanizadeh, A.; Lohr, M.; Roursgaard, M.; Messner, S.; Gunness, P.; Kelm, J. M.; Moller, P.; Stone, V.; Loft, S. *Particle and fibre toxicology* **2014,** 11, 56.
13. Wang, J.; Fang, X.; Liang, W. *ACS nano* **2012,** 6, (6), 5018-30.
14. Bregoli, L.; Chiarini, F.; Gambarelli, A.; Sighinolfi, G.; Gatti, A. M.; Santi, P.; Martelli, A. M.; Cocco, L. *Toxicology* **2009,** 262, (2), 121-9.
15. Zhang, H.; Wang, X.; Wang, M.; Li, L.; Chang, C. H.; Ji, Z.; Xia, T.; Nel, A. E. *Small* **2015,** 11, (31), 3797-805.
16. Luengo, Y.; Nardecchia, S.; Morales, M. P.; Serrano, M. C. *Nanoscale* **2013,** 5, (23), 11428-37.
17. Mukherjee, S. G.; O'Claonadh, N.; Casey, A.; Chambers, G. *Toxicol in Vitro* **2012,** 26, (2), 238-51.
18. Wang, Y.; Aker, W. G.; Hwang, H. M.; Yedjou, C. G.; Yu, H.; Tchounwou, P. B. *The Science of the total environment* **2011,** 409, (22), 4753-62.
19. Ekstrand-Hammarstrom, B.; Akfur, C. M.; Andersson, P. O.; Lejon, C.; Osterlund, L.; Bucht, A. *Nanotoxicology* **2012,** 6, (6), 623-34.
20. Kermanizadeh, A.; Gaiser, B. K.; Ward, M. B.; Stone, V. *Nanotoxicology* **2013,** 7, (7), 1255-71.
21. Shen, W. B.; Vaccaro, D. E.; Fishman, P. S.; Groman, E. V.; Yarowsky, P. *Contrast media & molecular imaging* **2016,** 11, (3), 222-8.
22. Soenen, S. J.; Himmelreich, U.; Nuytten, N.; De Cuyper, M. *Biomaterials* **2011,** 32, (1), 195-205.
23. Lei, H.; Nan, X.; Wang, Z.; Gao, L.; Xie, L.; Zou, C.; Wan, Q.; Pan, D.; Beauchamp, N.; Yang, X.; Matula, T.; Qiu, B. *J Nanosci Nanotechnol* **2015,** 15, (4), 2605-12.
24. Hahn, M. A.; Singh, A. K.; Sharma, P.; Brown, S. C.; Moudgil, B. M. *Analytical and bioanalytical chemistry* **2011,** 399, (1), 3-27.
25. Wu, Y. Y.; Mujtaba, T.; Rao, M. S. *Methods Mol Biol* **2002,** 198, 29-40.
26. Donato, R.; Miljan, E. A.; Hines, S. J.; Aouabdi, S.; Pollock, K.; Patel, S.; Edwards, F. A.; Sinden, J. D. *Bmc Neurosci* **2007,** 8, 36.
27. Seeger, R. C.; Rayner, S. A.; Banerjee, A.; Chung, H.; Laug, W. E.; Neustein, H. B.; Benedict, W. F. *Cancer research* **1977,** 37, (5), 1364-1371.

28. Ryder, E. F.; Snyder, E. Y.; Cepko, C. L. *J Neurobiol* **1990,** 21, (2), 356-375.
29. Klebe, R. J.; Ruddle, R. H. *Journal of Cell Biology* **1969,** 43, (2p2), A69-&.
30. Manshian, B. B.; Moyano, D. F.; Corthout, N.; Munck, S.; Himmelreich, U.; Rotello, V. M.; Soenen, S. J. *Biomaterials* **2014,** 35, (37), 9941-50.
31. Lin, C. A.; Sperling, R. A.; Li, J. K.; Yang, T. Y.; Li, P. Y.; Zanella, M.; Chang, W. H.; Parak, W. J. *Small* **2008,** 4, (3), 334-41.
32. Sun, S.; Zeng, H.; Robinson, D. B.; Raoux, S.; Rice, P. M.; Wang, S. X.; Li, G. *Journal of the American Chemical Society* **2004,** 126, (1), 273-9.
33. Caballero-Diaz, E.; Pfeiffer, C.; Kastl, L.; Rivera-Gil, P.; Simonet, B.; Valcarcel, M.; Jimenez-Lamana, J.; Laborda, F.; Parak, W. J. *Part Part Syst Char* **2013,** 30, (12), 1079-1085.
34. Soenen, S. J.; Parak, W. J.; Rejman, J.; Manshian, B. *Chemical reviews* **2015,** 115, (5), 2109-35.
35. Soenen, S. J.; Rivera-Gil, P.; Montenegro, J. M.; Parak, W. J.; De Smedt, S. C.; Braeckmans, K. *Nano today* **2011,** 6, (5), 446-465.
36. Wilkinson, K. E.; Palmberg, L.; Witasp, E.; Kupczyk, M.; Feliu, N.; Gerde, P.; Seisenbaeva, G. A.; Fadeel, B.; Dahlen, S. E.; Kessler, V. G. *ACS nano* **2011,** 5, (7), 5312-5324.
37. Schlinkert, P.; Casals, E.; Boyles, M.; Tischler, U.; Hornig, E.; Tran, N.; Zhao, J. Y.; Himly, M.; Riediker, M.; Oostingh, G. J.; Puntes, V.; Duschl, A. *J Nanobiotechnol* **2015,** 13.
38. George, S.; Xia, T.; Rallo, R.; Zhao, Y.; Ji, Z.; Lin, S.; Wang, X.; Zhang, H.; France, B.; Schoenfeld, D.; Damoiseaux, R.; Liu, R.; Lin, S.; Bradley, K. A.; Cohen, Y.; Nel, A. E. *ACS nano* **2011,** 5, (3), 1805-17.
39. Park, E. J.; Park, K. *Toxicol Lett* **2009,** 184, (1), 18-25.
40. Zhang, H.; Pokhrel, S.; Ji, Z.; Meng, H.; Wang, X.; Lin, S.; Chang, C. H.; Li, L.; Li, R.; Sun, B.; Wang, M.; Liao, Y. P.; Liu, R.; Xia, T.; Madler, L.; Nel, A. E. *Journal of the American Chemical Society* **2014,** 136, (17), 6406-20.
41. Sharma, G.; Kodali, V.; Gaffrey, M.; Wang, W.; Minard, K. R.; Karin, N. J.; Teeguarden, J. G.; Thrall, B. D. *Nanotoxicology* **2014,** 8, (6), 663-75.
42. Fujioka, K.; Hanada, S.; Inoue, Y.; Sato, K.; Hirakuri, K.; Shiraishi, K.; Kanaya, F.; Ikeda, K.; Usui, R.; Yamamoto, K.; Kim, S. U.; Manome, Y. *Int J Mol Sci* **2014,** 15, (7), 11742-59.
43. Huang, D. M.; Hsiao, J. K.; Chen, Y. C.; Chien, L. Y.; Yao, M.; Chen, Y. K.; Ko, B. S.; Hsu, S. C.; Tai, L. A.; Cheng, H. Y.; Wang, S. W.; Yang, C. S.; Chen, Y. C. *Biomaterials* **2009,** 30, (22), 3645-51.
44. Gao, L.; Zhuang, J.; Nie, L.; Zhang, J.; Zhang, Y.; Gu, N.; Wang, T.; Feng, J.; Yang, D.; Perrett, S.; Yan, X. *Nature nanotechnology* **2007,** 2, (9), 577-83.
45. Sabella, S.; Carney, R. P.; Brunetti, V.; Malvindi, M. A.; Al-Juffali, N.; Vecchio, G.; Janes, S. M.; Bakr, O. M.; Cingolani, R.; Stellacci, F.; Pompa, P. P. *Nanoscale* **2014,** 6, (12), 7052-61.
46. Petters, C.; Thiel, K.; Dringen, R. *Nanotoxicology* **2016,** 10, (3), 332-42.
47. Zhivotovsky, B.; Orrenius, S. *Cell calcium* **2011,** 50, (3), 211-21.
48. Clapham, D. E. *Cell* **2007,** 131, (6), 1047-58.
49. Ariano, P.; Zamburlin, P.; Gilardino, A.; Mortera, R.; Onida, B.; Tomatis, M.; Ghiazza, M.; Fubini, B.; Lovisolo, D. *Small* **2011,** 7, (6), 766-74.
50. Tseng, Y. C.; Yang, A.; Huang, L. *Molecular pharmaceutics* **2013,** 10, (11), 4391-4395.
51. Anguissola, S.; Garry, D.; Salvati, A.; O'Brien, P. J.; Dawson, K. A. *PloS one* **2014,** 9, (9), e108025.
52. Brookes, P. S.; Yoon, Y.; Robotham, J. L.; Anders, M. W.; Sheu, S. S. *American journal of physiology. Cell physiology* **2004,** 287, (4), C817-33.
53. Capiod, T.; Shuba, Y.; Skryma, R.; Prevarskaya, N. *Sub-cellular biochemistry* **2007,** 45, 405-27.
54. Fulda, S.; Galluzzi, L.; Kroemer, G. *Nature reviews. Drug discovery* **2010,** 9, (6), 447-64.
55. Ito, K.; Suda, T. *Nature reviews. Molecular cell biology* **2014,** 15, (4), 243-56.
56. Gottlieb, E.; Armour, S. M.; Harris, M. H.; Thompson, C. B. *Cell death and differentiation* **2003,** 10, (6), 709-17.
57. Heerdt, B. G.; Houston, M. A.; Wilson, A. J.; Augenlicht, L. H. *Cancer research* **2003,** 63, (19), 6311-9.

58. Buyukhatipoglu, K.; Clyne, A. M. *Journal of biomedical materials research. Part A* **2011,** 96, (1), 186-95.
59. Tay, C. Y.; Cai, P.; Setyawati, M. I.; Fang, W.; Tan, L. P.; Hong, C. H.; Chen, X.; Leong, D. T. *Nano letters* **2014,** 14, (1), 83-8.
60. Wu, Y. L.; Putcha, N.; Ng, K. W.; Leong, D. T.; Lim, C. T.; Loo, S. C. J.; Chen, X. D. *Accounts of chemical research* **2013,** 46, (3), 782-791.
61. Soenen, S. J.; Manshian, B.; Montenegro, J. M.; Amin, F.; Meermann, B.; Thiron, T.; Cornelissen, M.; Vanhaecke, F.; Doak, S.; Parak, W. J.; De Smedt, S.; Braeckmans, K. *ACS nano* **2012,** 6, (7), 5767-83.
62. Ware, M. J.; Godin, B.; Singh, N.; Majithia, R.; Shamsudeen, S.; Serda, R. E.; Meissner, K. E.; Rees, P.; Summers, H. D. *ACS nano* **2014,** 8, (7), 6693-6700.
63. Kirchner, C.; Liedl, T.; Kudera, S.; Pellegrino, T.; Javier, A. M.; Gaub, H. E.; Stolzle, S.; Fertig, N.; Parak, W. J. *Nano letters* **2005,** 5, (2), 331-338.
64. Ge, G. Y.; Wu, H. F.; Xiong, F.; Zhang, Y.; Guo, Z. R.; Bian, Z. P.; Xu, J. D.; Gu, C. R.; Gu, N.; Chen, X. J.; Yang, D. *Nanoscale research letters* **2013,** 8.

CHAPTER 7

Choose your cell model wisely: the *in vitro* nanoneurotoxicity of differentially coated iron oxide nanoparticles for neural cell labelling.

An adapted manuscript of this chapter is submitted as:

Freya Joris[▲], Daniel Valdepérez[†], Beatriz Pelaz[†], *Tianqiang Wang[†], Shareen H. Doak[§]*, Bella B. Manshian[◊], Stefaan J. Soenen[◊], Wolfgang J. Parak[†], Stefaan C. De Smedt[▲,1,], Koen Raemdonck[▲,1]. Choose your cell model wisely: the in vitro nanoneurotoxicity of differently coated iron oxide nanoparticles for neural cell labelling. *Acta Biomaterialia January* 2016.

[▲] Lab of General Biochemistry and Physical Pharmacy, Faculty of Pharmaceutical Sciences, Ghent University, Ottergemsesteenweg 460, B-9000 Ghent, Belgium.

[†] Philipps University of Marburg, Department of Physics, Renthof 7, D-35037 Marburg, Germany.

[§] Institute of Life Sciences, Swansea University Medical School, Singleton Park, Swansea, Wales, SA2 8PP, UK.

[◊] Biomedical MRI Unit/MoSAIC, Department of Medicine, KULeuven, Herestraat 49, B-3000 Leuven, Belgium.

Table of contents

ABSTRACT

Currently, there is a large interest in the labeling of neural stem cells (NSCs) with iron oxide nanoparticles (IONPs) to allow MRI-guided detection after transplantation in regenerative medicine. For such biomedical applications, excluding nanotoxicity is key. Nanosafety is primarily evaluated *in vitro* where an immortalized or cancer cell line of murine origin is often applied, which is not necessarily an ideal cell model. Previous work revealed clear neurotoxic effects of PMA-coated IONPs in distinct cell types that could potentially be applied for nanosafety studies regarding neural cell labeling. Here, we aimed to assess if DMSA-coated IONPs could be regarded as a safer alternative for this purpose and how the cell model impacted our nanosafety optimization study. Hereto, we evaluated cytotoxicity, ROS production, calcium levels, mitochondrial homeostasis and cell morphology in six related neural cell types, namely neural stem cells, an immortalized cell line and a cancer cell line from human and murine origin. The cell lines mostly showed similar responses to both IONPs, which were frequently more pronounced for the PMA-IONPs. Of note, ROS and calcium levels showed opposite trends in the human and murine NSCs, indicating the importance of the species. Indeed, the human cell models were overall more sensitive than their murine counterpart. Despite the clear cell type-specific nanotoxicity profiles, our multiparametric approach revealed that the DMSA-IONPs outperformed the PMA-IONPs in terms of biocompatibility in each cell type. However, major cell type-dependent variations in the observed effects additionally warrant the use of relevant human cell models.

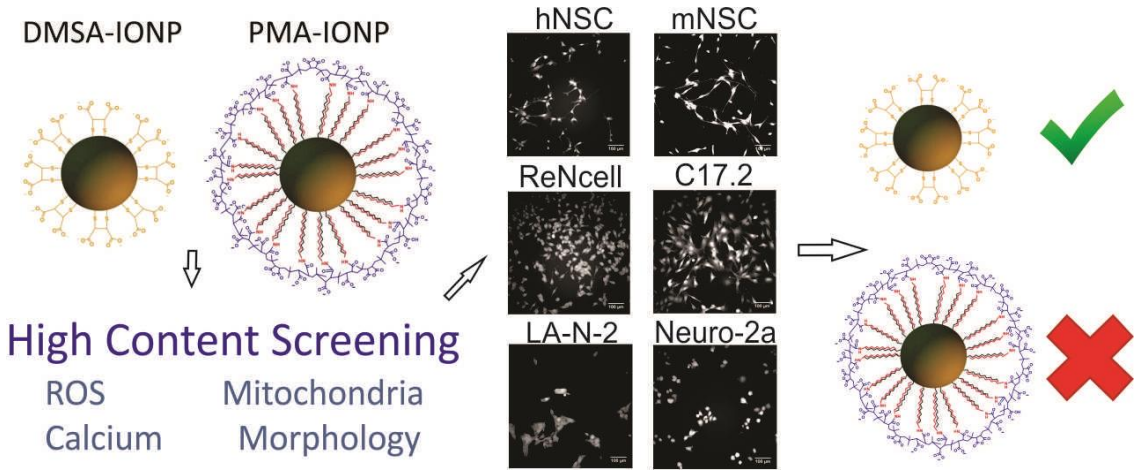

1. INTRODUCTION

Nanotechnology yields numerous nanomaterials with interesting properties, which can be exploited in a plethora of possible applications. The biomedical field, for instance, aims to apply these materials to develop novel or improve existing diagnostic and/or therapeutic strategies.[1-4]

A category of inorganic nanoparticles (NPs) for biomedical use that has received much attention over the last two decades, are iron oxide (IO)NPs.[5] By creating nanosized iron oxide particles, the material acquires superparamagnetic properties, which allows its implementation in biomarker and pathogen detection assays[6-8], protein sequestration[8], cell sorting[9], drug delivery[10] and cancer treatment through hyperthermia.[5, 11] Importantly, IONPs can also be applied as contrast agents for magnetic resonance imaging (MRI).[12, 13] In this regard, FDA-approved dextran-coated IONPs (USA: Feridex®, EU: Endorem®) have been clinically applied for the MRI-guided detection of liver lesions and tumors, before the production was discontinued in 2009.[14, 15] This MRI susceptibility can furthermore be exploited for regenerative cell therapy, where stem cells are transplanted into damaged tissues to replace the latter or promote cell survival and tissue repair *via* the secretion of specific factors.[16, 17] To monitor the cell distribution and engraftment, such therapies require a non-invasive method to track the transplanted cells *in vivo*, which can be accomplished by *ex vivo* cell labeling prior to the transplantation.[16, 18]

In the context of regenerative medicine, there is a large interest in IONP labeling of neural stem cells before transplantation into the neural trauma site.[17, 19, 20] Since cell survival is an inherent drawback to this therapeutic modality and IONPs should persist inside the cells to allow long-term cell tracking, the IONPs should not negatively affect cellular homeostasis.[18] Hence, IONP optimization in terms of nanosafety is of key importance. Previous work from our group on IONPs coated with poly(isobutylene-*alt*-maleic anhydride) grafted with dodecylamine (PMA) (Figure 7.1) showed a disturbed cellular homeostasis at sublethal doses, making this construct less ideal for the labeling of neural cells.[21] Coating with the ligand 2,3-meso-dimercaptosuccinic acid (DMSA) (Figure 7.1) could be a valuable alternative to improve the nanosafety profile. Indeed, DMSA is an FDA-approved chelator applied in case of lead intoxication and DMSA-IONPs show good biocompatibility both to neural cells *in vitro* and neural tissue *in vivo*.[22-24]

In general, many hazard identification studies are initially performed *in vitro* applying cell lines given their easy accessibility and applicability.[25-28] However, we and other groups have demonstrated that primary cells or stem cells often respond differently to NP exposure as compared to the cell line counterpart.[21, 29-31] In addition, murine cell types are regularly applied despite reported species-related variations in NP-induced effects, which impede the extrapolation of results towards possible human scenarios.[32-34] Although several groups investigated either the species or cell type associated diversity in NP-evoked responses,[35-37] such studies remain rare for neural cell types. Previous work from our group revealed cell type specific neurotoxicity profiles in response to PMA-IONPs.[21] Given the clear perturbation of cell homeostasis, the PMA-IONPs were considered less fit for neural stem cell labeling in the context of regenerative medicine. Hence, we set out to optimize the IONPs by applying a different coating. To investigate whether the cell type equally impacts nanosafety optimization studies we compared the nanosafety profile of DMSA-coated IONPs to the previously applied PMA-IONPs. Please note that the same PMA-IONP sample was applied as described in our previous work.[21] In short, we evaluated the cellular responses in neural cell types that could possibly be selected as an *in vitro* model for neural stem cell labeling prior to transplantation in regenerative medicine, namely neural stem cells (NSCs), a neural immortalized (progenitor) cell line and neuroblastoma (cancerous) cell line from both humans and mice.[25-27] This setup will allow us to rationally guide the cell type selection for future nanosafety studies in the context of biomedical applications.

2. MATERIALS & METHODS

2.1. IONP synthesis and characterization

The lab of Prof. W.J. Parak synthesized and coated the IONPs with either the meso-2,3-dimercaptosuccinic acid (DMSA) ligand or the polymer poly(isobutylene-alt-maleic anhydride) (PMA) grafted with dodecylamine.[21, 24, 38-40] IONP synthesis and characterization occurred as described in **Appendix A**.

2.2. Cell culture

The same cell types and cell culture protocol were applied as described in **Chapter 6**.

2.3. NP-cell interactions

A similar method was applied as detailed in **Chapter 6**. In short, the investigated parameters were cell viability, ROS production, mitochondrial and calcium homeostasis and cell morphology. Cell viability was assessed with the CellTiter GLO® assay (Promega, Belgium) whereas the other parameters were evaluated with high content imaging upon labeling with appropriate probes. In this case data were obtained with the IN Cell Analyzer 2000 and analysed with the IN Cell Developer Toolbox software. Detailed information on the staining procedure, data acquisition and data analysis is provided **Chapter 6**.

2.4. Statistics

Cytotoxicity data are expressed as the mean ± standard error of the mean (SEM, n=3). IN Cell data are presented as the mean normalized against the untreated control ± SEM for two independent replicates, with a minimum of 10000 cells being analysed per replicate. Statistical analysis was performed using the 6th version of the GraphPad Prism software. Treated samples were compared with the untreated control by means of one-way ANOVA combined with the post-hoc Dunnett test. Additionally, responses induced by the differently coated IONPs were compared with two-way ANOVA followed by the Bonferroni post-hoc test.

3. RESULTS

3.1. IONP characterization

The core diameter (d_c) of the synthesized IONPs was quantified with transmission electron microscopy (TEM), which showed a mean value of 3.8 nm (Figure 7.1c & 7.1d). Next, the IONPs were coated with a ligand or polymer, respectively meso-2,3-dimercaptosuccinic acid (DMSA) and poly-(isobutylene-*alt*-maleic) anhydride grafted with dodecylamine (PMA).[21] As measured with dynamic light scattering, the hydrodynamic diameter in number distribution (d_h) was 11.83 ± 0.61 and 12.33 ± 0.75 nm with a polydispersity index of 0.185 and 0.308 for the DMSA- and polymer-coated IONPs, respectively. In addition, both IONPs showed a strong, negative charge of -55.5 ± 0.9 mV for the IONP-DMSA and -54 ± 2.2 mV for the IONP-PMA.[21]

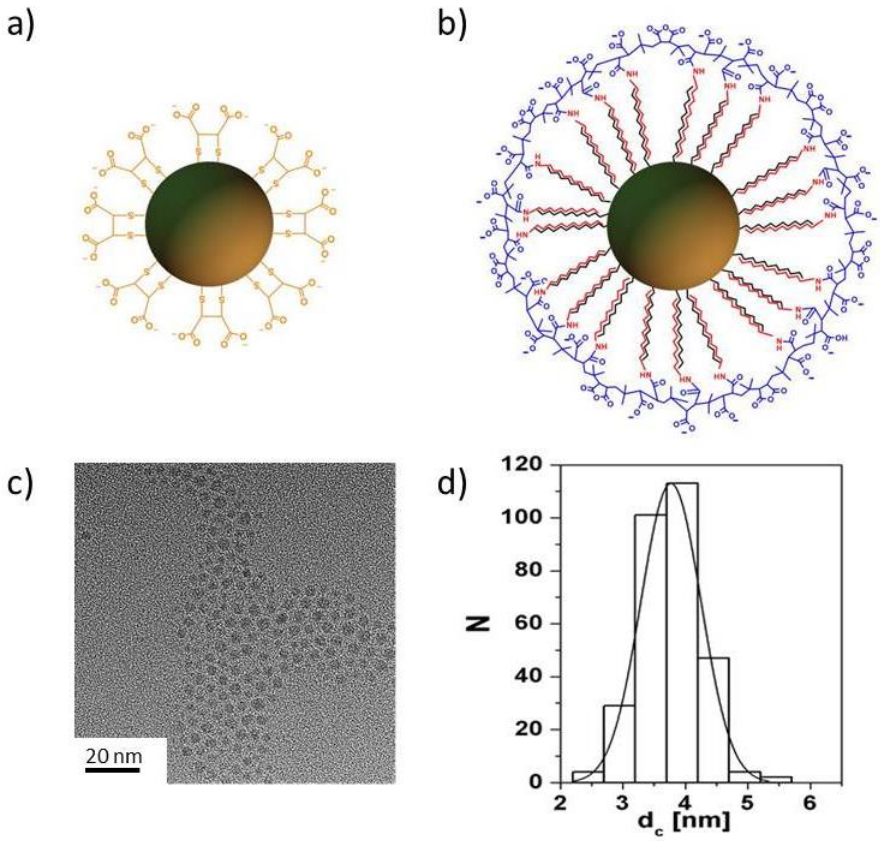

Figure 7.1. (a) DMSA-IONPs, (b) PMA-IONPs, (c) TEM image (scale bar corresponds to 20 nm) of the bare IONPs and (d) the corresponding size distribution histogram of the iron oxide cores N(d_c).

3.2. Cytotoxicity

In a first set of cell-based experiments we evaluated the IONP-induced cell injury. Upon exposure to higher doses, several cell types experienced cell damage, which was most pronounced in the hNSCs (Figure 7.2). In contrast, the murine Neuro-2a neuroblastoma cell line was most resilient to IONP exposure, as only the highest dose of PMA-IONPs evoked a minor, though significant, effect. In the majority of the cell types (the hNSCs, mNSCs and the murine C17.2 and Neuro-2a cell lines), the PMA-IONPs induced more severe effects than the DMSA-IONPs. However, in the ReNcell and LA-N-2 cell line, the opposite was true. Finally, when comparing the human cell types to their murine counterpart, the former appeared to be more sensitive, irrespective of the coating.

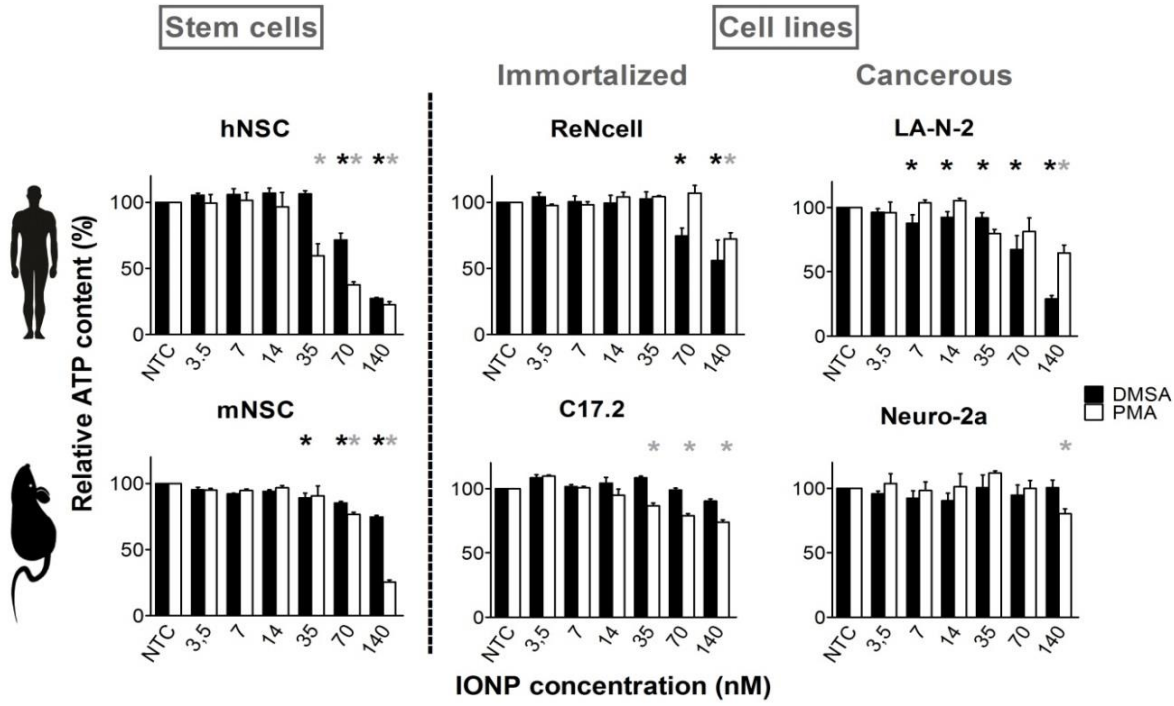

Figure 7.2. Cytotoxicity as determined with the CellTiter GLO® assay following 24 hours exposure to DMSA- (black) and PMA-coated (white) IONPs. Statistical significance with regard to the untreated control is indicated when appropriate ($p < 0.05$) in black for the DMSA-IONPs and grey for the PMA-coated IONPs. (NTC = not treated control)*

3.3. ROS production

To assess whether IONP exposure could affect the cell homeostasis at sublethal doses, we first looked into the effect of ROS production *via* staining with the CellROX® green probe.[41] This is especially important in neural cells since (i) ROS is a key player in the initiation and

progression of several neurodegenerative disorders and (ii) neural cells are especially sensitive to oxidative stress given their high metabolic rate and low anti-oxidative capacity.[42]

Three responses could be distinguished; an increase, a decline or a steady state (Figure 7.3). In case of the first two responses, the induced effects were IONP-concentration dependent. Similar to the cell damage, the observed changes in ROS levels were most pronounced in the NSCs. For instance, in the hNSCs the DMSA-coated IONPs evoked a three-fold ROS induction at the highest concentration tested, whereas a decline was induced by the IONP-PMA. Notably, exact opposite trends were obtained in the mNSCs, indicating species-specific effects. Likewise, in the human progenitor cell line (ReNcell), both IONPs caused ROS induction whereas a decline was seen in the murine counterpart (C17.2). In contrast, in both neuroblastoma cell lines only the PMA-coated IONPs significantly reduced ROS. Overall, the PMA-IONPs evoked more severe effects in the included cell lines but no general statements can be made on the interspecies variations.

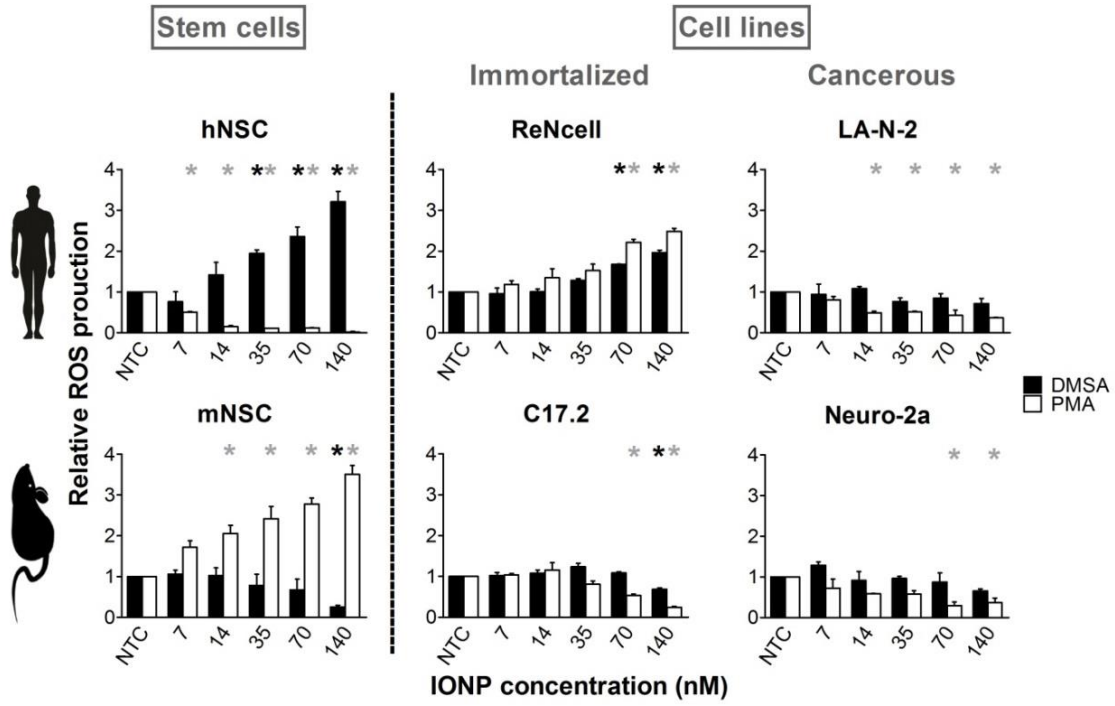

Figure 7.3. The influence of 24 hours DMSA-IONP (black bars) and PMA-IONP (white bars) exposure on reactive oxygen species (ROS) production as detected with the CellROX® green probe, with the latter generally evoking stronger responses. When appropriate, statistical significance with respect to the untreated control is indicated in grey for the PMA-IONPs and in black for the DMSA-IONPs (p < 0.05). (NTC = not treated control)*

3.4. Cytoplasmic calcium signal

Next, we evaluated the Ca^{2+} homeostasis in terms of the cytosolic free calcium concentration ($[Ca^{2+}]_c$) through Rhodamine-2 AM staining.[41] The latter is an important indicator of cell function, especially in neural cells, given its involvement in numerous intracellular processes (metabolic activity, gene expression, neurotransmitter release, cell proliferation and cell death, *etc*.).[43-46]

Similar to the results on ROS production, we found either a concentration dependent decline or augmentation in $[Ca^{2+}]_c$ or no significant changes (Figure 7.4). In both NSCs and the C17.2 cell line, the differentially coated IONPs induced opposite effects. Where the PMA-IONPs caused an elevated $[Ca^{2+}]_c$ in the hNSCs and C17.2 cells, a significant decrease was noted for the DMSA-IONPs. Again, the opposite was true for the mNSCs. In the human progenitor cell line (ReNcell), Ca^{2+}-levels were significantly elevated by both IONPs and the PMA-IONPs, which once more evoked stronger responses. In the murine Neuro-2a cell line, both IONPs induced a significant decline, which was significantly greater for the IONP-DMSA. In the LA-N-2 cell line this response was only observed for the PMA-IONPs, as the DMSA-IONPs did not induce a significant effect. Here, less pronounced responses were detected in the murine NSCs and C17.2 cell line compared to their human counterparts.

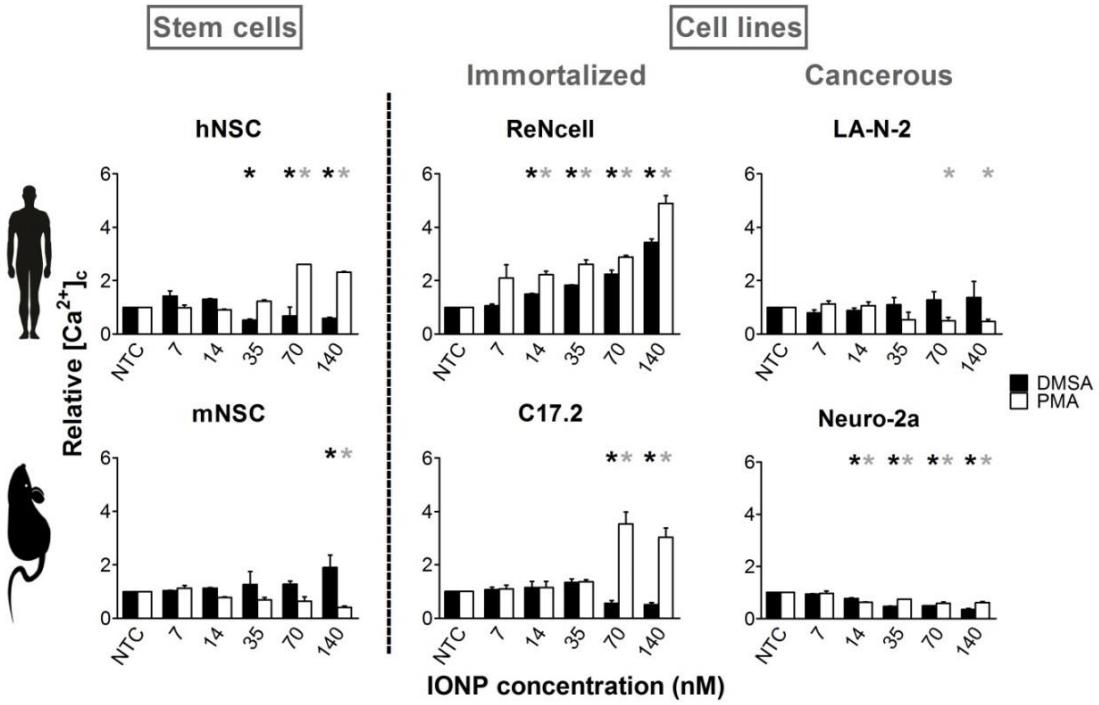

*Figure 7.4. The cytosolic free calcium concentration ($[Ca^{2+}]_c$) was visualized with Rhod-2 AM following 24 hours exposure to DMSA-IONPs (black bars) and PMA-IONPs (white bars). Grey and black * represent significant alterations when compared to the untreated control (* $p < 0.05$) induced by respectively PMA-IONPs and DMSA-IONPs. (NTC = not treated control)*

3.5. Mitochondrial homeostasis

In turn, the mitochondria provide the bulk of the cellular energy, require Ca^{2+} signaling for their function, produce significant amounts of ROS and are associated with programmed cell death.[47, 48] In addition, the $\Delta\psi_m$ is a known effector in neurodegenerative disorders.[49] When the $\Delta\psi_m$ is compromised, the mitochondria fail to produce ATP and cytochrome C can be released, followed by the initiation of apoptosis.[47, 50] These organelles were labeled with Mitotracker® CMX-ROS Red, which accumulates in the organelle based on the mitochondrial membrane potential ($\Delta\psi_m$). When the $\Delta\psi_m$ is compromised due to NPs directly interacting with the mitochondrial membrane or ROS-induced membrane damage, the dye can no longer accumulate and the mitochondrial signal area relative to the total cell area decreases.[51]

Figure 7.5 shows the relative signal area to be reduced or unaffected by IONP exposure. The latter was true for both IONPs in the Neuro-2a cell line and the C17.2 cells exposed to DMSA-IONPs. In all other cases the IONPs significantly reduced the $\Delta\psi_m$. Notably, the ReNcells were most severely affected by both IONPs, followed by the hNSCs. Similar to the cytotoxicity

observations, the human cell types were more sensitive to IONP exposure than the murine counterparts. On the whole, the onset of the effect occurred at lower doses for the IONP-PMA and effects were significantly more severe as compared to the DMSA-IONPs, except in the LA-N-2 neuroblastoma cells where no significant differences were detected between both IONPs.

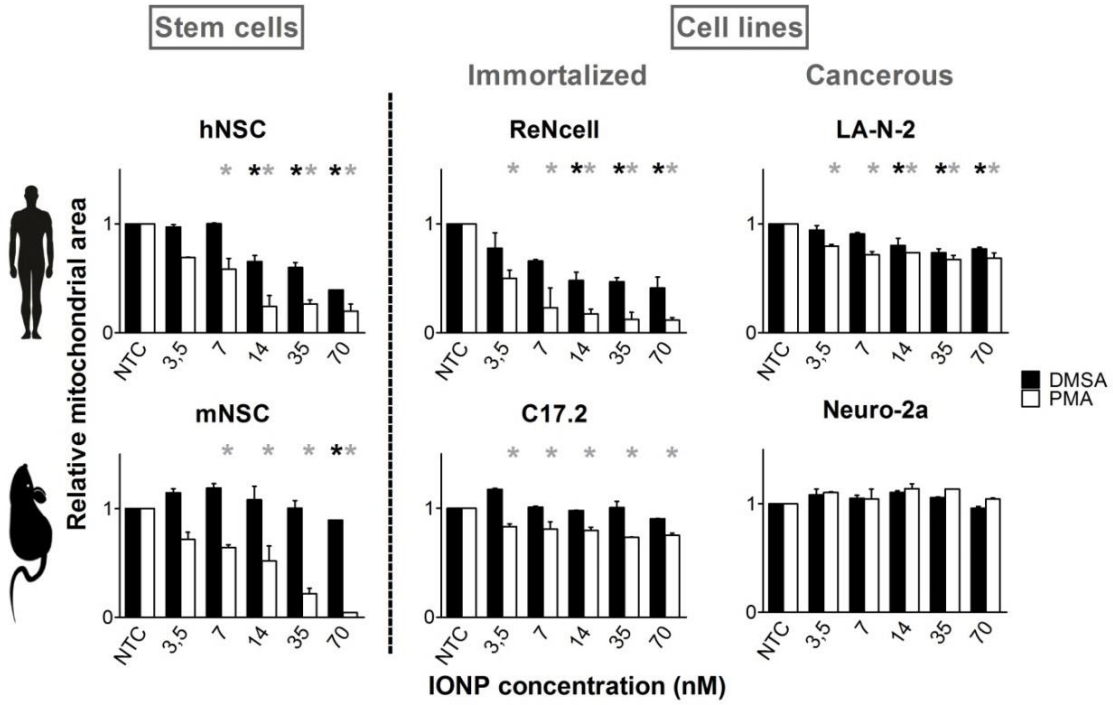

Figure 7.5. DMSA-IONP (black bars) and PMA-IONP (white bars) induced effects on mitochondrial homeostasis in terms of the relative mitochondrial area as visualized with Mitotracker® CMX-ROS. Statistical significance with regard to the untreated control is indicated when appropriate ($p < 0.05$), in black for significant effects evoked by IONP-DMSA and in gray for the PMA-coated IONP. (NTC = not treated control)*

3.6. Cell morphology

Following cell labeling with HCS CellMask™ Blue, cell morphology was evaluated in terms of cell area and cell circularity.[21] The latter is defined as a value between zero and one, with one representing a perfect sphere. Thus, a lower value corresponds to a more complex cell morphology whereas an increase due to IONP exposure points to cell rounding and loss of specific morphological features, such as neurite outgrowths.[21] Cell morphology is a convenient parameter to include in a multiparametric analysis, as cell death has specific morphological features whereas minor alterations to cytoskeleton building blocks can impair cell functions that require signaling *via* these components.[42, 44, 52, 53]

Figure 7.6 and 7.7 reveal that the effect of the PMA-IONPs on cell morphology was overall more severe, with the exception of the mNSCs. In the latter, both cell area and circularity were significantly affected by the lowest and highest dose of DMSA-IONPs and PMA-IONPs, respectively. Likewise, the hNSCs and ReNcells became smaller and more spherical starting from 14 nM PMA-IONPs, whereas DMSA-IONPs only significantly altered morphology at 70 nM. Cell circularity of the C17.2 cells was not significantly affected but the PMA-IONPs and DMSA-IONPs did reduce the cell area starting from the lowest and highest dose tested, respectively. The cell circularity of the Neuro-2a cells was elevated by both IONPs, while only the PMA-IONPs reduced the cell area at higher doses.

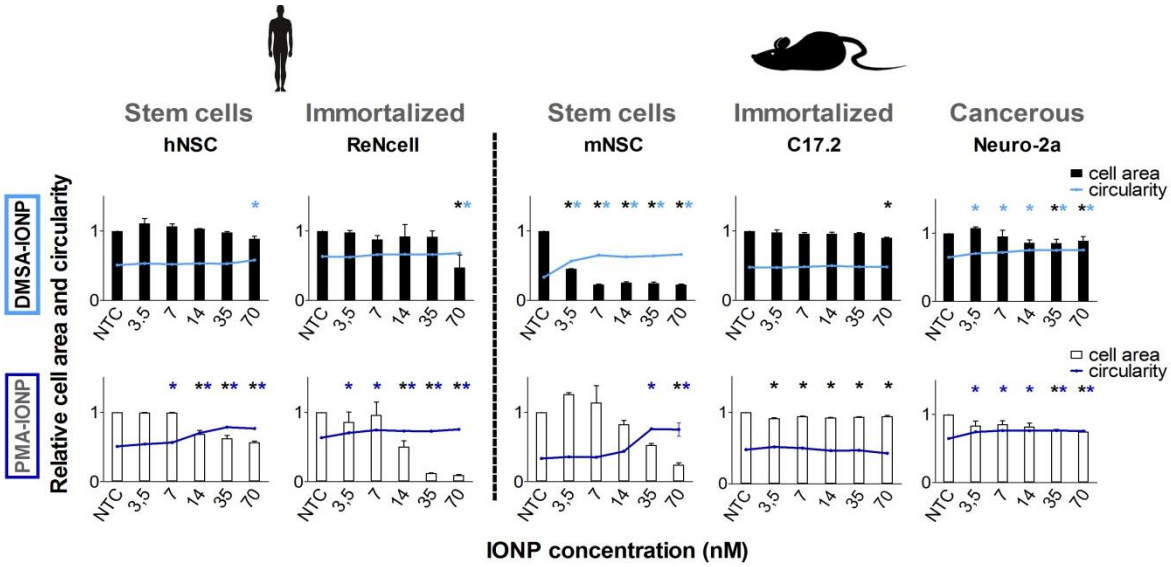

Figure 7.6. The effect on cell morphology of 24 hours exposure to DMSA-IONPs (top row) and PMA-IONPs (lower row) represented as changes in relative cell area (black bars) and cell circularity (blue lines). In general cell circularity is a more sensitive parameter and DMSA-IONPs induce least severe effects. Statistical significance with regard to the untreated control is indicated when appropriate in the corresponding color, black for cell area and blue for circularity ($p < 0.05$). (NTC = not treated control)*

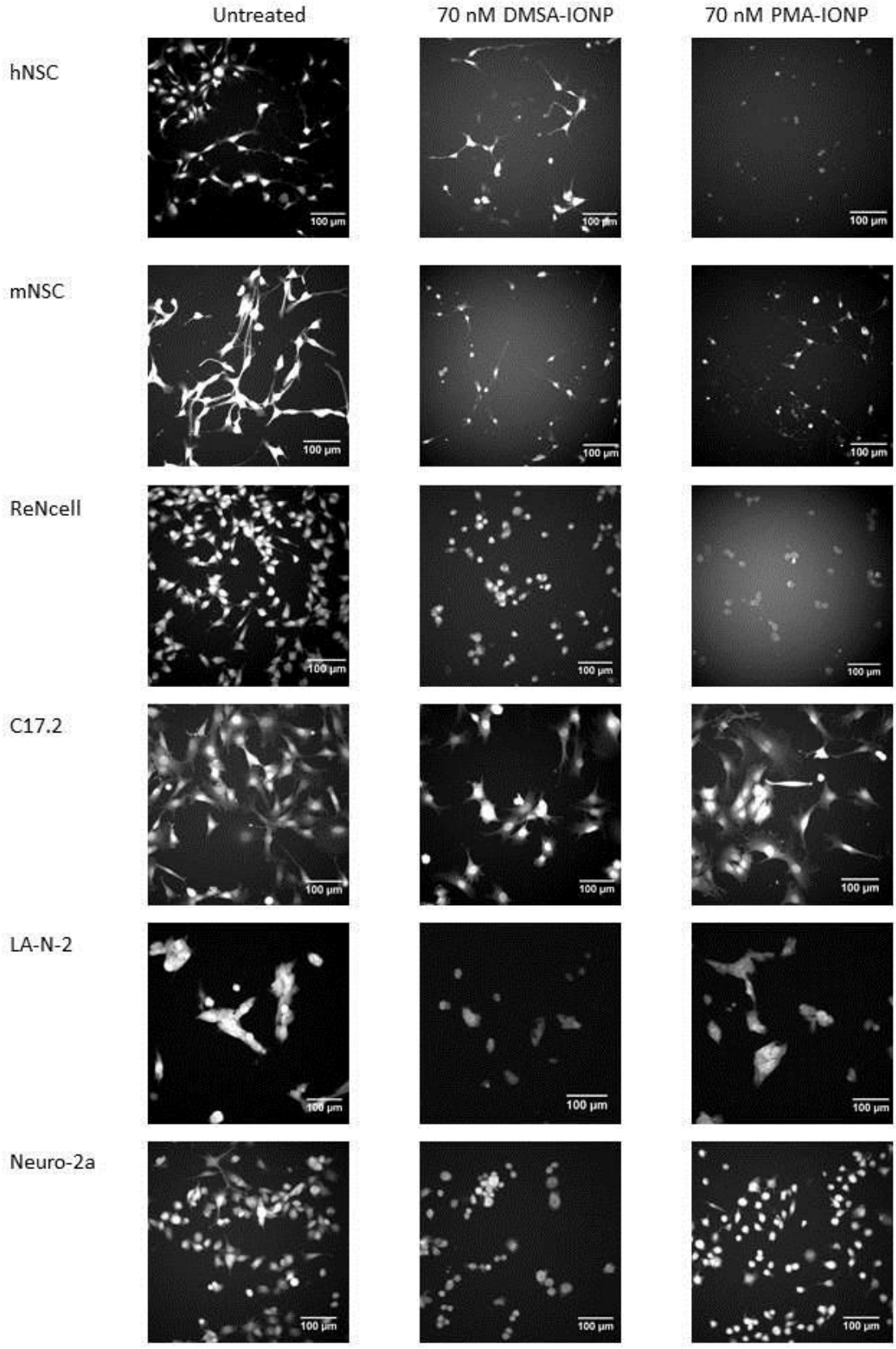

Figure 7.7. Representative images of HCS CellMask™ Blue-labeled untreated cells and cells treated with 70 nM DMSA-IONPs or PMA-IONPS. The scale bar corresponds to 100 µm.

Finally, since LA-N-2 cells tend to grow in clusters, the morphology was analyzed in terms of cluster area and cells per cluster. Here, the PMA-IONPs caused a significant concentration dependent decrease in both the average cluster area and number of cells per cluster at lower doses compared to the DMSA-IONPs (Figure 7.8).

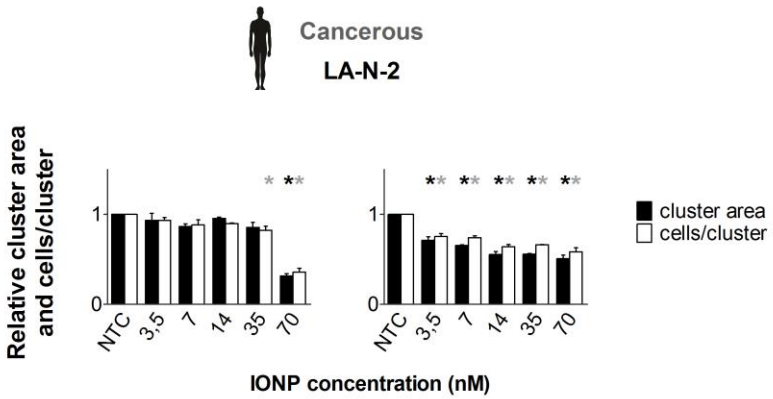

*Figure 7.8. The effect of both IONPs on the LA-N-2 cell line in terms of the total cluster area (black bars) and cells per cluster (white bars). Grey and black * represent significant alterations when compared to the untreated control (* $p < 0.05$) for respectively cluster area and cells per cluster. (NTC = not treated control)*

4. DISCUSSION

In this study, we evaluated the extent at which DMSA- and PMA-coated IONPs induced adverse effects in six neural cell types, namely NSCs, a progenitor cell line and a cancer cell line from murine and human origin. Please note that the same PMA-IONP sample was applied as in previous work, where we observed clear dose- and cell type-dependent neurotoxicity.[21] The specific aim of this work was to evaluate if such adverse effects could be similarly alleviated in the distinct cell types by applying a different coating strategy. The cell types were selected based on an important future application of the IONPs, i.e. neural cell labeling to allow MRI-guided *in vivo* cell tracking following transplantation in the context of regenerative cell therapy for neural lesions. Multiple studies regarding this topic apply various cell models without clearly specifying the species and or cell type (immortalized or cancer cell line, primary cells, stem cells).[25-27] Since NP-evoked effects can differ widely amongst various cell models[32, 34], we evaluated the impact of the cell model on nanosafety optimization studies. Hereto, we looked into the impact of both the cell type and species in one single study in contrast to previous reports focusing on a single variable.[33, 36, 37]

IONP characterization showed that DMSA- and PMA-IONPs had similar basic physicochemical properties, in line with previous reports.[21, 24, 38, 54] This was desirable as potentially distinct cell responses could be explained in terms of how the cell models interact with the NPs, rather than by the intrinsic physicochemical properties of the IONPs.

Overall, we found the DMSA-IONPs to evoke less extensive responses than the PMA-IONPs. In four out of six cell types DMSA-IONPs induced less cytotoxicity than the PMA-IONPs, as expected based on recent literature.[22-24] However, the observed toxicity for DMSA-IONPs was slightly more severe than anticipated possibly due to the greater sensitivity of neural cells towards NP exposure in general.[16] Cell homeostasis was furthermore perturbed at sublethal IONP doses in nearly all combinations tested. Indeed, in correspondence with previous reports, we witnessed decreased, induced or unaffected ROS levels.[49, 55, 56] In case of ROS induction or scavenging, the PMA-IONPs evoked more severe effects. The latter response can be explained in terms of the intrinsic scavenging potential of intact IONPs.[57, 58] The steady state observed for DMSA-IONPs in the cancer cell lines can be contributed to the chelating capacity of DMSA, preventing leached iron ions from inducing ROS.[14, 22, 24] Still, the DMSA-IONPs were found to significantly induce ROS in the hNSCs and ReNcells, possibly

indicating that the extent of ion leaching outweighed the DMSA chelating capacity or that ROS induction in part occurred through alternate mechanisms. In addition, the DMSA-IONPs most often showed less pronounced responses on the level of the calcium and mitochondrial homeostasis and cell morphology. Since all responses can to a certain extent be correlated to ROS production,[59, 60] the chelating capacity of DMSA may in part be accountable for the improved nanosafety profile. However, the capacity of DMSA to chelate iron ions is limited compared to its propensity to bind lead and cadmium ions. The capacity to catch iron ions may further be reduced by the ominously present calcium ions, although it slightly prefers to bind iron ions.[61] Hence, the exact mechanism of the improved biocompatibility of the DMSA-IONPs warrants further research.

From the multiparametric data set in each cell type alone it would be concluded that the DMSA-IONPs are the preferred candidate for further optimization since they generally evoked less severe effects, regardless of the distinct culture medium composition for the different cell types. The cell media could potentially influence IONP uptake through an impact on colloidal stability and the formation of a protein corona.[62, 63] The latter parameters were not investigated in detail in this work as we focused on investigating how various cell models (*i.e.* the cell type and its optimal medium) would respond to IONP exposure. Furthermore, adequate IONP uptake and colloidal stability were previously documented for the applied coating materials.[23, 41, 64] Nevertheless, further characterization of the protein corona and IONP uptake in the applied cell models would improve our understanding of the observed adverse events.[65]

Most importantly, a correct conclusion on the preferable IONP coating for the envisioned application could only be reached when a multiparametric approach was applied, as in rare cases the DMSA-IONPs more severely perturbed cell homeostasis.

Overall, a distinct nanotoxicity profile was obtained in each applied cell model. The sensitivity of the cell model was furthermore clearly species-related, as human cell types were more sensitive towards DMSA-IONP-induced effects. Likewise, Zhang *et al.* found human macrophages to be more sensitive towards DMSA-IONPs than the murine alternative.[66] Secondly, the cell type was a major factor since for both the human and murine cell types the NSCs were found to be most sensitive towards both IONPs, whereas

the cancer cell lines were most resilient. This is in agreement with the observation that tumor cells have several characteristics making them less prone to NP-induced effects, as cell transformation or immortalization is accompanied by phenotypical changes on the level of cell morphology, metabolic rate, proliferation rate, *etc*.[32, 67] Finally, not all cell models showed a similar sensitivity on all evaluated end points. For instance, no significant differences could be detected in IONP-induced mitochondrial damage in the cancer cell lines, while this was true for all other cell types. Hence, nanosafety screenings to define suitable NPs for a certain application should be performed in a multiparametric fashion evaluating sensitive and informative end points in sufficiently sensitive cell types.

Prior to the possible application of the investigated DMSA-IONPs, further testing would be required to (i) certify that a sufficient MRI signal could be detected at non-toxic doses, (ii) establish the importance of the detected adverse events on long-term cell function (e.g. differentiation in case of pluripotent stem cells) and (iii) rule out delayed cytotoxicity, as this was previously observed for the DMSA-IONP labeling of primary neurons.[68] Based on our observations we suggest that NSCs are the preferred model for further investigation given the selected application. In preference the hNSCs should be applied since both NSCs showed opposite effects on the level of ROS and Ca^{2+} in response to DMSA-IONP labeling. Finally, it would be interesting to compare the obtained responses to those evoked by commercially available IONPs, as clinical translation of the latter for a novel application might be more efficient than for novel IONPs.

5. CONCLUSION

IONPs are of interest as MRI contrast agents for the labeling of transplanted neural stem cells (NSCs), albeit that nanotoxicity remains a concern. Cell-nanoparticle interactions of DMSA- and PMA-coated IONPs were investigated in human and murine NSC, neural progenitor and neuroblastoma cells. The overall nanosafety profile of the DMSA-IONPs was superior compared to the PMA-IONPs. Importantly, a multiparametric approach was required to reach this conclusion. In the cell lines we predominantly found both IONPs to evoke similar responses. In contrast, clear interspecies variations were detected on ROS production and Ca^{2+} homeostasis in the NSCs, where both IONPs were found to evoke opposite effects. This is an important observation, as the hNSCs are considered to be the most representative model for the envisioned application. Thus, the DMSA-coating could not in all cell types equally alleviate the induced nanotoxicity compared to the PMA-IONPs. Overall, sufficiently sensitive cell lines can be applied when performing a multiparametric screening to define suitable candidates for a certain biomedical application. However, further thorough safety evaluations should be performed on a non-cancerous human cell model most closely resembling the target cell or tissue whenever possible.

ACKNOWLEDGEMENTS

F.J. is a doctoral fellow of the Agency for Innovation by Science and Technology in Flanders (IWT). K.R. and S.J.S. are postdoctoral fellows of the Research Foundation-Flanders (FWO). B.P. acknowledges the Alexander von Humboldt Foundation for a postdoctoral fellowship. We thank Sebastian Munck and Nicky Corthout (VIB Centre for Biology of Disease, Belgium) for use of the IN Cell Analyzer 2000 and IN Cell Developer Toolbox software. Additionally we wish to thank Karsten Kantner for the performed ICP measurements. Parts of this work were supported by DFG Germany (grant PA 794/25-1 to W.J.P.).

REFERENCES

1. Canfarotta, F.; Piletsky, S. A. *Advanced healthcare materials* **2014,** 3, (2), 160-75.
2. Kim, T.; Hyeon, T. *Nanotechnology* **2014,** 25, (1), 012001.
3. Zarschler, K.; Rocks, L.; Licciardello, N.; Boselli, L.; Polo, E.; Garcia, K. P.; De Cola, L.; Stephan, H.; Dawson, K. A. *Nanomedicine : nanotechnology, biology, and medicine* **2016,** 12, (6), 1663-701.
4. Chan, W. C. W.; Udugama, B.; Kadhiresan, P.; Kim, J.; Mubareka, S.; Weiss, P. S.; Park, W. J. *ACS nano* **2016,** 10, (9), 8139-8142.
5. Wu, W.; Changzhong, J.; Roy, V. A. *Nanoscale* **2015,** 7, (1), 38-58.
6. Busquets, M. A.; Sabate, R.; Estelrich, J. *Nanoscale research letters* **2014,** 9, (1), 538.
7. Wang, E. C.; Wang, A. Z. *Integr Biol (Camb)* **2014,** 6, (1), 9-26.
8. Gu, H.; Xu, K.; Xu, C.; Xu, B. *Chemical communications* **2006**, (9), 941-9.
9. Majewski, A. P.; Schallon, A.; Jerome, V.; Freitag, R.; Muller, A. H.; Schmalz, H. *Biomacromolecules* **2012,** 13, (3), 857-66.
10. Laurent, S.; Saei, A. A.; Behzadi, S.; Panahifar, A.; Mahmoudi, M. *Expert Opin Drug Deliv* **2014,** 11, (9), 1449-70.
11. Lim, E. K.; Kim, T.; Paik, S.; Haam, S.; Huh, Y. M.; Lee, K. *Chemical reviews* **2015,** 115, (1), 327-94.
12. Bakhtiary, Z.; Saei, A. A.; Hajipour, M. J.; Raoufi, M.; Vermesh, O.; Mahmoudi, M. *Nanomed-Nanotechnol* **2016,** 12, (2), 287-307.
13. Casula, M. F.; Floris, P.; Innocenti, C.; Lascialfari, A.; Marinone, M.; Corti, M.; Sperling, R. A.; Parak, W. J.; Sangregorio, C. *Chem Mater* **2010,** 22, (5), 1739-1748.
14. Soenen, S. J.; Parak, W. J.; Rejman, J.; Manshian, B. *Chemical reviews* **2015,** 115, (5), 2109-35.
15. Bobo, D.; Robinson, K. J.; Islam, J.; Thurecht, K. J.; Corrie, S. R. *Pharm Res* **2016**.
16. Mahmoudi, M.; Hosseinkhani, H.; Hosseinkhani, M.; Boutry, S.; Simchi, A.; Journeay, W. S.; Subramani, K.; Laurent, S. *Chemical reviews* **2011,** 111, (2), 253-80.
17. Levy, M.; Boulis, N.; Rao, M.; Svendsen, C. N. *Brain Res* **2016,** 1638, (Pt A), 88-96.
18. Taylor, A.; Wilson, K. M.; Murray, P.; Fernig, D. G.; Levy, R. *Chemical Society reviews* **2012,** 41, (7), 2707-17.
19. Chen, C. C. V.; Ku, M. C.; Jayaseema, D. M.; Lai, J. S.; Hueng, D. Y.; Chang, C. *PloS one* **2013,** 8, (2).
20. Stoll, E. A. *Mol Cell Ther* **2014,** 2, 12.
21. Joris, F. V., D.; Pelaz, B.; Soenen, S.J.; Manshian, B.B.; Parak, W.J.; De Smedt, S.C.; Raemdonck, K. *Journal of Nanobiotechnology* **2016**.
22. Vasconcelos Braz, S.; Monge-Fuentes, V.; Rodrigues da Silva, J.; Tomaz, C.; Tavares, M. C.; Pereira Garcia, M.; Nair Bao, S.; Paulino Lozzi, S.; Bentes de Azevedo, R. *PloS one* **2015,** 10, (11), e0140233.
23. Kim, Y.; Kong, S. D.; Chen, L. H.; Pisanic, T. R.; Jin, S.; Shubayev, V. I. *Nanomed-Nanotechnol* **2013,** 9, (7), 1057-1066.
24. Mejias, R.; Gutierrez, L.; Salas, G.; Perez-Yague, S.; Zotes, T. M.; Lazaro, F. J.; Morales, M. P.; Barber, D. F. *Journal of controlled release : official journal of the Controlled Release Society* **2013,** 171, (2), 225-33.
25. Shen, W. B.; Vaccaro, D. E.; Fishman, P. S.; Groman, E. V.; Yarowsky, P. *Contrast media & molecular imaging* **2016,** 11, (3), 222-8.
26. Egawa, E. Y.; Kitamura, N.; Nakai, R.; Arima, Y.; Iwata, H. *Biomaterials* **2015,** 54, 158-67.
27. Neri, M.; Maderna, C.; Cavazzin, C.; Deidda-Vigoriti, V.; Politi, L. S.; Scotti, G.; Marzola, P.; Sbarbati, A.; Vescovi, A. L.; Gritti, A. *Stem Cells* **2008,** 26, (2), 505-16.
28. Joris, F.; Manshian, B. B.; Peynshaert, K.; De Smedt, S. C.; Braeckmans, K.; Soenen, S. J. *Chem Soc Rev* **2013,** 42, (21), 8339-8359.

29. Bregoli, L.; Chiarini, F.; Gambarelli, A.; Sighinolfi, G.; Gatti, A. M.; Santi, P.; Martelli, A. M.; Cocco, L. *Toxicology* **2009,** 262, (2), 121-9.
30. Feng, W.; Guo, J.; Huang, H.; Xia, B.; Liu, H.; Li, J.; Lin, S.; Li, T.; Liu, J.; Li, H. *PloS one* **2015,** 10, (4), e0123520.
31. Schlinkert, P.; Casals, E.; Boyles, M.; Tischler, U.; Hornig, E.; Tran, N.; Zhao, J. Y.; Himly, M.; Riediker, M.; Oostingh, G. J.; Puntes, V.; Duschl, A. *J Nanobiotechnol* **2015,** 13.
32. Luengo, Y.; Nardecchia, S.; Morales, M. P.; Serrano, M. C. *Nanoscale* **2013,** 5, (23), 11428-37.
33. Wang, Y.; Aker, W. G.; Hwang, H. M.; Yedjou, C. G.; Yu, H.; Tchounwou, P. B. *The Science of the total environment* **2011,** 409, (22), 4753-62.
34. Zhang, H.; Wang, X.; Wang, M.; Li, L.; Chang, C. H.; Ji, Z.; Xia, T.; Nel, A. E. *Small* **2015,** 11, (31), 3797-805.
35. Wilkinson, K. E.; Palmberg, L.; Witasp, E.; Kupczyk, M.; Feliu, N.; Gerde, P.; Seisenbaeva, G. A.; Fadeel, B.; Dahlen, S. E.; Kessler, V. G. *ACS nano* **2011,** 5, (7), 5312-5324.
36. Ekstrand-Hammarstrom, B.; Akfur, C. M.; Andersson, P. O.; Lejon, C.; Osterlund, L.; Bucht, A. *Nanotoxicology* **2012,** 6, (6), 623-34.
37. Kermanizadeh, A.; Gaiser, B. K.; Ward, M. B.; Stone, V. *Nanotoxicology* **2013,** 7, (7), 1255-71.
38. Sun, S.; Zeng, H.; Robinson, D. B.; Raoux, S.; Rice, P. M.; Wang, S. X.; Li, G. *Journal of the American Chemical Society* **2004,** 126, (1), 273-9.
39. Lin, C. A.; Sperling, R. A.; Li, J. K.; Yang, T. Y.; Li, P. Y.; Zanella, M.; Chang, W. H.; Parak, W. J. *Small* **2008,** 4, (3), 334-41.
40. Schweiger, C.; Hartmann, R.; Zhang, F.; Parak, W. J.; Kissel, T. H.; Rivera Gil, P. *J Nanobiotechnol* **2012,** 10.
41. Manshian, B. B.; Moyano, D. F.; Corthout, N.; Munck, S.; Himmelreich, U.; Rotello, V. M.; Soenen, S. J. *Biomaterials* **2014,** 35, (37), 9941-50.
42. Wu, Y. L.; Putcha, N.; Ng, K. W.; Leong, D. T.; Lim, C. T.; Loo, S. C. J.; Chen, X. D. *Accounts of chemical research* **2013,** 46, (3), 782-791.
43. Clapham, D. E. *Cell* **2007,** 131, (6), 1047-58.
44. Zhivotovsky, B.; Orrenius, S. *Cell calcium* **2011,** 50, (3), 211-21.
45. Jan, E.; Byrne, S. J.; Cuddihy, M.; Davies, A. M.; Volkov, Y.; Gun'ko, Y. K.; Kotov, N. A. *ACS nano* **2008,** 2, (5), 928-38.
46. Ariano, P.; Zamburlin, P.; Gilardino, A.; Mortera, R.; Onida, B.; Tomatis, M.; Ghiazza, M.; Fubini, B.; Lovisolo, D. *Small* **2011,** 7, (6), 766-74.
47. Brookes, P. S.; Yoon, Y.; Robotham, J. L.; Anders, M. W.; Sheu, S. S. *American journal of physiology. Cell physiology* **2004,** 287, (4), C817-33.
48. Fulda, S.; Galluzzi, L.; Kroemer, G. *Nature reviews. Drug discovery* **2010,** 9, (6), 447-64.
49. Imam, S. Z.; Lantz-McPeak, S. M.; Cuevas, E.; Rosas-Hernandez, H.; Liachenko, S.; Zhang, Y.; Sarkar, S.; Ramu, J.; Robinson, B. L.; Jones, Y.; Gough, B.; Paule, M. G.; Ali, S. F.; Binienda, Z. K. *Mol Neurobiol* **2015,** 52, (2), 913-26.
50. Gottlieb, E.; Armour, S. M.; Harris, M. H.; Thompson, C. B. *Cell death and differentiation* **2003,** 10, (6), 709-17.
51. Pendergrass, W.; Wolf, N.; Poot, M. *Cytometry. Part A : the journal of the International Society for Analytical Cytology* **2004,** 61, (2), 162-9.
52. Buyukhatipoglu, K.; Clyne, A. M. *Journal of biomedical materials research. Part A* **2011,** 96, (1), 186-95.
53. Tay, C. Y.; Cai, P.; Setyawati, M. I.; Fang, W.; Tan, L. P.; Hong, C. H.; Chen, X.; Leong, D. T. *Nano letters* **2014,** 14, (1), 83-8.
54. Quarta, A.; Curcio, A.; Kakwere, H.; Pellegrino, T. *Nanoscale* **2012,** 4, (11), 3319-3334.
55. Harris, G.; Palosaari, T.; Magdolenova, Z.; Mennecozzi, M.; Gineste, J. M.; Saavedra, L.; Milcamps, A.; Huk, A.; Collins, A. R.; Dusinska, M.; Whelan, M. *Nanotoxicology* **2015,** 9 Suppl 1, 87-94.
56. Lindemann, A.; Ludtke-Buzug, K.; Fraderich, B. M.; Grafe, K.; Pries, R.; Wollenberg, B. *International journal of nanomedicine* **2014,** 9, 5025-40.

57. Gao, L.; Zhuang, J.; Nie, L.; Zhang, J.; Zhang, Y.; Gu, N.; Wang, T.; Feng, J.; Yang, D.; Perrett, S.; Yan, X. *Nature nanotechnology* **2007,** 2, (9), 577-83.
58. Huang, D. M.; Hsiao, J. K.; Chen, Y. C.; Chien, L. Y.; Yao, M.; Chen, Y. K.; Ko, B. S.; Hsu, S. C.; Tai, L. A.; Cheng, H. Y.; Wang, S. W.; Yang, C. S.; Chen, Y. C. *Biomaterials* **2009,** 30, (22), 3645-51.
59. Soenen, S. J.; Manshian, B.; Montenegro, J. M.; Amin, F.; Meermann, B.; Thiron, T.; Cornelissen, M.; Vanhaecke, F.; Doak, S.; Parak, W. J.; De Smedt, S.; Braeckmans, K. *ACS nano* **2012,** 6, (7), 5767-83.
60. Nel, A.; Xia, T.; Madler, L.; Li, N. *Science* **2006,** 311, (5761), 622-627.
61. Flora, S. J.; Pachauri, V. *Int J Environ Res Public Health* **2010,** 7, (7), 2745-88.
62. Mahmoudi, M.; Laurent, S.; Shokrgozar, M. A.; Hosseinkhani, M. *ACS nano* **2011,** 5, (9), 7263-76.
63. Rivera-Gil, P.; De Aberasturi, D. J.; Wulf, V.; Pelaz, B.; Del Pino, P.; Zhao, Y. Y.; De La Fuente, J. M.; De Larramendi, I. R.; Rojo, T.; Liang, X. J.; Parak, W. J. *Accounts of chemical research* **2013,** 46, (3), 743-749.
64. Pisanic, T. R., 2nd; Blackwell, J. D.; Shubayev, V. I.; Finones, R. R.; Jin, S. *Biomaterials* **2007,** 28, (16), 2572-81.
65. Maiolo, D.; Del Pino, P.; Metrangolo, P.; Parak, W. J.; Bombelli, F. B. *Nanomedicine : nanotechnology, biology, and medicine* **2015,** 10, (21), 3231-3247.
66. Zhang, L.; Wang, X.; Zou, J.; Liu, Y.; Wang, J. *J Nanobiotechnology* **2015,** 13, 3.
67. Wang, J.; Fang, X.; Liang, W. *ACS nano* **2012,** 6, (6), 5018-30.
68. Petters, C.; Dringen, R. *Neurochemistry international* **2015,** 81, 1-9.

CHAPTER 8

Broader international context, relevance and future perspectives.

Freya Joris, Stefaan C. De Smedt, Koen Raemdonck

Lab of General Biochemistry and Physical Pharmacy, Faculty of Pharmaceutical Sciences, Ghent University, B9000 Ghent, Belgium.

Table of contents

ABSTRACT

In the first part of this thesis we showed that by repurposing cationic amphiphilic drugs, siRNA-mediated gene silencing could significantly be improved upon nanogel transfection. In the second part of this thesis we focused on the impact of the cell model on the *in vitro* hazard assessment of inorganic nanoparticles. In short, we showed that the cell model selection in terms of the cell type and species influences the outcome of nanotoxicity evaluations and should not be overlooked in the optimization and standardization of *in vitro* nanosafety testing. In this final chapter we discuss the broader international context of our findings, the relevance of the work and the future perspectives. Hereto we first look into the commercial development of siRNA, RNAi therapeutics and inorganic nanoparticles. Secondly, we focus on the current clinical development of RNAi therapeutic en inorganic nanoparticles. Since we repurpose cationic amphiphilic drugs to improve siRNA delivery, both the concept of drug repurposing and combining drugs with siRNA to obtain an improved therapeutic outcome are discussed. Finally, we identify unmet challenges and suggest how research on both topics should be continued, with a focus on the importance of bridging the *in vitro-in vivo* gap.

1. NANOTECHNOLOGY

Nanotechnology has become indispensable to technological advances in the 21st century. By fabricating constructs in the nanometer range, many materials acquire unique and hard to obtain properties thereby unlocking a whole new world of novel applications and/or product improvements. Through the enlarged surface area, nanoparticles (NPs) may for instance contain improved catalytic properties (gold NPs), increased strength (graphene) and augmented antibacterial action (silver NPs) compared to their bulk materials. Semiconductor nanocrystals furthermore show excellent conducting properties and iron oxide NPs are superparamagnetic.[1] Upon the discovery of these unique nano-features, NPs became the driving force behind the rapid progress of various sectors in the past decade, such as the chemical, energy and electronics industry.[2, 3] As of today, nanotechnology has reached the consumer through various products, with many more still on the way. A general inventory of NP-containing consumer products can be found on the website of the Project on Emerging Nanotechnologies (www.nanotechproject.org).[4]

Besides the avid use in consumers products, various NPs are being developed for distinct biomedical applications.[5] In this regard, organic NPs are often applied as nanocarriers for macromolecules or molecules with a limited solubility. Several inorganic NPs are similarly being tested for their delivery potential, whereas their unique properties furthermore allow their development as contrast agents or radioenhancers in cancer therapy (section 3.1), besides improved biomarker detection.

2. NANOCARRIERS FOR siRNA DELIVERY

2.1. The industry perspective on siRNA therapeutics

The pharmaceutical industry connection with RNA interference (RNAi) could be perceived as a love-hate relationship. In retrospect four phases can be noted[6, 7]:

- 2002 – 2005 the RNAi discovery phase
- 2005 – 2008 the boom of RNAi
- 2008 – 2012 the burst of the RNAi bubble and the funding crisis
- 2012 – now the reinforced interest in RNAi

RNAi was first reported in *C. elegans* in 1998 by Fire and Mello.[8] Soon afterwards evidence of RNAi in mammalian and human cells was reported concurrent to the elucidation of the molecular RNAi pathway and how this pathway can be harnessed using RNAi triggers.[9, 10] This set of seminal data revealed the great potential of RNAi as a lab tool and as a therapeutic agent for a myriad of disorders. Indeed, theoretically any disease-causing gene could be silenced with high specificity and selectively.[11, 12] Hence, it was even proposed that RNAi would allow personalized cancer treatment.[13] In these early days, risk taking biotechnology companies such as Tekmira and Silence Therapeutics invested in the commercial development of the RNAi technique. In addition, the current leading RNAi company, Alnylam, was founded in the initial RNAi discovery phase.[6]

The interest in RNAi as a therapeutic modality fiercely increased upon the positive *in vitro* and *in vivo* proof-of-concept data and the first successful clinical study where naked siRNA was intravitreally injected for the treatment of age-related macular degeneration.[10, 11, 14, 15] Up until then the big pharmaceutical companies (Big Pharma) mainly regarded RNAi as a research tool, but now companies like Merck, Roche and Novartis invested large amounts in both the intellectual property and therapeutic development of RNAi.[16] Big Pharma was no longer watching from the side lines, but invested an estimated US$ 2.5 – 3.5B.[6] In retrospect, the expectations of Big Parma were unrealistically high, as it was anticipated that the development of an RNAi therapeutic would take no longer than 15 months.[17] Thus, Big Pharma envisioned RNAi to quickly boost their pipeline and thereby be a 'magic' solution to the ever-increasing cost and time required for drug development. In this enthusiasm it was even anticipated that RNAi therapeutics would rival with monoclonal antibodies.[6, 18]

Disillusionment soon followed since technical barriers to successful therapeutic RNAi applications were initially largely underestimated. Indeed, the initial wave of clinical trials did not yield marketable products, but revealed issues of delivery, safety and selectivity.[19] Since the anticipated quick return of investments held off, RNAi became a bad career strategy in Big Pharma. This was consolidated by a report stating that the positive effects observed in the 2004 trial on age-related macular degeneration was a consequence of the immune response to the injected siRNA rather than a sequence-specific RNAi effect.[20] At this point, the RNAi bubble burst with several Big Pharma players retreating from RNAi

development. Roche, Pfizer and Abbott Labs terminated their in-house RNAi development, whereas Merck and AstraZeneca strongly reduced their activities.[6]

In turn, smaller biotech companies and academia did not lose their faith in RNAi. For one, the siRNA structure was engineered to reduce immunogenicity and improve target specificity.[21] The inclusion of a 2'OH methyl group enhanced the stability and reduced the chances of an innate immune response. Off-target effects of the guide strand were reduced by applying asymmetric siRNA molecules with less thermodynamically stable base pairs at the 5' end.[21] Smaller biotechnology companies further recognized poor siRNA delivery as a main factor holding back therapeutic RNAi development and refocused their actions on the development of more efficient delivery platforms.[6] Tekmira for instance developed stable nucleic acid lipid nanoparticles (SNALP) and Alnylam established the GalNAc-conjugate with enhanced stabilization chemistry (ESC-)siRNA.[19, 22] Although various successful delivery strategies were developed, it is recognized that only a small fraction of the internalized dose is active inside the cytosol and that the delivery work should not be halted at this stage.

Various formulations are currently evaluated in clinical trials (Table 8.1). Consequently, it is expected that the first FDA-approved RNAi therapeutic will enter the market before 2020.[23] Although it may not be likely that RNAi therapeutics will immediately rival with monoclonal antibodies, such as Humira® and Remicade® (two of the currently largest selling drugs), as first anticipated, the RNAi market is expected to grow with the approval of the first RNAi therapeutic.[18, 24] In this regard, it should be kept in mind that monoclonal antibodies required several waves of innovation prior to the development of marketable products, similar to the situation RNAi therapeutics are currently facing. The enhanced clinical pipeline and overall quality of the RNAi science indeed fanned renewed interest into RNAi as a therapeutic modality. To ensure their share when RNAi therapeutics hit the market, Big Pharma players entered into collaborations with smaller biotech companies to outsource R&D activities on delivery strategies and siRNA therapeutics.[6]

A final note should be made on the rivalry between the RNAi and clustered regularly interspaced short palindromic repeats (CRISPR) technology, as both can be applied to sequence specifically silencing genes. Some anticipate that CRISPR may overrule RNAi as it has the potential to create stable gene knockouts whereas transient gene silencing is

obtained through RNAi.[25] This is potentially an exaggerated statement, as it is expected that both techniques will coexist with each their specific therapeutic applications. Certainly since CRISPR mediated gene silencing is less homogeneous compared to RNAi. Hence, CRISPR may pose advantages in chronic genetic diseases or in the context of cancer immunotherapy. CRISPR may for instance be the weapon of choice to tackle Duchenne muscular dystrophy where partial reversal of the diseased phenotype leads to muscle recovery. In contrast, RNAi would be beneficial as a temporary treatment for transient disorders (e.g. asthma) or if more homogeneous gene silencing is required (e.g. in endothelial cells).[25] The development of CRISPR is furthermore not as advanced as for RNAi.[14, 26] Although CRISPR may be delivered through similar delivery strategies as RNAi, delivery challenges for CRISPR may be even greater since both a ˜100 nucleotide single stranded RNA molecule and a Cas9-expressing mRNA or pDNA need to be delivered and translocated to nucleus. Hence, it is expected that RNAi therapeutics will be applied sooner and will create sufficient revenue prior to potential overruling by CRISPR therapeutics, for which clinical evaluation is yet to commence.[25]

2.2. Clinical development of siRNA therapeutics

The first clinical trial with an RNAi therapeutic candidate was conducted in 2004 where naked siRNA was injected intravitreally. The siRNA targeted the vascular endothelial growth factor (VEGF) to treat age-related macular degeneration. This product was successful in Phase I to III trials with the anti-angiogenic effect of the anti-VEGF siRNA leading to improved vision. However, Kleinman *et al.* showed that this was not an siRNA sequence-specific effect, as scrambled control siRNA and anti-luciferase siRNA induced similar improvements. In turn, the anti-angiogenic effect was related to the induction of an innate immune response upon siRNA recognition by toll like receptor 3.[20] On second thought, this observation was not surprising since naked siRNA shows poor uptake and can consequently not effectively alter VEGF expression.

A first wave of clinical trials evaluating RNAi therapeutics was initiated in 2008. These initial trials generally applied naked siRNA and failed to render marketable therapeutics.[13] However, they provided valuable information on the major obstacles towards efficient RNAi therapies being safety, efficacy and delivery.[19] Subsequent innovations on the siRNA structure and delivery modalities led to a second wave of clinical trials, which is anticipated to bring forth marketable RNAi-based therapeutics.[19] Anno 2017, ˜25 RNAi candidate

therapeutics are being evaluated in Phase I to III clinical trials (Table 8.1).[19, 27] The majority of the RNAi therapeutic candidates are investigated in the context of hereditary diseases, viral infections and cancer. Most therapeutics target hereditary orphan diseases given the advantageous FDA and EMA fast track for approval.[27] It is expected that a successful delivery method should fairly easy be repurposed for a different disorder in the same target tissue. Hence, once an RNAi therapeutic is approved for an orphan disease, applications for more generally occurring disorders in the same tissue may soon follow. However, this may be a simplistic view since alterations in the siRNA sequence may in turn be responsible for unexpected adverse events.

The organs that are currently most targeted in RNAi trials are the eye and the liver. The eye is a privileged site given its low nuclease activity and immunosensitivity.[19] At the time of writing, 4 ongoing trials are evaluating naked siRNA administered either topically or through intravitreal injections.[19, 28] However, the current absolute n° 1 target organ for RNAi therapy is the liver, which can chiefly be attributed to the preferential hepatic accumulation of the applied constructs.[27] The majority of the clinical trials for hepatic targets evaluate products developed by Alnylam to treat hypercholesterolemia, hemophilia, hepatic porphyria and paroxysmal nocturnal hemoglobinurua.[29-31] Alnylam's current lead component is Patisiran. This LNP containing transthyretin (TTR)-targeting siRNA is applied in familial amyloidotic polyneuropathy due to TTR amyloidosis and is currently tested in Phase III studies.[19] In contrast, the Phase III trial for Revusiran (a GalNAc conjugate applied for familial amyloidotic cardiomyopathy) was prematurely terminated, as reanalysis of the Phase II data revealed more deaths in the Revusiran treated group.[32] Besides Alnylam, Arrowhead and Nitto Denko are evaluating their RNAi therapeutics for alpha-I trypsin deficiency and hepatic fibrosis, respectively.[19] Further studies evaluate the safety and potency of RNAi therapeutics in the context of cancer immunotherapy or as a direct anti-cancer agent.[19, 33] A final set of hepatic RNAi indications for which RNAi therapeutics are currently clinically evaluated are viral infections, such as Ebola and Hepatitis B and C.[34-36]

Table 8.1. siRNA therapeutic candidates in clinical evaluation. (Adapted from [19])

Target tissue	Disease	siRNA target	Delivery	Clinical status	Company
Eye	Dry eye	TRPV1	Topical Naked siRNA	Phase I/II	Sylentis
	Ocular hypertension, open-angle glaucoma	ADRB2	Topical Naked siRNA	Phase II	Sylentis
	Angle closure glaucoma	CASP2	Intravitreal injection Naked siRNA	Phase II/III	Quark
	Ocular hypertension, open-angle glaucoma	RTP801 REDD1	Intravitreal injection Naked siRNA	Phase II	Quark/Pfizer
Liver	Hypercholesterolemia	PCSK9	Subcutaneous injection LNP	Phase I	Alnylam
	Hemophilia (Fitusiran)	AT	Subcutaneous injection ESC-siRNA-GalNAc	Phase I	Alnylam
	Hepatic porphyrias	ALAS1	Subcutaneous injection ESC-siRNA-GalNAc	Phase I	Alnylam
	Paroxysmal nocturnal hemoglobinuria	C5	Subcutaneous injection ESC-siRNA-GalNAc	Phase I /II	Alnylam
	Familial amyloidotic polyneuropathy (Patisiran)	TTR	IV infusion LNP	Phase I-III	Alnylam
	Alpha-1 antitrypsin deficiency	AAT	Subcutaneous injection ESC-siRNA-GalNAc	Phase I /II	Alnylam
	Alpha-1 antitrypsin deficiency	AAT	IV injection DPC	Phase I	Arrowhead
	Hepatic fibrosis	HSP47	IV injection vitamin A targeting LNP	Phase I/II	Nitto Denko
	Advanced/ metastatic cancer	STMN	Intratumoral injection LNP	Phase I	Gradalis

	Advanced recurrent cancer	EPHA2	IV injection DOPC LNP	Phase I	MD Anderson
	Hepatitis B	Three conserved regions of HBV	IV infusion LNP	Phase I	Arbutus
	Hepatitis B	Conserved region of HBV	IV injection DPC	Phase II	Arrowhead
	Hepatitis C	Three conserved regions of HCV	IV infusion AVV	Phase I/II	Benitec
	Ebola	VP24; VP35; Ebola L-polymerase	IV infusion LNP	Phase II	Arbutus
Cancer	Cancer immunotherapy	Cbl-b/DC cancer vaccine	IV infusion of ex vivo electroporation	Phase I	Apeiron
	Cancer immunotherapy	Furin/DC cancer vaccine	IV infusion of ex vivo electroporation	Phase III	Gradalis
	Neural endocriene cancer	PLK1	IV infusion LNP	Phase I/II	Arbutus
	Pancreatic cancer	KRAS-G12D	Surgical implementation LODER-polymer	Phase II/III	Silenseed
	Solid tumor, melanoma, lymphoma	MYC	IV infusion LNP	Phase I/II	Dicerna
Skin	Pachyonychia congenita	K6a	Intradermal injection naked siRNA	Phase I	TransDerm SomaGenetics
	Scar prevention, keloid formation	CTGF	Intradermal injection rxRNA	Phase II	Rxi Pharmaceuticals
GI tract	Familial adenomatous polyposis	Beta-catenin	Oral administration of bacteria (trans kingdom RNAi)	Phase I	Marina

With several RNAi candidates in Phase III studies, it will likely only be a matter of time before the first one is granted FDA-approval. Current applications are mainly limited to easily reachable tissues by local application (eye, skin, mucosa) and the liver upon systemic administration.[19, 27] Hence, the need for additional delivery methods able to target more difficult to access organs could not be more stringent. Since nanomedicines show preferential hepatic accumulation and targeting efforts towards extra-hepatic tissues have limited success[37], the focus of delivery research may benefit from a switch towards siRNA-conjugates, being an order of magnitude smaller in size than most nanocarriers. Ideally, such conjugates would target an ominously expressed receptor that quickly recycles back to the cell surface, after release of its ligand, to ensure maximal internalization of the conjugate.[27] Given the smaller size of the conjugates, tissue penetration might be less troublesome as for nanomedicines.[7] In any case, the development of more stable and potent delivery systems is required to enhance the efficiency of siRNA therapeutics. Here, our proposed adjuvant strategy might pose a solution.

2.3. Drug repurposing and drug-siRNA combinations

2.3.1. Drug repurposing

Ashburn and Thor were the first to apply the term drug repurposing in 2004, although various cases were described by that time.[38] In the context of drug repurposing, also known as drug repositioning or rescue, approved, withdrawn or abandoned drugs or drug candidates are evaluated for different indications than they were initially developed for.[38, 39] Thus, drug candidates previously underwent at least Phase I clinical investigations and data regarding the pharmacokinetics, drug safety and possible interactions are already available. Furthermore, potential issues with bulk manufacturing and formulation were often previously dealt with.[40] Based on this foreknowledge, drug repurposing is generally considered a risk- and cost-cutting strategy with a more rapid turnout.[38, 41] Currently, *de novo* drug discovery and development requires approximately 15 years and several billion US$. The upward trend in cost and development time does not coincide with an increasing amount of drugs reaching the market. In contrast, a historically low 6% of all investigated compounds reaches the market, with the development mainly being discontinued in late phase clinical assessments. Drug repurposing is expected to boost the product pipelines, as drug development should take no longer than 12 years with costs below US$ 1B.[42]

Before 2011, drug repurposing was mainly based on serendipitous clinical observations. Probably the most well-known example is sildenafil (Viagra®), which was developed to treat angina pectoris but is now applied for erectile dysfunctions.[38] From 2011 onwards, drug repurposing became an independent drug development strategy, driven by the availability of novel screening techniques and appropriate compound libraries.[40] The boom in drug repurposing can be clearly recognized by the vast increase of publications on the subject, with a record of nearly 500 reports published in 2016.

Currently, most repurposing strategies focus on repositioning drugs for oncologic applications[39, 43, 44], with the star of the show being metformin. The latter is an orally applied biguanide for the treatment of type II diabetes, as it reduces gluconeogenesis and insulin resistance. Nowadays metformin is tested in combination with available chemotherapeutic agents given its anti-mitotic, anti-angiogenic and anti-inflammatory actions.[43] In addition, many efforts focus on drug repositioning to treat infectious diseases, such as Zika virus[45, 46], Ebola virus[47], tuberculosis[48, 49] and other bacterial and parasite infections.[50] Further efforts are reported on drug repurposing for neurological disorders, inflammatory disorders (IBD, COPD), etc.[39, 51-54] Finally, various groups evaluated new drug combinations to meet the shortcoming of the low potency of newly identified hits. Sun *et al.* for instance suggested treating Ebola with a mixture of three lysosome-targeting compounds to reduce viral replication.[47]

In the current optimistic spirit, it is anticipated that 30% of the yearly FDA-approved products will stem from drug repurposing.[42] However, repurposing may, just like RNAi, not be the magical solution Big Pharma is hoping it to be. Indeed, many identified hits suffer from relatively weak efficiencies and will therefore potentially not outperform current standard treatments in clinical investigations.[40] In turn, not all repurposing strategies may be desirable. For instance, certain adverse effects may be acceptable in the context of an anti-cancer strategy but not when treating a chronic disorder.[40] Finally, repurposing does not always imply that preliminary clinical testing can be skipped. When different doses , formulations or novel drug combinations are applied, Phase I clinical trials are still required.[38, 40] Overall, drug repurposing will not replace the development of new compounds, but both strategies will continue to be applied to nourish Big Pharma's pipelines.

Our proposed adjuvant approach also fits in this context of drug repurposing. Of utmost interest, several cationic amphiphilic antihistamines (loratidine and ebastine) were recently shown to improve sensitivity towards chemotherapy and reduce multidrug resistance in Danish patients with non-small cell lung carcinoma.[44] Although similar clinical results were not observed for desloratadine, this compound may still be an applicable delivery adjuvant. In any case will the application of known CADs be advantageous in respect to both time and costs when bringing our concept from bench to bedside.

2.3.2. Drug-siRNA combinations

In the first section of this thesis, small molecules were applied to improve the nucleic acid therapeutic potential. In addition, a significantly larger amount of studies report on the combination of siRNA and small molecular drugs, where siRNA is applied to enhance the therapeutic potential of an anti-cancer treatment. The most reported combinations comprise doxorubicin or paclitaxel with a specific siRNA based on the tumor type.[55-57] In addition, the low molecular weight drug can be either administered as a free drug, in a nanocarrier or co-included with siRNA in the same carrier.[58]

The rationale to apply siRNA can be two-fold. On the one hand, siRNA can silence multidrug resistance proteins thereby increasing the drug concentration at the target site and ensuring enhanced tumor killing efficacy. On the other hand, a synergetic apoptotic effect can be obtained when applying siRNA targeting anti-apoptotic proteins or proteins involved in cell cycle regulation or cell proliferation.[57, 58] If apoptosis can be induced by the siRNA through a different pathway than the drug-induced apoptosis, a synergistic effect may be obtained. A second advantage to this strategy is that required doses of the chemotherapeutic may be reduced. Since these compounds often suffer from a narrow therapeutic range, adverse effects could potentially be scaled down.[57] Ideally a combination strategy is applied where the therapeutic anticancer agent enhances siRNA delivery, which in turn boosts the small molecule-induced cell death.

2.4. Where to go from here with the adjuvant concept

2.4.1. How do CADs promote siRNA-mediated gene silencing?

We previously showed that the apparent endo-lysosomal volume increases upon CAD treatment, most likely as a consequence of phospholipid accumulation, which was in turn correlated to enhanced siRNA-mediated gene silencing (**Chapter 3**). This Niemann-Pick disease-like phospholipidosis phenotype is in all probability induced through CAD-mediated acid sphingomyelinase (ASM) inhibition, although this was not experimentally verified. Sahay *et al.* showed that the Niemann-Pick C1 (NPC1) cholesterol transporter protein has a major role in retrograde transport and exocytosis. Indeed, LNP exocytosis in NPC1$^{-/-}$ cells was blocked, which significantly improved the LNP transfection efficiency.[59] However, our sequential CAD treatment, which causes secondary cholesterol accumulation through NPC2 inhibition, did not have a similar potentiating effect on LPS delivery. Both differences in carrier (lipidoid LNP vs LPS) and incubation schemes (NPC1$^{-/-}$ vs phenotype induction post transfection) could be responsible for this discrepancy. Despite the fact that Sahay *et al.* showed a clear impact on LNP trafficking in NPC1$^{-/-}$ cells[59], we were not yet able to evaluate whether sequential CAD treatment alters siNG trafficking. Such observations might enhance our understanding of the mechanism(s) through which CADs may improve siRNA delivery. It would furthermore we interesting to evaluate if CAD treatments prior to transfection could improve LPS-mediated siRNA delivery as observed in NPC1$^{-/-}$ cells. Further investigation of the effect of CAD pre- or co-incubation on nanocarrier uptake and siRNA-mediated gene silencing could provide valuable information on the mechanism of action and guide the definition of *in vivo* dosing schemes.

Based on the data presented in **Chapter 3**, we assumed that the improved cytosolic release occurred through lysosomal membrane permeabilization (LMP). However, this remains to be experimentally verified. Here, experiments should be performed to confirm the lysosomal lipid accumulation and LMP. In addition, siramesine should be applied as a control as this CAD is reported to induce LMP in cancer cells both *in vitro* and *in vivo*. However, improved siRNA release was not correlated to severe cytotoxicity. This suggests that the ˜34 kDa cathepsins often responsible for lysosomal cell death mainly retained their lysosomal localization, while the ˜12 kDa siRNA managed to escape. Cathepsins may in turn leak to the cytosol concurrent to the siRNA, although to a limited extent with cytosolic cathepsins levels

not saturating the cytosolic hydrolase inhibitors and inducing cytotoxicity.[60] Immunostaining of cathepsins would provide clarification on this topic. In any case, the hypothesis of minor LMP furthermore implies that only free siRNA (*i.e.* siRNA detached from its carrier) can transfer from the lysosomal to the cytosolic compartment upon CAD treatment. It would be interesting to probe the effective size of macromolecules for which CADs may enhance cytosolic delivery.

It would be equally interesting to further assess the impact of CADs on the lysosomal compartment. Uncertainty for instance lingers around their effect on the lysosomal pH.[61-64] Interestingly, lysosomal lipid accumulation may equally affect the lysosomal pH, depending on the phospholipidosis phenotype.[61, 62] It would furthermore be interesting to understand how lipid accumulation affects lysosomal membrane stability to promote cytosolic release.

Finally, we solely applied our adjuvant method to a single cancer cell line in this thesis. Preliminary experiments revealed that the CAD adjuvant approach was effective in the SKOV-3 and HeLa cancer cell lines (data not shown). By testing additional cancer cell lines we could establish if the CADs can generally be applied as adjuvants in cancer cells. Several reports furthermore state that cancer cell lysosomes are more easily perturbed and that CADs selectively induce LMP in cancer cells.[44, 64-66] Hence, it would be highly interesting to confirm whether this is also true for our adjuvant method by comparing the CAD effect in cancer cell lines and primary cells, thereby establishing the therapeutic indication(s) where this CAD strategy could be of use.

2.4.2. Applicable small molecules and their combinations

In **Chapter 3**, we showed that four CADs improved siRNA-mediated gene silencing in a similar concentration-dependent way (Figure 3.4C). However, not all CADs are expected to be active in the same dose range since higher and lower doses of dextromethorphan (Figure 3.5C) and terfenadine (data not shown) respectively provided similar adjuvant effects as the first four molecules. The doses applied in **Chapter 3** are relatively high, which may limit their applicability. Hence, more potent FIASMAs should be identified *via* a larger scale screening.

An additional strategy might be to evaluate chemical inhibitors of ASM since lower concentrations are potentially required to directly inhibit ASM through the key-lock mechanism than the large quantities required for functional ASM inhibition. A recent report

stated that bisphosphonates directly inhibit ASM in cell lysates. However, zolendronate was not as successful as our CADs in preliminary tests (data not shown), which may be attributed to the unfavorable properties for uptake trough passive diffusion. In any case, further experiments are required to confirm this observation.

Various compounds are furthermore reported to negatively influence the lysosomal membrane stability. Compounds that induce lysosomal membrane permeabilization without severe concurrent cytotoxicity due to cathepsins release may be equally applicable delivery adjuvants. In the general context of drug repurposing it would be interesting to screen larger commercially available libraries to identify additional delivery enhancers, which may act through distinct mechanisms. Subsequently, we should evaluate drug combinations, as synergetic combinations may be identified.[40] In this case, lower doses of each component would be required, thereby reducing the risk of adverse effects.

2.4.3. Applicable nanocarriers

In this thesis we showed that the proposed adjuvant strategy can strongly potentiate siRNA-mediated gene silencing upon NG transfection (**Chapter 3**), but not upon transfection with LPS or commercial lipid formulations (**Chapter 4**). Hence, it would be highly interesting to combine our adjuvant strategy with distinct polymer-based carriers to truely establish the broader applicability in terms of the nanocarrier. It would furthermore be of utmost interest to evaluate if CAD adjuvants can potentiate the effect of clinically tested formulations, such as SNALP and dynamic polyconjugates (DPC). If this were true, required siRNA doses and potential off-target effects could be dramatically reduced.

As previously noted, we expect that solely siRNA detached from its carrier is able to transfer from the lysosomal to the cytosolic compartment. Hence, carrier degradation and/or siRNA release are potentially of key importance to our adjuvant method. This should be confirmed by combining non-biodegradable NGs or enzyme resistant cyclodextrins with a sequential CAD treatment, where we would not expect to witness improved transfection efficiencies. This feature may indeed explain why our approach worked well for the biodegradable NGs, but not for the lipid-based formulations. Unfortunately, relatively little is known regarding the degradation of lipid-based carriers in the lysosomal compartment. However, it is generally assumed that carrier and cargo face degradation since the lysosomes are regarded as the cell's 'stomach'. Liposomal lipids are most likely digested by lysosomal lipases, such as

phospholipase A2 (PLA2), which are known to have a preference for phosphatidylcholine (PC) and –ethanolamine (PE) moieties.[67] The kinetics of this degradation process are potentially of key importance to our sequential adjuvant approach. Indeed, sufficient amounts of free (nuclease-stabilized) siRNA need to be present when initiating the sequential adjuvant treatment. Thus, the timing of the latter could be optimized based on degradation kinetics of the lipid nanocarrier. An additional solution could be to apply bioresponsive carriers - such as PLA2 sensitive LPS[68-70] - or biodegradable carriers (f.i. SNALP, Lipidoids, PLGA)[15, 71, 72]. In general a more in depth understanding of intracellular trafficking, the mechanism of escape and carrier degradation would stimulate the rational combination of nanocarriers and small molecular adjuvants.

2.4.4. New constructs

Two main strategies can be envisioned for the development of new constructs based on our adjuvant approach. The first implies the co-encapsulation of siRNA and small molecules in a single carrier, whereas the second focusses on the synthesis of CAD-siRNA conjugates.

The main advantage of introducing the small molecular adjuvant into the formulation is the reduction of the total required dose. In a first attempt, where we prepared DOPE:NT LPS (Figure 4.9), no beneficial effect of the NT could be detected since it was not able to induce a PLD phenotype. Hence, the challenge will be to prepare a formulation where both the CAD and siRNA are released in the lysosomal compartment, which may for instance be achieved through pH sensitive linkers.

Secondly, effort should be put into the synthesis of a CAD-siRNA conjugate in analogy with the GalNAc conjugate. This conjugate shows high hepatic transfection efficiency and is easier and cheaper to produce than nanocarrier alternatives. In addition, such conjugates are regarded as relatively save, although a Phase III clinical trial on GalNAc conjugates was recently halted.[32] Still such conjugates are dwarfed by nanocarriers and may show improved tissue penetration and pose opportunities to reach extra-hepatic tissues.[7]

2.4.5. A final critical note

A shortcoming to the presented work may be the lack of an *in vivo* proof-of-concept experiment. As discussed in **Chapter 3** it is not straightforward to evaluate our adjuvant approach in an *in vivo* setting. For one, the applied NGs are not stable upon systemic administration. Thus the use of NGs to deliver siRNA would solely be feasible through intratumoral injections, which are very rarely applied in the clinic. In addition, intratumoral injections are most often administered to xenograft tumors, which may not be an ideal model given the poor representation of human solid tumors.[73] Thus, we should first identify a suitable carrier both able to transport siRNA throughout the body and sensitive to our CAD adjuvant approach, and identify a more complex and representative tumor model to evaluate our approach *in vivo*. When performing an in vivo evaluation of our concept it would be advisable to include siramesine as a control in both the *in vitro* and *in vivo* experiments since this molecules was shown to induce LMP in both models.[64]

The safety of our current approach may be one of the biggest hurdles towards translation, as the *in vitro* effective doses can maybe not be achieved *in vivo* with therapeutic CAD doses, despite the large distribution volumes, preferential accumulation at acidic tumor sites and successful LMP induction by siramesine *in vivo*.[44, 64] Careful modeling of the pharmacokinetic profile of the adjuvant and safety assessments could provide clarification. In addition, one needs to be sure that other CADs consumed by the patient will not impact the siRNA release, as excess siRNA release would increase the risk of off-target effects and immune responses. On the other end of the spectrum, it should be ensured that the CAD does not negatively affect (off-)target tissue(s).

The majority of the current clinical trials locally apply siRNA formulations to the eye or skin or target the liver upon systemic administration. Despite research efforts in the past 20 years, little progress has been achieved on targeted delivery, as nanocarriers still predominantly accumulate in the liver. A sobering report by Chan's group revealed that a median 0.7% of the nanocarrier dose reaches solid tumor cells.[37] Although a recent communication stated that we should not as much look at the numbers but rather focus on the benefits for patients[74], we should still aim higher by developing more efficient delivery approaches able to target difficult to reach target tissues. In this regard, we may need a different approach to delivery keeping simplicity at the front of our minds.[75] According to

Haussecker: “Small polyconjugates bringing together active endosomal release chemistries and RNAi-triggers may strike the balance between size and cell penetration though at the cost of adding further chemical complexity.”[7] In this view we believe that a CAD-siRNA conjugate may be an important strategy to explore.

3. INORGANIC NANOPARTICLES IN MEDICINE

3.1. Clinical use and development of inorganic nanoparticles

At the time of writing, approved biomedical applications of inorganic NPs are chiefly limited to diagnostic tools. In this regard, various NPs (gold NPs, silver NPs, iron oxide NPs, quantum dots etc.) are applied to enhance the signal read-out or to improve bioseparation to ensure pathogen or biomarker detection with improved specificity and sensitivity.[76, 77] While such applications were initially developed by academia, various big pharmaceutical and medical device companies soon showed interest by investing in large R&D initiatives to develop nano-enabled *in vitro* and *ex vivo* diagnostic tools.[78] In contrast, inorganic NPs are as of today rarely applied for therapeutic purposes or *in vivo* imaging-mediated diagnostic strategies, despite numerous proof-of-concept studies.[79] Overall, the uncertainty regarding the safe use of inorganic NPs does not favor regulatory agencies to move an investigational new drug into clinical evaluation or to approve a new drug application. Consequently, the return of investments is highly insecure and investment in inorganic NP-based nanomedicines remains low. Several discontinued NP-containing contrast agents and imminent issues with bulk manufacturing further hinder the commercial incentive.[80-82]

The sole inorganic nanomaterial that managed to reach the clinic is iron oxide (Table 8.2). The best known application of iron oxide (IO)NPs is as an MRI contrast agent, where IONPs were administered systemically to image liver lesions or lymphatic abnormalities[83, 84] or orally as a gastro-intestinal contrast agent.[85, 86] Despite the clinical approval, many of the contrast agents failed to reach widespread use and production was discontinued by 2009.[87] The intraveneous injection of carbohydrate-coated IONPs is in contrast still successfully applied for the management of chronic anemia in chronic kidney disease.[88, 89] Aminosilane-coated IONPs are a final IONP-formulation that obtained EU approval and is applied to treat glioblastoma through hyperthermia following intratumoral injection.[90, 91]

An additional material currently proceeding in clinical evaluations is nano-sized gold. Interestingly, colloidal gold has since long been used in the treatment of rheumatoid arthritis before being outclassed by newer drugs.[92, 93] Currently, AuNPs coupled to tumor necrosis factor alfa (TNF_α) are evaluated for the treatment of solid tumor metastasis.[94] Silica-Au nanoshells coated with PEG are in turn investigated as a hyperthermia agent.[76, 95] Finally, the local application of silica-Au nanoshells, followed by low frequency ultrasound and laser irradiation, is investigated for the treatment of severe acne.[96] Cornell dots (silica NPs) can furthermore enhance PET imaging and are evaluated for the imaging of metastatic melanoma and the intraoperative mapping of sentinel lymph nodes.[97] Finally, hafnium oxide nanocrystals (NBTXR3) are investigated for their potential as radioenhancing agents in soft tissue sarcoma and head and neck cancer.[98, 99]

Table 8.2. Clinical use and development of inorganic nanoparticles.

NP	Application	Product	Route	Tissue	Availability / Clinical status
IONP	MRI	Endorem Feridex Resovist	IV	Liver	Discontinued
		Combidex Sinerem	IV	Lymphography	Discontinued
		Gastromark Lumirem	Oral	Upper GI tract	Discontinued
		Ferristene	Oral	GI tract	Discontinued
	Iron supplement	Feraheme	IV	Chronic anemia in chronic kidney disease	Available
	Hyperthermia	NanoTherm	IT	Glioblastoma	Available
AuNP	TNF_α delivery	Aurimune	IV	Solid tumor metastasis	Phase I
	Hyperthermia	AuroLase	IT	Recurrent head & neck cancer	Phase I
				Primary & metastatic lung cancer	Phase I
	Acne	Sebashells	Local	Skin	Phase I
Silica NP	PET Imaging	Cornell dots	Local	Metastatic melanoma	Phase I
			IT	Sentinel lymph node mapping	Phase I
Hafnium oxide NP	Radioenhancer	NBTXR3	IT	Soft tissue sarcoma	Phase I
				Head and neck cancer	Phase I

Although the current perception may not be in favor of a widespread use of inorganic NPs for biomedical applications, a solution may be found in altering the delivery method. Nanotoxicity can indeed nearly completely be circumvented by delivering NPs directly into the cytosol.[100, 101] When the NPs are not exposed to the acidic environment of the endo-lysosomes they are less prone to dissolution – which is a main determinant to NP toxicity – and can potentially be safely applied.[102, 103] Hence, scientists seeking to biomedically apply inorganic NPs may also need to identify efficient cytosolic delivery strategies.

3.2. How to advance in the field of *in vitro* nanotoxicology

In the first phase of research into nanotechnology, scientists mainly focused on the discovery of the unique nano-features and their potential implementation. In a second phase, concerns were raised regarding increasing exposure to inorganic NPs given the ever increasing number of NP-containing consumer products entering the market.[80] Consequently, scientists started looking into the safety of NPs. Initially, nanotoxicology was a small niche within the general toxicology field, but it soon became a discipline on its own and started to boom.[104] Due to this sudden explosion of reports, consistency in terms of dose metrics, NP characterization, applied assays etc. was staggeringly low. Currently, we face an enormous pool of uncorrelated nanosafety data from which little general conclusions are to be drawn. On the upside, this explosion in nanotoxicology data did reveal important weaknesses to the *in vitro* nanohazard assessment paradigm. At this stage, *in vitro* nanotoxicology should enter a new phase of harmonization where efforts are truly focused on the development, evaluation, standardization and implementation of appropriate methods. A set of standard NPs should furthermore be defined, which can subsequently be included as controls in the optimization and validation of *in vitro* methods.

The issue of inconsistent data troubles biomedical scientist seeking to rationally design a NP, but also hinders regulatory bodies aiming to ensure safe NP use. In the past decades, regulatory bodies and concerted multicenter projects therefore aimed to standardize nanohazard testing, exposure evaluation and risk assessment schemes. The NANoREG project, for instance, provided standard operating protocols for NP characterization and NP dispersion preparation, guidelines on harmonized data reporting and risk assessment schemes. Their highly concerted action in terms of applied NPs, methods, cell models and quality controls allowed obtaining meaningful data. As a result, various guidelines for NP

testing in the context of regulatory nanosafety testing were established and made available to the public. In addition, the organization for economic cooperation and development (OECD) enumerates which toxicological end points require investigation (f.i. skin and eye irritation[105, 106], chronic toxicity[107], carcinogenicity[108] etc.) by which assays and in which (animal) model(s) in the context of hazard assessment. These guidelines were initially developed for chemical compounds, but were found appropriate for NP hazard assessment upon minor adaptations of the methods. Thus, although these methods were developed to evaluate NP toxicity in the context of risk assessment, many of these methods will be appropriate to evaluate the toxicity of NPs for biomedical applications. These methods and guidelines must therefore increasingly clearly be communicated to the nanotoxicology community to urge harmonization. Journal boards should play their part by applying stricter guidelines on the minimum set of NP characterization data required for correct data interpretation and harmonized data representation. This would allow future meta-analysis and may prevent the pool of uncorrelated data from overflowing. On the downside, many of the OECD methods involve animal testing. To enable more rapid safety screening during NP optimization, credible scientific bodies should provide harmonized guidance on *in vitro* assays in terms of how NP dispersions should be prepared, the dose metric and which endpoints to study through which (combination of) assay(s) in which cell models. Although the field would significantly benefit from more harmonized research, scientists should never be discouraged to identify further shortcomings and file for additional improvements to the methodologies in place.

It is clear that nanotoxicology is becoming an increasingly complex field. Therefore, we believe that the field would benefit from the establishment of multidisciplinary knowledge centers who apply standardized methods in compliance to regulatory guidelines. A recent example is the European Nanomedicine Characterization Laboratory, where selected promising NP samples can be sent to for standardized characterization and safety testing.[109] Since the number of NPs that are selected for analysis is limited, more knowledge centers should be created, as we believe it would be challenging to bring all this knowledge and the required high end equipment together in an academic setting.

The setting where *in vitro* evaluations can be of use should finally be defined. We envision that *in vitro* tests may provide a first indication of NP cytotoxicity and allow NP ranking, since

in vitro evaluations largely neglect potential systemic interactions. However, at this point *in vitro* data are often questioned due to the *in vitro-in vivo* gap. Hence, current *in vitro* methods require further adaptations to enhance their predictivity, which is not straightforward when the true toxicity of the tested NP is uncertain.[110] Hence, it may be necessary to perform *in vivo* studies to acquire knowledge on the *in vivo* behavior of NPs. With such data sets, scientists can go back to the drawing board to develop reliable predictive *in vitro* models while balancing throughput and model complexity. At this point, the nanotoxicology community should more closely inspect the work of *in vitro* toxicologists, whom are often quite advanced in the development of *in vitro* models to evaluate the toxicity of chemical compounds. With several adaptations, such models may also be applicable to estimate NP toxicity.

4. BRIDGING THE *IN VITRO-IN VIVO* GAP

Research on both topics discussed in this thesis was performed on *in vitro* cell models, more specifically 2D cell monolayers. The latter are often selected for preliminary proof-of-concept studies given their simplicity and convenience. However, when applying such simplified models the question remains how the obtained data can be extrapolated first to *in vivo* effects and subsequently to observations in humans. The discrepancy between *in vivo* data and effects in humans is for instance largely responsible for the many compounds failing in late stage clinical trials. Similarly, effects obtained *in vitro* will not necessarily correlate with *in vivo* responses given the *in vitro-in vivo* gap.

It is proposed that the use of more complex models could provide a bridge between *in vitro* and *in vivo* studies given the improved representation of the *in vivo* environment.[111] Such models include co-cultures, 3D spheroids, organoids, histocultures etc. As mentioned in **Chapter 5**, the use of more complex models indeed allows an improved evaluation of intricate processes, such as inflammation and the metabolization of xenobiotic. In addition, the predictive value of such models must be validated by side-by-side comparisons with *in vivo* data. An interesting approach could be to first assess NP toxicity *in vivo* and go back to the drawing board to develop reliable predictive *in vitro* models while balancing throughput and model complexity.

Besides the use of more intricate models, it is of utmost important to build bridges between *in vitro* and *in vivo* models through the definition of correlations between *in vitro* end points and *in vivo* observations. This is true for both simplified 2D models and intricate 3D models. Zhang *et al.* for instance showed that ROS production in a 2D pulmonary cell model can be correlated to inflammation in the lung.[112] Similar correlations should increasingly be identified. However contrary to the 3R principle by Russel and Burch, it may thus again be necessary to first perform *in vivo* studies to understand the *in vivo* NP behavior and interactions. Next, relevant *in vitro* end points could be defined and analyzed to potentially identify correlations. Of note, various groups showed that the success of identifying correlations may be linked to the use of proper dose metrics.[113, 114] When correlations were defined using specific compounds or NPs, at least one of them should be applied as a positive control in subsequent experiments. This way, the extent of the potential *in vivo* effects could be estimated based on the *in vitro* result. In case of nanotoxicity assessments, standard NPs should ideally be applied as positive and negative controls. In case of therapeutic approaches, the optimal experiment would include a comparison between the proposed therapeutic and the current therapeutic standard for the specific disease. Many drug candidates fail in late phase clinical testing, as they do not outperform the therapeutic standard. This number may be reduced by earlier direct comparisons between the standard and proposed therapy. In our case specifically, it would be interesting to evaluate the effect of siramesine *in vitro*, as this compunds has been shown to induce LMP *in vivo*. At lower doses, siramesine may be applicable as a delivery adjuvant. The use of the same biomarkers in *in vitro* and *in vivo* experiments may furthermore reduce the *in vitro-in vivo* gap. The replication of relevant exposure scenario's may furthermore aid this process. When NPs are for instance expected to be inhaled it is more representative to apply an aerosol exposure than to simple add NPs to the culture medium of submerged lung cells.[115] Finally, physiology based pharmacokinetic modeling will provide information on the *in vivo* distribution of the of the novel drug or nanocarrier, which will allow more rational design of the *in vivo* experiment in terms of dosing schemes.

Overall, bridging the *in vitro-in vivo* gap can be achieved by increasing the model complexity but mainly by identifying correlations between effects observed in both model systems, which can be obtained through side-by-side comparisons.

5. CONCLUSION

Nanoparticles (NPs) are avidly investigated in the context of biomedical application. In the first part of this thesis we provided an *in vitro* proof-of-concept that CAD adjuvants can significantly enhance siRNA-mediated gene silencing upon nanogel-mediated transfection. However, further research is required to (i) identify CADs with greater functionality and/or additional delivery enhancers that can be applied either alone or combined with CADs, (ii) establish the importance of the carrier degradation and siRNA release and the subgroup of nanocarriers to which our approach is applicable and (iii) create new nanocarriers with both the CAD and siRNA present as cargo or synthesize CAD-siRNA conjugates, which may more easily reach extra-hepatic tissues. Although a long road still lies ahead, the great potential of our adjuvant approach warrants further investigation. The repurposing strategy may lead to accelerated approval especially when our strategy would combine well with currently clinically evaluated delivery platforms. Finally, it may strongly enhance the efficiency of siRNA therapeutics through lowering the required siRNA dose, thereby significantly improving the safety profile. Clinical translation of inorganic NPs is on the contrary severely limited by their ambiguous safety profile. Overall, the main challenge to nanotoxicology remains the harmonized implementation of characterization and testing guidelines to reduce the generation of conflicting data. Both in the development of nanocarriers and nanosafety studies, the question remains how the obtained *in vitro* data will translate to *in vivo* responses. In the interest of bridging the *in vitro*-*in vivo* gap, more complex *in vitro* models are being applied to evaluate responses in models that more closely represent the *in vivo* microenvironment. Most importantly, future side-by-side comparisons should be performed to define correlations between *in vitro* and *in vivo* parameters to improve the predictive capacity of *in vitro* models.

REFERNCES

1. Stark, W. J.; Stoessel, P. R.; Wohlleben, W.; Hafner, A. *Chem Soc Rev* **2015,** 44, (16), 5793-805.
2. Platt, J. R., Nanotechnology: Big Opportunities for Those Who Think Small. The Institute: 2012.
3. *Nanotechnology Industry Review and Prospects: Key technologies and markets in 2015 and beyond*; Future Markets: 2014.
4. The Project on Emerging Nanotechnologies. http://www.nanotechproject.org/ (7/12/2016),
5. Wicki, A.; Witzigmann, D.; Balasubramanian, V.; Huwyler, J. *J Control Release* **2015,** 200, 138-57.
6. Haussecker, D. *Mol Ther Nucleic Acids* **2012,** 1, e8.
7. Haussecker, D. *J Control Release* **2014,** 195, 49-54.
8. Fire, A.; Xu, S.; Montgomery, M. K.; Kostas, S. A.; Driver, S. E.; Mello, C. C. *Nature* **1998,** 391, (6669), 806-11.
9. Elbashir, S. M.; Harborth, J.; Lendeckel, W.; Yalcin, A.; Weber, K.; Tuschl, T. *Nature* **2001,** 411, (6836), 494-8.
10. Morris, K. V.; Chan, S. W.; Jacobsen, S. E.; Looney, D. J. *Science* **2004,** 305, (5688), 1289-92.
11. Whitehead, K. A.; Langer, R.; Anderson, D. G. *Nat Rev Drug Discov* **2009,** 8, (2), 129-38.
12. Juliano, R. L. *Nucleic Acids Res* **2016,** 44, (14), 6518-48.
13. Wu, S. Y.; Lopez-Berestein, G.; Calin, G. A.; Sood, A. K. *Sci Transl Med* **2014,** 6, (240), 240ps7.
14. Song, E. W.; Lee, S. K.; Wang, J.; Ince, N.; Ouyang, N.; Min, J.; Chen, J. S.; Shankar, P.; Lieberman, J. *Nature Medicine* **2003,** 9, (3), 347-351.
15. Zimmermann, T. S.; Lee, A. C.; Akinc, A.; Bramlage, B.; Bumcrot, D.; Fedoruk, M. N.; Harborth, J.; Heyes, J. A.; Jeffs, L. B.; John, M.; Judge, A. D.; Lam, K.; McClintock, K.; Nechev, L. V.; Palmer, L. R.; Racie, T.; Rohl, I.; Seiffert, S.; Shanmugam, S.; Sood, V.; Soutschek, J.; Toudjarska, I.; Wheat, A. J.; Yaworski, E.; Zedalis, W.; Koteliansky, V.; Manoharan, M.; Vornlocher, H. P.; MacLachlan, I. *Nature* **2006,** 441, (7089), 111-4.
16. Lundin, P. *Nat Biotechnol* **2011,** 29, (6), 493-7.
17. Krieg, A. M. *Molecular Therapy* **2011,** 19, (6), 1001-1002.
18. LaMattina, J., Big Pharma's turn on RNAi shows that new technologies don't guarantee R1D success. *Forbes* 15/4/2014, 2014.
19. Bobbin, M. L.; Rossi, J. J. *Annu Rev Pharmacol* **2016,** 56, 103-122.
20. Kleinman, M. E.; Yamada, K.; Takeda, A.; Chandrasekaran, V.; Nozaki, M.; Baffi, J. Z.; Albuquerque, R. J. C.; Yamasaki, S.; Itaya, M.; Pan, Y. Z.; Appukuttan, B.; Gibbs, D.; Yang, Z. L.; Kariko, K.; Ambati, B. K.; Wilgus, T. A.; DiPietro, L. A.; Sakurai, E.; Zhang, K.; Smith, J. R.; Taylor, E. W.; Ambati, J. *Nature* **2008,** 452, (7187), 591-U1.
21. de Fougerolles, A.; Vornlocher, H. P.; Maraganore, J.; Lieberman, J. *Nat Rev Drug Discov* **2007,** 6, (6), 443-453.
22. Akinc, A.; Querbes, W.; De, S.; Qin, J.; Frank-Kamenetsky, M.; Jayaprakash, K. N.; Jayaraman, M.; Rajeev, K. G.; Cantley, W. L.; Dorkin, J. R.; Butler, J. S.; Qin, L.; Racie, T.; Sprague, A.; Fava, E.; Zeigerer, A.; Hope, M. J.; Zerial, M.; Sah, D. W.; Fitzgerald, K.; Tracy, M. A.; Manoharan, M.; Koteliansky, V.; Fougerolles, A.; Maier, M. A. *Mol Ther* **2010,** 18, (7), 1357-64.
23. Visiongain *RNAi for therapeutic applications: technology and market forecast 2015-2025*; 24/06/2015, 2015; p 174.
24. Research, G. V. *Antisense and RNAi Therapeutics Market Analysis By Technology (RNA interference, siRNA, miRNA, Antisense RNA), By Application (Oncology, Cardiovascular, Renal, Neurodegenerative, Respiratory, Genetic, Infectious Diseases), By Route of Administration (Pulmonary, Intravenous, Intra-dermal, Intra-peritoneal, Topical) And Segment Forecasts To 2022*; Grand View Research: March 2016, 2016; p 148.
25. Haussecker, D. *FEBS J* **2016,** 283, (17), 3249-60.

26. Ran, F. A.; Cong, L.; Yan, W. X.; Scott, D. A.; Gootenberg, J. S.; Kriz, A. J.; Zetsche, B.; Shalem, O.; Wu, X.; Makarova, K. S.; Koonin, E. V.; Sharp, P. A.; Zhang, F. *Nature* **2015,** 520, (7546), 186-91.
27. Wittrup, A.; Lieberman, J. *Nat Rev Genet* **2015,** 16, (9), 543-52.
28. Martinez, T.; Gonzalez, M. V.; Roehl, I.; Wright, N.; Paneda, C.; Jimenez, A. I. *Molecular Therapy* **2014,** 22, (1), 81-91.
29. Fitzgerald, K.; Frank-Kamenetsky, M.; Shulga-Morskaya, S.; Liebow, A.; Bettencourt, B. R.; Sutherland, J. E.; Hutabarat, R. M.; Clausen, V. A.; Karsten, V.; Cehelsky, J.; Nochur, S. V.; Kotelianski, V.; Horton, J.; Mant, T.; Chiesa, J.; Ritter, J.; Munisamy, M.; Vaishnaw, A. K.; Gollob, J. A.; Simon, A. *Lancet* **2014,** 383, (9911), 60-68.
30. Borodovsky, A.; Yucius, K.; Sprague, A.; Banda, N. K.; Holers, V. M.; Vaishnaw, A.; Maier, M.; Kallanthottathil, R.; Charisse, K.; Kuchimanchi, S.; Manoharan, M.; Salant, D. J.; Fitzgerald, K.; Meyers, R.; Sorensen, B. *Blood* **2014,** 124, (21).
31. Yasuda, M.; Gan, L.; Chen, B.; Kadirvel, S.; Yu, C. L.; Phillips, J. D.; New, M. I.; Liebow, A.; Fitzgerald, K.; Querbes, W.; Desnick, R. J. *P Natl Acad Sci USA* **2014,** 111, (21), 7777-7782.
32. Reuters Alnylam Pharma says discontinues revusiran development. http://www.reuters.com/article/idUSFWN1CB0ML (23/11/2016),
33. Nemunaitis, J.; Barve, M.; Orr, D.; Kuhn, J.; Magee, M.; Lamont, J.; Bedell, C.; Wallraven, G.; Pappen, B. O.; Roth, A.; Horvath, S.; Nemunaitis, D.; Kumar, P.; Maples, P. B.; Senzer, N. *Oncology-Basel* **2014,** 87, (1), 21-29.
34. Wooddell, C. I.; Rozema, D. B.; Hossbach, M.; John, M.; Hamilton, H. L.; Chu, Q. L.; Hegge, J. O.; Klein, J. J.; Wakefield, D. H.; Oropeza, C. E.; Deckert, J.; Roehl, I.; Jahn-Hofmann, K.; Hadwiger, P.; Vornlocher, H. P.; McLachlan, A.; Lewis, D. L. *Molecular Therapy* **2013,** 21, (5), 973-985.
35. Geisbert, T. W.; Lee, A. C. H.; Robbins, M.; Geisbert, J. B.; Honko, A. N.; Sood, V.; Johnson, J. C.; de Jong, S.; Tavakoli, I.; Judge, A.; Hensley, L. E.; MacLachlan, I. *Lancet* **2010,** 375, (9729), 1896-1905.
36. Thi, E. P.; Mire, C. E.; Lee, A. C. H.; Geisbert, J. B.; Zhou, J. Z.; Agans, K. N.; Snead, N. M.; Deer, D. J.; Barnard, T. R.; Fenton, K. A.; MacLachlan, I.; Geisbert, T. W. *Nature* **2015,** 521, (7552), 362-+.
37. Wilhelm, S.; Tavares, A. J.; Dai, Q.; Ohta, S.; Audet, J.; Dvorak, H. F.; Chan, W. C. W. *Nat Rev Mater* **2016,** 1, (5).
38. Ashburn, T. T.; Thor, K. B. *Nat Rev Drug Discov* **2004,** 3, (8), 673-83.
39. Ishida, J.; Konishi, M.; Ebner, N.; Springer, J. *J Transl Med* **2016,** 14, 269.
40. Sun, W.; Sanderson, P. E.; Zheng, W. *Drug Discov Today* **2016,** 21, (7), 1189-95.
41. Strittmatter, S. M. *Nat Med* **2014,** 20, (6), 590-1.
42. Nosengo, N. *Nature* **2016,** 534, (7607), 314-316.
43. Gadducci, A.; Biglia, N.; Tana, R.; Cosio, S.; Gallo, M. *Crit Rev Oncol Hemat* **2016,** 105, 73-83.
44. Ellegaard, A. M.; Dehlendorff, C.; Vind, A. C.; Anand, A.; Cederkvist, L.; Petersen, N. H. T.; Nylandsted, J.; Stenvang, J.; Mellemgaard, A.; Osterlind, K.; Friis, S.; Jaattela, M. *Ebiomedicine* **2016,** 9, 130-139.
45. Xu, M.; Lee, E. M.; Wen, Z.; Cheng, Y.; Huang, W. K.; Qian, X.; Tcw, J.; Kouznetsova, J.; Ogden, S. C.; Hammack, C.; Jacob, F.; Nguyen, H. N.; Itkin, M.; Hanna, C.; Shinn, P.; Allen, C.; Michael, S. G.; Simeonov, A.; Huang, W.; Christian, K. M.; Goate, A.; Brennand, K. J.; Huang, R.; Xia, M.; Ming, G. L.; Zheng, W.; Song, H.; Tang, H. *Nat Med* **2016,** 22, (10), 1101-1107.
46. Cheng, F.; Murray, J. L.; Rubin, D. H. *Trends Mol Med* **2016**.
47. Sun, W.; He, S.; Martinez-Romero, C.; Kouznetsova, J.; Tawa, G.; Xu, M.; Shinn, P.; Fisher, E.; Long, Y.; Motabar, O.; Yang, S.; Sanderson, P. E.; Williamson, P. R.; Garcia-Sastre, A.; Qiu, X.; Zheng, W. *Antiviral Res* **2016**.
48. Shen, H.; Wang, F.; Zeng, G.; Shen, L.; Cheng, H.; Huang, D.; Wang, R.; Rong, L.; Chen, Z. W. *Sci Rep* **2016,** 6, 32725.

49. Ramon-Garcia, S.; Gonzalez Del Rio, R.; Villarejo, A. S.; Sweet, G. D.; Cunningham, F.; Barros, D.; Ballell, L.; Mendoza-Losana, A.; Ferrer-Bazaga, S.; Thompson, C. J. *Sci Rep* **2016,** 6, 34293.
50. Ferreira, L. G.; Andricopulo, A. D. *Drug Discovery Today* **2016,** 21, (10), 1699-1710.
51. Walton, G. M.; Stockley, J. A.; Griffiths, D.; Sadhra, C. S.; Purvis, T.; Sapey, E. *J Clin Med* **2016,** 5, (10).
52. Collij, V.; Festen, E. A.; Alberts, R.; Weersma, R. K. *Inflamm Bowel Dis* **2016,** 22, (11), 2562-2570.
53. Loesche, A.; Wiese, J.; Sommerwerk, S.; Simon, V.; Brandt, W.; Csuk, R. *Eur J Med Chem* **2016,** 125, 430-434.
54. Mehdi, S. J.; Rosas-Hernandez, H.; Cuevas, E.; Lantz, S. M.; Barger, S. W.; Sarkar, S.; Paule, M. G.; Ali, S. F.; Imam, S. Z. *Int J Mol Sci* **2016,** 17, (9).
55. Reddy, T. L.; Garikapati, K. R.; Reddy, S. G.; Reddy, B. V. S.; Yadav, J. S.; Bhadra, U.; Bhadra, M. P. *Sci Rep-Uk* **2016,** 6.
56. Meng, H.; Mai, W. X.; Zhang, H. Y.; Xue, M.; Xia, T.; Lin, S. J.; Wang, X.; Zhao, Y.; Ji, Z. X.; Zink, J. I.; Nel, A. E. *Acs Nano* **2013,** 7, (2), 994-1005.
57. Saraswathy, M.; Gong, S. Q. *Mater Today* **2014,** 17, (6), 298-306.
58. Yhee, J. Y.; Son, S.; Lee, H.; Kim, K. *Curr Pharm Design* **2015,** 21, (22), 3158-3166.
59. Sahay, G.; Querbes, W.; Alabi, C.; Eltoukhy, A.; Sarkar, S.; Zurenko, C.; Karagiannis, E.; Love, K.; Chen, D.; Zoncu, R.; Buganim, Y.; Schroeder, A.; Langer, R.; Anderson, D. G. *Nat Biotechnol* **2013,** 31, (7), 653-8.
60. Aits, S.; Jaattela, M. *J Cell Sci* **2013,** 126, (Pt 9), 1905-12.
61. Lloyd-Evans, E.; Platt, F. M. *Traffic* **2010,** 11, (4), 419-28.
62. Canfran-Duque, A.; Barrio, L. C.; Lerma, M.; de la Pena, G.; Serna, J.; Pastor, O.; Lasuncion, M. A.; Busto, R. *Int J Mol Sci* **2016,** 17, (3), 404.
63. Otomo, T.; Higaki, K.; Nanba, E.; Ozono, K.; Sakai, N. *J Biol Chem* **2011,** 286, (40), 35283-90.
64. Petersen, N. H.; Olsen, O. D.; Groth-Pedersen, L.; Ellegaard, A. M.; Bilgin, M.; Redmer, S.; Ostenfeld, M. S.; Ulanet, D.; Dovmark, T. H.; Lonborg, A.; Vindelov, S. D.; Hanahan, D.; Arenz, C.; Ejsing, C. S.; Kirkegaard, T.; Rohde, M.; Nylandsted, J.; Jaattela, M. *Cancer Cell* **2013,** 24, (3), 379-93.
65. Gulbins, E.; Kolesnick, R. N. *Cancer Cell* **2013,** 24, (3), 279-281.
66. Saftig, P.; Sandhoff, K. *Nature* **2013,** 502, (7471), 312-313.
67. Schulze, H.; Kolter, T.; Sandhoff, K. *Bba-Mol Cell Res* **2009,** 1793, (4), 674-683.
68. Davidsen, J.; Vermehren, C.; Frokjaer, S.; Mouritsen, O. G.; Jorgensen, K. *International Journal of Pharmaceutics* **2001,** 214, (1-2), 67-69.
69. Andresen, T. L.; Jorgensen, K. *Bba-Biomembranes* **2005,** 1669, (1), 1-7.
70. Foged, C.; Nielsen, H. M.; Frokjaer, S. *J Liposome Res* **2007,** 17, (3-4), 191-6.
71. Wang, H.; Tam, Y. Y.; Chen, S.; Zaifman, J.; van der Meel, R.; Ciufolini, M. A.; Cullis, P. R. *Mol Ther* **2016**.
72. Sandor, M.; Mehta, S.; Harris, J.; Thanos, C.; Weston, P.; Marshall, J.; Mathiowitz, E. *J Drug Target* **2002,** 10, (6), 497-506.
73. Mitragotri, S. L., T.; Bae, Y.H.;, Schwendeman, S.; De Smedt, S.C.; Leroux, J.C.; Peer, D.; Kwon, I.C.; Harashima, K.; Kikuchi, A.; Oh, Y.K.; Torchilin, V.; Hennink, W.; Hanes, J.; Park, K. *J Control Release* **2017**.
74. Lammers, T.; Kiessling, F.; Ashford, M.; Hennink, W.; Crommelin, D.; Storm, G. *Nat Rev Mater* **2016,** 1, (9).
75. Raemdonck, K.; De Smedt, S. C. *Nat Biotechnol* **2015,** 33, (10), 1026-7.
76. Anselmo, A. C.; Mitragotri, S. *AAPS J* **2015,** 17, (5), 1041-54.
77. Chinen, A. B.; Guan, C. M.; Ferrer, J. R.; Barnaby, S. N.; Merkel, T. J.; Mirkin, C. A. *Chemical reviews* **2015,** 115, (19), 10530-74.

78. Research, G. V. *Healthcare Nanotechnology (Nanomedicine) Market Analysis By Application (Drug Delivery System, Molecular Diagnostics, Clinical Oncology, Clinical Neurology, Clinical cardiology, Anti-inflammatory, Anti-infective) And Segment Forecasts To 2020*; 978-1-68038-039-2; 2014.
79. Kim, T.; Hyeon, T. *Nanotechnology* **2014,** 25, (1).
80. Bobo, D.; Robinson, K. J.; Islam, J.; Thurecht, K. J.; Corrie, S. R. *Pharm Res* **2016,** 33, (10), 2373-87.
81. Min, Y.; Caster, J. M.; Eblan, M. J.; Wang, A. Z. *Chemical reviews* **2015,** 115, (19), 11147-90.
82. Hofmann-Amtenbrink, M.; Grainger, D. W.; Hofmann, H. *Nanomedicine : nanotechnology, biology, and medicine* **2015,** 11, (7), 1689-94.
83. Canfarotta, F.; Piletsky, S. A. *Adv Healthc Mater* **2014,** 3, (2), 160-175.
84. Tanoura, T.; Bernas, M.; Darkazanli, A.; Elam, E.; Unger, E.; Witte, M. H.; Green, A. *AJR. American journal of roentgenology* **1992,** 159, (4), 875-81.
85. Johnson, W. K.; Stoupis, C.; Torres, G. M.; Rosenberg, E. B.; Ros, P. R. *Magnetic resonance imaging* **1996,** 14, (1), 43-9.
86. Rinck, P. A.; Smevik, O.; Nilsen, G.; Klepp, O.; Onsrud, M.; Oksendal, A.; Borseth, A. *Radiology* **1991,** 178, (3), 775-9.
87. Wang, Y. X. J. *World J Gastroentero* **2015,** 21, (47), 13400-13402.
88. Spinowitz, B. S.; Kausz, A. T.; Baptista, J.; Noble, S. D.; Sothinathan, R.; Bernardo, M. V.; Brenner, L.; Pereira, B. J. *J Am Soc Nephrol* **2008,** 19, (8), 1599-605.
89. Hetzel, D.; Strauss, W.; Bernard, K.; Li, Z.; Urboniene, A.; Allen, L. F. *Am J Hematol* **2014,** 89, (6), 646-50.
90. Thiesen, B.; Jordan, A. *Int J Hyperther* **2008,** 24, (6), 467-474.
91. Maier-Hauff, K.; Ulrich, F.; Nestler, D.; Niehoff, H.; Wust, P.; Thiesen, B.; Orawa, H.; Budach, V.; Jordan, A. *J Neurooncol* **2011,** 103, (2), 317-24.
92. Sanders, M. *J Rheumatol* **2000,** 27, (2), 523-529.
93. Kean, W. F.; Kean, I. R. *Inflammopharmacology* **2008,** 16, (3), 112-25.
94. Libutti, S. K.; Paciotti, G. F.; Byrnes, A. A.; Alexander, H. R.; Gannon, W. E.; Walker, M.; Seidel, G. D.; Yuldasheva, N.; Tamarkin, L. *Clinical Cancer Research* **2010,** 16, (24), 6139-6149.
95. Stern, J. M.; Stanfield, J.; Kabbani, W.; Hsieh, J. T.; Cadeddu, J. A. *J Urol* **2008,** 179, (2), 748-53.
96. Paithankar, D.; Hwang, B. H.; Munavalli, G.; Kauvar, A.; Lloyd, J.; Blomgren, R.; Faupel, L.; Meyer, T.; Mitragotri, S. *Journal of controlled release : official journal of the Controlled Release Society* **2015,** 206, 30-6.
97. Phillips, E.; Penate-Medina, O.; Zanzonico, P. B.; Carvajal, R. D.; Mohan, P.; Ye, Y. P.; Humm, J.; Gonen, M.; Kalaigian, H.; Schoder, H.; Strauss, H. W.; Larson, S. M.; Wiesner, U.; Bradbury, M. S. *Sci Transl Med* **2014,** 6, (260).
98. Marill, J.; Anesary, N. M.; Zhang, P.; Vivet, S.; Borghi, E.; Levy, L.; Pottier, A. *Radiat Oncol* **2014,** 9.
99. Bonvalot, S.; Le Pechoux, C.; De Baere, T.; Kantor, G.; Buy, X.; Stoeckle, E.; Terrier, P.; Sargos, P.; Coindre, J. M.; Lassau, N.; Ait Sarkouh, R.; Dimitriu, M.; Borghi, E.; Levy, L.; Deutsch, E.; Soria, J. C. *Clinical cancer research : an official journal of the American Association for Cancer Research* **2016**.
100. Xiong, R. H.; Joris, F.; Liang, S. Y.; De Rycke, R.; Lippens, S.; Demeester, J.; Skirtach, A.; Raemdonck, K.; Himmelreich, U.; De Smedt, S. C.; Braeckmans, K. *Nano letters* **2016,** 16, (10), 5975-5986.
101. Guarnieri, D.; Sabella, S.; Muscetti, O.; Belli, V.; Malvindi, M. A.; Fusco, S.; De Luca, E.; Pompa, P. P.; Netti, P. A. *Nanoscale* **2014,** 6, (17), 10264-10273.
102. Petters, C.; Thiel, K.; Dringen, R. *Nanotoxicology* **2016,** 10, (3), 332-42.
103. Soenen, S. J.; Parak, W. J.; Rejman, J.; Manshian, B. *Chemical reviews* **2015,** 115, (5), 2109-35.
104. Donaldson, K.; Stone, V.; Tran, C. L.; Kreyling, W.; Borm, P. J. *Occup Environ Med* **2004,** 61, (9), 727-8.

105. OECD, OECD GUIDELINE FOR THE TESTING OF CHEMICALS. In *In Vitro Skin Irritation: Reconstructed Human Epidermis Test Method*, 2010; Vol. OECD TG 439.
106. OECD, OECD GUIDELINE FOR THE TESTING OF CHEMICALS. In *Acute Eye Irritation/Corrosion*, 2002; Vol. OECD TG 405.
107. OECD, DRAFT OECD GUIDELINE FOR THE TESTING OF CHEMICALS. In *Test Guideline 453: Combined Chronic Toxicity\Carcinogenicity Studies*, 2008; Vol. OECD TG 453.
108. OECD, DRAFT OECD GUIDELINE FOR THE TESTING OF CHEMICALS. In *Test Guideline 451: Carcinogenicity Studies*, 2008; Vol. OECD TG 451.
109. Nijhara, R.; Balakrishnan, K. *Nanomedicine : nanotechnology, biology, and medicine* **2006,** 2, (2), 127-36.
110. Joris, F.; Manshian, B. B.; Peynshaert, K.; De Smedt, S. C.; Braeckmans, K.; Soenen, S. J. *Chem Soc Rev* **2013,** 42, (21), 8339-8359.
111. Pampaloni, F.; Reynaud, E. G.; Stelzer, E. H. *Nature reviews. Molecular cell biology* **2007,** 8, (10), 839-45.
112. Zhang, H.; Pokhrel, S.; Ji, Z.; Meng, H.; Wang, X.; Lin, S.; Chang, C. H.; Li, L.; Li, R.; Sun, B.; Wang, M.; Liao, Y. P.; Liu, R.; Xia, T.; Madler, L.; Nel, A. E. *Journal of the American Chemical Society* **2014,** 136, (17), 6406-20.
113. Kim, Y. H.; Boykin, E.; Stevens, T.; Lavrich, K.; Gilmour, M. I. *J Nanobiotechnology* **2014,** 12, 47.
114. Rushton, E. K.; Jiang, J.; Leonard, S. S.; Eberly, S.; Castranova, V.; Biswas, P.; Elder, A.; Han, X.; Gelein, R.; Finkelstein, J.; Oberdorster, G. *Journal of toxicology and environmental health. Part A* **2010,** 73, (5), 445-61.
115. Chortarea, S.; Clift, M. J.; Vanhecke, D.; Endes, C.; Wick, P.; Petri-Fink, A.; Rothen-Rutishauser, B. *Nanotoxicology* **2015,** 9, (8), 983-93.

APPENDIX A

Supporting information to Chapter 6 &7.

Table of contents

1. MATERIALS & METHODS

1.1. Nanoparticle (NP) synthesis

1.1.1. AuNP synthesis

The synthesis of gold nanoparticles (AuNPs) was performed according to previously reported protocols [1, 2]. First, 0.300 g of the aqueous gold precursor, chloroauric acid ($HAuCl_4$, Alfa Aesar, USA), was dissolved in 35 mL Milli-Q water. 80 mL of a 27.125 mg/mL tetraoctylammonium bromide (TOAB, Sigma-Aldrich, USA) solution in toluene was added and the mixture was vigorously stirred during 5 minutes to ensure gradual transfer of the $AuCl_4^-$ ions from the aqueous to the organic phase.

$$N(C_8H_{17})_4^+{}_{organic} + AuCl_4^-{}_{aqueous} \longrightarrow N(C_8H_{17})_4^+AuCl_4^-{}_{organic}$$

After carefully discarding the aqueous solution and transferring the organic phase to a 250 mL round bottom flask, 25 mL of a 13.36 mg/mL sodium borohydride ($NaBH_4$, Roth, Germany) solution was added drop-wise under vigorous stirring. This caused an immediate reduction of the gold precursor, which could be observed by a color shift from light orange to dark purple.

$$AuCl_4^-{}_{organic} \xrightarrow{+3\,e^-} Au_{organic} + 4 \cdot Cl^-_{aqueous}$$

Following one hour of additional stirring to allow complete reduction of the remaining Au^+ ions, the solution was transferred to a separation funnel. Here, the resulting AuNPs were washed under vigorous shaking with 25 mL 0.01 M HCl to remove the excess $NaBH_4$. After removal of the aqueous solution the same procedure was repeated with 25 mL 0.01 M NaOH (Roth, Germany) in order to eliminate the remaining acid. Finally, the AuNPs were washed up to four times with Milli-Q water to dispose residual salts created in the previous washing steps. In the interest of obtaining a thermodynamically stable size distribution, the obtained dispersion was stirred overnight to allow the Ostwald ripening process to take place. Next, 10 mL of the surfactant 1-dodecanethiol was added and the resulting mixture was placed at 65 °C for 3 hours to allow the attachment of the 1-dodecanethiol ligand to the AuNP surface. This occurred *via* the high affinity of the thiol groups for the AuNP surface, thereby replacing the residual Br^- ions. Subsequently, large agglomerates were removed by

centrifuging at 1000 rpm, followed by precipitation *via* methanol addition and a second centrifugation step at 1000 rpm to obtain the AuNP precipitate. This precipitate, containing dodecanethiol-coated AuNPs, was dispersed in chloroform and stored at room temperature until further use.

1.1.2. AgNP synthesis

Silver nanoparticles (AgNPs) were synthesized as previously reported [3,4]. First, the stabilizer sodium S-dodecylthiosulfate, was synthesized by adding 25 mmol sodium thiosulfate pentahydrate (Sigma-Aldrich, USA) in Milli-Q water to a solution of 25 mmol 1-bromododecane (Sigma-Aldrich, USA) in 50 mL ethanol, which was prepared at 50 °C. This solution was stirred and refluxed at 50 °C for 3 hours after which it was kept at 4 °C overnight. A white precipitate was formed and isolated *via* filtration and vacuum drying.

In order to synthesize the AgNPs, 1.68 mmol $AgNO_3$ (Aldrich, USA) was added to 1.26 mmol of sodium S-dodecylthiosulfate that was previously dissolved in ethanol at 50 °C. This mixture was stirred for 10 minutes, during which the solution became light brown. Next, a solution of 8.4 mmol $NaBH_4$ in 15 mL ethanol was added. As the Ag^+ ions were reduced by $NaBH_4$, a coating of the dodecylthiol ligand was formed around the AgNPs, which was visibly detected by the glooming of the dispersion into a dark brown shade. After a 5 minute incubation period, 0.42 mmol ascorbic acid (Sigma-Aldrich, USA) was added and the resulting dispersion was stirred for 3 hours. Next, the sample was slowly cooled down to room temperature and the resulting AgNPs were collected *via* centrifugation (15 minutes at 3000 rpm). After being washed with Milli-Q water, ethanol and acetone, the AgNPs were dried under vacuum and conserved dried until further use.

1.1.3. IONP synthesis

Iron oxide nanoparticles (IONPs) were synthesized according to the method described by Sun *et al.* [5]. In short, 2 mmol of the metal precursor, iron (III) acetylacetonate $Fe(acac)_3$ (Sigma-Aldrich, USA), was mixed with 10 mmol 1,2-hexadecanediol (Chemos GmbH, Germany) in the presence of 6 mmol oleic acid (Sigma-Aldrich, USA), 6 mmol oleylamine (Aldrich, USA) and 20 mL phenyl ether (Sigma-Aldrich, USA). The resulting mixture was stirred in water-free and oxygen-free conditions and consequently heated up to 200 °C during 30 minutes. Next, the temperature was increased to 265 °C for an additional 30

minutes. During the heating $Fe(acac)_3$ was reduced to IONPs *via* thermal decomposition, with 1,2-hexadecanediol acting as a reducing agent. Oleic acid and oleylamine were in turn applied as surfactants to stabilize the particles during the decomposition process. The resulting dispersion was slowly cooled down to room temperature and removed from the water- and oxygen-free glove box. Subsequently, 80 mL ethanol (Roth, Germany) was added, which resulted in the precipitation of a black NP powder that was separated *via* centrifugation at 4000 rpm for 40 minutes. Next, the NP powder was dissolved in 20 mL of an organic mixture consisting of hexane with 1 vol% oleic acid and 1 vol% oleylamine after which centrifugation during 30 minutes at 4000 rpm was applied to remove undispersed aggregates. Next, ethanol was added to the supernatant to precipitate the IONPs, which were concentrated in a third 30-minute centrifugation step at 4000 rpm. Finally, the resulting pellet was redispersed in hexane and stored until further use.

1.1.4. Synthesis of the amphiphilic polymer (PMA)

The amphiphilic polymer poly(isobutylene-*alt*-maleic anhydride)-graft-dodecyl (PMA), which is capable of transferring hydrophobic nanoparticles from an organic to an aqueous phase, was prepared according to a previously published protocol [6]. This polymer, of which the structure is depicted in Figure S1, consists of a poly(isobutylene-*alt*-maleic anhydride) hydrophilic backbone (6 kDa/mol, 531278, Sigma-Aldrich, USA) that has been modified with hydrophobic dodecylamine chains (D222208, Sigma-Aldrich, USA), which ensure linkage to the hydrophobic NPs. The dodecylamine chains were added in an amount that would ensure covalent binding with 75% of the anhydride rings of the poly(isobutylene-*alt*-maleic anhydride) *via* its amine groups. Note that covalent linkage is assumed, but not experimentally verified.

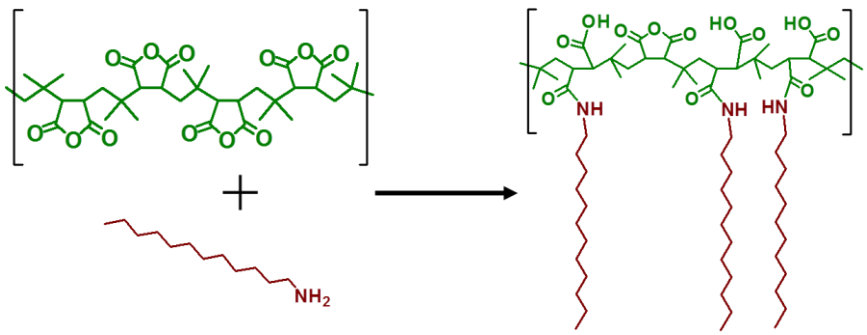

Figure S1. Structure of the amphiphilic poly(isobutylene-alt-maleic anhydride)-graft-dodecyl (PMA) with the green poly(isobutylene-alt-maleic anhydride) hydrophilic backbone and bordeaux hydrophobic dodecylamine chains.

In short a solution of 2.70 g (15 mmol) dodecylamine (Sigma-Aldrich, USA) in 100 mL tetrahydrofuran was added to 3.084 g (20 mmol monomer) of poly(isobutylene-*alt*-maleic anhydride) (Sigma-Aldrich, USA) powder in a round bottom flask. The resulting mixture was stirred until the solution became clear and subsequently heated to 60 °C under stirring conditions during two hours. Next, the solution was concentrated under vacuum to a final volume of approximately 40 mL, which was left at 55 °C under stirring conditions overnight. This volume decrease was necessary to allow the interaction between the anhydride rings and the amino groups. The following day the solution was dried and the powder was redispersed in 40 mL chloroform to a final concentration of 0.5 M.

1.1.5. Polymer coating of the NPs

The amount of PMA monomer required to coat the NP surface was determined *via* the following equation:

$$V_{polymer} = \frac{\pi \cdot d_{eff}^2 \cdot c_{NP} \cdot V_{NP} \cdot R_{p/area}}{c_{polymer}}$$

with d_{eff} being the effective diameter of the NP, which is defined as the sum of the NP core diameter (d_c) as determined by transmission electron microscopy (TEM), and two times the estimated thickness of the surfactant molecule layer (l_{surf} = 1.2 nm; $d_{eff} = d_c + 2 \bullet l_{surf}$).[6] c_{NP} and $c_{polymer}$ respectively correspond to the NP and the PMA monomer concentration. Each PMA molecule comprises on average 39 monomer units. The concentration determination of the NPs is explained in detail in section II.2. V_{NP} and $V_{polymer}$ stand for the volume of NP sample solution and polymer solution, respectively. $R_{p/area}$ refers to the amount of PMA monomers that have to be added per effective NP surface area in monomer units per nm^2 (in this study the value of 200 monomers PMA per nm^2 NP surface was used, which was experimentally optimized). The calculated volume $V_{polymer}$ was subsequently added to the preset amount of NPs in a 25 mL round bottom flask. Subsequent to the slow removal of the solvent under vacuum, 20 mL chloroform was added, which was repeated twice. After the third cycle, the dried PMA-coated NPs were dispersed in a 50 mM pH 12 sodium borate buffer (SBB 12). The opening of the anhydride rings and the origination of carboxylic groups in this basic environment ensured complete dispersion in an aqueous medium, as illustrated in Figure S2.

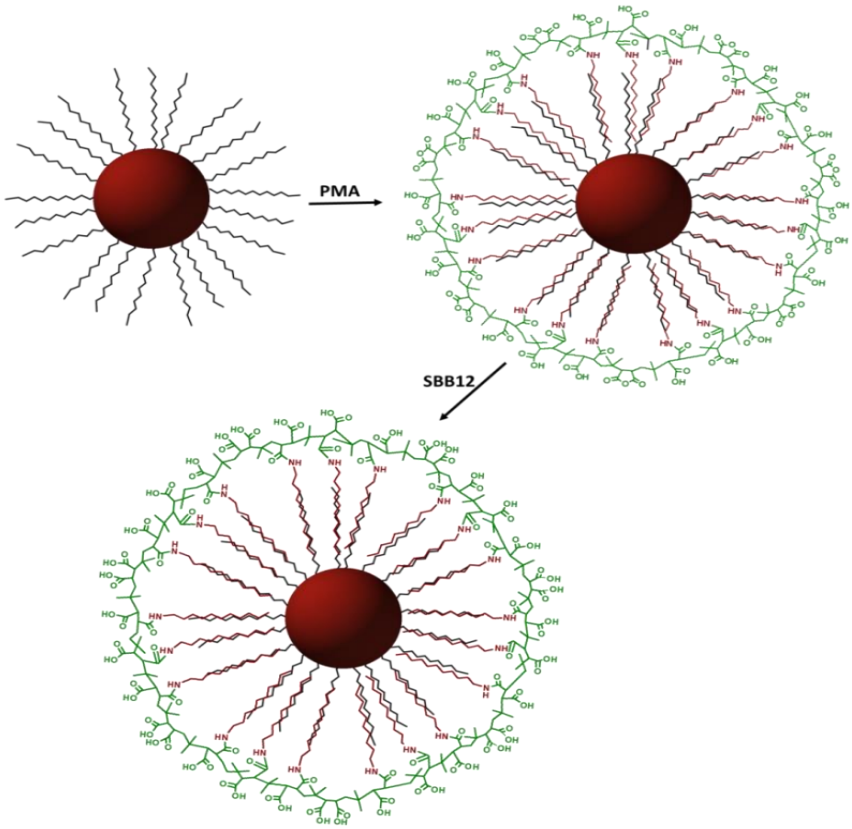

Figure S2. When the PMA polymer is added to the NPs, the dodecylamine chains (bordeaux) hydrophobically interact with the surfactant (black) on the NP surface. By adding sodium borohydrate buffer (pH = 12) the anhydride rings on the poly(isobutylene-maleic acid) backbone (green) are opened and carboxylic groups are formed. Hence, the NPs acquire hydrophilic properties and are transferred to the aqueous phase. [6]

1.1.6. Ligand coating of the IONPs

To coat the IONPs by the specific ligand of choice, in this case meso-2,3-dimercaptosuccinic acid (DMSA, #D7881, Sigma Aldrich, USA), a ligand exchange was performed, where the ligand applied during the IONP synthesis was replaced by DMSA. Hereto, 50 mg of the IONPs were dispersed in 10 mL chloroform. Subsequently, the IONPs were purified by the addition of 20 mL ethanol, vigorous shaking, and sonication during 3 minutes followed by a magnetic separation of the IONP aggregates.[7] After discarding the supernatant, the procedure was repeated until the supernatant became colorless. Consequently, the IONPs were dried under vacuum and redissolved in 20 mL toluene. Next, 90 mg DMSA was dissolved in 5 mL DMSO (#D4540, Sigma Aldrich, USA) to which the IONP dispersion in toluene was added. Following a 5-minute sonication of the resulting dispersion, it was left stirring on a rotary shaker for 4 days. During this period, the DMSA ligand was coupled to the IONP surface and the phase transfer took place. After 4 days, 2 phases could be distinguished in the sample: a black solid

phase containing the precipitated IONPs and a clear brownish supernatant. The latter was discarded and the IONPs were washed with 10 mL ethanol. Subsequently, the dispersion was placed in an ultrasonic bath and centrifuged at 9000 rpm during 20 minutes. These washing steps were repeated until the supernatant became colorless. Next, the IONPs were dried under vacuum. After redispersion in Milli-Q water, a heterogeneous dispersion was obtained that was homogenized by slowly raising the pH to 10 with diluted NaOH. Finally, a 3-day dialysis with a 50 kDa MWCO membrane was performed against Milli-Q water to remove the excess ligand and the sample was stored in Milli-Q water until further use.

1.1.7. Purification of the NPs

Subsequently the aqueous PMA-coated NP dispersions were concentrated by the use of centrifuge filters (100 kDa MWCO) for 30 minutes at 3000 rpm. Then, the NPs were injected in a 2% agarose gel in a Tris-Borate-EDTA buffer (TBE 0.5x) to remove empty polymer micelles from the samples *via* gel electrophoresis [8]. Before injection, a mixture of glycerol and orange G in a 1:8 proportion (v:v, glycerol + orange G solution: PMA-coated NPs) was added to improve injection into the wells of the gel (*i.e.* due the viscosity of glycerol) and to allow spotting of the front of the samples while running through the gel (*i.e.* due to the color of orange G). Once the gel was placed in the tray of the electrophoresis set-up and fully covered with TBE 0.5X, the NP samples were injected in the well and an electric field of 15 V/cm was applied during 60 minutes. The resulting NP bands on the gel (Figure S3 & S4) were cut away and transferred to a dialysis membrane (50 kDa molecular weight cut-off (MWCO)) with fresh TBE 0.5X. By applying the electric field for an additional 20 minutes the NPs were transferred out of the gel pieces into the TBE 0.5X solution. Subsequently, they were collected and washed 5 times *via* centrifugation at 3000 rpm for 20 minutes using centrifuge filters with 100 kDa MWCO membranes and Milli-Q water to remove the salts from TBE 0.5X solution. Finally, the NP dispersions were filtered with 0.2 µm syringe filter and stored in Milli-Q water until further use. Note that in our hands gel electrophoresis has so far turned out to be the best option to remove empty PMA micelles from PMA-coated NPs. However, some residual PMA micelles as impurities in the NP samples cannot be excluded.

Figure S3. Image of a gel in which AuNPs, AgNPs and IONPs had been run with gel electrophoresis. (1) 10 nm phosphine-coated AuNPs used as a control, (2) PMA-coated AuNPs, (3) PMA-coated AgNPs and (4) PMA-coated IONPs after 1 hour gel electrophoresis in a 2% agarose gel [9]. The yellow band corresponds to the loading buffer orange G used as gel front line. Due to their negative charge the NPs run towards the plus pole.

Figure S4: Image of (1) PMA-coated IONPs and (2) DMSA-coated IONPs after 1h of gel electrophoresis in a 2% agarose gel.[9]

2. RESULTS

2.1. Nanoparticle characterization

2.1.1. Transmission electron microscopy (TEM)

With the aim of obtaining the inorganic core diameter (d_c) of each batch of NPs, transmission electron microscopy (TEM) measurements were performed using a Jeol JEM3010. First, a drop of each NP sample (as dissolved in chloroform, *i.e.* before the PMA

coating) was added to a TEM grid and slowly dried. Finally, pictures were recorded and analyzed using Image J to obtain a d_c histogram of each sample (Figure S4). For all three NP samples a mean core diameter of d_c = 3.8 nm was achieved. Note that core diameters with exactly the same mean value of the 3 different NP types were obtained by chance (*i.e.* our synthesis does not allow to tune the NP diameter with a tenth of nm precise) and the values have to be seen in respect to the relatively broad size distributions (Figure S5).

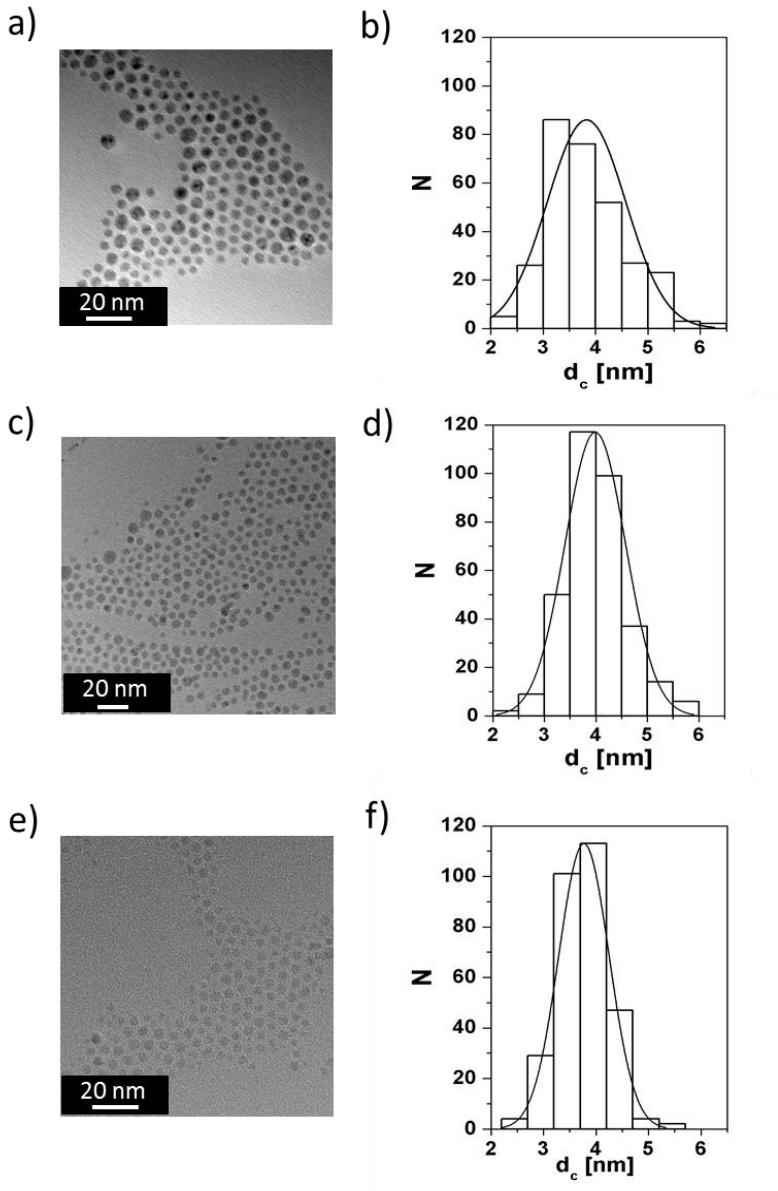

Figure S5. TEM images of (a) AuNPs, (c) AgNPs, and (e) IONPs, and the corresponding size distribution histograms N(d_c) (respectively (b), (d) and (f)). For all NPs a mean d_c of 3.8 nm was obtained. Note that due to the width of the bars in the histograms the accuracy in the determination of the d_c is limited to 0.5 nm. For TEM pictures, the scale bar corresponds to 20 nm.

2.1.2. Inductively coupled plasma mass spectrometry (ICP-MS)

The concentrations of the prepared NP dispersions were measured *via* inductively coupled plasma mass spectrometry (ICP-MS, 7700 Series ICP-MS from Agilent Technologies). For concentration determination, the aqueous samples were mixed with aqua regia (1:10, $V_{aqua\ regia}$: V_{NP}) and subsequently incubated at room temperature for 3 hours. These mixtures were further diluted 1:10 ($V_{mixture}$: V_{HCl}) in 2% HCl in water and the elemental concentrations (c_M) of the metals Au, Ag, and Fe were measured directly with ICP-MS. Subsequently the elemental metal concentrations (*i.e.* Au, Ag, or Fe) were converted into NP concentrations (c_{NP}). For this purpose the mass of a single NP core (m_{NP}) was first calculated *via* the equation below:

$$m_{NP} = \rho_M \cdot V_{c,NP}$$

in which ρ_M corresponds to the theoretical density of the NP core material (being 19.3 g/cm^3 for gold; 10.49 g/cm^3 for silver; and 5.18 g/cm^3 for iron oxide) and $V_{c,NP}$ refers to the volume of one NP core: $V_{NP}=(4/3)\cdot\pi\cdot(d_c/2)^3$. The molar NP concentration (c_{NP}) of the NP samples [mol/L] was obtained by dividing the elemental mass concentration [g/L] of the metals as obtained by ICP-MS (c_M) by the mass of one mole of NPs (referred as the Avogadro constant, N_A multiplied by the mass of a single core NP, m_{NP}). An additional factor F was added to the equation. For both pure metal nanoparticles (AuNPs and AgNPs) F corresponds to one. In the case of IONPs, F is the ratio of the molecular weight of iron oxide (231.53 g/mol) and the multiplication of the molecular weight of iron (55.84 g/mol) and the molar conversion factor 3 (3 moles of Fe per mol of Fe_3O_4). Thus for the IONPs the value of F is 1.38 (F=231.53/(55.84·3)=1.38).

$$c_{NP} = \frac{c_M}{m_{NP} \cdot N_A} \cdot F$$

The concentrations of the NP stock dispersions as determined by ICP-MS can be found in Table S1.

Table S1. NP dispersion concentration as determined *via* ICP-MS.

	C_{NP} [μM]
PMA-AuNPs	1.0432
PMA-AgNPs	2.0711
PMA-IONPs	4.2363
DMSA-IONPs	6.022

2.1.3. UV/Vis absorption spectroscopy

UV/Vis absorption spectra were recorded with an Agilent 8453 UV-visible Spectroscopy System, which allowed the identification of the surface plasmon resonance (SPR) peaks for the AuNPs and AgNPs in Milli-Q water (cf. Figure S6). As expected, the data depicted in Figure S6 show that surface plasmon peaks were found in the AuNP and AgNP samples around 517 nm and 430 nm, respectively, while no peak was observed in the IONP absorption spectrum.

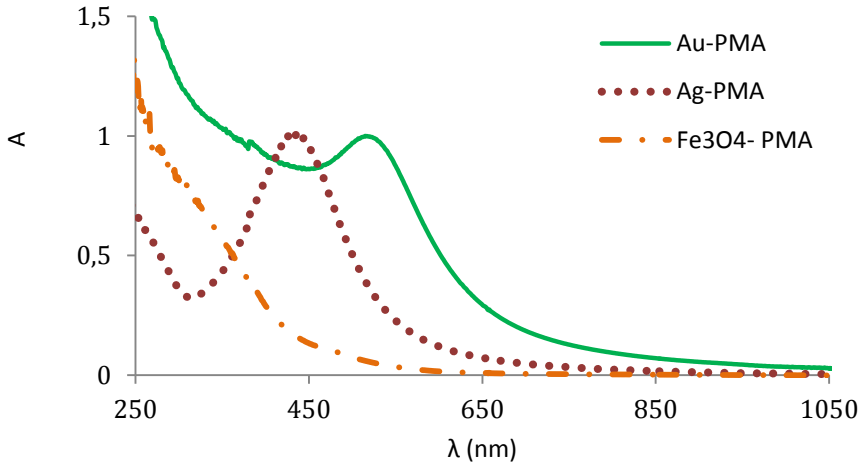

Figure S6. UV/Vis absorption spectra of the various NP dispersions in Milli-Q water.

Figure S7 shows that the coating did not have a major influence on the spectral properties since a good spectral overlap is observed for the differently coated IONPs.

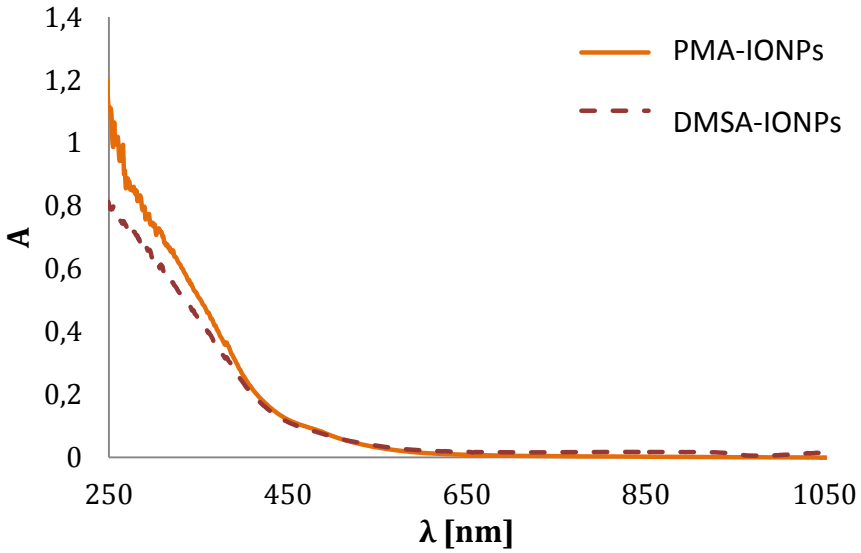

Figure S7: UV/Vis absorption spectra of the different IONPs in Milli-Q water dispersions.

For further characterization, series of minimum 4 dilutions were prepared for each NP type and analyzed with both UV/Vis absorption spectroscopy and ICP-MS, in order to experimentally determine of the extinction coefficients (ε_{NP}) of the NPs (Table S2). For AuNPs and AgNPs UV/Vis absorption measurements were performed at the SPR peak wavelength, namely 517 nm and 430 nm respectively, while a wavelength of 450 nm was selected for the IONPs. The ε_{NP} were retrieved from the slopes of the linear fittings of the molar NP concentrations (c_{NP}), as determined *via* ICP-MS (Table S1), and absorption values (A) measured in the same sample (with a cuvette of l = 1 cm path length). The linear fittings and ε_{NP} values can be found in Figure S8 and Table S2, respectively.

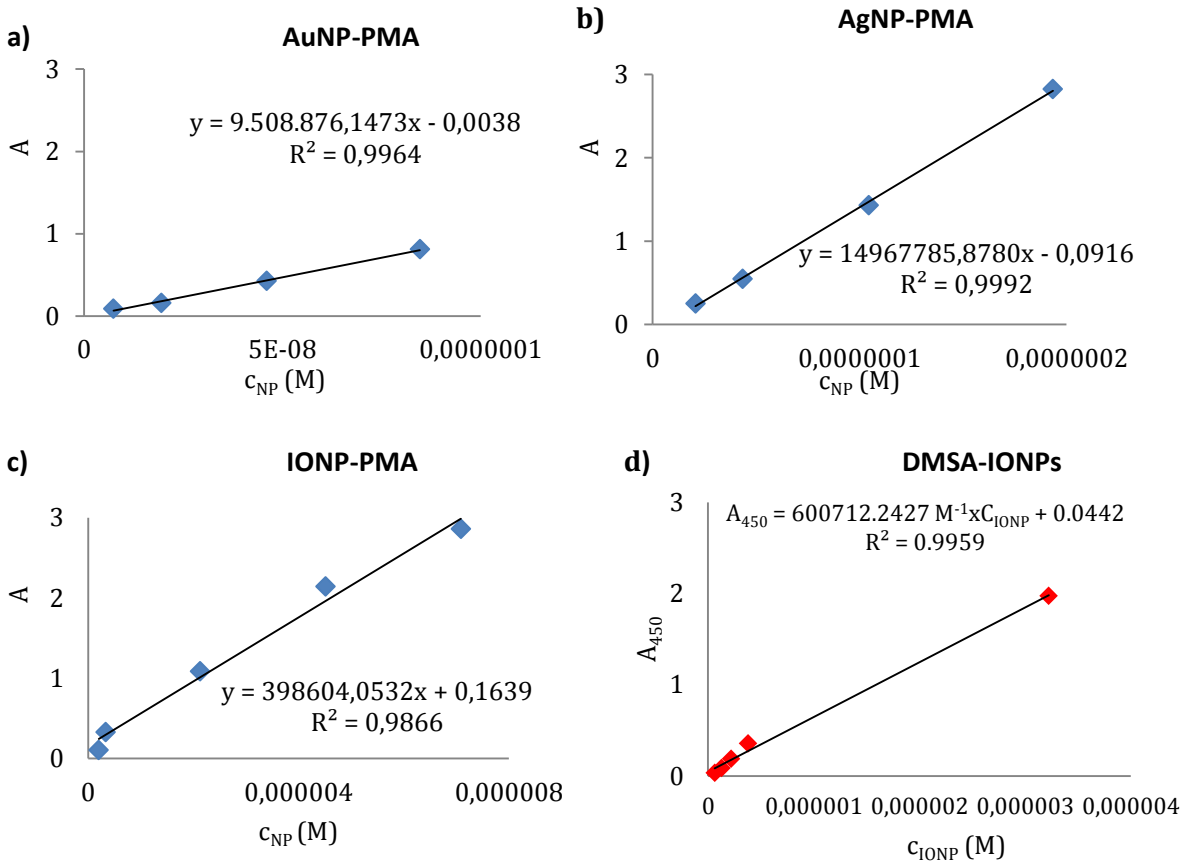

Figure S8. Linear fitting of NP absorbance measured at 517 nm, 430 nm, and 450 nm for the AuNPs, AgNPs, and IONPs, respectively, versus the molar concentration for different NP dispersion dilutions. According to the Lambert Beer law the slope $A/(c_{NP} \bullet 1cm) = \varepsilon_{NP}$ represents the ε_{NP} value for (a) AuNPs, (b) AgNPs, (c) PMA-IONPs and (d) DMSA-IONPs. R^2 is the coefficient of determination of the linear regression fit, which is an indication of the quality of the fit.[10]

Table S2: ε_{NP} values for the different NPs.

	ε_{NP} [$M^{-1}cm^{-1}$]
PMA-AuNPs	9510000
PMA-AgNPs	15000000
PMA-IONPs	398000
DMSA-IONPs	600000

2.1.4. Dynamic light scattering (DLS) and laser Doppler anemometry (LDA)

The NP hydrodynamic diameter (d_h) was measured *via* dynamic light scattering (DLS), while the zeta potential was measured *via* laser Doppler anemometry (LDA). Both measurements were performed in a Zetasizer Nano ZS (Malvern Instruments). The samples were filtered and diluted to a concentration of 10 nM in Milli-Q water. Samples were then equilibrated for 2-5 minutes at 25 °C to avoid interferences in NP movement due to temperature gradients. Measurements were performed in triplicates and the results are shown as the mean ± standard deviation (SD).

2.2. Cell-NP interactions

2.2.1. Cell morphology

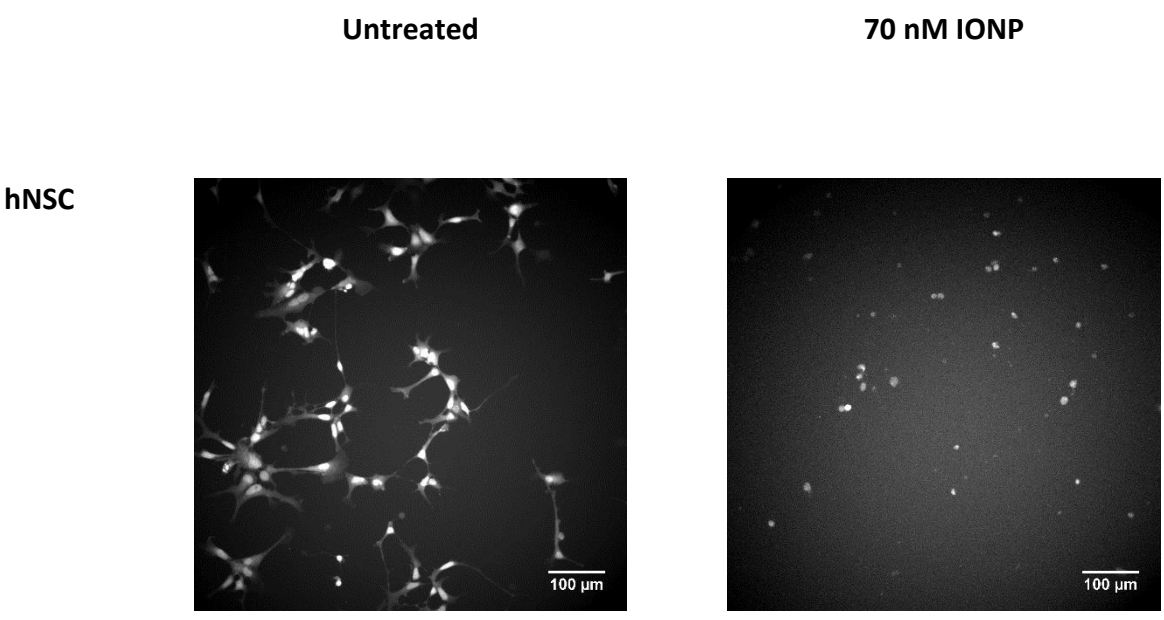

mNSC

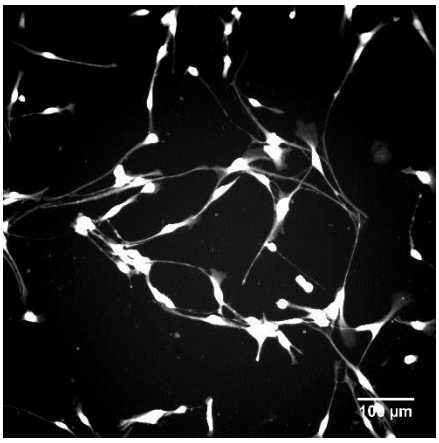

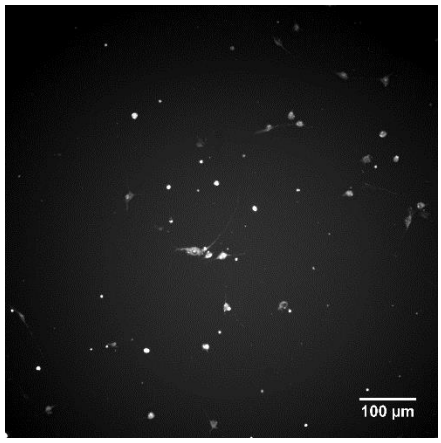

ReNcell

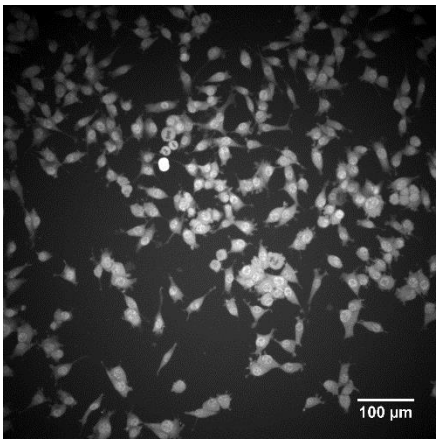

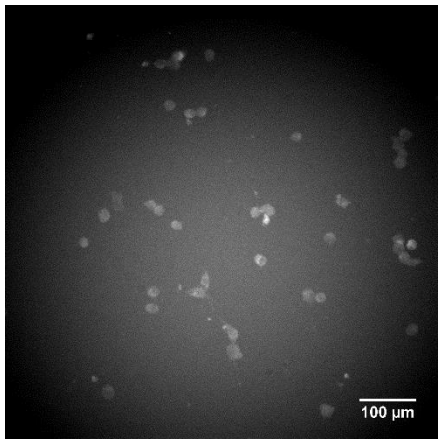

C17.2

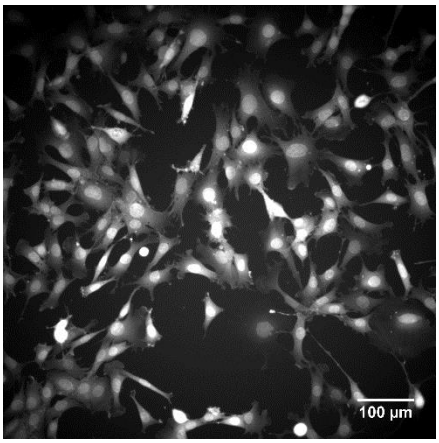

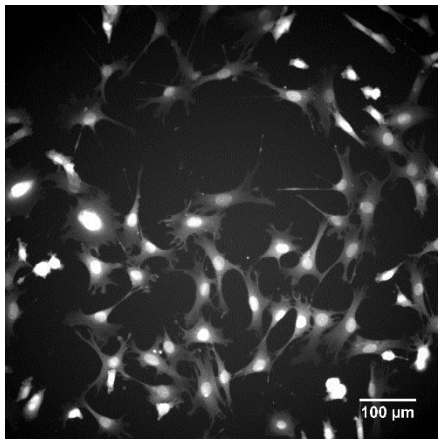

LA-N-2

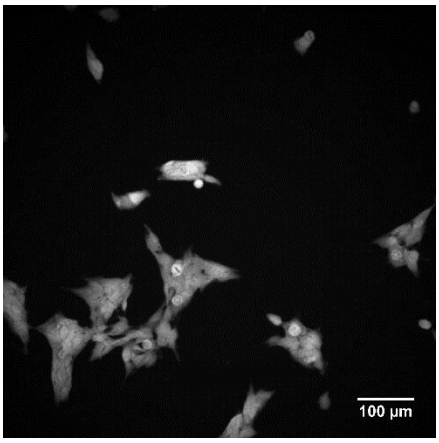

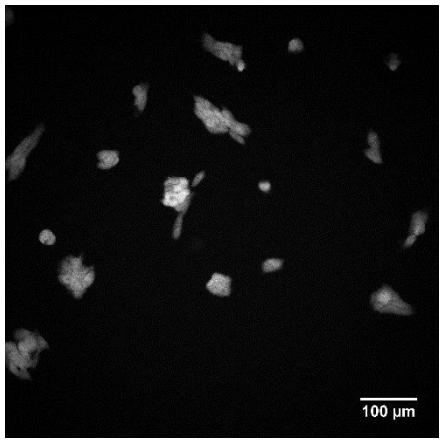

Neuro-2a

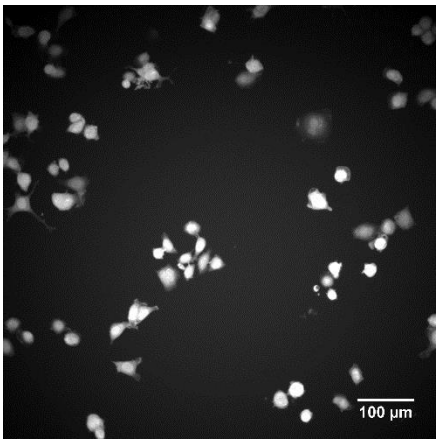

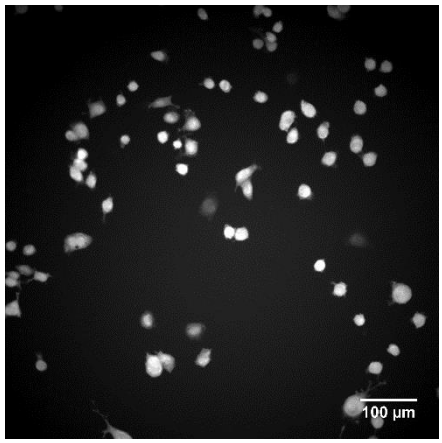

REFERENCES

1. Sperling, R. A.; Pellegrino, T.; Li, J. K.; Chang, W. H.; Parak, W. J. Electrophoretic Separation of Nanoparticles with a Discrete Number of Functional Groups. *Adv Funct Mater* 2006, 16, 943-948.
2. Brust, M.; Walker, M.; Bethell, D.; Schiffrin, D. J.; Whyman, R. Synthesis of Thiol-Derivatized Gold Nanoparticles in a 2-Phase Liquid-Liquid System. *J Chem Soc Chem Comm* 1994, 801-802.
3. Mari, A.; Imperatori, P.; Marchegiani, G.; Pilloni, L.; Mezzi, A.; Kaciulis, S.; Cannas, C.; Meneghini, C.; Mobilio, S.; Suber, L. High Yield Synthesis of Pure Alkanethiolate-Capped Silver Nanoparticles. *Langmuir : the ACS journal of surfaces and colloids* 2010, 26, 15561-15566.
4. Caballero-Diaz, E.; Pfeiffer, C.; Kastl, L.; Rivera-Gil, P.; Simonet, B.; Valcarcel, M.; Jimenez-Lamana, J.; Laborda, F.; Parak, W. J. The Toxicity of Silver Nanoparticles Depends on Their Uptake by Cells and Thus on Their Surface Chemistry. *Part Part Syst Char* 2013, 30, 1079-1085.
5. Sun, S.; Zeng, H.; Robinson, D. B.; Raoux, S.; Rice, P. M.; Wang, S. X.; Li, G. Monodisperse Mfe2o4 (M = Fe, Co, Mn) Nanoparticles. *Journal of the American Chemical Society* 2004, 126, 273-9.
6. Lin, C. A.; Sperling, R. A.; Li, J. K.; Yang, T. Y.; Li, P. Y.; Zanella, M.; Chang, W. H.; Parak, W. J. Design of an Amphiphilic Polymer for Nanoparticle Coating and Functionalization. *Small* 2008, 4, 334-41.
7. Mejias, R.; Gutierrez, L.; Salas, G.; Perez-Yague, S.; Zotes, T. M.; Lazaro, F. J.; Morales, M. P.; Barber, D. F. Long Term Biotransformation and Toxicity of Dimercaptosuccinic Acid-Coated Magnetic Nanoparticles Support Their Use in Biomedical Applications. *Journal of controlled release : official journal of the Controlled Release Society* 2013, 171, 225-33.
8. Fernandez-Arguelles, M. T.; Yakovlev, A.; Sperling, R. A.; Luccardini, C.; Gaillard, S.; Medel, A. S.; Mallet, J. M.; Brochon, J. C.; Feltz, A.; Oheim, M*., et al.* Synthesis and Characterization of Polymer-Coated Quantum Dots with Integrated Acceptor Dyes as Fret-Based Nanoprobes. *Nano letters* 2007, 7, 2613-7.
9. Pellegrino, T.; Sperling, R. A.; Alivisatos, A. P.; Parak, W. J. Gel Electrophoresis of Gold-DNA Nanoconjugates. *Journal of biomedicine & biotechnology* 2007, 2007, 26796.
10. Joris, F.; Valdeperez, D.; Pelaz, B.; Soenen, S. J.; Manshian, B. B.; Parak, W. J.; De Smedt, S. C.; Raemdonck, K. The Impact of Species and Cell Type on the Nanosafety Profile of Iron Oxide Nanoparticles in Neural Cells. *J Nanobiotechnology* 2016, 14, 69.

SUMMARY & CONCLUSION

Nanotechnology is one of the key enabling technologies of the 21st century. Various inorganic and organic materials show unique properties when engineered at the nanoscale, which opens up a myriad of novel applications. In the context of medicine, organic nanoparticles (NP) are often applied as carriers for insoluble drugs or macromolecules, such as nucleic acids (NA). The latter require packaging into a nanocarrier to ensure transportation to the target tissue and cellular internalization, while maintaining their functionality. In this regard, both viral and non-viral vectors were explored in parallel. Non-viral delivery vehicles are considered relatively safe but generally fall short in terms of transfection efficiency given the many extra- and intracellular barriers limiting NA delivery. At the intracellular level, endosomal escape is regarded to be the major bottleneck. Even for state-of-the-art carriers, a minor fraction of the internalized NA dose escapes to the cytosol whereas the bulk of the NA cargo is trafficked to the lysosomal compartment for degradation. Hence, current strategies aim to improve endosomal escape from the early or late endosomal compartment to avoid lysosomal entrapment. In contrast to this paradigm, we set out to specifically target the lysosomes to induce release of the accumulated NA cargo. In particular, we aimed to improve the cytosolic delivery of small interfering (si)RNA upon nanogel (NG)-mediated transfection using approved low molecular weight drugs, namely cationic amphiphilic drugs (CADs), which functionally inhibit acid sphingomyelinase (FIASMA). A general introduction into the use of siRNA to trigger the RNA interference pathway, nanogels as non-viral nanocarriers and FIASMAs as lysosomal delivery enhancers is provided in **Chapter 1**.

Since the early days of plasmid (p)DNA delivery through lipid-based nanocarriers, scientists explored the use of small molecules to boost the delivery potential. Our literature study **(Chapter 2)** revealed adjuvants can enhance tumor penetration or cellular internalization. In turn, some adjuvants boost endosomal escape, alter intracellular trafficking or directly promote the transgene expression of successfully delivered pDNA. Several small molecules can furthermore improve the transfection efficiency by reducing the innate immune response or facilitating pDNA nuclear entry. Finally, pleiotropic molecules such as

chloroquine, dexamethasone and other steroids, improve NA transfection by simultaneously influencing various delivery-related processes. Overall, this overview underscores the diversity small molecular adjuvant approaches to stimulate NA delivery. Of note, the activity of several adjuvants is limited to specific NA and/or nanocarriers and the moment of the adjuvant treatment relative to the transfection. Hence, further insights into nanocarrier uptake, intracellular trafficking and endosomal escape should allow to rationally combine adjuvants, NA and carriers in the future.

The data presented in **Chapter 3** show that the FIASMAs induce the accumulation of phospholipids, cholesterol and sphingomyelin. This transient phospholipidosis (PLD) phenotype was suggested to reduce the lysosomal membrane stability, leading to enhanced transfer of siRNA from the lysosomes into the cytosol. Of note, this assumed improved siRNA delivery drastically enhanced the gene silencing potential of the siRNA-loaded NGs. In addition, we showed that the lysosomes could be applied as a depot for prolonged and controlled siRNA release, underscoring the great potential of the CAD adjuvant approach. In **Chapter 4** we explored the broader applicability of this adjuvant strategy. First, we showed that the induction of PLD through mechanisms other than acid sphingomyelinase inhibition, does not necessarily improve siRNA delivery. In turn, distinct adjuvants might too greatly affect the lysosomal membrane stability wherefore the stimulated cytosolic siRNA release coincides with significant cytotoxicity. In addition, messenger (m)RNA delivery could not to a similar extent be improved and the delivery of siRNA by lipid-based transfection reagents was less prone to the FIASMA adjuvant effect.

In conclusion, we showed that a sequential FIASMA treatment is able to markedly improve the therapeutic potential of siRNA-loaded NGs. However, this effect was both carrier- and NA-dependent since neither mRNA delivery nor transfection by lipid-based carriers could equally be enhanced. Research on the subject could be continued by identifying more potent adjuvants through large-scale compound screenings. A more detailed elucidation of the cellular FIASMA effects will in turn clarify to which subgroup of NA and carriers this method can be applied. Finally, the co-inclusion of the FIASMA and NA into the nanocarrier or the synthesis of FIASMA-NA conjugates should be explored.

In addition to the use of organic nanocarriers as delivery vehicles for NA, inorganic NPs are being explored in a biomedical setting, with their unique properties allowing improvements to current detection and/or treatment strategies or the development of novel biomedical applications. Iron oxide (IO)NPs for instance allow magnetism-guided delivery, magnetic resonance imaging (MRI) and cancer treatment through hyperthermia. Despite extensive proof-of-concept studies, few inorganic NPs are currently clinically applied, which can largely be attributed to their elusive safety profiles given the inconsistent nanotoxicity data. **Chapter 5** summarizes cell-NP interactions suggested to elicit nanotoxicity, the current *in vitro* approaches to study nanotoxicity and their major limitations. We discuss novel methods and show that the complexity of the cell model influences NP uptake and toxicity, highlighting the need for optimization and standardization of the *in vitro* nanotoxicity testing paradigm.

In **Chapter 6**, we assessed how IONPs interact with six related neural cell types, namely murine and human neural stem cells (NSC), neuroblastoma and immortalized neural progenitor cells. Besides species-specific variations, the neuroblastoma cell line and NSCs were respectively least and most affected. Of note, we obtained cell type-specific nanotoxicity profiles in terms of the extent and nature of the effects, indicating that a single toxicity end point will not provide sufficient information on *in vitro* nanotoxicity. In a follow-up study (**Chapter 7**), we reported on the influence of the cell type on the optimization of NPs for biomedical applications. We showed that DMSA-coated IONPs outperformed PMA-coated IONPs in the same six neural cell types, although the differentially coated IONPs again elicited cell-type specific toxicity profiles. Hence, the major cell type-dependent variations in the observed effects warrant the use of relevant human cell models that mimic the envisioned target cells as closely as possible.

Overall, the optimization and standardization of *in vitro* hazard evaluations would significantly improve the quality of *in vitro* nanotoxicity research, which could boost the clinical development of inorganic NPs. In analogy with guidelines on *in vivo* methods established by regulatory bodies, a consensus should be reached on how to assess nanotoxicity *in vitro*. We showed that the cell type is a critical factor that should not be overlooked in the standardization process. Most importantly, correlations should be

established between *in vitro* effects and *in vivo* adverse events to allow extrapolation to possible adverse events in human.

SAMENVATTING & CONCLUSIE

Nanotechnologie is één van de drijfveren achter vele technologische ontwikkelingen in de 21ste eeuw. Vele anorganische en organische materialen vertonen immers unieke eigenschappen op nanoscopische schaal, hetgeen de deur opent naar nieuwe innovatieve producten. Op medisch vlak, worden organische nanopartikels (NPs) veelal gebruikt as dragers voor weinig oplosbare moleculen of marcomoleculen, zoals nucleïne zuren (NZ). Deze laatste groep wordt verpakt in nanoscopische dragers om transport tot zijn doelwit orgaan en opname in de cel te bewerkstelligen zonder verlies van NZ functie. In deze context werden zowel virale als niet-virale dragers in parallel ontwikkeld. Niet-virale dragers worden als relatief veilig beschouwd maar worden gekenmerkt door een beperkte transfectie efficiëntie door vele extra- en intracellulaire barrières die een efficiënte NZ aflevering belemmeren. Endosomale ontsnapping van de NZ wordt beschouwd als het belangrijkste intracellulaire knelpunt. Zelfs ingeval van transfectie met zeer efficiënte dragers, kan slecht een beperkte fractie van de NZ cargo in het cytoplasma afgeleverd worden. Het leeuwendeel van de NZ cargo wordt immers naar de lysosomen geleid, waar ze ten prooi vallen van degraderende enzymen. Om deze afbraak te voorkomen, focussen de meeste recente strategieën op het vermeiden van de lysosomen door vrijstelling van de NZ vanuit de vroege of late endosomen te faciliteren. In tegenstelling tot deze algemene trend, ontwikkelden wij een methode om NZ vrijstelling vanuit de lysosomen te bekomen. Meer specifiek, trachtten we om de afgifte van klein interfererend (si)RNA na transfectie met nanogelen (NG) te bevorderen met behulp van kationische amfifiele geneesmiddelen, meer specifiek functionele inhibitoren van het zure sphingomyelinase (FIASMAs). In **Hoofdstuk 1** werden siRNA, NZ aflevering met behulp van NG en het gebruik van FIASMAs als adjuvans uitgediept.

Initieel werd plasmide (p)DNA afgeleverd via liposomale formulaties. Sinds het gebruik van deze methode werd geëxperimenteerd met adjuvantia om de pDNA afleveringsefficiëntie te verhogen. In **Hoofstuk 2** werden zowel de initiële als recente studies belicht die gebruik maken van een adjuvans strategie. Bepaalde adjuvantia verbeteren de penetratie van de drager in de tumor, terwijl de cellulaire opname eveneens verbeterd kan worden. Enkele andere moleculen zullen specifiek de endosomale vrijstelling verbeteren, interfereren met de intracellulaire verdeling of rechtstreeks de transgen expressie van het afgeleverde pDNA

stimuleren. Twee bijkomende klassen van ajduvantia kunnen de immuun respons reduceren of pDNA translocatie naar de kern begunstigen. Finaal, zijn er bepaalde pleiotrope moleculen (chloroquine, dexamethason en andere steroïden) die simultaan verschillende processen beïnvloeden. Dit overzicht toont duidelijk de diversiteit van de adjuvans strategie aan hoewel het effect van bepaalde adjuvantia sterk afhangt van het NZ, de drager en het moment van toediening ten opzichte van de transfectie. Verdere inzichten in opname, intracellulaire verdeling en endosomale vrijstelling zullen in de toekomst toelaten om rationeel adjuvantia, NZ en dragers te combineren.

In **Hoofdstuk 3** werd aangetoond dat FIASMAs de accumulatie van fosfolipiden, cholesterol en sphingomyeline induceren. Deze kortstondige inductie van een fosfolipidosis fenotype zou vervolgens de stabiliteit van de lysosomale membraan verminderen, waardoor siRNA kan worden vrijgesteld in het cytosol. De vooropgestelde verbeterde afgifte van siRNA naar het cytosol zorgde op zijn beurt voor een sterke verhoging van het therapeutisch potentieel van de siRNA-beladen NG. Verder toonden we aan dat de lysosomen als depot voor gestimuleerde en verlengde siRNA vrijstelling konden dienen. In **Hoofdstuk 4** werd de bredere toepasbaarheid van de FIASMA adjuvans methode bestudeerd. Ten eerste bemerkten we dat een molecule die fosfolipidosis induceert, niet noodzakelijk een functioneel adjuvans is. Verder kunnen bepaalde moleculen de lysosomale membraan mogelijkst te sterk beschadigen waardoor verhoogde siRNA vrijstelling gepaard gaat met cytotoxiciteit. Verder kon de vrijstelling van mRNA niet in een zelfde mate verbeterd worden en waren lipide-gebaseerde transfectie methoden minder gevoelig voor het FIASMA effect.

Samengevat, hebben we aangetoond dat FIASMAs het therapeutisch potentieel van siRNA-belanden NG sterk verhogen maar dat dit effect zowel drager- als NZ-afhankelijk is. Een volgende stap in dit onderzoek is mogelijks het aanduiden van meer potente adjuvantia met behulp van een grootschalige screening. Verder kan de opheldering van het mechanisme waardoor de FIASMAs siRNA aflevering verbeteren uitsluitsel geven over voor welke NZ en dragers deze methode toepasbaar is. Een laatste element dat verder onderzoek vergt is de co-inclusie van zowel het adjuvans als het NZ in eenzelfde drager of de synthese van adjuvans-NZ conjugaten.

Naast het gebruik van organische nanoscopische dragers, worden mogelijke biomedische toepassingen van inorganische NPs uitgebreid bestudeerd. Bepaalde NPs kunnen immers toegepast worden om bestaande detectiemethoden of therapieën te verbeteren of om nieuwe biomedische applicaties te ontwikkelen. Ijzer oxide (IO)NPs kunnen bijvoorbeeld gebruikt worden in magnetisch-geleide aflevering van medicijnen, beeldvorming met magnetische resonantie en de bestrijding van kanker via hyperthermie. Ondanks de vele proof-of-concept studies worden slecht weinig anorganische NPs klinisch toegepast. Dit is in grote mate te wijten aan de onzekere veiligheid van anorganische NPs door de vele contradictorische resultaten van nanotoxiciteitsstudies. In **Hoofdstuk 5** werden NP-interacties op celniveau besproken die tot nanotoxiciteit kunnen leiden. Verder werden de meest gebruikte *in vitro* methoden en hun tekortkomingen aangehaald. Nieuwe methoden werden geïntroduceerd en we toonden aan dat de complexiteit van het *in vitro* cel model de NP opname en toxiciteit beïnvloed, hetgeen het belang van optimalisatie en standaardisatie van *in vitro* methoden benadrukt.

In **Hoofdstuk 6** bestudeerde we hoe IONPs interageren met zes neuronale celtypes, namelijk humane en muriene neuronale stam cellen (NSC), een geïmmortaliseerde neuronale progenitor cellijn en een neuroblastoma kankercellijn. Naast species-specifieke variaties, bemerkten we dat de kanker cellijn en NSC respectievelijk het minst en meest uitgesproken reageerden op de IONPs. Meer nog, elk celtype vertoonde een uniek toxiciteitsprofiel waarbij de mate en het type effect verschilden. Hieruit blijkt dat een enkel eindpunt onvoldoende informatie biedt omtrent de *in vitro* nanotoxiciteit. Vervolgens (**Hoofdstuk 7**) rapporteerden we hoe het celtype de optimalisatie van NPs kan beïnvloeden. Hoewel de DMSA-gecoate IONPs in het algemeen minder toxisch bleken dan de PMA-gecoate IONPs werd in elk celtype opnieuw een uniek nanotoxiciteitsprofiel bekomen. Daarom is het belangrijk om een celmodel te gebruikten dat de doelwitcel zo dicht mogelijk benaderd.

In het algemeen zou de optimalisatie en standaardisatie van *in vitro* nanohazard evaluaties de kwaliteit van nanotoxiciteisonderzoek sterk bevorderen. Hierdoor zou eveneens de klinische toepassing van NPs een boost kunnen krijgen. Naar analogie met richtlijnen omtrent *in vivo* experimenten, zouden regulatoren een consensus moeten bieden over hoe nanotoxiciteit *in vitro* geëvalueerd dient te worden. In dit werk hebben we aangetoond dat het celmodel een belangrijke invloed heeft en dat deze factor niet vergeten mag worden in

de optimalisatie en standaardisatie. Daarnaast dienen bruggen gebouwd te worden tussen *in vitro* toxiciteitseindpunten en *in vivo* waarnemingen aangezien dit zou betere extrapolatie toelaten naar mogelijke nadelige effecten in de mens.

CURRICULUM VITAE

PERSONALIA

Last name	Joris
First name	Freya
Nationality	Belgian
Date of birth	20th December 1989
Place of birth	Jette
Private address	Burg J Neyberghlaan 15A 29, 1090 Jette, Belgium
Private telephone	+32 473 23 12 67
Professional address	Laboratory for General Biochemistry and Physical Pharmacy, Faculty of Pharmaceutical Sciences, Ghent University, Ottergemsesteenweg 460, 9000 Ghent, Belgium
Professional telephone	+32 9 264 80 95
E-mail	freya.joris@ugent.be freya.joris@gmail.com
Websites	https://www.researchgate.net/profile/Freya_Joris https://be.linkedin.com/in/freya.joris

EDUCATION

2010-2012 Master of Science in Drug Development *(Magna cum laude)*

Faculty of Pharmaceutical sciences, Free University of Brussels, Belgium

Master thesis: Optimization of miR-143 transfection in primary rat hepatocytes and its influence on the cell cycle.
Promoter: Prof. T. Vanhaecke from Faculty of Pharmaceutical sciences, Free University of Brussels, Belgium

2007-2010 Bachelor of Science in Pharmaceutical Sciences *(Cum laude)*
Faculty of Pharmaceutical sciences, Free University of Brussels, Belgium

2001-2007 Latin & Sciences
Koninklijk Atheneum Grimbergen, Belgium

INTERNATIONAL PEER REVIEWED PUBLICATIONS

Accepted

Xiong R, **Joris F**, Liang S, Raemdonck K, Demeester J, Skirtach A, De Smedt SC, Himmelreich U, Braeckmans, K. "Cytosolic delivery of labels by photoporation prevents assymetric inheritance and enables extended quantitative *in vivo* cell imaging." *Nano Letters 2016 (IF: 13.78)*.

Joris F, Valdepérez D, Pelaz B, Manshian BB, Soenen SJ, Parak WJ, De Smedt SC, Raemdonck K. "The impact of species and cell type on the nanosafety profiles of iron oxide nanoparticles in neural cells." *Journal of Nanobiotechnology 2016 (IF: 3.74)*.

Peynshaert K., Manshian B.B., **Joris F**., Demeester J., De Smedt S.C., Braeckmans K., Soenen S.J. "Exploiting intrinsic nanoparticle toxicity: the pros and cons of nanoparticle-induced autophagy in biomedical research." *Chemical Reviews 2014 (IF: 37.37)*.

Joris F., Manshian B.B., Peynshaert K., De Smedt S.C., Braeckmans K., Soenen S.J. "Assessing nanoparticle toxicity in cell-based assays: influence of cell culture parameters and optimized models for bridging the *in vitro–in vivo* gap." *Chemical Society Reviews 2013 (IF: 34.09)*.

Submitted

Joris F., Bastiancich C., De Backer L., Van de Vyver T., De Smedt S.C., Raemdonck K.. Cationic amphiphilic drugs induce lysosomal siRNA escape in nanogel transfected cells: towards simple adjuvants of siRNA-mediated gene silencing. Submitted to *Nano Letters February 2017 (IF: 13.78)*

Joris F., Valdepérez D., Pelaz B., Doak S.H., Manshian B.B., Soenen S.J., Parak W.J., De Smedt S.C., Raemdonck K. "Choose Your Cell Model Wisely: The In Vitro Nanosafety Optimization of Differentially Coated Iron Oxide Nanoparticles for Neural Cell Labeling." *Revisions submitted to Acta Biomaterialia January 2017 (IF:6.01)*.

In preparation

Joris F., De Smedt S.C., Raemdonck K. "Boosting non-viral nucleic acid delivery and transfection efficiency: small molecules aid to convey big messages" *Manuscript in preparation for Nano Today (IF:13.16).*

CONFERENCE PROCEEDING

Xiong R., **Joris F**. De Cock I., Demeester J., De Smedt S.C., Skirtach A., Braeckmans K. Efficient delivery of quantum dots in live cells by gold nanoparticle mediated photoporation. Colloidal Nanoparticles for Biomedical Applications, *Proceedings of SPIE* 2015.

PATENT APPLICATION

Joris F., De Smedt S.C., Raemdonck K.. Molecular adjuvants for enhanced cytosolic delivery of active agents. Patent application n° EP17152264.2 (19/1/2017) .

NATIONAL AND INTERNATIONAL CONFERENCES WITH ORAL PRESENTATION

Joris F., Valdepérez D., Soenen S.J., De Smedt S.C., Raemdonck K. Multiparametric high content imaging reveals distinct cell type-specific nanotoxicity profiles.

- *BelTox/Invitrom Annual Scientific Meeting 2015*, Antwerp (Belgium), November 26th 2015.

Joris F., Braeckmans K., Demeester J., De Smedt S.C., Raemdonck K. High content imaging reveals cell type-specific nanotoxicity.

- *SENN 2015, Helsinki (Finland),* April 14th 2015
- *Meeting of the Belgian-Dutch Biopharmaceutical Society*, Vlaardingen (the Netherlands), December 12th 2014.

Joris F., Demeester J., Braeckmans K., De Smedt S.C., Raemdonck K. A comparison of iron oxide nanoparticle induced toxicity in stem cells, a long-lived cell line and a cancer cell line.

- *18th Congress of the European Society for Toxicology In Vitro ESTIV2014*, Egmond aan Zee (the Netherlands), June 12th 2014.

NATIONAL AND INTERNATIONAL CONFERENCES WITH POSTER PRESENTATION

Joris F., Valdepérez D., Pelaz B., Soenen S.J., Parak W.J., De Smedt S.C., Raemdonck K. The importance of the cell model in the optimization of nanoparticles for biomedical applications.

- *Meeting of the Belgian-Dutch Biopharmaceutical Society*, Ghent (Belgium), November 23rd 2015.

Joris F., Braeckmans K., Demeester J., De Smedt S.C., Raemdonck K. High content screening of cell-nanoparticle interactions reveals cell-type specific toxicity profiles.

- *NB-Photonics annual meeting*, Zwijnaarde (Belgium), August 28th 2014

Joris F., Soenen S.J., Demeester J., Braeckmans K., De Smedt S.C., Raemdonck K. Cell type specific IONP toxicity in stem cells, a long lived cell line and a cancer cell line.

- *Knowledge for growth*, Ghent (Belgium), May 8th 2014

Joris F., Soenen S.J., Demeester J., Braeckmans K., De Smedt S.C., Raemdonck K. Selecting a relevant cell type for *in vitro* nanotoxicity studies: a comparison of iron oxide nanoparticle induced toxicity in stem cells, a long-lived cell line and a cancer cell line.

- *7th International Nanotoxicology congress NANOTOX2014*, Antalya (Turkey), April 24th 2014
- *Meeting of the Belgian-Dutch Biopharmaceutical Society*, Ghent (Belgium), December 18th 2013.

INTERNATIONAL RESEARCH EXPERIENCE

DNA Damage Research group, Swansea University, Wales, UK

Subject: High content imaging to study cell-nanoparticle interactions.

Under supervision of Prof. S.H. Doak

May – August 2013.

TEACHING ACTIVITIES

2013 – 2016 Tutor Problem-based learning 2nd Bachelor
Unraveling the biochemistry of DNA

2014 – 2016 Tutor and lab instructor for the Pharmaceutical Bachelor Thesis (FaBaP)

2014 – 2016 Supervisor of:

Gust Nuyten, Master dissertation (Drug Development – Ghent University). The repurposing of small molecules to enhance cytosolic delivery of siRNA. (2016)

Veerle Peeters, Master dissertation (Industrial pharmacy – Ghent University). The use of small molecules to enhance siRNA delivery in cancer cells. (2014)

Lise Vandeputte, Master dissertation (Pharmaceutical care – Ghent University). Controle van de nanopartikelaggregatie voor de acute toxiciteitsbepaling *in vitro*. (2014)

SCHOLARSHIPS

2012 – 2016 IWT PhD fellowship
"Development and optimization of cell culture protocols for evaluation of cell nanoparticle interactions"
Promoters: Prof. Dr. Stefaan De Smedt & Dr. Koen Raemdonck

2014 Partial Fellowship NANOTOX2014
Funding for 7th international conference on nanotoxicology

2013 FCWO funding for long term stay abroad at Swansea University

COURSES

2014 Effective Scientific Communication (Ghent University)
Effective Graphical Displays (Ghent University)

2013 Creative Thinking (Ghent University)

2011 Intensive Course in Dermato-Cosmetic Sciences 2011
(Free University of Brussels)

ACKNOWLEDGEMENTS

Nu rest er enkel nog een woord van dank, want een doctoraat succesvol tot een einde brengen dat doe je ten slotte niet alleen.

Stefaan, jou wil ik in de eerste plaats bedankt voor de kans die je me gegeven hebt om in je lab van start te kunnen gaan. Ik heb ik veel opgestoken van de wijze waarop jij met een open en verwonderde blik naar wetenschap (en de wereld in het algemeen) kijkt en complexe materie in heldere metaforen giet. Daarnaast bewonder ik hoe jij het lab runt, op tijd en stond een luisterend oor biedt en ons al eens belangrijke levenslessen meegeeft. De bemoedigende woorden en het vertrouwen dat ik van je kreeg tijdens de eindspurt van dit doctoraat deden wonderen. Je oprechte interesse in de persoon en de wens dat je studenten goed terecht komen sieren je als persoon. Ik mag hopen dat ik in mijn verdere loopbaan het geluk heb zulke people managers te treffen.

Koen, bedankt om me bijna halfweg mijn doctoraat te adopteren. Het was een plezier om vanaf dan jouw inventieve FIASMA concept uit te werken. Jij bent een vat vol ideeën en bezit een enorme kennis omtrent de onderwerpen van je studenten. Via je zeer nauwgezette begeleiding zet je jouw studenten aan om de beste wetenschapper in hun naar boven te halen. Nu de samenwerking op zijn einde loopt, hoop ik dat jij even trost bent als ik op de resultaten die we samen bereikt hebben. Verder is je benoeming niet minder dan verdiend en wens ik je het allerbeste toe in je verdere academische carrière.

Kevin, ik hou goede herinneringen over aan de samenwerking omtrent de (as)symmetrische nanopartikelverdeling. We hebben een belangrijk nieuw inzicht kunnen aanleveren en ik ben trost dat ik mijn steentje hieraan heb kunnen bijdragen! Daarnaast heb ik zowel van jou als **Jo** belangrijke steun gekregen tijdens het eerste jaar van mijn doctoraat. In de monday meetings samen met **Stefaan (DS)** leerden jullie me dat er van een correcte hypothese vertrokken moet worden en het belang van het definiëren van het juiste experiment met de correcte controles. **Katrien** en **Ine** ook jullie wil ik bedanken voor de wetenschappelijke suggesties tijdens o.a. discussion groups. Daarnaast wil ik elk van jullie bedanken om het Labo Biochemie te maken tot wat het nu is: een aangename werkomgeving waar het de PhD

studenten zeker niet aan kansen ontbreekt en de gecombineerde expertises een brede ondersteuning bieden.

Katharine en **Ilse,** voor alle administratieve beslommeringen kon ik steeds jullie terecht. Oprecht bedankt om het 'minder fijne' papierwerk over te nemen en om steeds de bareel te openen als ik mijn batch weer eens vergeten was. Dan zijn er misschien wel dé meest onmisbare personen als het over praktische aangelegenheden gaat: **Bart & Hilde**. Ik denk dat we maar half beseffen hoeveel jullie doen om het lab draaiende te houden. **Hilde**, jouw hulp in het cellab is alleszins een geschenk uit de hemel. **Bart**, ik heb ontelbare keren aan jouw deur gestaan om een of ander 'probleem' te melden. Bovendien kon je me steeds uit de nood helpen als ik (weer net te laat) iets wou bestellen. Je staat verder steevast klaar met advies of het nu gaat over praktische of persoonlijke zaken. Laatst heb ik mogen ondervinden dat je ook nog is een absolute pro bent in het inbinden van thesissen! Die vier jaar hebben me geleerd dat je een prachtige persoon bent met het hart op de juiste plek en daarom terecht een steunpilaar voor velen als het even (experimenteel) niet mee wil. **Toon**, ook jij mag in dit rijtje niet ontbreken. Jij bent absoluut de reddende engel voor velen van ons. Ook ik heb menig maal gebeld omdat ik een probleem met één van de microscopen zelf niet opgelost kreeg. Je bent oprecht een aanwinst voor het lab.

Wat heb ik geluk gehad dat ik in een labo met zo'n TOP mensen terecht gekomen ben. Ik had me geen leukere bende kunnen wensen om deze vier jaar THUNDER mee te gaan. De jaarlijkse weekendjes, vele concerten, ongeplande uitstapjes naar de bar des amis & de charlatan, afterwork feestjes, housewarmings, uitgelopen traktaties en alles wat ik hier nu nog vergeet, hebben ervoor gezorgd dat jullie meer zijn geworden dan collega's.

First things first, second things second, third things third and the rest you can count on your own. Om te beginnen zijn er natuurlijk de bureau-maatjes. **Koen**, jij zat er al even toen **Elisa** en ik toekwamen. De Wim Helsen one-liners wilden al wel eens door de bureau vliegen en het was al snel duidelijk dat we over veel zaken op dezelfde lijn zitten. Het was dan ook onwennig toen je stoel een tijdje leeg bleef. Anderzijds ben ik content dat je een fijne nieuwe uitdaging gevonden hebt en ik wens jou en Suus een prachtige reis toe. Al kom ik graag eerst nog eens langs voor dat goed glas rood. **Elisa**, I will certainly remember your ability to find order in chaos. More importantly, you are a genuine and kind person and I

wish you the best of luck with everything life has in store for you now. **Lotte**, natuurlijk zal ik jou associëren met de manke swept field, maar er is veel meer dan dat. We hebben elkaar tonnen advies gegeven over experimenten, posters, presentaties, figuren etc. Belangrijker dan dat, we waren elkaars steun en toeverlaat en de gezellige babbels zal ik ontzettend missen. Ik wens je een beter vervolg van 2017 en daarna ontzettend veel succes met het afronden van je doctoraat! (Je hebt mijn nr als je raad nodig hebt ☺.) **Aranit**, Ik wens je toe dat je verder groeit in je onderzoek. **Felix**, I want to thank you a lot for the encouraging gestures during these final months. I wish you the best of luck with your FRAP-eye project and your further career.

Dan zijn er natuurlijk de (ex-)leden van Team Koen. **Lynn**, jou wil ik oprecht bedanken voor het delen van jouw kennis over de nanogelen. Zonder jouw expertise en advies had ik een hele tijd lopen klungelen. Ook nadien kon ik met al mijn vragen bij jou terecht. Je bent met stip één van de meest behulpzame personen van het lab. Nog zo iemand is **Laura**. Als ik jou in drie worden zou moeten omschrijven zouden het behulpzaam, zachtaardig en precies zijn. Ik heb sowieso goede herinneringen aan de vele momenten samen in het cellab, telkens op onze zelfde plek meezingen met de radio of met Roland Garros of De Tour op de achtergrond. **Stephan** (aka complex), ook bij jou kon ik steeds terecht voor advies over van alles en nog wat. Daarnaast ben je ook een echte doorzetter. Ik denk dat weinigen het je nadoen om zo'n werkijver aan de dag te blijven brengen terwijl de resultaten niet steeds meevallen. Ik moet toegeven, jouw thesis was mijn voorbeeld tijdens het schrijven van deze thesis. **Pieterjan**, ik denk niet dat ik al ooit iemand ontmoet heb die zo 'droog' is als jij. Ook jou wil ik bedanken voor de aanmoediging de laatste maanden. Daarnaast wou ik je dit nog meegeven: "Experience is what you obtain, when you don't achieve what you want". **Jelter**, Laura nr 2 en auteur van 'the rising of a new star…'. Je bent misschien niet de meest uitbundige persoon maar kan onverwacht grappig uit de hoek komen: dat pipet mysterie heeft toen echt mijn dag gemaakt! **Thijs**, ik denk dat het FIASMA project bij jou zeker in goede handen is. Succes ermee! Finally, **Roberta** and **Arianna**: the Italian reinforcements. I wish you both the best of luck in the four years to come.

"Like the legendary feeling" of "Like the legend of the phoenix"? **Karen**, wij zijn er 4 jaar geleden samen aan begonnen. Bijna hadden we elkaar al eerder gekend als we samen met Joker van Singapore naar Bangkok waren getrokken! Onze maanden in Swansea zal ik zeker

noot vergeten. Jij die ’s morgens niet uit je woorden komt en ik die voor de eerste koffie nog niet echt veel kan verdragen: top combo! In de eerste twee jaar hebben we ook op wetenschappelijk vlak enorm veel aan elkaar gehad. Daarna heb jij je oogproject uit de grond gestampt, waar ik tonnen respect voor heb. Ik had het je niet nagedaan. Nu begint het ook voor jou te korten. Geniet nog met volle teugen van Canada voor je aan de eindspurt begint! **Rita**, I truly admire your focus and persistence. No wonder you’re office buddies call you ‘the machine’. I’m sure you will do great in Portugal and I can’t wait to come to your defense in September ☺. **Eline**, nog zo’n harde werker, jij lijkt altijd alles onder controle te hebben en je project lijkt als een sneltrein te gaan. Ik heb veel respect voor de wijze waarop jij door je doctoraat lijkt te fietsen en je bijna eeuwig optimisme. **Gaëlle**, de nieuweling in de VNB groep, jou wens ik veel succes met je project.

Heleen, ook jij bent er al van het begin bij. Als een onwetende jonkie kon ik steeds bij jou terecht. Maar ook daarbuiten waren er vele leuke momenten; samen trainen voor de ekiden, I Love Techno, de labo-biochemie-doos,… Merci voor alles! **Joke**, de absolute sfeermaker en het nieuwe prijsbeest van het lab. Samen met Karen vorm je een top-oog-team. **Laurens**, de eerste die liever naar MNM luistert dan StuBru. Gelukkig komen we in zake wijn beter overeen. Alleszins merci voor de info omtrent CRISPR/Cas9. **Ranhua** I enjoyed our collaboration and trips to Leuven and am very happy with the result of our collaboration. **Rein**, jij bent zo mogelijk de meest gezapige mens die ik ken. Daarbuiten ben je oprecht geïnteresseerd in mensen en weet je wanneer een schouderklopje of bemoedigend woordje op zijn plaats is. **Juan**, you have such a bubbly personality! Your joy, optimism, Laura Pausini imitations and love for karaoke were exactly what the group needed. **Silke**, ik apprecieer je eerlijkheid en de wijze waarop je er de sfeer steeds weet in te houden**.** Ik duim mee dat je het noorderlicht ziet in IJsland! **Heyang**, I was truly surprised when I found out you like football! By the way, you and **Jing** make delicious dumplings. **Molood**, I wish you the best of luck with your project.

Thomas, Katrien, Ine DC en George jullie hebben het lab al een tijdje of pas sinds kort verlaten. Ook jullie wil ik bedanken voor de vele goede herinneringen. Thomas zijn (soms flauwe) grappen, Katrien haar photoshop kunsten, Ine haar kaasgunstigheid en George zijn dansmoves, zullen me steeds bijblijven.

Next, I wish to thank the collaborators with whom I worked together during the past four years. **Prof. Préat** and **Chiara**, thank you for the nice collaboration on the FIASMA project. I furthermore want to thank **Prof. Parak, Béatriz** and **Daniel** for the synthesis and characterization of the applied inorganic nanoparticles and straightforward communication afterwards. Finally, I thank **Prof. Doak** for the opportunity to perform research and use the IN Cell Analyzer at the DNA damage group at Swansea University.

Natuurlijk behoort ook een woord van dank toe aan **al mijn lieve vrienden**: de SNOW vrienden, de altijd-feest vriendinnetjes en aanhang, de VUB-vrienden en al degenen die niet in een vakje te schuiven zijn. Bedankt voor jullie interesse, het aanhoren van de vele verhalen en frustraties, de steun in de laatste maanden en zo veel meer…

Mama, papa jullie wil ik bedanken voor de kansen en steun die jullie me altijd gegeven hebben. **Thomas**, merci om te komen luisteren. Dit is normaal gezien de laatste keer dat je naar iets van mij zal moeten komen kijken ;). Ook aan de **Wilgenhof**-clan, merci.

Adriaan, ik weet niet of je beseft hoe groot jouw positieve impact op me is geweest de voorbije jaren. Toen ik me in het begin van mijn PhD dreigde te verliezen in de experimenten, vertelde je me het verhaal van het glas, de stenen, de keitjes en het zand. De moraal van het verhaal: " No matter how full the jar of life may seem, there is always room for a couple of beers with some friends". Hoewel dit de laatste maanden misschien minder het geval was, was het de voorbije jaren wel steevast het devies en zal het vanaf nu opnieuw zijn ingang nemen. Daarvoor alleen al kan ik je niet genoeg bedanken. We hebben samen vier prachtige jaren achter de rug met Laos, Cambodia, Southport Weekender, Namibië, Lapland en de aanschaf van ons appartement als absolute hoogtepunten. Nooit gedacht dat we na 9 jaar op dit punt zouden staan. Maar kijk, jij maakt me gelukkig. Je wenste me de laatste dagen voor het indienen telkens weer succes. Je brengt me aan het lachen, zet mijn favoriete nummers op als ik er nood aan heb, hebt een glas wijn voor me uitgeschonken als het een rotdag was… Je bent de laatste vier jaar mijn grootste steun en toeverlaat geweest en ik hoop dat je dat nog heel lang zal blijven.

Aan iedereen: carrément merci (-> zo gebruik je het dus Stephan)

Freya